



An Electrochemical Investigation of Platinum Group Minerals

By

Margreth Tadie

Thesis Presented in fulfilment of the requirements for the degree of
Doctor of Philosophy

Faculty of Engineering and the Built Environment
Department of Chemical Engineering

University of Cape Town

February 2015



The copyright of this thesis vests in the author. No quotation from it or information derived from it is to be published without full acknowledgement of the source. The thesis is to be used for private study or non-commercial research purposes only.

Published by the University of Cape Town (UCT) in terms of the non-exclusive license granted to UCT by the author.

Declaration

I hereby declare that:

1. This thesis is my own unaided work, both in concept and execution, and that apart from the normal guidance from my supervisor, I have received no assistance.
2. Neither the substance nor any part of the above thesis has been submitted in the past, or is being, or is to be submitted for a degree at this University or at any other university

Acknowledgements

I would like to thank and express my sincere gratitude to the following people and institutions;

- My supervisors, Dr Kirsten Corin and Mrs Jenny Wiese for their guidance, support, hard work editing and friendship when no one else understood me.
- My advisor Professor Cyril O'Connor for his invaluable insight, support throughout the entire PhD process and hours of thesis proof reading.
- My advisor Professor Mike Nicol for introducing me to electrochemistry and consistent willingness to answer questions and listen to ideas and theories.
- Dr Natalie Shackleton of Anglo American Research laboratories for manufacturing the electrodes used in this study
- The staff of the CMR laboratories, particularly Mrs Shireen Govender and Mr Moegsien Southgate who were always available to assist with experimental equipment.
- Colleagues and friends in the chemical engineering department at UCT, with special mention to Thandazile who has been my electrochemistry sounding board, Tanaka, Motena, Constance and Kas.
- My parents, my father Mr Steven Tadie and mother Mrs Esther Tadie who have believed in me from the beginning of this work and have never stopped supporting me.
- Special thanks go to my husband Edson Charikinya who has played the role of spouse, editor, friend and colleague.

List of Publications and Conferences

An investigation into the electrochemical interactions between platinum group minerals and xanthate and dithiophosphate collectors: Mixed Potential Study

M Tadie, K. C. Corin, J. G. Wiese, M. Nicol, C. T. O'Connor

Submitted

An investigation into electrochemical interactions between platinum group minerals and xanthate: Voltammetric Study

M Tadie, K. C. Corin, J. G. Wiese, M. Nicol, C. T. O'Connor

Minerals Engineering 70 (2015) 148–155

Electrochemical interactions of some platinum group minerals with flotation reagents

Margreth Tadie, Kirsten Corin, Jenny Wiese & Cyril O'Connor

Proceedings of XXVII International Mineral Processing Congress, 2014, Santiago Chile

Voltammetric study of the interaction between PGMs and sodium ethyl xanthate

M. Tadie, K. Corin, J. Wiese and C. O'Connor (University of Cape Town, South Africa)

Proceedings of Flotation '13, November 18 – 21 2013, Cape Town South Africa

An investigation into the electrochemical interactions between platinum group minerals and xanthate and dithiophosphate collectors: Mixed Potential Study.

M Tadie, K. C. Corin, J. G. Wiese and C. T. O'Connor

SAIMM Minerals Processing 13, August 2013 Cape Town, South Africa

Synopsis

The Bushveld complex is the largest ore body in the world hosting platinum group elements (PGEs). It is a stratified orebody with three major reefs namely, the Merensky reef, UG2 reef and the Platreef. Platinum and palladium are the most abundant PGEs found in the Bushveld complex. They occur in the form of minerals/mineral phases with elements such as sulphur, tellurium, arsenic and iron. These minerals/mineral phases are associated with base metal sulphides occurring along grain boundaries. Unlike the Merensky and UG2 reef, the Platreef is almost barren of PGE sulphides and the distribution of base metals sulphides and their association with PGMs is erratic.

Froth flotation targeted at the recovery of base metal sulphides is implemented in PGM concentrators to concentrate PGMs. Flotation of sulphide minerals is achieved with the use of thiol collectors to create hydrophobicity, and copper sulphate is often used to improve hydrophobicity and therefore recovery. Sodium ethyl xanthate (SEX) and sodium diethyl dithiophosphate (DTP) are commonly used as collectors on PGM concentrators. The erratic mineral variations in the Platreef ore, however, raise the question of the effectiveness of the application of sulphide mineral flotation techniques on this ore.

Previous work by Shackleton, (2007) investigated the flotation of PGE tellurides, sulphides and arsenides. The study highlighted that the mechanisms with which these minerals interact with collectors and with copper sulphate was poorly understood. It is as a result of the findings of Shackleton's work that this study aims to elucidate the fundamental interactions of telluride and sulphide PGMs with thiol collectors and with copper sulphate. Subsequently this work also aims to compare the behaviour of these reagents on sulphide PGMs and telluride PGMs.

Electrochemical techniques are a classical method for the study of collector-mineral interactions and represent an excellent technique for such studies. An electrochemical study was conducted using thiol collectors, sodium ethyl xanthate (SEX) and sodium diethyl dithiophosphate (DTP) and the minerals PtTe₂, PdTe₂, PtS and PdS. Due to the small grain size of PGMs discrete samples could not be obtained for the study but instead synthetic minerals were used. Synthetic minerals have previously been successfully applied to the study of the behaviour of naturally occurring PGMs by Shamaila and O'Connor, (2008) and Shackleton, (2007).

In this study it was hypothesized that the telluride PGMs would not interact with collectors in the same manner as sulphide PGMs due to their having different crystal structures. Tellurides belong to a melonite structure group whilst sulphides belong to a braggite structure group. It was found that rest potential and cyclic voltammograms in the presence of collector were indeed similar for PtTe₂ and PdTe₂ which have similar crystal structures. The same observation was made in the case of the sulphide minerals of Pt and Pd. It thus appears that there is some correlation between crystal structure of minerals and their electrochemical behaviour. In addition the lower electronegativity of the Te atom was expected

to contribute towards greater ease of oxidation of telluride minerals compared to that of sulphide minerals for which S atoms have higher electronegativity than Te atoms. This was observed in cyclic voltammetry measurements where large oxidation currents were measured for the telluride mineral compared to the sulphide mineral.

pH was found to be a significant factor determining the species formed on PtTe₂ in the presence of SEX. Dixanthogen was identified to be the dominant species formed at pH 5.2, and pH 7 whilst at pH 9.2 a metal thiolate was present alongside dixanthogen and at pH 11.2 a metal thiolate was the only species identified. On the other hand pH had no significant effect on the species formed on PtS which was dixanthogen.

It was also hypothesized that both the sulphide and telluride minerals would not behave in the same manner as their PGE constituents (Pt and Pd) but that they would be more significantly affected by mineral structure. Cyclic voltammetry results showed that in the presence of SEX PtTe₂ was more similar to Pt metal than in the absence of SEX. On the other hand PtS showed voltammograms to be more similar to Pt metal in the absence of SEX than in its presence.

In the study to investigate the effect of CuSO₄ on collector-mineral interactions it was found that at alkaline pH of 10, CuSO₄ was detrimental to the adsorption of collector on both telluride and sulphide mineral surfaces. Shackleton, (2007) also found CuSO₄ to be detrimental to the flotation of these PGMs.

These interactions between telluride minerals and sulphide minerals were investigated in the presence of solids since these conditions are more representative of the conditions prevalent in a flotation cell. Rest potential measurements were conducted for Pt, PtTe₂ and PtS. Results showed that compared to the case of the absence of solids, the rest potential of Pt metal and that of PtS were not significantly affected. The rest potential of PtTe₂ however became more cathodic and there was very little difference between the potential in the presence and absence of collector, thereby questioning whether there in fact had been any interaction on the mineral surface. Studies in the presence of solids were preliminary and present a new scope for the development of mineral-collector interactions going further.

Table of Contents

Declaration.....	i
Acknowledgements	ii
List of Publications and Conferences	iii
Synopsis.....	iv
Table of Contents	vi
List of Figures.....	ix
List of Tables	xvi
Nomenclature	xvii
1 Introduction.....	1
1.1 Background	1
1.2 Geology of the Bushveld Complex	3
1.2.1 Platreef	4
1.3 Mineralogy of the Bushveld Complex	5
1.3.1 Mineralogy of the Platreef	6
1.3.2 PGM Minerals	7
1.4 Flotation	13
1.5 Thiol – Collectors	15
1.5.1 Chemistry	15
1.5.2 Adsorption Mechanism of Thiol Collectors.....	17
1.5.3 Mixed Potential Model.....	19
1.5.4 Electrochemical Investigation of Adsorption Mechanism	21
1.6 Copper Activation.....	27
1.7 Flotation of and Electrochemical Investigations on PGMs.....	30
1.8 Summary and Hypotheses.....	31
2 Research Objectives.....	33
2.1 Objectives	33
2.2 Key Questions.....	33
2.3 Research Approach	34
3 Experimental Materials and Methods.....	35
3.1 Synthesis of Minerals.....	35
3.2 Electrode Manufacture.....	37
3.2.1 X-Ray CT Scan Analysis of Minerals.....	39
3.3 Reagents.....	41
3.4 Equipment	44

3.5	Procedures for Electrochemical Measurement.....	46
3.5.1	Mineral Working Electrode Preparation	46
3.5.2	Rest Potential Measurements	46
3.5.3	Cyclic Voltammetry Measurements.....	48
4	Results	50
4.1	Oxidation Potentials of Collectors	50
4.1.1	Oxidation Potential of SEX.....	50
4.1.2	Oxidation Potential of DTP.....	51
4.1.3	Oxidation Potentials of Modified Thiol Collectors (DTPI, MTP).....	52
4.2	Rest Potential Measurements	52
4.2.1	Validation of Rest Potential Measurement Techniques	52
4.2.2	Rest Potential Measurements of Galena and Pyrite	54
4.2.3	Rest Potential Measurements of Platinum Group Minerals in SEX	55
4.2.4	Rest Potentials of Platinum Group Minerals in DTP	62
4.2.5	Rest Potentials of platinum minerals in DTC, MTP and DTPI.....	66
4.3	Cyclic Voltammetry Study of Platinum Group Minerals with Thiol Collectors	67
4.3.1	Validation of Cyclic Voltammetry Experiments – Galena and Pyrite Measurements..	68
4.3.2	Sodium Ethyl Xanthate Study.....	69
4.3.3	Sodium Diethyl Dithiophosphate Study.....	89
4.4	Interaction of Platinum Group Minerals with Copper Sulphate (CuSO ₄).....	94
4.4.1	Mixed Potential measurements of PtS and PtTe ₂	94
4.4.2	Cyclic Voltammetry Measurements of PtTe ₂	97
4.4.3	Cyclic Voltammetry Measurements of PtS.....	100
5	Discussion.....	104
5.1	Equilibrium Potential Results	106
5.2	Rest Potential Measurements	107
5.2.1	Validation of rest potential measurement technique	107
5.2.2	Rest potentials of platinum minerals in the presence of SEX	108
5.2.3	Rest potential measurements of palladium minerals in SEX	111
5.2.4	Rest potential of platinum group minerals in the presence of DTP	113
5.2.5	Summary of Rest Potential Results.....	113
5.3	Cyclic Voltammetry Study.....	114
5.3.1	Validation and Reproducibility of Measurements	114
5.3.2	Cyclic voltammetry measurements using SEX.....	115
5.3.3	Reactions in DTP	127
5.3.4	Comparison of telluride and sulphide mineral reactions.....	128

5.4	Reactions of Pt Minerals with CuSO ₄	131
5.4.1	Mixed Potential Measurements of PtS and PtTe ₂ with CuSO ₄ and SEX addition.....	133
5.4.2	Cyclic Voltammetry Measurements for PtS and PtTe ₂ in the presence of CuSO ₄ and SEX	136
5.4.3	Summary	140
6	Conclusions.....	143
7	References.....	146
Appendix A	A-1	
CT-Scanning Images for PtS	A-1	
Appendix B	B-1	
Cyclic Voltammetry Results for Pt/Pd Minerals in De-aerated Solution.....	B-1	
Voltammograms measured with 600 mV Switching Potential	B-1	
Voltammograms Measured with 400 mV Switching Potential.....	B-2	
Appendix C	C-1	
Equilibrium Potential Calculations	C-1	
Equilibrium potential calculations for formation of metal xanthates.....	C-1	
Appendix D	D-1	
Collector coverage calculations	D-1	

List of Figures

Chapter 1

Figure 1.1. Factors affecting the flotation process with highlighted areas forming the focus of this study. Adapted from Kimpel, (1984).....	2
Figure 1.2. Aerial map of the Bushveld Complex (Schouwstra and Kinloch, 2000).....	3
Figure 1.3. Stratification of the Bushveld Complex and the relative positions of the Merensky, UG2 and Platreefs with respect to the complex and to each other (Schouwstra and Kinloch, 2000).	4
Figure 1.4. Map of the Northern Bushveld Limb showing the Platreef which is located above the Planknek fault (Holwell et al., 2005).	5
Figure 1.5. Mineral crystal structures. Structures obtained from (http://www.webminerals.com).	9
Figure 1.6. Eh – pH diagram for S-O-H ₂ O system (Pourbaix, 1974).	11
Figure 1.7. Eh – pH diagram of Pt-S-H ₂ O (Westland, 1981).....	11
Figure 1.8. Eh – pH diagram of Pd-S-H ₂ O (Westland, 1981).....	12
Figure 1.9. Eh – pH diagram of Te-O-H ₂ O (Pourbaix, 1974).....	13
Figure 1.10. Chemical structure of a Xanthate, thiol collector molecule.....	14
Figure 1.11. Schematic of a typical concentrator flow sheet (Shackleton, 2007).....	15
Figure 1.12. Schematic of chemisorbed Xanthate on a Galena surface (Woods, 2010).....	18
Figure 1.13. Schematic representation of a mixed potential model for two different redox couples ...	20
Figure 1.14. Schematics of the variation of potential and example of a voltammogram.....	23
Figure 1.15. Cyclic voltammogram of galena in the absence of collector (dotted line) and presence of collector (solid line) at pH 9, 0.1 M Borate solution, 10 mV/s sweep rate, 25 °C, EX concentration of 9.5 x 10 ⁻³ M by (Woods, 1971).	25
Figure 1. 16. Mixed potential model for the effect of copper addition to the rest potential of a mineral (Wang et al., 1989).....	28
Figure 1.17. Speciation diagram for Cu-H ₂ O system at a Cu ²⁺ concentration of 10 ⁻⁵ M (Wang et al., 1989).....	29
Figure 1.18. pE- pH diagram for the Cu – EX system for Cu and EX concentration of 10 ⁻⁴ M where pE=E°/0.059. (Wang et al., 1989).	29

Chapter 3

Figure 3.1. Galena (PbS) and Pyrite (FeS ₂) electrodes	37
Figure 3. 2. Platinum group mineral electrodes, PdTe ₂ , PtTe ₂ , PdS and PtS.....	37
Figure 3.3. Metrohm Pt wire electrode (model 60301100) and Pd metal electrode.	38
Figure 3.4. Electrode mount for electrochemical experiments.	38
Figure 3. 5. X-Ray CT Scans of PtS and Pt (a) and PtTe ₂ and Pt (b).	40

Figure 3.6. X-Ray CT Scans for PdS and Pd (a) and PdTe ₂ and Pd (b).....	41
Figure 3.7. Electrochemistry Equipment Set-Up.	45
Figure 3. 8. Schematic of Standard Rest potential measurement profile including the expected potentials of the dominant reactions affecting the rest potential viz. oxygen reduction, mineral oxidation, collector oxidation	47

Chapter 4

Figure 4.1. Repeated rest potential measurements for Galena in a solution containing 6.24×10^{-4} M SEX at a pH of 7.....	53
Figure 4.2. Repeated rest potential measurements for Pyrite in a solution containing 6.24×10^{-4} M SEX at a pH of 7.....	53
Figure 4.3. Rest potential of Galena and Pyrite at pH 9.2 in the presence and absence of SEX	54
Figure 4.4. Rest potential of Galena and Pyrite at pH 9.2 in the presence and absence of diethyl dithiophosphate.....	55
Figure 4.5. Rest potential of platinum minerals at pH 9.2 in the presence and absence of SEX.....	56
Figure 4.6. Rest potential of platinum minerals at pH 4.2 in the presence and absence of SEX.....	57
Figure 4.7. Rest potential results for PtTe ₂ under different anodising conditions at pH 9.2 and with SEX collector addition after 600 s.....	58
Figure 4.8. Rest potential results for PtS under different anodising conditions at pH 9.2 and with SEX collector addition after 600 s.....	58
Figure 4.9. Rest potential results for Pt minerals in pulp at pH 7 before and after collector addition of SEX.....	59
Figure 4.10. Rest potential of palladium minerals at pH 9.2 in the presence and absence of SEX	60
Figure 4.11. Mixed potential of palladium minerals at pH 4.2 in the presence and absence of SEX...	61
Figure 4.12. Rest potential results for PdTe ₂ under different anodising conditions at pH 9.2 and with SEX collector addition after 600 s	61
Figure 4.13. Rest potential results for PdS under different anodising conditions at pH 9.2 and with SEX collector addition after 600 s.....	62
Figure 4.14. Rest potential of platinum minerals at pH 9.2 in the presence and absence of diethyl dithiophosphate.....	63
Figure 4.15. Rest potential of platinum minerals at pH 4.2 in the presence and absence of diethyl dithiophosphate.....	64
Figure 4.16. Mixed potential of palladium minerals at pH 9.2 in the presence and absence of diethyl dithiophosphate.....	65
Figure 4.17. Mixed potential of palladium minerals at pH 4.2 in the presence and absence of diethyl dithiophosphate.....	65

Figure 4.18. Mixed potential of platinum minerals at pH 9.2 in the presence and absence of monothiophosphate.....	66
Figure 4.19. Mixed potential of platinum minerals at pH 9.2 in the presence and absence of diethyl dithiophosphate.....	67
Figure 4.20. Cyclic voltammograms for galena (PbS) with forward starting sweeps measured for a single sweep in the absence and presence of collector, 1×10^{-2} M SEX in an aerated solution of 0.1 M $\text{Na}_2\text{B}_4\text{O}_7$ (a) 10 mV/s sweep rate and (b) 40 mV/s sweep rate. The oxidation potential for dixanthogen is indicated as a dotted line at 0.15 V.	68
Figure 4.21. Cyclic voltammograms for Pt with forward starting sweeps measured for two sweeps in the absence and presence of collector, 6×10^{-4} M SEX (a) aerated solution conditions and (b) nitrogen saturated solution conditions. The oxidation potential for dixanthogen is indicated as a dotted line at 0.15 V.....	69
Figure 4.22. Cyclic voltammograms for PtTe_2 with forward starting sweeps measured for two sweeps in the absence and presence of collector, 6.24×10^{-4} M SEX (a) aerated solution conditions and (b) nitrogen saturated solution conditions. The oxidation potential for dixanthogen is indicated as a dotted line at 0.15 V.....	70
Figure 4.23. Cyclic voltammograms for PtTe_2 with a reverse starting sweep measured for two sweeps in the absence and presence of SEX, 6.24×10^{-4} M, in an aerated solution. The oxidation potential for dixanthogen is indicated as a dotted line at 0.15 V.....	71
Figure 4.24. Cyclic voltammograms for PtTe_2 with a forward starting sweep measured for one sweep in the absence and presence of 6.24×10^{-4} M SEX, in an aerated solution. The oxidation potential for dixanthogen is indicated as a dotted line at 0.15 V.....	72
Figure 4.25. Linear sweep voltammograms in the presence and absence of 6.24×10^{-4} M SEX collector in aerated solution (a) oxidation sweep and subsequent reduction sweep (b) reduction sweeps generated after applying an anodic potential of 0.207 V for 15 minutes.	73
Figure 4.26. Cyclic voltammogram for PtTe_2 with forward starting sweeps in the absence and presence of 6.24×10^{-4} M SEX measured in aerated solution conditions. Voltammograms presented for varying pH conditions, pH 5.2, pH 7, pH 9.2 and pH 11.2 (starting potential of 0.207 V).	74
Figure 4.27. Cyclic voltammograms for PtTe_2 in forward starting sweeps in the presence of (a) 2.5×10^{-2} M SEX measured for two sweeps and (b) 2.5×10^{-3} M SEX measured for a single sweep in aerated solution. The oxidation potential for dixanthogen is indicated as a dotted line at 0.15 V.	75
Figure 4.28. Cyclic voltammograms for PtTe_2 in a forward started sweep for a single sweep in the presence of 6.24×10^{-4} M SEX measured in an aerated solution. Voltammograms measured at sweep-rates of 1 mV/s, 10 mV/s and 50 mV/s.	76
Figure 4.29. Cyclic voltammograms for PtS with a forward starting sweep measured for two sweeps in the absence and presence of collector, 6.24×10^{-4} M under aerated solution conditions. The oxidation potential for dixanthogen is indicated as a dotted line at 0.15 V.	77

Figure 4.30. Cyclic voltammograms for PtS with a reverse starting sweep measured for two sweeps in the absence and presence of 6.24×10^{-4} M SEX, under aerated solution conditions. The oxidation potential for dixanthogen is indicated as a dotted line at 0.15 V.	78
Figure 4.31. Cyclic voltammograms for PtS with a forward starting sweep measured for one sweep in the absence and presence of 6.24×10^{-4} M SEX, under aerated solution condition. The oxidation potential for dixanthogen is indicated as a dotted line at 0.15 V.	79
Figure 4.32. Cyclic voltammogram for PtS with forward starting sweeps in 6.24×10^{-4} M SEX in aerated solution. Voltammograms are shown for varying pH conditions, pH 5.2, pH 7, pH 9.2 and pH 11.2 and the potential for dixanthogen formation is indicated as a vertical dotted line at 0.15 V.....	80
Figure 4.33. Cyclic voltammograms for PtS in forward starting sweeps in the presence of (a) 2.5×10^{-2} M SEX measured for 2 sweeps and (b) 2.5×10^{-3} M SEX measured for a single sweep in aerated solution. The reduction potential for xanthate to dixanthogen is superimposed at the potential of 0.15 V as a dotted line.	81
Figure 4.34. Cyclic voltammogram for PtS with forward starting sweeps in the presence of 6.24×10^{-4} M SEX for forward starting sweeps at sweep-rates of 1 mV/s, 10 mV/s and 50 mV/s measured in an aerated solution.	82
Figure 4.35. Cyclic voltammograms for Pd with reverse starting sweep measured for two sweeps in the absence and presence of 6.24×10^{-4} M SEX (a) in aerated solution conditions and (b) nitrogen saturated solution conditions. The oxidation potential for dixanthogen is indicated as a dotted line at 0.15 V... ..	82
Figure 4.36. Cyclic voltammograms for PdTe ₂ with forward starting sweep measured for two sweeps in the absence and presence of 6.24×10^{-4} M SEX (a) in aerated solution conditions and (b) nitrogen saturated solution conditions. The oxidation potential for dixanthogen is indicated as a dotted line at 0.15 V.....	83
Figure 4.37. Cyclic voltammograms for PdTe ₂ with reverse starting sweep measured for two sweeps in the absence and presence of 6.24×10^{-4} M SEX (a) in aerated solution conditions and (b) nitrogen saturated solution conditions. The oxidation potential for dixanthogen is indicated as a dotted line at 0.15 V.....	84
Figure 4.38. Cyclic voltammograms for PdTe ₂ with a reverse starting sweep measured for two sweeps in the absence and presence of 6.24×10^{-4} M SEX, in aerated solution. The oxidation potential for dixanthogen is indicated as a dotted line at 0.15 V.....	85
Figure 4.39. Cyclic voltammograms for PdTe ₂ with a forward starting sweep measured for one sweep in the absence and presence of 6.24×10^{-4} M SEX, in aerated solution. The oxidation potential for dixanthogen is indicated as a dotted line at 0.15 V.....	86
Figure 4.40. Cyclic voltammograms for PdS with forward starting sweep measured for two sweeps in the absence and presence of 6.24×10^{-4} M SEX (a) in aerated solution conditions and (b) nitrogen saturated solution conditions. The oxidation potential for dixanthogen is indicated as a dotted line at 0.15 V.....	87

Figure 4.41. Cyclic voltammograms for PdS with a reverse starting sweep measured for two sweeps in the absence and presence of collector 6.24×10^{-4} M SEX, in aerated solution. The oxidation potential for dixanthogen is indicated as a dotted line at 0.15 V.	88
Figure 4.42. Cyclic voltammograms for PdS with a forward starting sweep measured for one sweep in the absence and presence of 6.24×10^{-4} M SEX, under aerated solution conditions. The oxidation potential for dixanthogen is indicated as a dotted line at 0.15 V.	88
Figure 4.43. Cyclic voltammograms for PtTe ₂ with a forward starting sweep at a sweep rate of 10 mV/s measured for one sweep in the absence and presence of 6.24×10^{-4} M DTP, under aerated solution conditions. The oxidation potential for DTP ₂ is indicated as a dotted line at 0.388 V.	90
Figure 4.44. Cyclic voltammograms for PtTe ₂ with a forward starting sweep at a sweep rate of 1 mV/s measured for a single sweep in the absence and presence of 6.24×10^{-4} M DTP, (a) in aerated solution conditions (b) in Nitrogen saturated solution conditions. The oxidation potential for DTP ₂ is indicated as a dotted line at 0.388 V.	91
Figure 4.45. Cyclic voltammograms for PtS with a forward starting sweep at a sweep rate of 10 mV/s measured for a single sweep in the absence and presence of 6.24×10^{-4} M DTP, in aerated solution. The oxidation potential for DTP ₂ is indicated as a dotted line at 0.388 V.	92
Figure 4.46. Cyclic voltammograms for PtS with a forward starting sweep at a sweep rate of 1 mV/s measured for a single sweep in the absence and presence of 6.24×10^{-4} M DTP, in aerated solution conditions. The oxidation potential for DTP ₂ is indicated as a dotted line at 0.388 V.	92
Figure 4.47. Cyclic voltammograms for PdTe ₂ with a forward starting sweep at a sweep rate of 10 mV/s measured for a single sweep in the absence and presence of 6.24×10^{-4} M DTP, in aerated solution. The oxidation potential for DTP ₂ is indicated as a dotted line at 0.388 V.	93
Figure 4.48. Cyclic voltammograms for PdS with a forward starting sweep at a sweep rate of 10 mV/s measured for a single sweep in the absence and presence of 6.24×10^{-4} M DTP, in aerated solution conditions. The oxidation potential for DTP ₂ is indicated as a dotted line at 0.388 V.	94
Figure 4.49. Mixed potential of platinum minerals at pH 10 in the absence of SEX and CuSO ₄ followed by the addition of CuSO ₄ and SEX.	95
Figure 4.50. Mixed potential of platinum minerals at pH 8 in the absence of SEX and CuSO ₄ followed by the addition of CuSO ₄ and SEX.	96
Figure 4.51. Rest potential of platinum minerals at pH 6 in the absence of SEX and CuSO ₄ followed by the addition of CuSO ₄ and SEX.	96
Figure 4.52. Cyclic voltammograms for PtTe ₂ with a forward starting sweep at a sweep rate of 10 mV/s measured for a single cycle in the absence and presence of 1×10^{-4} M SEX, in the presence of 1×10^{-4} M CuSO ₄ and in the presence of both 1×10^{-4} M SEX and 1×10^{-4} M CuSO ₄ in de-aerated solution at pH 10.	97
Figure 4.53. Cyclic voltammograms for PtTe ₂ with a forward starting sweep at a sweep rate of 10 mV/s measured for a single cycle in the absence and presence of 1×10^{-4} M SEX, in the presence of 1×10^{-4}	

M CuSO ₄ and in the presence of a both 1 x 10 ⁻⁴ M SEX and 1 x 10 ⁻⁴ M CuSO ₄ in de-aerated solution at pH 8.....	98
Figure 4.54. Cyclic voltammograms for PtTe ₂ with a forward starting sweep at a sweep rate of 10 mV/s measured for a single cycle in the absence and presence of 1 x 10 ⁻⁴ M SEX, in the presence of 1x10 ⁻⁴ M CuSO ₄ and in the presence of a both 1 x 10 ⁻⁴ M SEX and 1 x 10 ⁻⁴ M CuSO ₄ in de-aerated solution at pH 6.....	100
Figure 4.55. Cyclic voltammograms for PtS with a forward starting sweep at a sweep rate of 10 mV/s measured for a single cycle in the absence and presence of 1 x 10 ⁻⁴ M SEX, in the presence of 1x10 ⁻⁴ M CuSO ₄ and in the presence of a both 1 x 10 ⁻⁴ M SEX and 1 x 10 ⁻⁴ M CuSO ₄ in de-aerated solution at pH 10.....	101
Figure 4.56. Cyclic voltammograms for PtS with a forward starting sweep at a sweep rate of 10 mV/s measured for a single cycle in the absence and presence of 1 x 10 ⁻⁴ M SEX, in the presence of 1x10 ⁻⁴ M CuSO ₄ and in the presence of a both 1 x 10 ⁻⁴ M SEX and 1 x 10 ⁻⁴ M CuSO ₄ in de-aerated solution at pH 8.....	102
Figure 4.57. Cyclic voltammograms for PtS with a forward starting sweep at a sweep rate of 10 mV/s measured for a single cycle in the absence and presence of 1 x 10 ⁻⁴ M SEX, in the presence of 1x10 ⁻⁴ M CuSO ₄ and in the presence of a both 1 x 10 ⁻⁴ M SEX and 1 x 10 ⁻⁴ M CuSO ₄ in de-aerated solution at pH 6.....	103

Chapter 5

Figure 5.1. Mixed potential response to the addition of reductive and oxidative reactions.....	105
Figure 5.2. Oxidation potentials of the thiolate/dithiolate formation potential of SEX, DTP, MTP and DTPI at pH 9.2.....	106
Figure 5.3. Cyclic voltammograms for PtTe ₂ in an aerated solution in the absence of collector over varied pH levels.	117
Figure 5.4. Current – time curves for PtTe ₂ anodically polarised at 0.207 V in an aerated solution for Figure 4.25b. The solid line and dotted line represent repeat measurements.	118
Figure 5.5. Cyclic voltammograms for PtS in an aerated solution in the absence of collector over varied pH levels.	122
Figure 5.6. Cyclic voltammograms for PtS in an aerated solution in the absence of collector over varied pH levels.	122
Figure 5. 7 Speciation diagram for copper species in solution at a collector concentration of 1x10 ⁻⁴ M CuSO ₄	132
Figure 5. 8 pE- pH diagram for the Cu – EX system for Cu and EX concentration of 10 ⁻⁴ M where pE=E°/0.059 (Wang et al., 1989).	134

Appendix A

Figure A.1. PtS CT-Scanning surface image, 220kV, 20 micron resolution and 1hour scan.A-1

Figure A.2. Cross sectional slice through PtS electrode, 220 kV scan.A-1

Appendix B

Figure B.1. Cyclic voltammograms for (a) PtTe₂ with a forward starting sweep and (b) PdTe₂ in a reverse starting sweep with two sweeps measured in the absence and presence of collector 6×10^{-4} M. The oxidation potential for dixanthogen is indicated as a dotted line at 0.15 V. B-1

Figure B.2. Cyclic voltammograms for (a) PtS with a forward starting sweep and (b) PdS in a reverse starting sweep with two sweeps measured in the absence and presence of collector 6×10^{-4} M. The oxidation potential for dixanthogen is indicated as a dotted line at 0.15 V. B-2

Figure B.3. Cyclic voltammograms for (a) PtTe₂ with a reverse starting sweep measured for two sweeps and (b) PdTe₂ with a forward starting sweep measured for one sweep in the absence and presence of collector 6×10^{-4} M. The oxidation potential for dixanthogen is indicated as a dotted line at 0.15 V. B-2

Figure B.4. Cyclic voltammograms for PdTe₂ (a) with a reverse starting sweep measured for two sweeps and (b) with a forward starting sweep measured for one sweep in the absence and presence of collector 6.24×10^{-4} M. The oxidation potential for dixanthogen is indicated as a dotted line at 0.15 V. B-2

Figure B.5. Cyclic voltammograms for PtS (a) with a reverse starting sweep measured for two sweeps and (b) with a forward starting sweep measured for one sweep in the absence and presence of collector 6.24×10^{-4} M. The oxidation potential for dixanthogen is indicated as a dotted line at 0.15 V. B-2

Figure B.6. Cyclic voltammograms for PdS (a) with a reverse starting sweep measured for two sweeps and (b) with a forward starting sweep measured for one sweep in the absence and presence of collector 6.24×10^{-4} M. The oxidation potential for dixanthogen is indicated as a dotted line at 0.15 V. B-3

Appendix D

Figure D.1. Gamry software source file for PtTe₂ indicating integrated peaks.D-2

List of Tables

Chapter 1

Table 1.1. Mineralogy and Platinum distribution of the Platreef, Merensky Reef and UG-2 Reef in the Bushveld Complex. Adapted from (Shamaila and O'Connor, 2008).....	6
Table 1.2. Common Platinum and Palladium, Sulphides and Tellurides and their unit cell dimensions. Information compiled from (Berlincourt et al., 1981)	8
Table 1.3. Structures of some common thiol collectors.....	17
Table 1.4. Results of rest potentials of various minerals and the surface species on the mineral surface in solution of 6×10^{-4} M potassium ethyl xanthate by Allison et al., (1972).....	21

Chapter 4

Table 4.1. Equilibrium potentials of SEX at different concentrations	50
Table 4.2. Equilibrium potential of SEX compared to literature values.....	51
Table 4.3. Results of measured equilibrium potentials of diethyl dithiophosphate	51
Table 4.4. Equilibrium potential of diethyl dithiophosphate compared to literature values	51
Table 4.5. Results of the equilibrium potential measurements of sodium dithiophosphate (DTPI) ..	52
Table 4.6. Summary of the rest potential values for Galena and Pyrite after 600 s compared to values reported in literature for the same system.....	54

Chapter 5

Table 5. 1. Calculation of fractional coverage of SEX on PtTe ₂ surfaces. Γ (mol) denotes total coverage in mols and (Γ/Γ_m) denotes the fraction of a monolayer that the collector coverage results in.	130
Table 5.2. Summary of XPS data obtained by Shackleton, (2007) for PtS and PtTe ₂ adapted from (Shackleton, 2007)	142

Appendix C

Table C.1. Electrochemical reactions with their standard equilibrium potentials and calculated equilibrium potentials for the conditions measured.....	C-1
--	-----

Nomenclature

A	Amperes
a_{ox}	Activity of oxidised species
a_{red}	Activity of reduced species
AgCl	Silver chloride
$A_{mineral}$	Surface Area
ATR	Attenuated Infrared
BMS	Base metal sulphides
DTC	Diethyl dithiocarbamate
DTP	Diethyl dithiophosphate
DTPI	Diethy di-isobutyl dithiophosphate
E	Equilibrium potential at given conditions
E°	Standard equilibrium potential
E_h	Solution equilibrium potential
F	Faradays Constant
FeS ₂	Pyrite
ΔG_r°	Standard Gibbs energy of reaction
ΔG_f°	Standard Gibbs energy of formation
GNPA	Grasvally norite-pyroxenite-anorthosite
Γ	Surface coverage
IR	Infra-red
IUPAC	International
KCl	Potassium chloride
KEX	Potassium ethyl xanthate

MTP	Monothiophosphate
MX	Metal xanthate
n	Number of moles
OCP	Open circuit potential
PbS	Galena
Pd	Palladium
PdS	Vysotskite
PdTe ₂	Merenskyite
PGM	Platinum group minerals
PGE	Platinum group elements
ppm	Parts per million
Pt	Platinum
PtS	Cooperite
PtTe ₂	Moncheite
Q	Charge
ROM	Run of Mine
SEX	Sodium ethyl xanthate
SHE	Standard hydrogen electrode
t	Time
Th	Thiolate
ToF SIMS	Time of flight secondary ion mass spectrometry
UG2	Upper Group 2
UV-Vis Spectroscopy	Ultra violet visual spectroscopy
V	Volts

w/w%	Weight percent
X ₂	Dixanthogen
XPS	X-Ray Photo spectroscopy

Chapter 1

1 Introduction

1.1 Background

The Bushveld Complex is the largest natural reserve of platinum group elements (PGE's) in the world. From it, South Africa contributes up to 80% of the world's platinum (Cawthorn et al., 2002). This large reserve of ore is comprised of three main reefs, the Merensky reef, Upper Group 2 (UG2) reef and the Platreef. Despite early discovery (1925), mining operations on the Platreef only seriously commenced in 1992 (Kinnaird and McDonald, 2005). Interest in the Platreef has increased because next to the Merensky and UG2 reefs, it is one of the largest ore reserves of platinum group elements (PGEs) in the world. According to a study by Cawthorn, (1999) the platinum and palladium reserves of the Bushveld complex, probable and proven, are estimated at 204 and 116 million ounces respectively over a depth of only 2km. It is further shown that platinum and palladium in the Merensky, UG2 and Platreef's make up 55% and 32%, 44% and 36%, and 46% and 30% respectively, of total platinum group minerals (PGMs) (Cawthorn, 1999). These figures illustrate the importance of studying the extraction of these PGEs from these reefs.

PGEs form complexes (minerals) with three groups of elements, viz. semimetals (Bi, Te, Sb, Se, As, and S), metals (Pb, Cu, Zn) and other transition elements (Fe, Co, Ni) (Daltry and Wilson, 1997). The most significant platinum group minerals are tellurides, sulphides, arsenides and Fe alloys (Viljoen and Schurmann, 1998). Distribution of these PGMs in the Bushveld complex occurs in three modes, viz locked in base metal sulphides (BMS), locked in silicate minerals and occurring on the grain boundaries of these minerals (Penberthy et al., 2000; Viljoen and Schurmann, 1998).

Metallurgical treatment of the ores from the Bushveld complex involves concentration by flotation yielding a high grade product (concentrates). These concentrates are smelted followed by converting and then refining to produce pure PGEs as a final product. The concentration process is necessary in order to optimise the cost of smelting which is expensive. Higher recoveries in the flotation circuit translate to larger amounts of product and higher concentrate grades translate to purer products. Flotation is therefore an important part of the metallurgical treatment of PGM ores. Performance of this process is dependent on three main components; operation, chemistry and equipment.

This study focuses on the chemical component of flotation with specific reference to collector chemistry as is illustrated in Figure 1.1 which is adapted from Klimpel, (1984). The highlighted sections form the focus of this work. In the chemical component, collectors impart hydrophobicity to the mineral once attachment has taken place. As a result the attachment of a collector and the selectivity of the collector,

i.e. how strongly the chemical is able to attach to a mineral, are significant properties of the collector. Mechanisms of attachment of collectors, thiol collectors specifically, have been studied and found to be electrochemical reactions. As a result electrochemical techniques such as rest potential measurements and cyclic voltammetry are used to study the attachment of collectors on mineral surfaces.

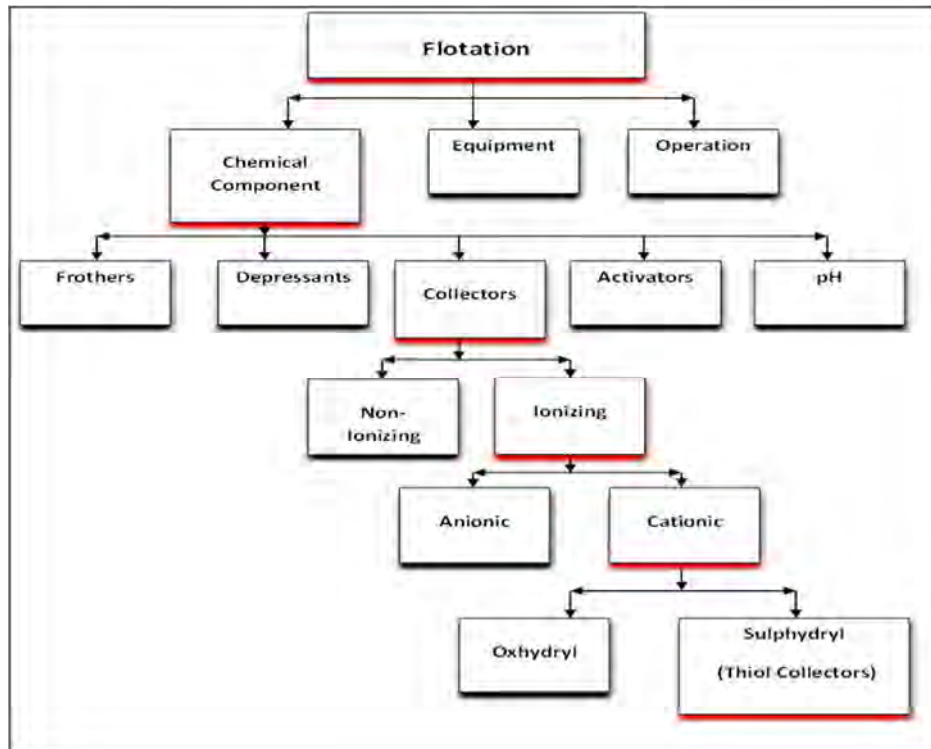


Figure 1.1. Factors affecting the flotation process with highlighted areas forming the focus of this study. Adapted from Kimpel, (1984).

Currently flotation practice is designed for the recovery of sulphide minerals Shackleton, (2007) and it is assumed that all PGMs will respond to the reagent chemistry in a manner similar to the sulphides. The chemistry involves the use of sulphydryl collectors (thiol collectors), to create hydrophobicity on sulphide minerals. The most common of these types of collectors are xanthates which have been used to float sulphide minerals since their discovery in 1920. Xanthates are used as either a single collector or as part of a mixed collector system in which a more selective collector such as dithiophosphate is used as a secondary collector (Wiese et al., 2005). A high proportion of sulphide minerals within Merensky and UG2 reefs have made the use of collectors such as these, widely used in industry. The use of these same collectors for flotation of the Platreef does not effectively translate however due to the fact that the Platreef is almost barren of sulphide minerals in some areas. Under such reagent suites, PGMs within the Platreef have been found to report to flotation tailings (Shackleton, 2007; Shamaila and O'Connor, 2008). Given the size of the reef, these are significant losses of value material. It is therefore important to understand whether the choice of reagent suite has an effect on these losses by studying collector mineral interactions.

1.2 Geology of the Bushveld Complex

The Bushveld complex is a siliceous body of ore that arose from a magmatic intrusion in the earth's crust (Figure 1.2). The complex covers an area of 65000 km² and has a thickness of 7 – 9 km (Cawthorn, 1999; Schouwstra and Kinloch, 2000). Solidification of magma occurred in layers which are enriched in various minerals with varying compositions (Cawthorn, 1999; Cawthorn, 2011; Schouwstra and Kinloch, 2000).

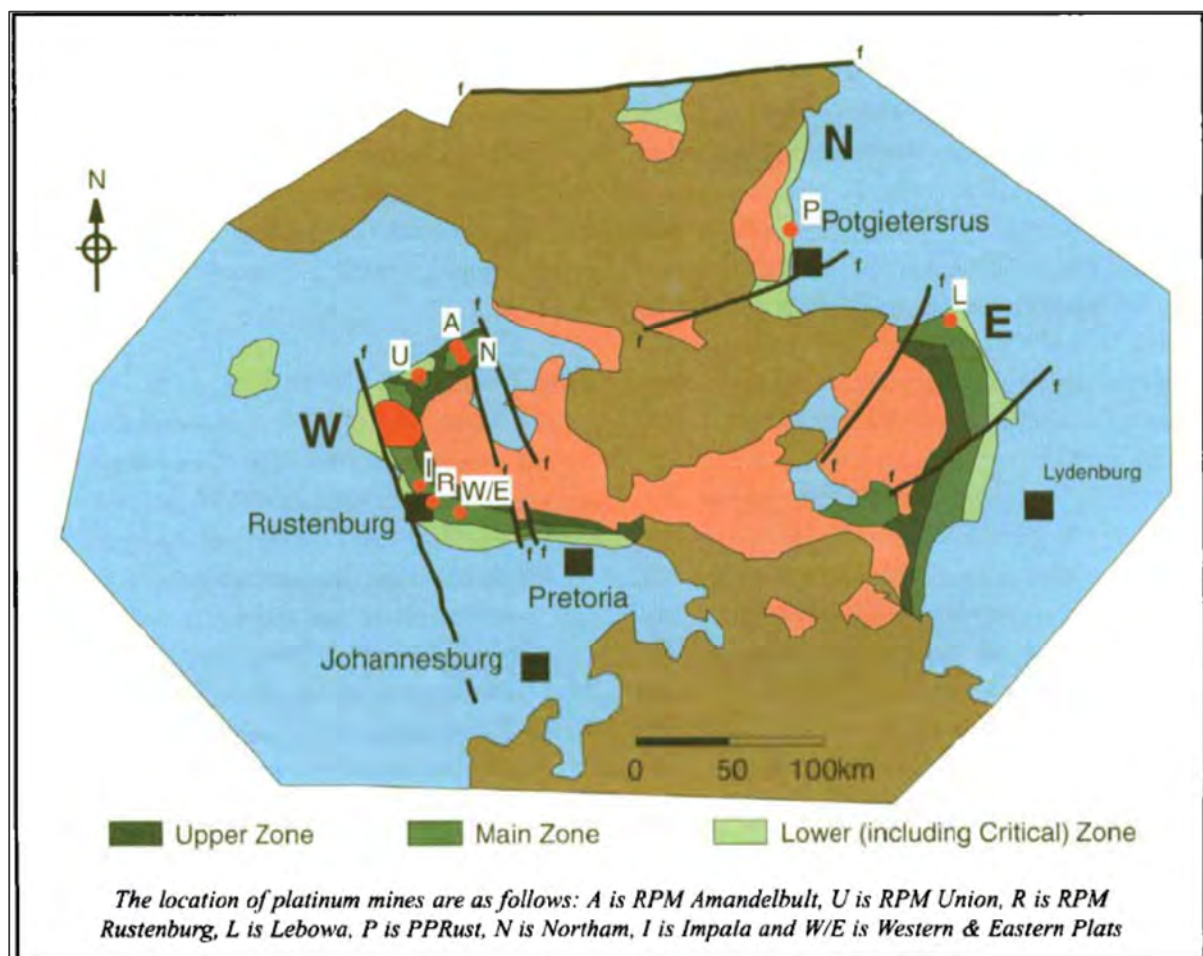


Figure 1.2. Aerial map of the Bushveld Complex (Schouwstra and Kinloch, 2000).

Three major sections (limbs) make up the complex viz. Northern, Eastern and Western limbs. Various mechanisms for the formation of the complex are proposed by researchers (Barnes, 2004; Barnes et al., 2004; Cawthorn et al., 2002; Cawthorn, 2011; Holwell et al., 2006; Kinloch, 1982; McDonald et al., 2005). These mechanisms all suggest the intrusion of magma over different time periods resulting in layered formation with stratified mineralogy. Differences in the layers of the complex are attributed to the intrusion of different magmas at different times. PGMs are concentrated within the different layers and the mechanism by which this took place is a source of contradiction between researchers. It is proposed that percolation of a sulphide liquid carrying dissolved PGEs through solidifying rock resulted in the formation of PGMs and their concentration in regions such as the chromite rich regions

(Cawthorn, 2011). This theory is presumed to account for the mineralisation within the Merensky and UG2 reefs.

Of the mineralised layers referred (reefs) the most economically viable with regard to PGE mineralisation are the Merensky reef and the UG2 reefs in the Eastern and Western limbs, and Platreef only present in the Northern limb. These reefs occur in zones subdivided into the Upper Zone, Critical Zone and Lower Zone (Figure 1.3).

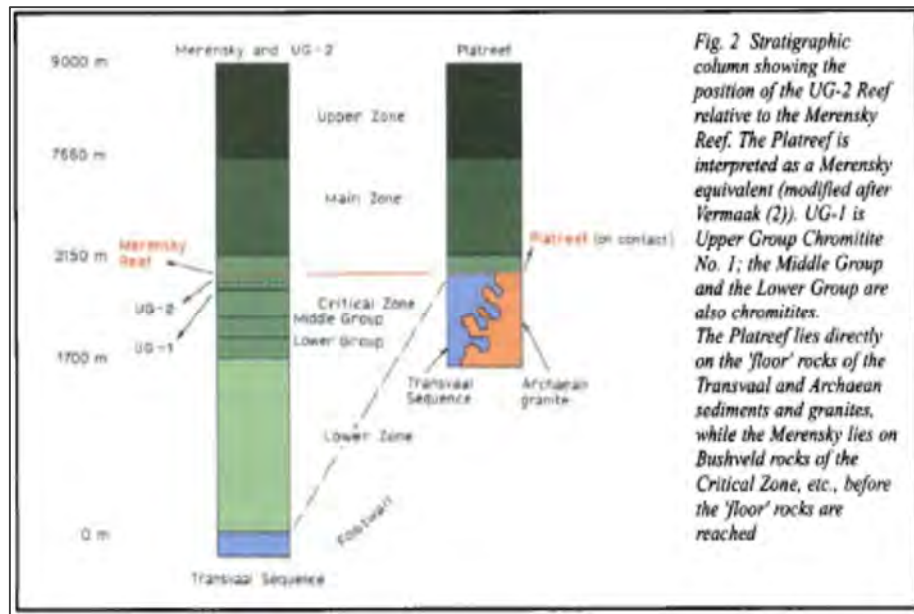


Figure 1.3. Stratification of the Bushveld Complex and the relative positions of the Merensky, UG2 and Platreefs with respect to the complex and to each other (Schouwstra and Kinloch, 2000).

1.2.1 Platreef

Located in the Northern limb of the Bushveld Complex, it can be traced for 35 km and has stratigraphy similar to that of the rest of the Bushveld complex. Minerals in the lower zone are harzburgites and pyroxenites, the critical zone (Grasvally norite-pyroxenite-anorthosite GNPA) is made of layered orthopyroxene-chromite-clinopyroxene-plagioclase cumulates, the main zone of gabbros and gabbronorites whilst the upper zone is made up of ferrogabbros with magnetite (Kinnaird and McDonald, 2005). Within the Northern limb (c.f. Figure 1. 4) the Platreef can be defined as the “mafic units that occur between the Archaean granite – gneiss basement or Transvaal Supergroup and the gabbros gabbronorites of the Main Zone which are north of the Planknek Fault (Kinnaird and McDonald, 2005). PGE mineralisation within this reef is heterogenous but main mineralisation in the Platreef occurs near the footwall of the reef and just below the gabbronorite hanging wall (Holwell et al., 2005). Division of the reef is in three main sections the first being a ‘C’ Reef which is in contact with the hanging wall of the main zone, a ‘B Reef’ which is comprised of coarse grained pyroxenites and an ‘A’ reef which is a feldspathic pyroxenite reef in contact with the footwall (Transvaal

Supergroup or Archaean Granite) (Armitage et al., 2002). Reefs A and B host the major PGE mineralisation of the Platreef.

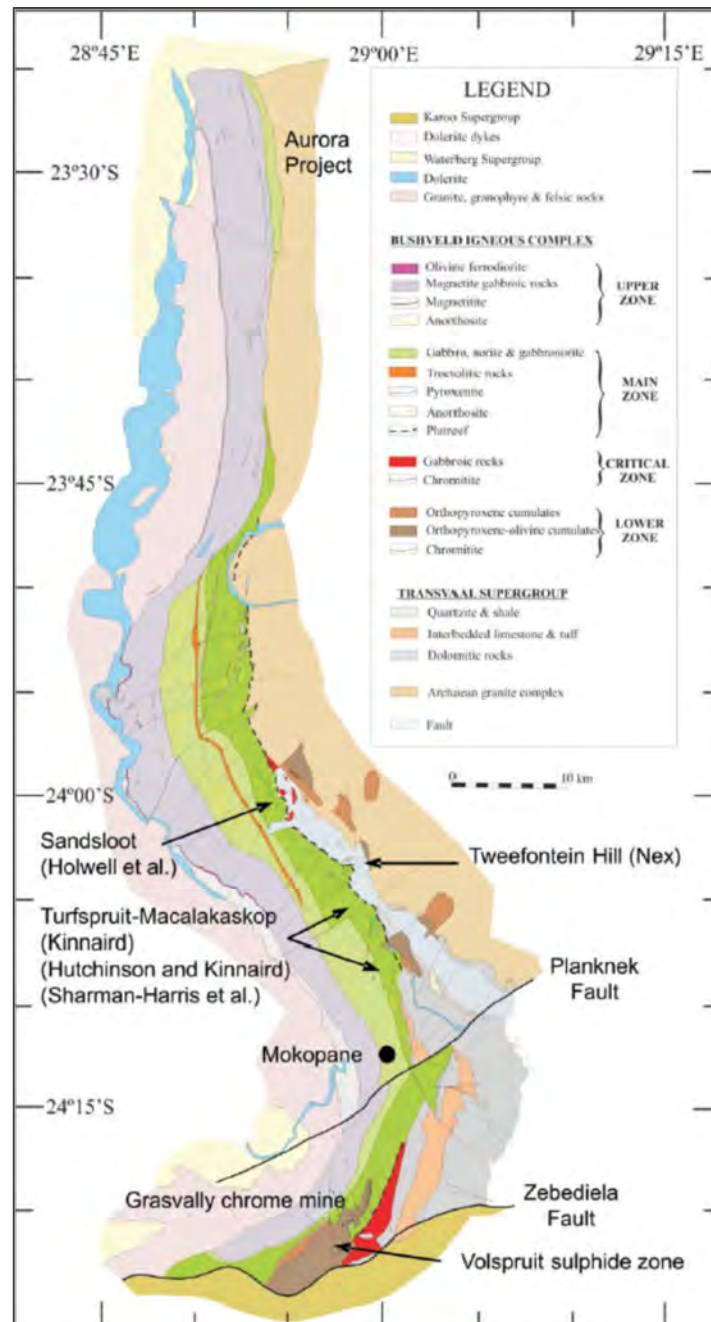


Figure 1. 4. Map of the Northern Bushveld Limb showing the Platreef which is located above the Planknek fault (Holwell et al., 2005).

1.3 Mineralogy of the Bushveld Complex

Value minerals in the Bushveld complex are base metal sulphides (BMS) and platinum group minerals such as PGE sulphides, tellurides, arsenides, platinum – iron alloys and bismuths (Daltry and Wilson,

1997; Kinloch, 1982). PGMs in the Merensky reef occur in three textural associations namely; enclosed in or attached to BMS, enclosed in silicate minerals and enclosed in or attached to chromite or iron oxides. The PGMs locked in or attached to BMS can account for 36 % to 97 % of occurrences (Viljoen and Schurmann, 1998). Grain sizes can range from 10 – 31 μm and 50 – 350 μm (Viljoen and Schurmann, 1998). Base metal sulphides common to this reef are chalcopyrite, pentlandite and pyrrhotite.

In the UG2 reef the most abundant BMS are pentlandite and chalcopyrite with minor phases of other BMS such as pyrrhotite, pyrite, arsenopyrite and galena (in order of decreasing abundance) (Viljoen and Schurmann, 1998). According to Viljoen and Schurmann, (1998) about 86.5% of these BMS are found along grain boundaries. The PGMs are dominated by the sulphide minerals and laurite. These minerals are found to occur in the same textural associations that are present in the Merensky reef (Penberthy et al., 2000; Viljoen and Schurmann, 1998). Grain sizes of the PGM's in the UG2 are much smaller than in the Merensky reef with maximum grain sizes reaching 50 μm (Schouwstra and Kinloch, 2000; Viljoen and Schurmann, 1998) but averaging at 10 μm (Penberthy et al., 2000; Schouwstra and Kinloch, 2000; Viljoen and Schurmann, 1998).

The abundances of the minerals in the Bushveld complex have been summarised in Table 1.1 as compiled by (Shamaila and O'Connor, 2008).

Table 1.1. Mineralogy and Platinum distribution of the Platreef, Merensky Reef and UG-2 Reef in the Bushveld Complex. Adapted from (Shamaila and O'Connor, 2008).

	Platreef	Merensky	UG-2
Bulk mineralogy	Pyroxene Serpentine Calcium silicates Base metal sulphides	Pyroxene Feldspar Base metal sulphides	Chromite Pyroxene Feldspar Base metal sulphides
PGE distribution	Tellurides 30% Arsenides 21% Alloys 26% Sulphides 3% Rest 20%	Tellurides 30% Arsenides 7% Alloys 7% Sulphides 36% Rest 20%	Tellurides < 5% Arsenides < 5% Alloys 20% Sulphides 70% Rest < 5%

1.3.1 Mineralogy of the Platreef

PGM mineralization of the Platreef is erratic and variable along the reef resulting in areas that are richer in some PGMs than others. This has been determined from studies of different sections of the reef. It has been proposed that the reason behind the variation in PGM types is the change in footwall

mineralogy which played a role in the mechanism that resulted in PGM mineralisation of the Platreef (Schouwstra and Kinloch, 2000). In the Drenthe region, which is the extreme Northern region, the dominant PGM's are the Tellurides (up to 80 %) followed by Arsenides (≈ 18 %) (Viljoen and Schurmann, 1998). In Overysel, Kinloch, (1982) found that sulphides were present up to 23% which is less than the tellurides which were present up to 40 % in abundance. Sulphides are also present in Tweefontein North (25 %) (Kinloch, 1982). Armitage et al. (2002) studied the PGMs in the Sandsloot area and found this section of the reef to be virtually free of sulphides and dominated by tellurides and arsenides. Holwell et al. (2006) have confirmed that this area of the reef is virtually free of sulphide PGMs but is dominated by tellurides. The Macalacaskop and Turfspruit areas have similarly been found to be virtually free of PGM sulphides and are dominated by the bismuthotellurides and the arsenide PGMs (Holwell et al., 2006). Viljoen and Schurmann, (1998) have concluded that the major PGMs in the Platreef are by far the tellurides which can constitute up to 80 % of the PGM concentration in some areas followed in order of decreasing abundance by the arsenides, alloys and then sulphides.

The grain sizes of the PGM's in the Platreef are larger than that of the Merensky reef. According to Viljoen and Schurmann, (1998) the tellurides and arsenides are predominantly enclosed in silicate gangue although this is in close proximity to BMS. Holwell et al. (2006) also found the PGMs to occur as single phase grains within the silicate reef and some instances interstitial to BMS. Viljoen and Schurmann, (1998) also determined that up to 62 % of PGMs are associated with silicate gangue and the rest with BMS.

The significant differences between the Merensky reef, UG2 reefs and the Platreef are therefore the form of the PGEs in each of the reefs. Table 1.1 shows clearly that the PGE mineralization of the Platreef is significantly different from that of the other two reefs.

1.3.2 PGM Minerals

Over 600 PGMs have been identified, with a small fraction of these being recognised as minerals (Daltry and Wilson, 1997). This section will only focus on the major PGM types found in the Platreef, some of which occur in minor phases in the Merensky and UG2 reefs. The platinum group elements are Pt, Pd, Rh, Ru, Ir and Os. These PGMs are transition metals and form complexes with other transition metals e.g. Pb, Ni and Cu, semi metals e.g. Te, Sb, As and Bi, other transition metals such as Fe and Co as well as S (Daltry and Wilson, 1997). Varying geochemistry of formation has resulted in each of the minerals having differing elemental compositions, and hence the large number of platinum group phases identified.

Some common sulphide platinum group minerals are, cooperite (Pt,Pd,Ni)S, braggite (Pt,Pd,Ni)S₂, malanite (Pt,Ir)₂CuS₄ and laurite (Ru,Os)S₂ (Daltry and Wilson, 1997; Penberthy et al., 2000). Amongst the Telluride minerals the most common are; moncheite PtTe₂ merenskyite PdTe₂, melonite (Ni,Pd)Te₂ and kotulskite (Pd,Ni)Te (Helmy et al., 2007). These also include the bismuthotellurides; michenerite PdTeBi, slobolevskite Pd(Bi,Te), maslovite (Pt,Pd)BiTe and stibnite bearing tellurides such as borovskite Pd₃SbTe₄ (Helmy et al., 2007). Of the arsenides the most common are sperrylite PtAs₂ and palladoarsenide Pd₂As (Daltry and Wilson, 1997; Viljoen and Schurmann, 1998).

1.3.2.1 Mineral Structures

It has been found that the PGMs mostly form cubic structures or hexagonal and orthorhombic structures (Daltry and Wilson, 1997). The minerals of interest in this study are platinum and palladium sulphides and tellurides of which common minerals are Vysotskite (PdS), Kotulskite (PdTe), Merenskyite (PdTe₂), Cooperite (PtS), and Moncheite (PtTe₂). Table 1.2 gives the names of some of the PGMs relevant to this study with their crystal data. Sulphides studied in this work are monochalcogens and the tellurides are dichalcogens of platinum and palladium. Chalcogen referring to the group 8 elements of which S and Te are a part of.

Table 1.2. Common Platinum and Palladium, Sulphides and Tellurides and their unit cell dimensions. Information compiled from (Berlincourt et al., 1981)

Crystal Grouping	Mineral	Simplest Formula	Crystal Symmetry	Unit Cell Å
Braggite	Vysotskite	PdS	Tetragonal	a = 6.43 c = 6.63
	Cooperite	PtS	Tetragonal	a = 3.4700 c = 5.0388
Melonite	Merenskyite	PdTe ₂	Hexagonal	a = 4.0425 c = 5.124
	Moncheite	PtTe ₂	Hexagonal	a = 4.0259 c = 5.2209

Metal dichalcogens have a CdI₂ structure (Westland, 1981). This is an octahedron structure that is layered. It is also called a melonite structure and is made up of sheets of edge sharing M/MQ₆ (Q = S, Se, Te) octahedron which are held together by Van der Waals forces, Figure 1.5a (Dai et al., 2003; Strunz and Nickel, 2001). This layered structure of metal dichalcogens is unique to transition metals with group 6 element bonds (Dai et al., 2003). Dichalcogenide bonding occurs between transition metal

d-orbitals and p-orbitals in group 6 elements. A study by Dai et al. (2003) showed that the energy level of the p-orbitals increases from O to Te resulting in the 5d-5p bond transforming from ionic character to covalent character in that order. As a result there is a transition from semi-conductor properties in $M-O_2$ and $M-S_2$ to semi-metallic in $M-Se_2$ and metallic properties in $M-Te_2$, where M denotes a metal (Dai et al., 2003). According to Westland, (1981) the change in metallic properties is due to the difference in metallic nature between S and Te. This metallic property of $PtTe_2$ and $PdTe_2$ will enable their electrochemical investigation. Van der Waals forces holding these telluride mineral structures together provide a likely point of cleavage (a-b plane, Figure 1.5(a)) as opposed to the covalent bonds between octahedron in sulphide minerals. This cleavage is likely to expose tellurium atoms at the surface to the prevailing solution environment.

Monochalcogens on the other hand have a braggite crystal structure. This structure is square planar with ligand atoms being tetragonally coordinated to platinum or palladium metal atoms (Strunz and Nickel, 2001). Bonding within the structure is completely covalent making it difficult to predict the line of cleavage or fracture. This complexity can be seen in Figure 1.5b.

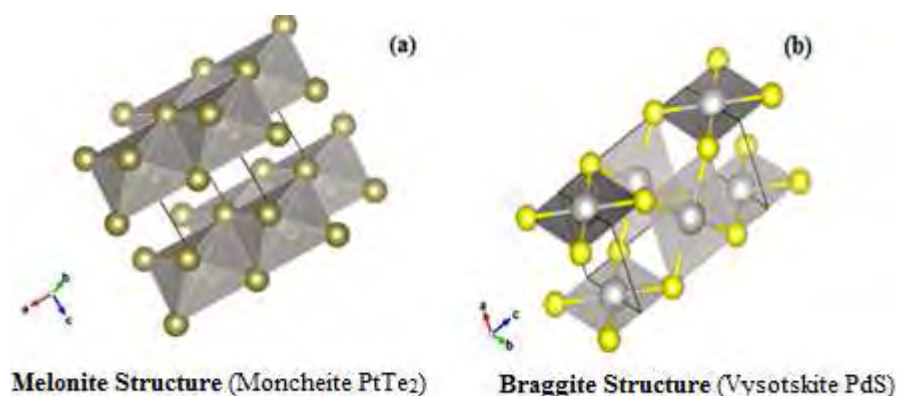


Figure 1.5. Mineral crystal structures. Structures obtained from (<http://www.webminerals.com>).

1.3.2.2 Mineral Reactivity

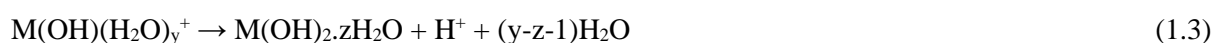
Mineral reactivity is dependent on the strength of bonds within the crystal structure of the mineral. Both telluride and sulphide minerals have covalent bonds between molecules and atoms. Strength of the PGE chalcogen bond is perhaps more significant and this is a function of the polarizability of both the central and ligand atom. Pt and Pd have strong polarizability and therefore the effect of the central atom to both sulphide and telluride minerals is uniform. The polarizability of Te and S is significantly different however with Te having lower polarizability than S owing to a larger ionic radius (Livingstone, 1965; Westland, 1981). It is therefore expected that Pt/Pd -S will have stronger intra molecular bonds than Pt/Pd -Te which will in turn affect reactions of these different minerals.

Semi-conductor properties of sulphide minerals and metallic properties of the telluride minerals make these minerals capable of being electron acceptors and donors. They can therefore participate in oxidation and reduction reactions. The noble property of PGE's however means that the significant reactions involving PGMs are reactions involving a change in the oxidation state of the adjoining ligand i.e. S and Te (Elvy et al., 1996; Gardner and Woods, 1979).

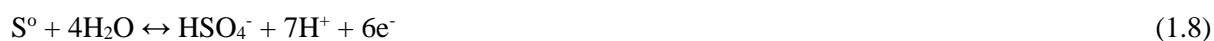
The reactions for both tellurides and sulphides in solution are a result of and a combination of the redox behaviour of sulphur and tellurium in solution and the thermodynamic stability regions for each mineral (PtS, PdS, PtTe₂ and PdTe₂). These reactions as reported in the literature will be highlighted further. A knowledge of the redox behaviour of these minerals in solution is key to understanding and predicting the interactions between the mineral surface and flotation reagents.

1.3.2.2.1 Sulphides

Reactions of sulphide PGMs do not differ significantly from those of base metal sulphides and therefore it is useful to understand the reactions of base metal sulphides. Oxidation of sulphide minerals in the application of mineral processing has been studied in order to determine oxidation products which can possibly be detrimental towards flotation. Reaction in an aqueous solution results in the formation of a hydrolysed metal ion which can result in the formation of a metal hydroxide species (Rao and Leja, 2004). Such a mechanism is according to Reactions (1.1), (1.2) and (1.3) which show a three step hydrolysis reaction.



It is clear from Reaction (1.1) that sulphur undergoes oxidation. In as much as Reactions (1.2) and (1.3) are pertaining to the metal atom oxidation of sulphur which occurs simultaneously is also significantly important. Species formed are a function of pH and Eh of the solution as indicated in the Pourbaix diagram for sulphur (Figure 1.6). The dominant reactions for sulphur in an oxygenated system are represented by Reactions (1.4) to (1.8) (Westland, 1981);



The coexistence of these reactions with the minerals PtS and PdS are illustrated on the Eh-pH diagrams in Figure 1.7 and Figure 1.8 reconstructed from Pourbaix, (1974) by Westland, (1981).

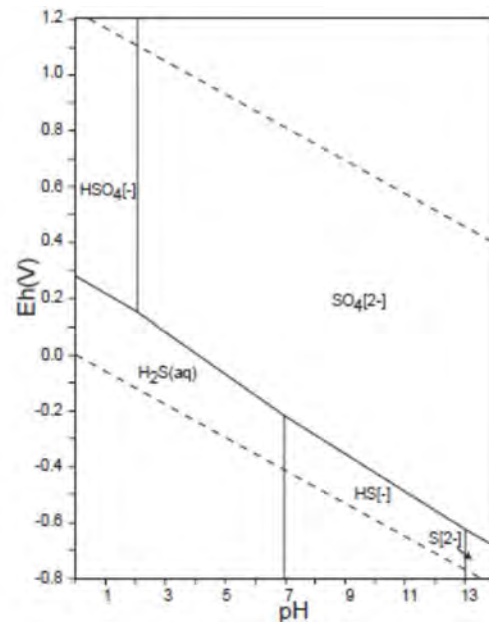


Figure 1.6. Eh – pH diagram for S-O-H₂O system (Pourbaix, 1974).

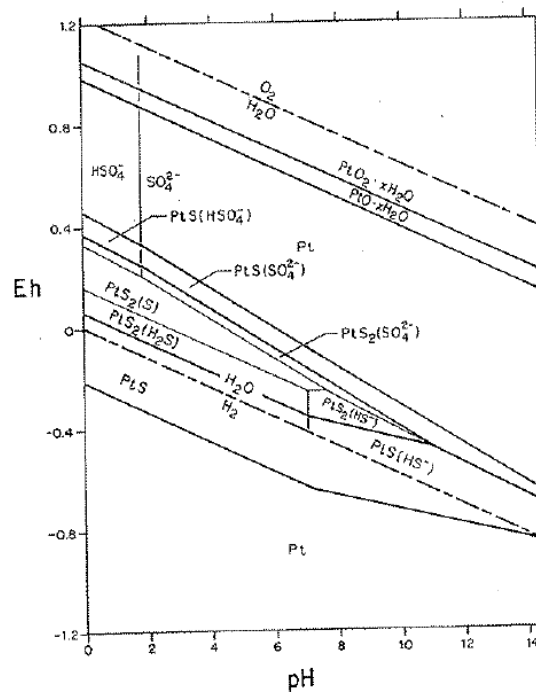


Figure 1.7. Eh – pH diagram of Pt-S-H₂O (Westland, 1981).

Tellurides

Information regarding the oxidation behaviour of Pt and Pd Tellurides is not extensive within the literature. Perhaps the most significant work is that of Elvy et al., (1996). This was a study conducted on PdTe, PdTeBi, PdBi regarding their oxidation in air. It was determined that the initial oxidation of the PdTe was the preferential oxidation of tellurium to yield a tellurium deficient metal surface according to Reaction (1.11).



A Pourbaix diagram for the reactions of tellurium in aqueous solution is given in Figure 1.9. From this diagram it is evident that at typical flotation pH, the TeO_3^{2-} ion is stable across a wide Eh range. In a study on PdTe (Vermaak et al., 2005) generated voltammograms which were corresponded to the oxidation of Te to a TeO_3^{2-} species and thus identifying similar oxidation behaviour of the mineral solution to that of the mineral in air.

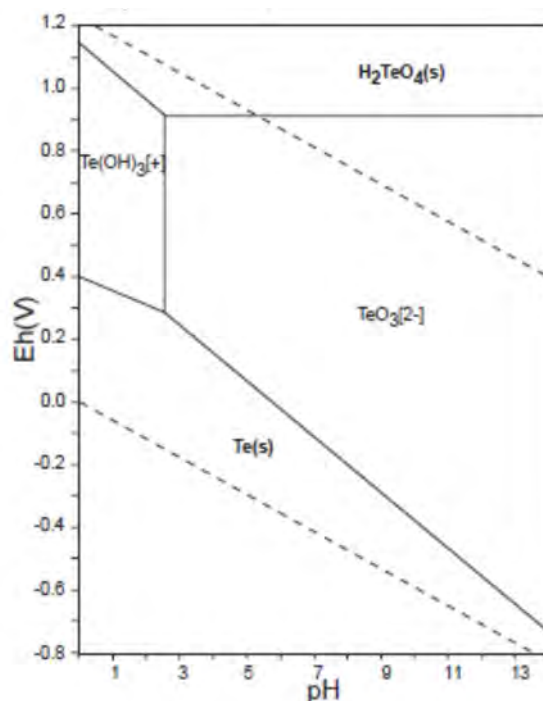


Figure 1.9. Eh – pH diagram of Te-O-H₂O (Pourbaix, 1974).

1.4 Flotation

Flotation is a physico-chemical process which takes advantage of differences in surface properties between value minerals and gangue material in order to effect separation (Wills and Napier-Munn, 2005). In order to exploit the differences in surface properties between the minerals being separated, the ore is treated with reagents that selectively alter the hydrophobicity of the value minerals. Air is

introduced into the pulp and hydrophobic value minerals attach to them forming a froth at the top of the vessel. Hydrophobicity is achieved by the use of collectors. Collectors are polarisable organic compounds that are comprised of two active parts; a polarised head and an aliphatic hydrocarbon body which is un-polarised (e.g. Figure). The polar group, sometimes referred to as the solidophilic/minerophilic group, is responsible for attachment to the mineral surface whilst the non-polar hydrocarbon chain creates hydrophobicity (Bulatovic, 2007). Although collector attachment alone does not ensure recovery of minerals it is a vital first step towards recovery of PGE's in the ore. Other factors contributing to successful recovery of valuable minerals via froth flotation are summarised in Klimpel's Triangle (cf. Figure 1.1).

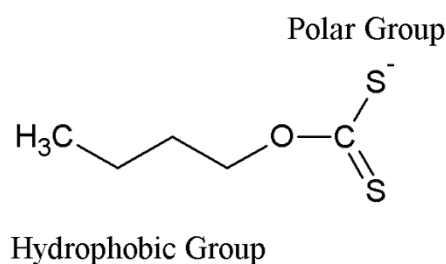


Figure 1.10. Chemical structure of a Xanthate, thiol collector molecule.

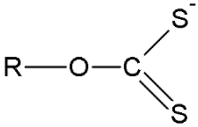
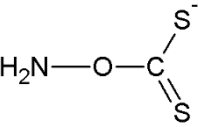
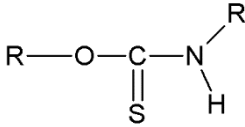
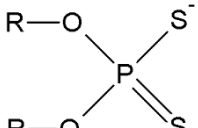
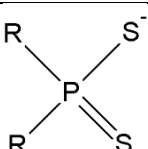
In mineral processing flow-sheets froth flotation follows the comminution stage (crushing and primary milling). Circuits include different stages of flotation designed to systematically upgrade the concentration of valuable minerals within the product (concentrate). Since liberation plays a crucial role to the recovery of minerals via flotation a secondary milling stage is often incorporated into the circuit as shown in Figure 1.11 (Shackleton, 2007). Collectors are sometimes introduced into the circuit via the primary mill before oxidation products inhibit attachment of collector. Collector can be subsequently added at various stages downstream to ensure that all exposed mineral surfaces have contact with collector molecules and hydrophobicity is achieved.

having lower electronegativity than oxygen and nitrogen, sulphur has characteristics that make it particularly useful as a donor atom. Sulphur possesses 3d orbitals in its outer electron shell that are readily available for bonding and make the atom readily polarizable thereby enabling physical or chemical adsorption of the molecules at mineral surfaces.

The polarity of the minerophilic head of a collector molecule is also determined by the structure of the molecule. The structure of the molecule in turn is comprised of various molecular groups which have varying effects on the electron density surrounding the bonding atom. This affects the polarizability of a collector molecule. An example of such an effect is that of an oxygen atom bonded to a bonding atom such as sulphur. Oxygen being a strongly electronegative molecule creates strong inductive effects that withdraw electrons from sulphur weakening its bonding capability (Somasundaran, 2006). Inductive effects of constituent groups on collector molecules are similarly responsible for variations in the strength and therefore solubility of collector-metal bonds for different thiol collectors. Xanthate and dithiophosphate collectors which have different structures which in turn affect the polarisability of the polar head. Structures for these collectors as well as some other well-known thiol collectors are shown in Table 1.3, where the constituent atoms comprising each thiol collector can be seen.

With regards to hydrophobicity it has been found that the dimer form of a thiol collector is the most hydrophobic species. This is because once the dimer has been formed the molecule becomes strongly non-polar. The metal thiolate species is considered to be less hydrophobic and its solubility is a function of the solubility of the species. Low solubility species are strongly hydrophobic and the hydrophobicity is a function of the collector molecule as well as the mineral (Rao and Leja, 2004).

Table 1.3. Structures of some common thiol collectors.

Thiol Collector	Structure
Dithiocarbonates/Xanthates – central atom is carbon and the donor atom is Sulphur.	
Thiocarbamates – in place of hydrocarbon an amyl group separated from primary carbon by O atom	
Thionocarbamates – bonding takes place through the thiono (C=S) group.	
Thiophosphates – The central carbon atom is replaced with Phosphorus (P) and alkyl groups are bonded by an oxygen bridge.	
Thiophosphinates – Alkyl groups are bonded directly to Phosphorous.	

1.5.2 Adsorption Mechanism of Thiol Collectors

Theories for adsorption mechanisms of thiol collectors have been developed over a number of years from as early as the 1920's. Theories have ranged from chemical reaction to adsorption and ion exchange. Finally it was determined that the adsorption mechanism is a function of a combination of a number of chemical processes which are all brought together in the electrochemical reaction theory by Nixon (Rao and Leja, 2004).

The electrochemical mechanism proposed by Nixon describes the adsorption of thiol collectors as occurring through the anodic oxidation of the thiol collector with the oxidised collector species subsequently adsorbing on the mineral surface. The role of the mineral is to provide a path for the electrons released by the thiol collector (Woods, 2010). The electron acceptor in solution has been accepted to be oxygen. The role of oxygen has been studied extensively as the electron acceptor species in the mechanism of oxidation of collector. The consensus has however become that oxygen is the electron acceptor in the absence of other oxidising agents in a reduction reaction according to Reaction (1.12) (Rao and Leja, 2004).



Three straightforward reactions have been proposed in the literature for the oxidation of the collector. The first reaction involves adsorption of the thiol collector on the surface through a chemisorption reaction. Chemisorption occurs through the solidophilic group on the collector and usually the metal atoms on the mineral surface as shown in Figure 1.12. The role of the mineral surface is to transfer the electron released by the collector to be accepted by oxygen (Woods, 2010).

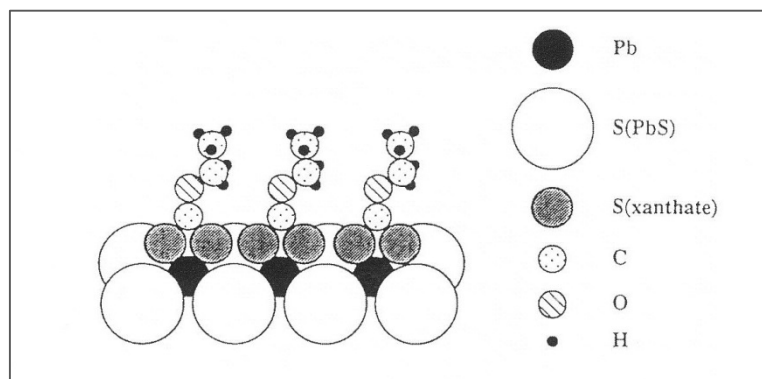


Figure 1.12. Schematic of chemisorbed Xanthate on a Galena surface (Woods, 2010).

Reaction (1.13) represents the chemisorption reaction in question. This reaction has been identified via electrochemistry and is indicated in voltammograms as a pre-wave to larger anodic currents denoting bulk collector adsorption (Woods et al., 1992). XPS has also been used to identify this reaction on the mineral surface. Buckley and Woods, (1990) studied fresh galena surfaces using XPS and they identified chemisorbed xanthate at the mineral surface. This reaction was also found to be coupled with oxygen reduction. The rate of reaction is found to be of the order of 10s of seconds being 30 seconds from the work of Buckley and Woods, (1990).



Overall Reaction;



Another oxidation reaction in which the collector can undergo is the formation of a metal thiolate species. Short chain alkyl xanthates are soluble in water whilst the heavy metal xanthate complexes are insoluble in water (Poling, 1976). It has been found that the insolubility of heavy metal xanthates is not dependent on the properties of the xanthate molecule but rather the properties of the heavy metal. The order of decreasing solubility of metal xanthates has been found to be $Hg_2X_2 > Cu_2X_2 > PbX_2 > ZnX_2$ (Poling, 1976). The solubility's of PtX_2 and PdX_2 have been reported in (Chanturiya and Vigdergauz, 2008) to be $\approx 10^{-54}$ and 3×10^{-53} respectively. These values are both larger than that reported in the same work for Hg_2X_2 , indicating that the metal thiolate species for PtX_2 and PdX_2 are likely to be more hydrophobic than the former heavy metal thiolate. The reaction for formation of metal thiolate species

has been suggested to occur for sulphides according to Reaction (1.15), where M denotes a heavy metal atom.



Overall Reaction;



Dithiolate is the dimerised form of a thiol collector resulting from oxidation. Dixanthogen, the dimerised form of xanthates has been long considered to be the most important hydrophobic species formed by xanthates (Chanturiya and Vigdergauz, 2008; Poling, 1976; Woods, 2010). This species is the third oxidative species that can be formed by the collector at the mineral surface in solution.

The oxidation of thiol collectors to their dithiolate form can occur as an anodic process (Reaction 1.17) to the cathodic reduction of an oxidising agent such as oxygen (Reaction 1.12), or other oxidising agents such as potassium iodide and hydrogen peroxide (Poling, 1976). Coupled with the reduction of oxygen the overall reaction can be represented by Reaction (1.18).

An alternative to the mechanism is the formation of the dithiolate species in the bulk solution coupled with the reduction of a metal species such as Cu^{2+} (Poling, 1976) or Ferric ions Fe^{3+} . In the former the resulting species formed are a cuprous xanthate and dixanthogen which are both precipitates (Poling, 1976). A study by Usul and Tolun, (1974) showed that in an oxygen free environment dixanthogen did not adsorb onto the mineral surface and did not produce a hydrophobic surface. From this result they concluded that oxygen was an important component of the mechanism by which dixanthogen creates a hydrophobic surface.



Overall Reaction;



1.5.3 Mixed Potential Model

From the previous discussion it has been identified that oxygen reduction is a reaction in order to create hydrophobicity on the mineral surface. It has also been determined that the mineral surface behaves as a catalytic surface for the reactions to occur with part of the mechanism involving the transfer of electrons. With the reactions being electrochemical in nature and comprising of oxidation/reduction (redox) couples it follows therefore that electrochemical potential is a driving force for the reactions to occur.

In the principle of corrosion, metals are known to oxidise under oxidising conditions and in the presence of an electron acceptor or oxidant giving off metal ions. For sulphide minerals in solution this corrosion reaction has been proposed to be according to Reaction (1.19) (Rao and Leja, 2004);



The electrons released are accepted by an electron acceptor such as oxygen forming a redox couple. A potential is achieved at the mineral surface where the rate of oxidation is matched by an equal and opposite reduction rate. This is known as the rest potential of the mineral in solution.

The mixed potential model was proposed after recognising the chemical complexity of the solution surrounding a mineral. Multiple reactions occur at the mineral surface which act as an electro-catalyst for these reactions (including collector oxidation) to occur. The theory assumes that at open circuit potential the potential measured occurs as a result of the sum of rates of oxidation reactions matching the sum of the rates of all reduction reactions taking place at the mineral surface. The mixed potential therefore lies between the reversible potentials of these oxidation and reduction reactions (Poling, 1976). On a current potential diagram, where current is a measure of the rate of reaction, the mixed potential model can be diagrammatically represented as in Figure 1.13.

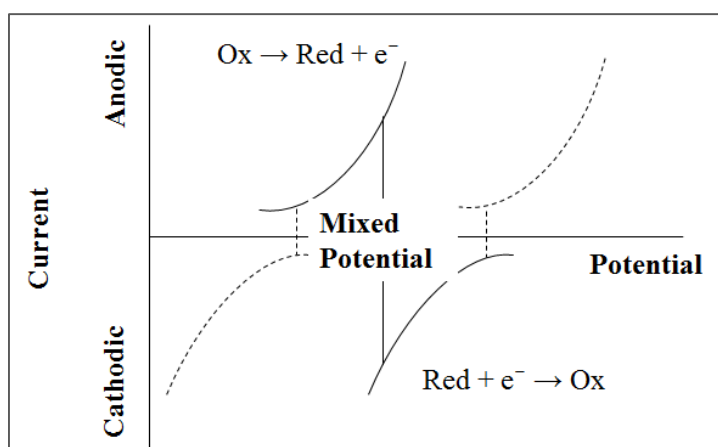


Figure 1.13. Schematic representation of a mixed potential model for two different redox couples

In determining adsorption of collector species at the mineral surface, it has been determined that when the mixed potential/rest potential of a mineral is higher in potential than the equilibrium reduction potential of dixanthogen formation, then this species is present at the surface (Poling, 1976; Rao and Leja, 2004). A study by Allison et al. (1972) of the rest potentials of several minerals in a solution of 6.25×10^{-4} M potassium ethyl xanthates (KEX) at pH 7, showed that minerals with rest potentials above the potential of the dixanthogen couple showed evidence of the dixanthogen species being present at the surface. Some of the results of this study are given in Table 1.4.

Table 1.4. Results of rest potentials of various minerals and the surface species on the mineral surface in solution of 6×10^{-4} M potassium ethyl xanthate by Allison et al. (1972).

Mineral	Adsorbed Species	Rest Potential 10min v NHE
Galena	MX	+0.06
Chalcocite	X ₂	+0.06
Covellite	X ₂	+0.05
Chalcopyrite	X ₂	+0.14
Molybdenite	X ₂	+0.16
Pyrrhotite	X ₂	+0.21
Pyrite	X ₂	+0.22
Arsenopyrite	X ₂	+0.22

MX – metal xanthate, X₂ – dixanthogen

Allison et al. (1972) discovered that minerals with rest potentials below the potential of the dixanthogen couple had metal thiolate species as the dominant species present at the surface. This study has become one of the most important studies in the determination of adsorption mechanisms for thiol collectors. This work showed that by measurement of the mixed/rest potential it is possible to surmise the manner of species present at the mineral surface. The work also demonstrates the differences in electro-catalytic properties of different mineral species.

The species formed by thiol collectors when oxidised are consistently the same i.e. dixanthogen, metal thiolate formation and chemisorbed thiolate species. What is varied is the interaction between the oxidised species and the mineral surfaces.

1.5.4 Electrochemical Investigation of Adsorption Mechanism

The previous section describes the adsorption mechanism of thiol collectors on mineral surfaces as being electrochemical in nature. As such, electrochemical techniques are frequently used to study the species that occur at the mineral surface. Electrochemistry is often complemented with other techniques such as spectroscopic techniques to attempt to detect the exact species present at the mineral surface. As these techniques have not been used in this study this review will not be dedicated to these techniques but will only make mention of them where necessary. Though there are various electrochemical techniques that can be used to study these adsorption mechanisms, in this work cyclic voltammetry and the measurement of rest potential have been used and this review will be dedicated to outlining how these types of measurements have contributed to the knowledge on adsorption mechanisms of thiol collectors.

1.5.4.1 Mixed Potential/ Rest potential

Owing to the mixed potential theory (cf.1.4.3) the measurement of the mixed potential of a mineral, also known as the rest potential of a mineral can yield valuable information. The classic work of Allison et al. (1972) was one of the first studies measuring rest potentials to yield information regarding the species present at mineral surface. Mixed potential was used to determine the final oxidised species present at the mineral surface. This work was complemented by infrared and ultraviolet spectroscopy to give the widely accepted conclusion that the mixed potential of a mineral in solution determines the oxidised species present at the mineral surface. Similar work was conducted by Finkelstein and Goold, (1972) for an extended range of collectors which included dithiophosphate, dithiocarbamate, mercaptobenzothiazole and thionocarbamate; rest potentials were used to successfully predict the adsorbed thiol collector species on a range of minerals. Infrared (IR) spectroscopy was used to identify the collector species at the surface.

The mixed potential of a mineral gives indication of the type of electrochemical surface that is created by a mineral in solution. In regard to galvanic interaction between minerals it is found that where two minerals are in contact with one another the mineral with more anodic rest potential becomes a cathode and reduction occurs at the surface whilst the mineral that is more cathodic in equilibrium potential becomes the anode and is oxidised (Rao and Leja, 2004). This galvanic interaction can be seen in the mineral couple of pentlandite; a nickel hosting mineral and pyrrhotite. For recovery of nickel it is preferable to float pentlandite whilst depressing pyrrhotite. Bozkurt et al. (1998) measured the rest potentials of pentlandite and pyrrhotite in the presence and absence of xanthate. The rest potentials indicated that in the absence of xanthate pyrrhotite would be more readily oxidised than pentlandite. However, in the presence of sodium isobutyl xanthate the rest potentials indicate that xanthate is more readily oxidised to dixanthogen on pentlandite than on pyrrhotite, a result corroborated by ATR spectroscopy. In most of the rest potential studies that have been undertaken two key characteristics of the rest potential have been used viz;

- The comparison of the rest potential with the oxidation potential of the collector to enable prediction of the adsorbed species (Allison et al., 1972; Buswell, 1998; Buswell et al., 2002; Finkelstein and Goold, 1972; Khan and Kelebek, 2004; Moslemi et al., 2011)
- The difference in rest potential of minerals in the absence of collector and in the presence of collector. This has been used to allude to the extent at which the collector reacts at the mineral surface (Bozkurt et al., 1998; Buswell et al., 2002; Buswell and Nicol, 2002)

In conclusion, the study of the rest potential has provided information on the oxidising or reducing characteristics of the minerals in question (Buswell et al., 2002).

1.5.4.2 Cyclic Voltammetry

1.5.4.2.1 Technique

Cyclic voltammetry has been used to study the adsorption mechanisms of electrochemically active species over a wide range of scientific applications. One of the special interests in cyclic voltammetry is its capability to provide quick information regarding the redox behaviour of electrodes and species at the surface over a wide potential range. Potential is varied from one value E_1 to a limit E_2 which is also known as a switching potential (Mabbott, 1983). Potential acts as an electrochemical driving force for electrochemical reactions and in so doing as the reaction equilibrium potential is reached a current response can be measured which is the flow of electrons (Wang, 2006). The change in potential from one potential limit to the switching potential is illustrated in Figure 1.14 and the resulting voltammogram is included.

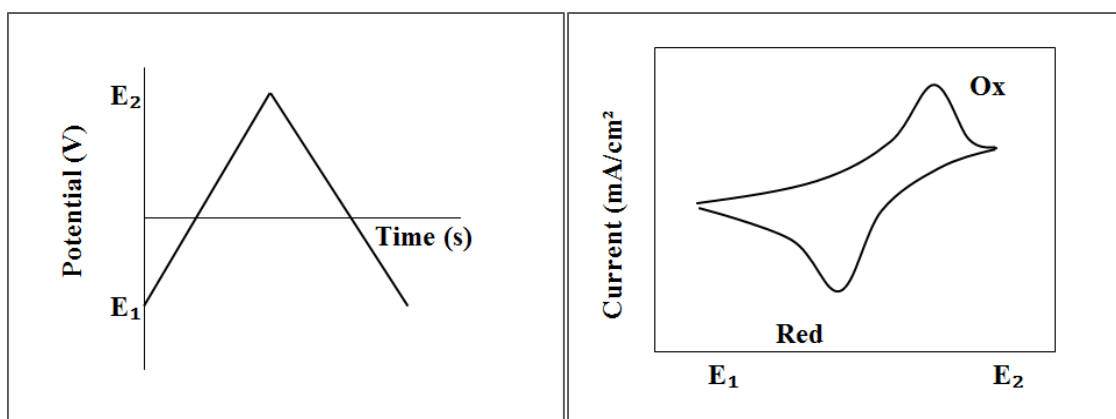


Figure 1.14. Schematics of the variation of potential and example of a voltammogram

The integral of the area under the voltammogram gives a measure of the charge transferred in a reaction process. This is according to Reaction 1.20.

$$Q/A_{\text{mineral}} = \int_0^t \text{Current Density } dt \quad (1.20)$$

According to Faradays law this charge translates to the number of moles of chemical species reacted by the Reaction (1.21).

$$\Gamma = Q/nFA_{\text{mineral}} \quad (1.21)$$

where: Q – charge transferred in Coulombs

F – Faradays constant in Coulombs per mol

Γ – Surface coverage in moles

A_{mineral} – Area of minerals in cm^2

n – number of moles of electrons transferred

There are two electrode processes that dominate the measurement of voltammograms;

- Mass transfer of reacting species to the surface of the working electrode
- Electron transfer reaction

As reaction potential is reached a reaction occurs for the species present at the electrode surface. The electron transfer process is the dominant rate determining step. Mass transport soon becomes the rate determining step and the current measured reaches a peak which dissipates as the species at the electrode surface depletes. The advantage of voltammetry is the accumulation of an oxidised species at the surface which can be reduced during the reduction process. This allows for the identification of a reduction reaction as well as an oxidation reaction.

The electrode potential for a reversible process can be estimated from the distance between the oxidation and reduction peaks. It has been found that for perfectly reversible processes the difference between the oxidation and reduction peak potentials is close to $58 / n$ (Kissinger and Heineman, 1983; Mabbott, 1983). Not all electrode processes are reversible however and the further the redox peak potentials become apart the less reducible the redox couple is. Irreversibility of reactions is caused by various factors including (Mabbott, 1983);

- Extensive bond breaking
- Loss of substituents to solution
- Reversible charge transfers followed by an irreversible chemical reaction

It stands to reason that given the corrosive nature of mineral oxidation then voltammograms generated during the oxidation of minerals should be irreversible. Indeed, this has been observed in the use of cyclic voltammetry to investigate the oxidation behaviour of sulphide minerals (Gardner and Woods, 1979).

Cyclic voltammetry experiments are now commonly conducted using the three electrode system where potential is applied using a potentiostat. The three electrodes involved are the working electrode, reference electrode and the auxiliary electrode. A potential is applied by the potentiostat between the reference electrode and the working electrode. The auxiliary electrode is included in the circuit in order to prevent current from flowing through the reference electrode and to maintain a current at the working electrode that sustains reactions taking place (Bard and Faulkner, 1980; Kissinger and Heineman, 1983; Mabbott, 1983; Wang, 2006). Platinum due to its inert nature is often used as the auxiliary electrode in order to prevent the electrode from taking part in any of the reactions. The reference electrode used can be a standard calomel electrode or a silver/silver chloride reference electrode (Wang, 2006).

1.5.4.2.2 Cyclic Voltammetry in Mineral Processing

In mineral processing and the study of adsorption mechanisms voltammetry has contributed a significant amount of knowledge regarding the oxidation and reduction behaviour of minerals. Much of what is known regarding the oxidation or corrosion behaviour of some base metal sulphides has been developed through the use of cyclic and linear sweep voltammetry. For example the oxidation reactions of galena in alkaline and acidic conditions (Gardner and Woods, 1979), the reactions of pyrite and pyrrhotite (Buckley and Woods, 1987; Hamilton and Woods, 1981) and the natural floatability of chalcopyrite (Gardner and Woods, 1979).

Electrochemical studies using voltammetry have elucidated what is currently known about the adsorption mechanisms of thiol collectors. One of the principal works on determination of adsorption mechanisms of thiol collectors on minerals was by Woods, (1971), where the reaction of ethyl xanthate on platinum metal, gold, copper and galena were studied. With particular emphasis on galena this work showed evidence of Reactions (1.13), (1.16) and (1.17) to be occurring on the galena surface. The voltammogram generated is given in Figure 1.15 for the conditions specified.

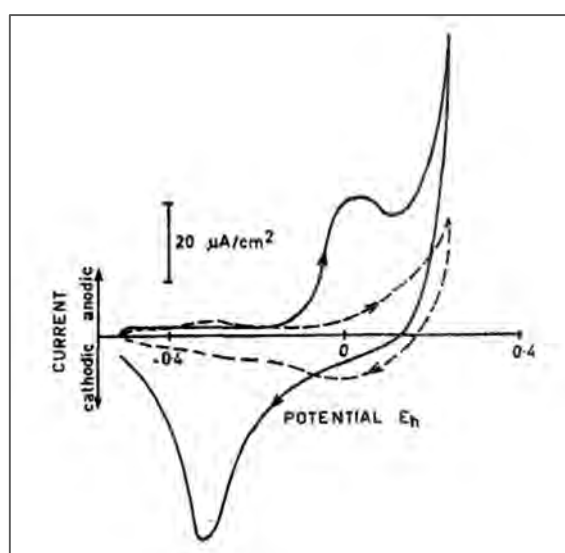


Figure 1.15. Cyclic voltammogram of galena in the absence of collector (dotted line) and presence of collector (solid line) at pH 9, 0.1 M Borate solution, 10 mV/s sweep rate, 25 °C, EX concentration of 9.5×10^{-3} M by (Woods, 1971).

Since this work, other researchers have taken the cyclic voltammetry technique and used it to postulate the occurrence of Reactions (1.13), (1.16) and (1.17) on other metals and sulphide minerals. Reaction (1.13) has been identified as what is referred to as the under-potential deposition or chemisorption of thiol collectors at the mineral surface; under potential in this context referring to the chemisorption of the thiol collector at potentials below the thermodynamic potential for formation of multi-layers.

Using voltammetry this reaction has been identified as occurring as a pre-wave. That is, there is a charge associated with the adsorption of the thiol species that occurs before charge associated to bulk formation of dithiolates and metal thiolate species during voltammetric potential sweeps (Buckley and Woods, 1997). This has been identified by example for ethyl xanthate on galena (Buckley and Woods, 1994; Woods, 1971) and on metals such as silver, platinum and gold (Woods, 1971; Woods et al., 1992). It has also been identified electrochemically for dithiophosphates on platinum, copper and chalcocite (Buckley and Woods, 1993; Chander and Fuerstenau, 1974). Calculations of charge, which has already been discussed, is an indicator of the number of moles transferred has led to the determination that this chemisorption reaction results in up to only a single monolayer of collector coverage. Where it is possible to determine the number of molecules of collector adsorbed to the mineral surface the adsorption isotherm can be determined. A Frumkin isotherm is used to describe electrochemical adsorption processes relating fractional surface coverage to the activity of ions in solution as well as the interaction effects of adsorbed molecules (Bockris and Reddy, 1973). A connection was made by Woods et al. (1990) between the adsorption isotherm of ethyl xanthate on chalcocite which followed a Frumkin Isotherm and flotation recoveries of chalcocite. From this work they were able to conclude that chemisorption of ethyl xanthate is sufficient for flotation having achieved 90% recovery at a collector coverage of 90%.

The study of the interaction of DTP on minerals using cyclic voltammetry has yielded two different responses that are characteristic of voltammetry measurements. Voltammetry measurements either provide information from the changes in current density (peak occurrence), or the absence of changes in current density. Typically in order to determine adsorption mechanisms, voltammograms of minerals in the absence of collector are compared with those generated in the presence of collector. Using this approach Güler et al. (2005) determined the interaction of DTP with chalcopyrite using cyclic voltammetry. They observed that current densities measured in the absence of collector were lower than those measured in the presence of collector. This result indicated a passivation layer formed by DTP that is not identified by electron discharge. Using this same approach of comparing voltammograms in the absence and presence of collector Güler et al. (2004) also identified a passivation effect of dithiophosphate (DTPI) on the same chalcopyrite mineral.

Cyclic voltammetry has also been coupled with thermodynamic calculations to validate the postulated mechanisms from voltammograms. These thermodynamic calculations are very useful although they have their limitations which arise from assumptions that need to be made. In work conducted by Chander and Fuerstenau, (1974) to study the interaction of DTP with platinum, copper and chalcocite they compared experimental results to a theoretical model for the anodic peak potential by Nicholson and Shain and by Delahay for an irreversible electrode process. The assumptions in this work were firstly that the oxidation of the collector is a single step irreversible reaction and that the rate determining step is electron transfer and not mass transport. The model was capable of validating the behaviour of

only some of the peaks generated in the voltammograms as other measurements did not produce distinct anodic peaks. The model was also only applied to platinum and copper. This highlights another limitation of models aside from assumptions and that is the possible lack of distinct peaks to provide the information required to feed into the model.

Other use of thermodynamics to validate cyclic voltammetry results is the estimation of and comparison of voltammograms with E_h values, where E_h refers to the reduction potential of the reaction at the experimental conditions. E_h is determined from the standard reduction potential and corrected for pH and activity of species at the experimental conditions using the Nernst Equation (Equation 1.22).

$$E_h \leftrightarrow E^\circ - 0.0592\text{pH} - (0.0592/n) \text{Log} [a_{\text{ox}}/a_{\text{red}}] \quad (1.22)$$

This approach was also used by Güler et al., (2004), Güler et al. (2005) Pecina et al. (2006) to validate the identification of the reactions from voltammograms against the work of previous authors such as Gardner and Woods, (1979) and Hamilton and Woods, (1981).

Although extensively used, cyclic voltammetry has its limitations. It was proposed by Yoon and Basilio, (1993) that the interaction of large collector molecules with mineral surfaces cannot be identified through cyclic voltammetry after they attempted to study the interaction of thionocarbamates. These collectors in themselves are not readily oxidised and therefore electrochemical interactions with minerals do not yield a vast amount of information. The same applies for all collectors that are not readily oxidised. Owing to the complexity of the nature of reactions it is also evident that cyclic voltammetry alone cannot give definitive information of the species available at the mineral surface. At the same time the spectroscopic techniques that are also used to complement voltammetry have their weaknesses, the largest of which being that almost all are ex-situ techniques which means that adsorbed species can be subject to alteration before measurement.

1.6 Copper Activation

Copper activation is a process that has been used in the mineral processing industry dating back as far as the advent of flotation. Finkelstein and Allison, (1976) define activation as being, “a process whereby the surface of a mineral particle is modified so as to make it react more readily or more strongly with collector.” It has been found that copper activation can result in the floatability of poorly floating sulphide minerals. One such mineral is sphalerite which is not readily floated using thiol-collectors but in the presence of copper sulphate (CuSO_4) it has been found that the mineral becomes floatable in the presence of thiol collectors (Finkelstein and Allison, 1976; Finkelstein, 1997). Studies have also shown that acidic conditions favour the activation by copper, whilst the verdict on alkaline conditions is still subject to interpretation?

Heavy metals other than copper are capable of activation of sulphide minerals, for example lead. The overall mechanism has been assumed to involve an ion exchange mechanism at acidic pH, in which the driving force of the ion exchange is the difference in free energy of the sulphides in question. For sphalerite activation with copper the ratio of Cu^{2+} to Zn^{2+} involved in the exchange was found to be almost 1:1 (Finkelstein and Allison, 1976). This however is believed to be an oversimplified explanation of the interactions of Cu with sulphide minerals (Wang et al., 1989).

The nature of the adsorbed species on the mineral surface after activation has been a matter of contest. Owing to observed successful activation of sulphide minerals under acidic pH conditions, much work regarding the mechanism of interaction has been done under acidic conditions. One theory based on the ion exchange mechanism is the presence of CuS as the activating species present on the sulphide mineral surface. However it is also believed that subsequent to the absorption of CuS, Cu (II) is reduced to Cu (I) which is the formation of covellite occurring as a slow reaction. This does indicate that electrochemical experiments can be used to identify the adsorbed species on the sulphide mineral surfaces. Experiments conducted in oxygen free solutions have indicated that the dominant reduction process is the reduction of Cu (II). In oxygenated solutions therefore, the addition of Cu (II) to the mineral solution interface results in an increase in mixed potential (Wang et al., 1989) and can be represented in a mixed potential model as shown in Figure 1. 16.

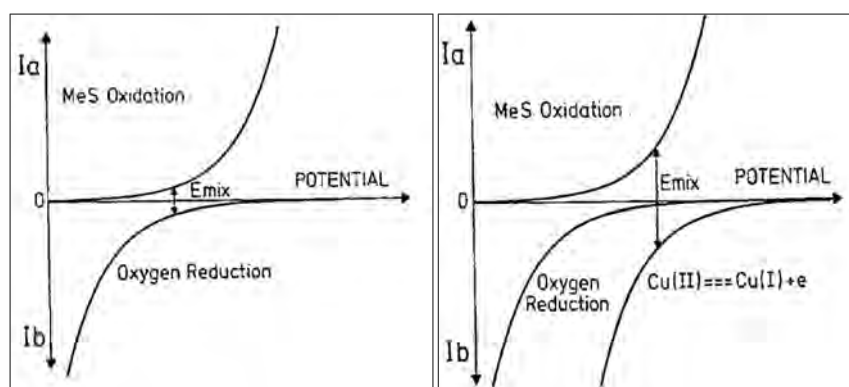


Figure 1. 16. Mixed potential model for the effect of copper addition to the rest potential of a mineral (Wang et al., 1989)

The pH dependent hydrolysis of heavy metal ions specifically copper in solution is of interest to how the metal ion behaves as an activator. Cu (II) spontaneously forms the following species; $\text{Cu}(\text{OH})^+$, $\text{Cu}_2(\text{OH})_2^{2+}$, $\text{Cu}(\text{OH})_2(\text{aq})$, $\text{Cu}(\text{OH})_2(\text{s})$, $\text{Cu}(\text{OH})_3^-$, $\text{Cu}(\text{OH})_4^{2-}$. The distribution of hydrolysed species as a function of pH is shown in Figure 1.17 for a Cu^{2+} concentration of 10^{-5} M. It is noted from this figure that copper ions only exist at very low pH and at alkaline pH the hydroxyl form of the copper is more stable.

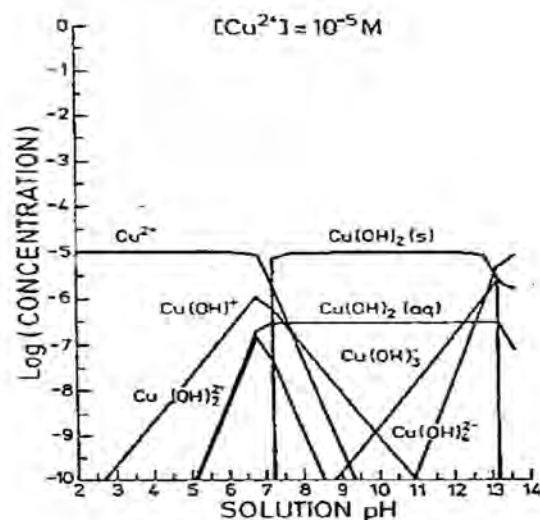


Figure 1.17. Speciation diagram for Cu-H₂O system at a Cu²⁺ concentration of 10⁻⁵ M (Wang et al., 1989)

Under alkaline conditions Wang et al. (1989) suggest that the activation mechanism initiates with precipitation of a hydroxide at the sulphide mineral surface. The second step is proposed to be a surface conversion, in which the hydroxide reacts with the surrounding sulphur species to form the accepted species of activation, CuS and Cu₂S. This is a slow reaction which requires sufficient conditioning time for the hydroxide to convert to the sulphide form.

It is the sulphide form of the activating copper which enables stronger interaction with ethyl xanthate. Wang et al., (1989) suggest that poor activation results at high pH are a result of the ethyl xanthate forming a complex with copper hydroxide (Cu-OH-EX) rather than copper sulphide (CuEX). The former complex would have a lower degree of hydrophobicity due to the presence of OH, than the latter. This species is dependent both on pH and potential and as shown in Figure 1.18 the stability region of this species is quite large.

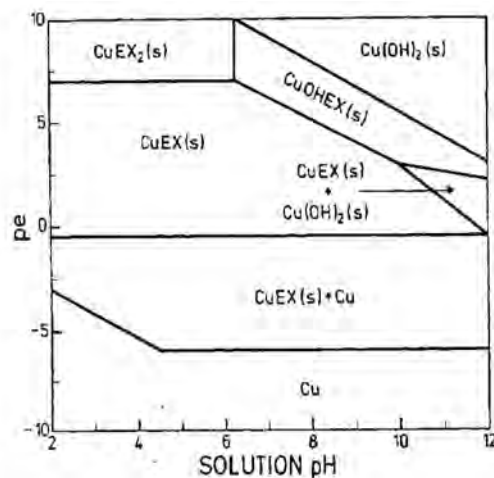


Figure 1.18. pE- pH diagram for the Cu - EX system for Cu and EX concentration of 10⁻⁴M where pE=E°/0.059. (Wang et al., 1989).

In Figure 1.18 it is shown that the species Cu-OH-EX is stable across the potential range E° of 0.148 V – 0.590 V and pH 6 – 12. A study of the oxidation conditions at the mineral surface can therefore determine whether this species is indeed a source of the poor activating capability of copper under high alkalinity.

1.7 Flotation of and Electrochemical Investigations on PGMs

Concentration of PGMs from their ores within the Bushveld complex is directed towards the recovery of base metal sulphides which float readily with thiolate collectors being used as collectors. Many studies have taken place with regards to the floatability of base metal sulphides (Finkelstein and Poling, 1977; Hanson and Fuerstenau, 1991; Miller et al., 2005; Wiese et al., 2005). Due to their association with base metal sulphides the floatability of PGMs has not been a subject that has been extensively researched.

However, significant work by Penberthy et al. (2000) showed the floating of discrete particle PGMs to be possible. This investigation was done on a UG-2 ore and a key finding was the order of floatability of PGMs. In decreasing order this was found to be; braggite, cooperite, malanite, ferroplatinum, other non-sulphide PGMs and laurite, thereby showing that sulphide PGMs are the most readily floating of the group. Telluride and arsenide PGMs are characterised as ‘other non-sulphide’ PGMs.

One of the major challenges of studying PGMs is their unavailability for study due to their very small size. Work subsequent to that of Penberthy et al. (2000) has used synthetic PGMs to study the surface characteristics of these minerals. The applicability of synthetic PGMs as a proxy for the naturally occurring minerals has been shown to be feasible by Shamaila and O’Connor, (2008). By using naturally occurring minerals on flexi float experiments, they showed that with regards to non-sulphide PGMs the order of floatability is tellurides followed by arsenides, thereby corroborating the findings of Penberthy and co-workers. They produced the same flotation response for synthetic tellurides and sperrylite as their natural counterparts thereby proving the significance of synthetic minerals as a diagnostic for the behaviour of natural minerals.

Regarding telluride PGMs some work has been done by Vermaak and co-workers. Their work investigated the interaction of ethyl xanthate, a common thiol collector and various forms of tellurides. Vermaak et al. (2007) used a number of investigative techniques to determine the interactions between ethyl xanthate and two synthetic minerals; Pt-Bi-Te and PtTe₂. They measured open circuit potentials (OCP) and found that the OCP’s were much higher than the oxidation reduction potential of dixanthogen formation. These OCP’s were measured in oxygenated solution, and high reactivity of platinum with oxygen in solution was proposed to account for the very high OCP values. Raman

Spectroscopic studies were conducted to analyse the surface species of the minerals after contact with the collector. Both mineral surfaces were found to indicate the predominant presence of dixanthogen. In earlier and similar work Vermaak et al. (2005) found the presence of dixanthogen on the surface of Pd-Bi-Te. In these studies contact angles were measured and Pt-Bi-Te and Pd-Bi-Te both showed maximum contact angles of 60° (Vermaak et al., 2007; Vermaak et al., 2005).

In addition to the work done on telluride minerals in the work of Vermaak et al. (2007) the interaction of ethyl xanthate and synthetic sperrylite was studied. This time, in addition to identifying the presence of dixanthogen on the mineral surface, they also noted that the contact angle measured was independent of the charge transfer at the surface, implying that even at low potentials there was sufficient coverage of dixanthogen to produce hydrophobicity of the mineral.

The flotation response of various PGMs to thiol collectors was studied by Shackleton et al. (2007) and Shackleton, (2007), using sodium isobutyl xanthate as collector. For telluride PGMs, it was found that the order of floatability between merenskyite and moncheite was merenskyite producing recoveries between 60% and 75% from natural floatability in comparison to between 40% and 50% for moncheite under the same conditions. Sulphide and arsenide PGMs were also studied for their flotation response and it was believed that differences in crystal structure and morphology would result in differences in flotation response, however, the results showed no indication of this being the case. Another significant finding by Shackleton was the effect of CuSO₄ as an activator to possibly promote the interaction between collectors and these PGMs, and the result of that study showed it to be detrimental to the recovery of the PGMs. It was believed that the cause was the presence of Cu(OH)₂ at mineral surfaces, this species had been identified via XPS and ToF SIMS.

The consensus between these studies has been that PGMs interact with collectors and float, albeit at slower rates than base metal sulphides. Adsorption mechanisms for the telluride minerals have been proposed however they have not been compared to those of other PGMs including sulphide minerals. The work of Penberthy et al. (2000) and Shackleton, (2007) both show that there is a difference in flotation response however with regards to whether this difference in floatability of these minerals is due to the adsorption mechanism of collectors is still to be elucidated.

1.8 Summary and Hypotheses

It has been shown in this review that the platinum group minerals in the Platreef ore body of the Bushveld complex are predominantly non sulphide minerals. The state of knowledge with regard to flotation of platinum group minerals is limited to what knowledge is available regarding base metal sulphides especially galena, pyrite, chalcopyrite, pyrrhotite and pentlandite. Very little work has been

done with regards to understanding the adsorption mechanisms and the flotation behaviour of the non-sulphide platinum group minerals. Literature gives an indication that sulphhydryl collectors, which are considered to be most suited for sulphide mineral flotation, can be used to float non-sulphide platinum group minerals. It has been established in the literature that the behaviour of thiol collectors when adsorbing onto mineral surfaces is essentially the same. Therefore, through the use of electrochemistry, more specifically open circuit potential measurements as well as cyclic voltammetry, the oxidation and reduction reactions involving various thiol collectors on mineral surfaces can be investigated.

Hypotheses

- Although the PhD work of Shackleton, (2007) showed that there was no evident relationship between crystal structure or morphology and the flotation response, this could have been as a result of a large number of interacting variables masking the effect of crystal structure. At a mechanistic level of interaction between collector molecules and mineral surface the crystal structure should have an effect on the way collector molecules dock on the surface. This is because crystal structure will affect the atoms available at the surface through orientation and arrangement of molecules as well as cleavage patterns. PGM sulphides and tellurides belonging to different crystal structure groups (cf. Section 1.2.2.1) will in turn interact differently with thiol collectors.
- PGEs particularly Pt and Pd have partially occupied d-orbitals which allow them to bond reversibly with ligands and makes them good catalysts. They are also able to take on variable oxidation states and form covalent as well as coordinate bonds. These properties of the metals allows them to not only form multiple bonds but makes them good reaction sites for reaction with suitably polarised ligands such as is the case with thiols. Therefore given availability of metal atoms on the mineral surface, the reaction of thiol collector molecules on the mineral surfaces will take place with the metal atoms present and not the adjacent ligand atoms in the mineral as they do not have available bonding electrons.
- For CuSO_4 interaction with the PGMs, Cu is less reactive than Pt or Pd and is therefore not expected to take part in any ion exchange mechanism, instead the catalytic properties of both Pt and Pd will catalyse the reduction of Cu^{2+} to Cu^+ in its hydroxyl form. With no interaction between the Cu and the PGM surfaces the interaction of collector with the mineral surface in the presence of CuSO_4 will remain the same.

Chapter 2

2 Research Objectives

2.1 Objectives

The main objective of this work was to determine the electrochemical interactions between PGMs viz. Vysotskite, Cooperite, Moncheite and Merenskyite with typical flotation reagents viz thiol collectors, Sodium ethyl xanthate and sodium diethyl dithiophosphate as well as copper sulphate. Vysotskite and Cooperite are representative of sulphide PGMs whilst Merenskyite and Moncheite are representative of telluride PGMs.

Specific objectives within the study were;

- To determine the interaction reactions between thiol collectors and PGMs studied.
- To determine the likely interactions between copper sulphate and PGMs studied.
- To compare the interactions taking place on telluride PGMs with those of sulphide PGMs and determine and qualify the differences if any.

2.2 Key Questions

The key question which forms the driver for this work is formed from the variability in mineralogy within the Platreef (cf. Section 1.2.1). This is that;

‘Can Telluride PGMs be treated in the same manner as sulphide PGMs with regards to the flotation reagent suite?’

From this some other key questions which would guide the research towards answering this question are;

- Do thiol collectors interact with telluride PGMs in the same manner as sulphide PGMs?
- Do sulphide PGMs interact with copper sulphate in the same manner as base metals?
- Does copper sulphate interact with telluride PGMs to produce the typical species of hydrophobicity?

2.3 Research Approach

Work was done by Shackleton, (2007) to study the floatability of several sulphide and telluride PGMs using ToF-SIMS, UV-Vis Spectroscopy, Electrophoresis Tests and micro-flotation. The first two methods used are ex-situ techniques used to determine the surface species at the mineral surface and although they are able to provide this information they have the drawback of exposing the surface to external conditions that can alter the original species at the surface of the mineral. Electrophoretic tests are also very useful for determining the charge behaviour of the mineral under different conditions but do not provide information on the specific species present. Micro-flotation which is essentially flotation in the absence of a froth phase is an excellent measure for the hydrophobicity of a mineral exposed to flotation reagents. In Shackleton's work the emphasis was not on determining the mechanisms of interaction but to determine floatability. This work has a wealth of information which can be used to validate work done to determine the interaction mechanisms of both xanthate collectors and copper sulphate.

Due to the ability to track reactions occurring at the mineral surface as they occur, electrochemical measurements are an excellent technique to determine the reactions taking place at the mineral surface. The measurements made by Shackleton, (2007) can therefore act as corroboration of the observations made from electrochemical measurements. Rest potential measurements are therefore made in order to determine the bulk species produced at the mineral surface in the presence of collector or copper sulphate which is representative of species present during flotation under those conditions. Cyclic voltammetry measurements allow for the identification of multiple species present at the mineral surface if any, and enable the determination of the order of formation of multiple species. In addition to that information it is also possible to determine the electrochemical activity of species formed which can be of importance in determining the reversibility of the reactions and stability of the species at the surface. All this information may then explain the hydrophobic behaviour of the minerals.

Chapter 3

3 Experimental Materials and Methods

This chapter describes the materials and experimental methodology used in this study. The reagents studied all belong to the thiol group of collectors and the activator studied was copper sulphate. Varying pH levels were studied and in most cases all experiments were conducted in synthetically controlled solution conditions. The minerals studied were naturally occurring and synthesised minerals which were constructed into electrodes in order to measure potentials and currents.

3.1 Synthesis of Minerals

Galena (PbS) and Pyrite (FeS₂), two well-studied minerals were used to establish an electrochemical basis for this study and for validation of experimental methods used in this study. These minerals were obtained as high purity samples from Murdoch University Museum.

Pure palladium used in this study was obtained from Goodfellow, United Kingdom, and platinum was obtained in the form of an electrode from Metrohm. Platinum group minerals (PGMs); Moncheite - PtTe₂, Cooperite - PtS, Merenskyite - PdTe₂ and Kotulskite - PdS were synthesised at Anglo American Research Laboratories by Dr Natalie Shackleton. The procedures for manufacture of the synthetic minerals are detailed in (Shackleton, 2007) and are summarised in Table 3. 1 and Table 3. 2.

Table 3. 1 Synthesis procedure for sulphide minerals used in this study (Shackleton, 2007)

Mineral	Stoichiometric Composition Selected	Thermal Treatment	Product Produced
Cooperite PtS	$Pt_{2.00}S_{2.00}$ (34.35 g Pt, 5.65 g S)	Ampoule heated to 1000 °C at a rate of 20 °/min, held for 96 hours, then allowed to cool naturally at a rate of 10 °/min. Tube broken, reground, resealed and reheated to 1000 °C at a rate of 20 °/min, held for 96 hours, then allowed to cool naturally at a rate of 10 °/min	40 g @ >99% purity
Vysotskite PdS	$Pd_{8.00}S_{8.00}$ (30.74 g Pd, 9.26 g S)	Ampoule heated to 800 °C at a rate of 20 °/min, held for 30 minutes and subjected to a controlled linear slow-cooling to 350 °C over 60 hours.	40 g @ 97.4% purity

Table 3. 2. Synthesis procedure for telluride minerals used in this study (Shackleton, 2007)

Mineral	Stoichiometric Composition Selected	Thermal Treatment	Product Produced
Moncheite PtTe ₂	$Pt_{1.00}Te_{2.00}$ (20 g Pt, 40 g Te)	Ampoule heated to 1150 °C at a rate of 20 °/min, held for 30 minutes, and subjected to a controlled linear slow-cooling to 350 °C over 60 hours then slowly cooled to ambient temp at a rate of 10 °/min.	60 g @ 75.7% purity
Merenskyite PdTe ₂	$Pd_{1.00}Te_{2.00}$ (20 g Pd, 40 g Te)	Ampoule heated to 800 °C at a rate of 20 °/min, held for 30 minutes and subjected to a controlled linear slow-cooling to 350 °C over 60 hours then slowly cooled to ambient temp at a rate of 10 °/min.	60 g @ 68.7% purity

3.2 Electrode Manufacture

Electrodes were manufactured at Murdoch University, Perth Western Australia. The mineral was attached to a threaded copper support using silver conductive glue. This was then embedded in an epoxy mould leaving a section of the surface exposed. Resulting electrodes were approximately 15 mm x 20 mm in diameter (Figure 3.1, Figure 3.2 and Figure 3.4).

Each electrode was attached to a portable holder from which connection to the potentiostat was made. The holder comprised a threaded copper adaptor attached to a copper wire. These were insulated in a plastic casing sealed with epoxy to ensure no solution contact with the conducting wire (Figure 3.4).

The platinum electrode used in this work was obtained from Metrohm and was a Model 60301100 Pt wire electrode as shown in Figure 3.3.

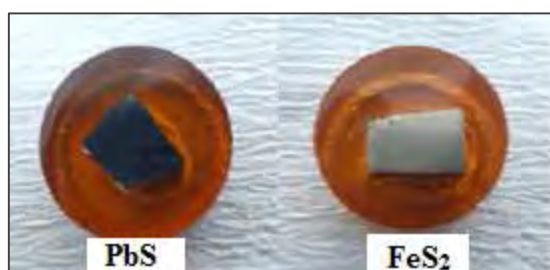


Figure 3.1. Galena (PbS) and Pyrite (FeS₂) electrodes

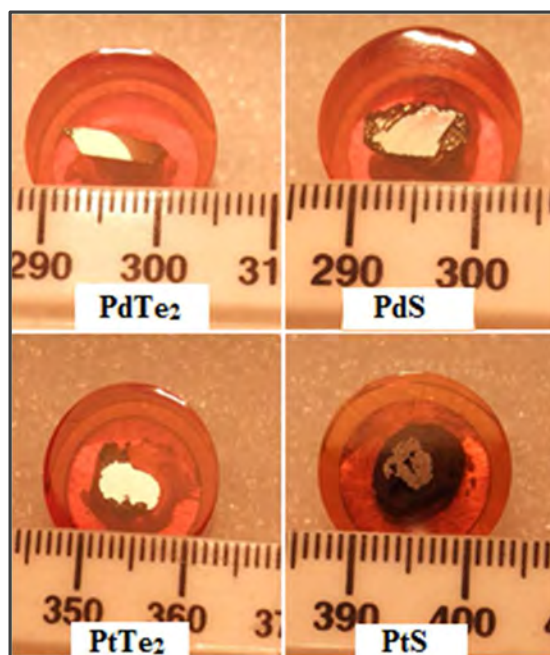


Figure 3.2. Platinum group mineral electrodes, PdTe₂, PtTe₂, PdS and PtS.

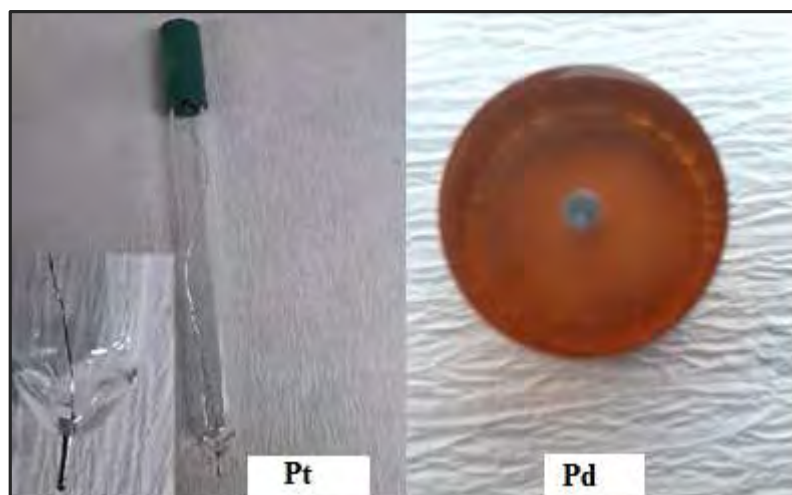


Figure 3.3. Metrohm Pt wire electrode (model 60301100) and Pd metal electrode.



Figure 3.4. Electrode mount for electrochemical experiments.

The surface area of each electrode was measured using an open access image processing program; ImageJ (Research Services Branch, National Institute of Mental Health USA, 2013). The surface area was checked at regular intervals to ensure that it remained constant throughout the study. Average surface areas are given in Table 3.3. These surface areas do not take into account roughness of the mineral surface.

Table 3. 3. Average surface areas of the mineral samples used in this study

Name	Formula	Area cm ²
Moncheite	PtTe ₂	0.168
Cooperite	PtS	0.129
Merenskyite	PdTe ₂	0.116
Vysotskite	PdS	0.199
Palladium	Pd	0.126
Platinum	Pt	0.148
Galena	PbS	0.477
Pyrite	FeS ₂	0.557

3.2.1 X-Ray CT Scan Analysis of Minerals

The synthetic PGMs were analysed for homogeneity by X-Ray Computed Tomography (CT-Scans). X-ray computed tomography is a non-destructive technique that allows for multiple phase analysis using the difference in the densities of the phases. High density phases do not absorb x-rays and appear as bright white colours whilst low density phases allow x-rays to pass through readily and appear as dark grey according to the grey scale used.

Measurement and analysis of the minerals by X-ray CT was conducted using a General Electric Phoenix VTomex L240 with NF180 additional x-ray tube (CT Scanner Unit, Central Analytical Facilities at the University of Stellenbosch). Scans were conducted under the following settings;

- X-ray energy (Nano-tube voltage) -200 kV
- X-ray intensity (Nano-tube current) - 150 μ A
- Scan resolution - 20 μ m

Image analysis of the scans was done using VG Studio Max 2.1 (Volume Graphics Solutions and Voxels).

Figure 3. 5 shows the X-Ray CT-Scans for PtS and PtTe₂. These were measured alongside a pure Pt electrode as a standard comparison for the presence of pure Pt. The grey scales in the scans indicate that there was no metallic Pt in the synthetic mineral phases. PtS showed evidence of porosity; however the sample was shown to be uniform in mineral phase. Scans for the PtTe₂ also indicate that no pure metallic Pt was found within the sample. The scan, however, indicates that there were two phases present, the similarity in grey scale infers a variation of Pt-Te phase, possibly one of the following; PtTe, Pt₃Te₄, Pt₂Te₃ along with PtTe₂ which is the phase favoured by the synthesis conditions.

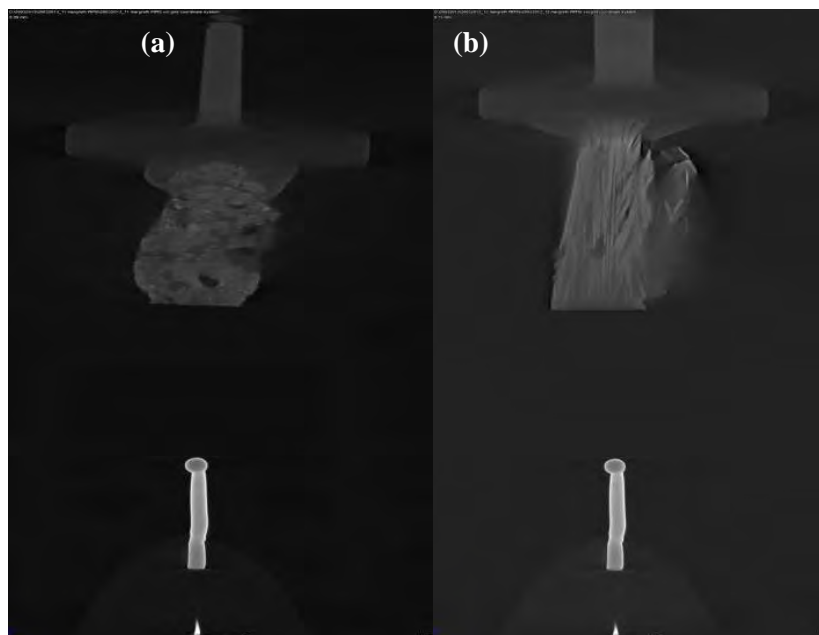


Figure 3. 5. X-Ray CT Scans of PtS and Pt (a) and PtTe₂ and Pt (b).

Figure 3.6 shows the X-ray CT-Scans for the Pd minerals. These have been measured alongside pure Pd as a comparison in order to detect the presence of pure metallic Pd. The scans clearly show that there was no pure metallic Pd present in the synthetic minerals. The scan for PdS indicated that two phases were present. The mineral was therefore comprised of PdS with possible phases of PdS₂, Pd₄S, Pd₃S, Pd₁₆S₇ and PdS₂. Pure elemental sulphur would have resulted in a darker grey scale, which was not seen in this sample.

The scan for PdTe₂ indicated that the mineral did not contain pure metallic Pd. The mineral was uniform throughout without any indication of a second phase.

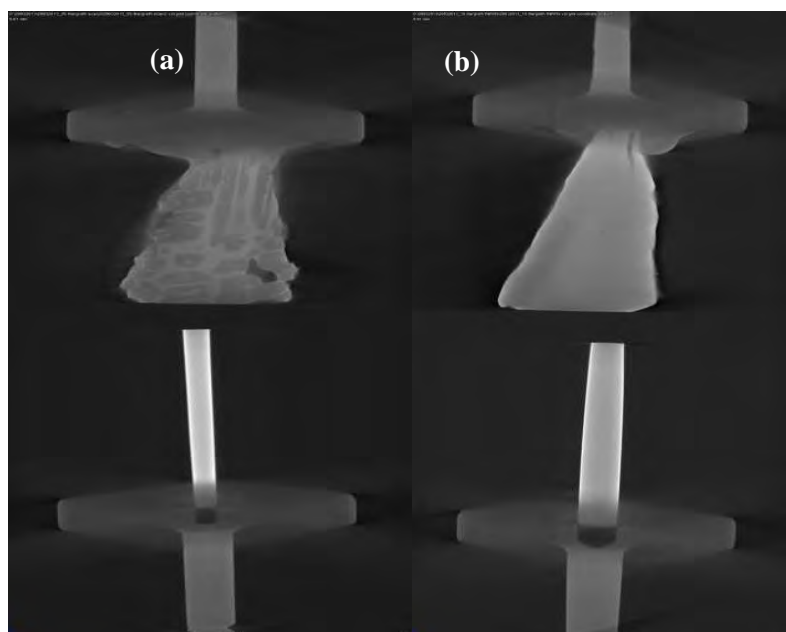


Figure 3.6. X-Ray CT Scans for PdS and Pd (a) and PdTe₂ and Pd (b).

3.3 Reagents

Reagent concentrations were calculated based on the mass of the active ingredient i.e. purity of the reagent was accounted for in calculation of all concentrations. Sodium sulphate (Na₂SO₄) was obtained from Associated Chemical Enterprises, Sodium tetraborate decahydrate (Na₂B₄O₇·10H₂O) from Merck, potassium dihydrogen orthophosphate (KH₂PO₄) from Merck and copper sulphate pentahydrate (CuSO₄·5H₂O) from Associated Chemical Enterprises all in the form of powders. Sodium hydroxide was obtained as pellets from Merck and Sulphuric acid in liquid form was obtained from Kimix.

Sodium ethyl xanthate (SEX) was obtained in powder form, Sodium di-ethyl dithiophosphate (Senkol 3) in liquid form buffered in a solution of sodium hydroxide and Sodium diethyl dithiocarbamate (Senkol 5) in liquid form buffered in an alkaline solution. These collectors were supplied by Senmin. The buffer solutions were not expected to affect measurements in this work. Sodium diisobutyl dithiophosphinate (Aerophine 3418A Promoter) and Sodium monothiophosphinate (Aero 6697) were obtained from Cytec in liquid form. Table 3.4 shows the reagents used in this study and their purities.

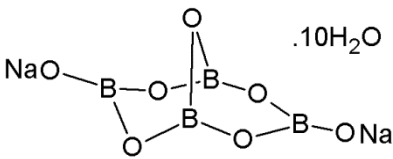
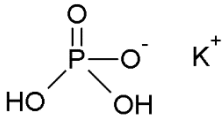
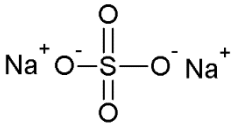
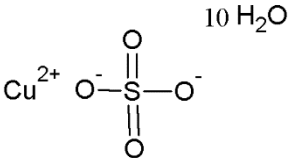
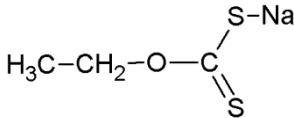
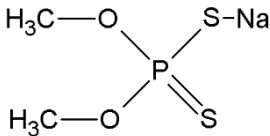
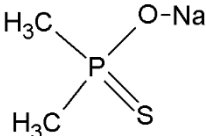
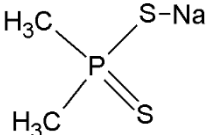
All electrochemical solutions were made using deionised water. The resistivity of the water was above 10 MΩ/cm². Na₂SO₄ was added as an electrolyte at a concentration of 0.1 M. Different buffer solutions were used to achieve various pH values. In experiments investigating collector interactions, the collector concentration was maintained at 6.24 x 10⁻⁴ M.

- pH 11.2 was achieved by using 0.05 M $\text{Na}_2\text{B}_4\text{O}_7$ in a 0.1 M solution of Na_2SO_4 and adjusting the pH level using 1M NaOH
- pH 9.2 was achieved by using 0.05 M $\text{Na}_2\text{B}_4\text{O}_7$ in a 0.1 M solution of Na_2SO_4
- pH 7.0 was achieved using 0.1 M KH_2PO_4 and 0.1 M NaOH
- pH 5.2 was achieved using 0.1 M KH_2PO_4 , 0.1 M NaOH and 0.01 M H_2SO_4
- pH 4.2 was achieved using 0.01 M H_2SO_4 in 0.1 M Na_2SO_4

In experiments investigating the effect of copper sulphate addition, the concentration of CuSO_4 was maintained at 1×10^{-4} M and collector concentration was maintained at 1×10^{-4} M. Potassium dihydrogen orthophosphate was not used to make buffer solutions in this study due to the reactivity of the chemical with CuSO_4 which resulted in the formation of a precipitate. The following buffer solutions were used for the different pH levels studied;

- pH 10 was achieved using 0.05 M $\text{Na}_2\text{B}_4\text{O}_7$ and 1M NaOH in a 0.1 M solution of Na_2SO_4
- pH 8 was achieved using 0.05 M $\text{Na}_2\text{B}_4\text{O}_7$ and 0.01 M H_2SO_4 in 0.1 M solution of Na_2SO_4
- pH 6 was achieved using 0.1 M NaOH in a solution of 0.1 M Na_2SO_4 and 0.01 M H_2SO_4 was used to adjust pH.

Table 3.4 Reagents used in this study and their purities

Reagent	Chemical Formula	Molecular Weight	Purity (w/w %)
Sodium Tetraborate Decahydrate		381.38	99.0 %
Potassium Dihydrogen Orthophosphate		136.09	99.0 %
Sodium Sulphate		142.04	99.5 %
Copper Sulphate Pentahydrate		249.69	99.0 %
Sodium Ethyl Xanthate		144.19	99.0 %
Sodium Di-Ethyl Dithiophosphate		208.21	50.0 %
Sodium Monothiophosphate		180.03	50.0 %
Sodium di-isobutyl Dithiophosphate		232.32	51.0 %

3.4 Equipment

The electrochemical equipment set-up is shown in Figure 3.7. Electrochemical measurements were conducted in a 500 ml jacketed glass vessel (C) which was agitated using a 15mm magnetic stirrer bar. The vessel was mounted on a Freed Electric magnetic stirrer/hotplate (B). An ABB water bath using a Shinha DCS Model 300 (A) temperature controller was used to regulate the water temperature within the vessel at 25 °C.

A three electrode system was used for electrochemical measurements. The counter electrode was a Pt wire electrode and the reference electrode was a double junction Ag/AgCl reference electrode supplied by Metrohm with a potential of -0.207 V against the standard hydrogen electrode (SHE). This reference electrode was filled with 3 M KCl solution. The reference solution was changed once every month. The electrode was then measured against a standard Ag/AgCl electrode to ensure that the reference electrode was measuring the correct potential. These electrodes and electrode solutions were obtained from Metrohm. The construction of the working electrode has been discussed in Section 3.2.

A Gamry Instruments Reference 600TM Potentiostat/Galvanostat/Zero Resistance Ammeter (D) was used for all electrochemical measurements. The potentiostat was interfaced to a computer (F) via USB connection. The user interface used with the potentiostat is the Gamry Framework which enables calibration of the instrument, measurement of open circuit potential and measurement of current. Electrochemistry software is sold separately and run through Gamry framework. The electrochemistry module used with the instrument was module PHETM 200. Module PHETM 200 had nine different experimental set-up techniques viz;

- Chronoamperometry
- Chronocoulometry
- Chronopotentiometry
- Controlled Potential Coulometry
- Cyclic Voltammetry
- Linear Sweep Voltammetry
- Repeating Chronoamperometry
- Repeating Chronopotentiometry
- Multiple-Step Chronoamperometry

Connection between the potentiostat and electrodes was made through a cell cable (E) that comprised of six connections.

- A blue banana plug, for the working sense electrode which sensed the voltage of the working electrode
- A green banana plug, for the working electrode which carried the cell current
- A red banana plug, for the counter or auxiliary electrode
- An orange banana plug which sensed the counter electrode potential used in ZRA mode
- White pin Jack, for the reference electrode
- Black Pin Jack, for the floating ground which either connects to a Faraday cage or can be left open

Analysis of results was conducted using Gamry Instruments Echem™ Analyst Software. All potentials were corrected to Standard Hydrogen Electrode potential within the software and subsequently exported to Microsoft Excel for further data processing. The charge transferred under each peak was obtained using the Cyclic Voltammetry tool 'Peak Integration' which is present within Echem analyst. The tool enables selection of a peak and returns the charge transferred.

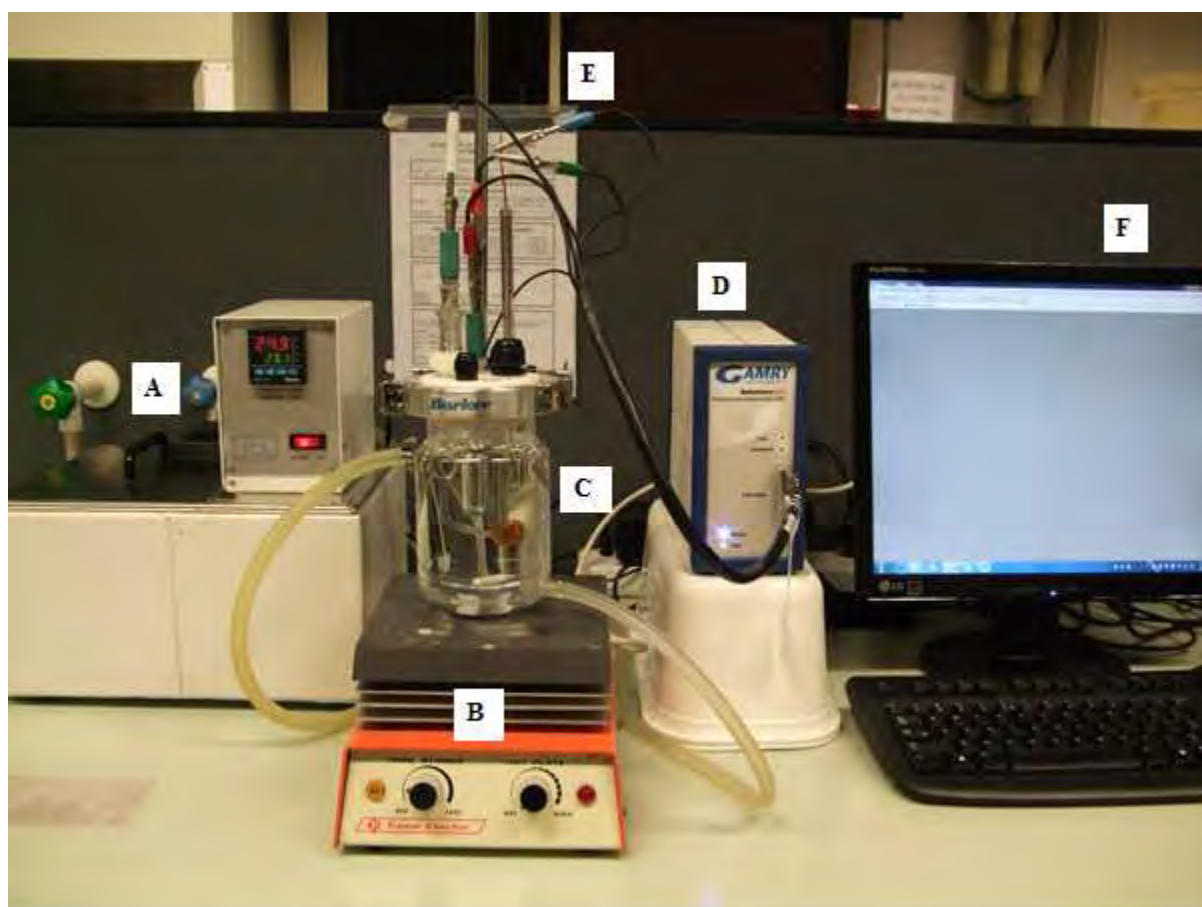


Figure 3.7. Electrochemistry Equipment Set-Up.

3.5 Procedures for Electrochemical Measurement

3.5.1 Mineral Working Electrode Preparation

The mineral electrodes were polished prior to each electrochemical measurement using the following procedure. The mineral was initially wet ground on 600 Grit Silica Carbide paper after which it was immediately wet polished on alumina powders starting with the most coarse (1 μm) and ending with the finest (0.05 μm). The mineral was then washed with deionised water and dried with a paper towel by lightly dabbing the surface. 1 μm , 0.3 μm and 0.05 μm alumina powders were obtained from IMP Scientific and Precision (Pty) Ltd.

3.5.2 Rest Potential Measurements

3.5.2.1 Standard Procedure for Rest Potential Measurements

Measurements were made to determine the rest/open circuit potentials of the minerals in solution. 450 ml of an electrolyte solution was charged to the vessel for each rest potential measurement. Measurements of rest potential were conducted in the absence and presence of collector. After 600s collector was injected into the reaction vessel for the measurement of rest potential in the presence of collector. Table 3.5 summarises the sequence of measurement of the mixed potentials.

Table 3. 5 Sequence of mixed potential measurement

Mixed potential of mineral in collectorless solution	10 minutes
Mixed potential of mineral in collector solution	10 minutes

A schematic of the rest potential profile that is expected for the case of collector addition which forms the basis of this study is shown in Figure 3. 8. Mixed potential theory determines that the rest potential lies between the equilibrium potential of the dominant reduction reaction and the equilibrium potential of the oxidation reactions taking place at the mineral surface. In the absence of collector the mixed potential is a result of the balance between oxygen reduction rates and mineral oxidation rates. In the presence of collector the mixed potential at the mineral surface is a balance of oxygen reduction and both mineral oxidation and collector oxidation. As a result a shift in the original rest potential prior to collector introduction is indicative of the interaction of collector with the mineral surface.

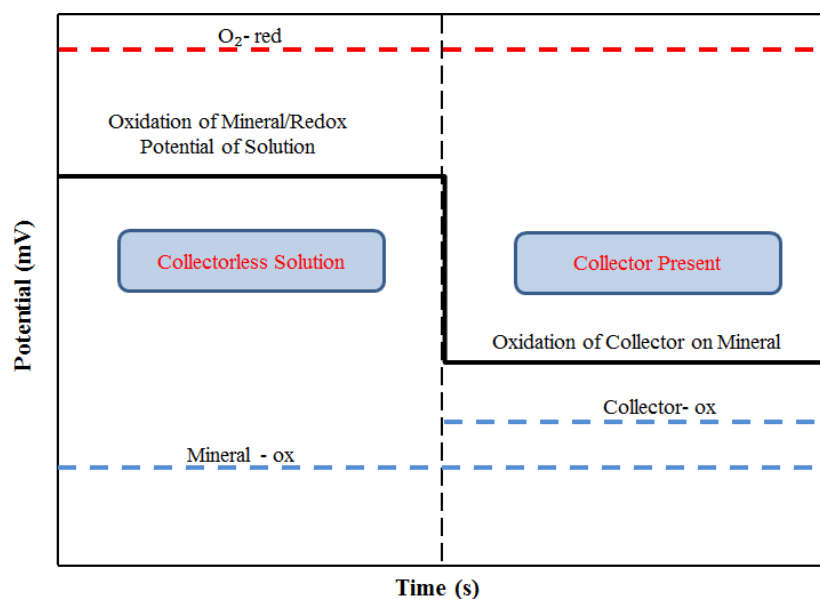


Figure 3. 8. Schematic of Standard Rest potential measurement profile including the expected potentials of the dominant reactions affecting the rest potential viz. oxygen reduction, mineral oxidation, collector oxidation

3.5.2.2 Rest Potential Measurements in the Presence of Solids

Measurements of the mixed potential were made in the presence of solids in order to simulate plant conditions. The pulp was made up using Platreef ore milled to 80% passing 75 μm . 1 kg of solids were milled for 15 minutes in a rod mill. The milled pulp was then removed and dried under infrared light. These solids were then split using a rotary splitter into size fractions of approximately 100 g. Synthetic plant water was used to reconstitute a pulp which had a solids concentration of 33 w/w %. The ionic concentration of synthetic plant water is summarised in Table 3. 6. The same collector concentration was used in the pulp tests as was used for the tests without solids.

Table 3. 6. Ionic composition of synthetic plant water

Ion	Concentration (ppm)
Ca^{2+}	80
Mg^{2+}	70
Na^{+}	153
Cl^{-}	287
SO_4^{2-}	240
NO_3^{-}	176
CO_3^{2-}	17
TDS	1023

3.5.2.3 Rest Potential Measurements of a Polarised Mineral Surface

Oxidation of the mineral surface was investigated by polarising the mineral at different potentials, anodic and cathodic. Using the chronoamperometry module on PHETM200 the mineral was polarised at potentials of +0.6 V, +0.4 V, -0.4 V and -0.6 V for 15 seconds and immediately afterwards the standard procedure used for rest potential measurements was applied c.f. Section 3.5.2.1.

3.5.2.4 Rest Potential Measurements in the presence of CuSO₄

Rest potential measurements in the presence of CuSO₄ were measured over a period of 1800 s. The same electrode preparation procedure as described in Section 3.5.1 was utilised. The rest potential of the mineral was measured in a solution without CuSO₄ or SEX for 600s and then 1 ml of a 1% solution of CuSO₄ was added to the vessel. The rest potential of the mineral was subsequently measured for a further 600 s at which point, 1 ml of a 0.1 % solution of SEX was added to the vessel with rest potential being measured for a further 600 s to obtain a rest potential profile over 1800 s.

3.5.3 Cyclic Voltammetry Measurements

Cyclic voltammetry measurements were determined in both the absence and presence of collector. Measurements were made under atmospheric oxygen which was measured to have an average dissolved oxygen concentration of 6.98 ppm and this has been referred to as an 'Aerated Condition'. In order to investigate the effect of dissolved oxygen the vessel was purged with N₂ to de-aerate the solution. Nitrogen was purged for 30 minutes prior to measurements and the vessel was maintained under nitrogen atmosphere by continuously purging the airspace at the top of the vessel with nitrogen during measurements. The dissolved oxygen concentration achieved was < 0.50 ppm. All voltammograms were measured in quiescent solutions (absence of stirring). The current measured was normalized by dividing it by the surface area of the mineral to obtain the current density which is reported on all the voltammograms. Cyclic voltammetry measurements were conducted immediately after polishing of the mineral surface.

3.5.3.1 Cyclic Voltammetry Procedure

Measurements were controlled via Gamry software by setting the required parameters;

- Under de-aerated solution conditions, the vessel was purged with nitrogen gas for 30 min from the base of the solution. Prior to measurements the nitrogen line was removed from solution and the gas was allowed to purge the air space above the liquid level within the vessel.
- The mineral was wet polished as described in Section 3.5.1, immediately placed in the vessel and the connections to the potentiostat were made.
- 10 seconds were allowed for the electrode equilibration time prior to sweep measurements.
- The starting potential was 0 V versus Open Circuit Potential.
- The potential limits were set to be the required potential limit minus 0.207 V (Ag/AgCl potential).
- The final potential was set to be 0 V versus open circuit potential.
- Sweep rate, number of sweeps and current limit were also set prior to measurement

Table 3.7 shows the parameters investigated for cyclic voltammetry measurements.

Table 3. 7 Cyclic Voltammetry Parameters

Potential Limits	± 0.4 V and ± 0.6 V
Scan Rates	1 mV/s , 10 mV/s, 50 mV/s
Number of Scans	1 Sweep and 2 Sweeps
Oxygenation of Solution	Aerated and Deaerated Solution

3.5.3.2 Interpretation of Voltammograms

Voltammograms were generated in forward going sweeps (increasing potential in the positive direction) and reverse going sweeps (decreasing potential in the negative direction). Currents generated during positive potential sweeps are due to electron losing processes. These are indicative of oxidation and are therefore anodic. Currents that are generated during negative going potential sweeps are indicative of electron gaining processes and are therefore cathodic.

The equilibrium potential at which a reaction takes place is the potential at which rates of cathodic and reduction reactions are balanced. Any potential above the equilibrium potential creates a driving force (over- potential) for oxidation to occur. Likewise electrochemically active species will be reduced when a potential is applied which is below the equilibrium potential of the reduction of the species. Reduction currents therefore arise.

Chapter 4

4 Results

In this chapter the results for this work are presented. The Chapter begins with a presentation of the mixed or rest potential results for galena and pyrite so as to validate the experimental procedure against results reported in the literature. This is followed by the rest potential results obtained for the interactions of the thiol collectors of interest with pure Pt and Pd as well as the tellurides and sulphides of these metals. Cyclic voltammetry results for these same systems are then presented. The chapter concludes with the results obtained in an investigation of the effect of the presence of copper sulphate in the system. In some instances results are contained in an appendix where such results are not critical to the development of the major investigation.

4.1 Oxidation Potentials of Collectors

The equilibrium potential for the formation of a dimer for various collectors was determined experimentally on a Pt electrode. The relevant reaction is as follows;



where X denotes a thiol

4.1.1 Oxidation Potential of SEX

Table 4.1 shows the results of experimental measurements for the oxidation potential of sodium ethyl xanthate (SEX). Three different collector concentrations were used and from these a standard electrode potential for the oxidation of the collector to its dimer form was calculated using the Nernst equation. A standard deviation of 0.001 V on the calculated standard potential was calculated.

Table 4.1. Equilibrium potentials of SEX at different concentrations

Concentration	6.24 x 10⁻⁴ M	1.00 x 10⁻³ M	2.00 x 10⁻³ M
Potential E (V)	0.150	0.137	0.120
Standard Potential E° (V)	-0.039	-0.041	-0.040

At a collector concentration of 6.24x10⁻⁴ M the standard potential measured in this work was compared to that of Majima and Takeda, (1968) in Table 4.2.

Table 4.2. Equilibrium potential of SEX compared to literature values

	Literature*	Experimental
Potential E (V)	0.140	0.150
Standard Potential E° (V)	-0.049	-0.039

*(Majima and Takeda, 1968)

The results obtained indicate that the system used in this work provides similar results to those previously reported.

4.1.2 Oxidation Potential of DTP

Equilibrium potentials for the formation of a dimer from this collector at various concentrations are shown in Table 4.3. From the measured equilibrium potentials standard potentials were once again calculated using the Nernst Equation. The calculated standard deviation was 0.011 V.

Table 4.3. Results of measured equilibrium potentials of diethyl dithiophosphate

Concentration	5 x 10⁻³ M	4 x 10⁻³ M	2 x 10⁻³ M
Potential E (V)	0.338	0.353	0.348
Standard Potential E° (V)	0.202	0.209	0.188

An average standard potential for diethyl dithiophosphate was calculated from Table 4.3 and used to determine the equilibrium potential for the formation of a dimer for a collector concentration of 6.24×10^{-4} M using the Nernst Equation. A standard potential for DTP is reported to be 0.250 V by Finkelstein and Goold, (1972). Comparison of this value and the calculated potential at a concentration of 6.24×10^{-4} M with that measured in this work is shown in Table 4.4.

Table 4.4. Equilibrium potential of diethyl dithiophosphate compared to literature values

	Literature*	Experimental
Potential E (V)	0.439	0.388
Standard Potential E° (V)	0.250	0.199

*(Finkelstein and Goold, 1972)

4.1.3 Oxidation Potentials of Modified Thiol Collectors (DTPI, MTP)

Of the ‘modified’ thiol collectors studied in this work the standard potential for dimer formation for sodium monothiophosphate and sodium dithiophosphate collector were determined experimentally. The measured equilibrium potentials and calculated standard potentials for these collectors are shown in Table 4.5. The oxidation potentials were observed to be significantly higher than found for xanthate and dithiophosphate.

Table 4.5. Results of the equilibrium potential measurements of sodium dithiophosphate (DTPI)

Collector Concentration	Equilibrium Potential	MTP	DTPI
6.24 x 10 ⁻⁴ M	Potential E (V)	0.595	0.709
	Standard Potential E° (V)	0.405	0.520
2.00 x 10 ⁻³ M	Potential E (V)	0.608	0.749
	Standard Potential E° (V)	0.448	0.590
1.00 x 10 ⁻³ M	Potential E (V)	0.643	0.768
	Standard Potential E° (V)	0.465	0.591

4.2 Rest Potential Measurements

Rest potential measurements were made for all the minerals used in this study i.e PbS, FeS₂, PtTe₂, PdTe₂, PtS and PdS. Rest potentials for Pyrite (FeS₂) and Galena (PbS) were measured to validate the technique used in this work by comparing the results with those previously reported in the literature. The effect of different thiol collectors on the rest potential of the mineral under varying solution conditions c.f. Section 3.5.2 was also investigated. A shift in the rest potential of the mineral was observed as indication of the interaction between the collector and the mineral surface.

4.2.1 Validation of Rest Potential Measurement Techniques

Rest potential measurement techniques were validated against the results reported by (Allison et al., 1972). The rest potentials for galena and pyrite were measured at pH 7 at a collector concentration of 6.24x10⁻⁴ M sodium ethyl xanthate (SEX). Rest potential profiles generated are shown in Figure 4.1 and Figure 4.2 for galena and pyrite respectively.

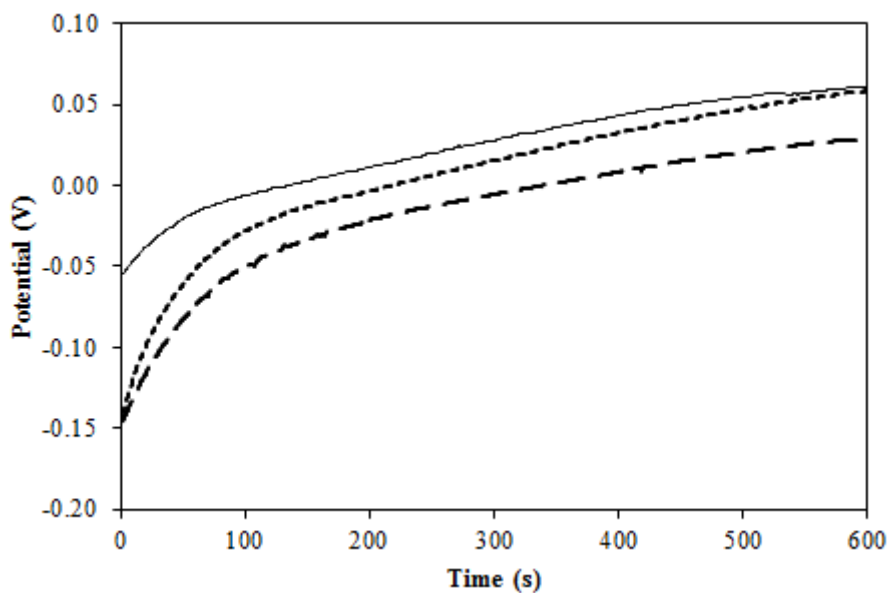


Figure 4.1. Repeated rest potential measurements for Galena in a solution containing 6.24×10^{-4} M SEX at a pH of 7.

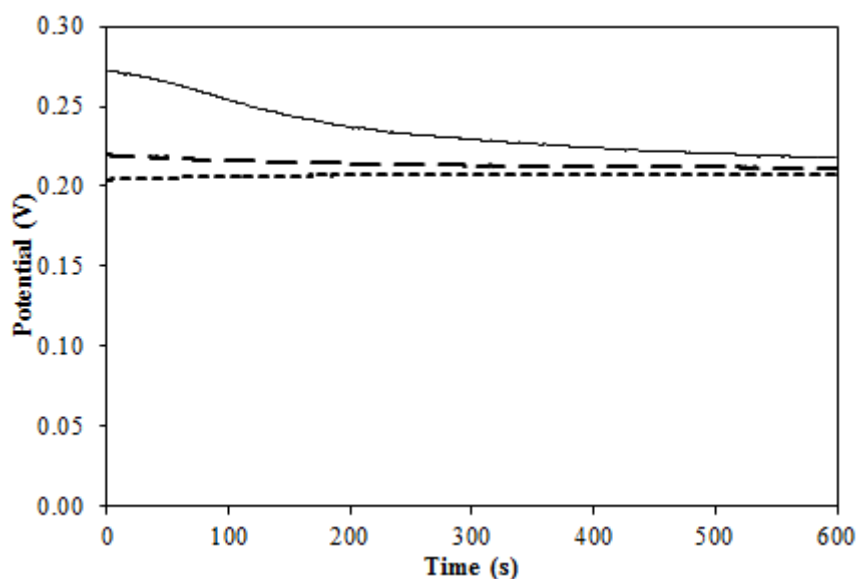


Figure 4.2. Repeated rest potential measurements for Pyrite in a solution containing 6.24×10^{-4} M SEX at a pH of 7.

The rest potential measurements were repeated three times with the standard deviation being calculated as the error for the rest potential after 600 s on each mineral. These values were compared to those obtained by (Allison et al., 1972) under the same conditions. These values are shown in Table 4.6.

Table 4.6. Summary of the rest potential values for Galena and Pyrite after 600 s compared to values reported in literature for the same system

Rest Potential (mV)		
	Pyrite	Galena
1	0.218	0.067
2	0.207	0.072
3	0.210	0.040
Average	0.212	0.060
StDev	0.005	0.017
Literature*	0.220	0.060
Deviation	0.008	0.000

* (Allison et al., 1972)

4.2.2 Rest Potential Measurements of Galena and Pyrite

Figure 4.3 shows the mixed potentials for galena and pyrite with SEX addition after 600 s. As can be seen, pyrite was shown to have a rest potential more positive than that for Galena. In this figure these rest potentials before and after collector addition are separated by the dixanthogen oxidation potential which is indicated in both figures as a solid line. When the rest potential of a mineral in the presence of collector lies above the dixanthogen line this is indicative of thermodynamically favourable conditions at the mineral solution boundary for the formation of dixanthogen.

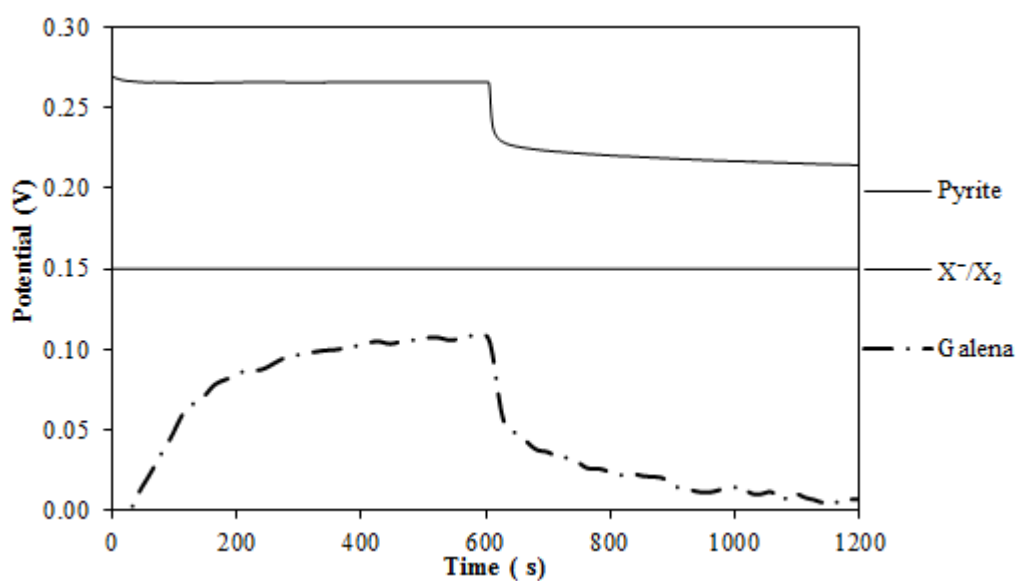
**Figure 4.3. Rest potential of Galena and Pyrite at pH 9.2 in the presence and absence of SEX**

Figure 4.4 shows the rest potentials for pyrite and galena shown when DTP is the collector and is added after 600 s. The oxidation potential for the reaction of DTP to its dimer is shown on Figure 4.4 as a solid line at 0.388 V. The rest potential profiles of both minerals are below this equilibrium potential. Interaction between DTP and both mineral surfaces is indicated by changes in the mixed potential of the minerals after 600 s.

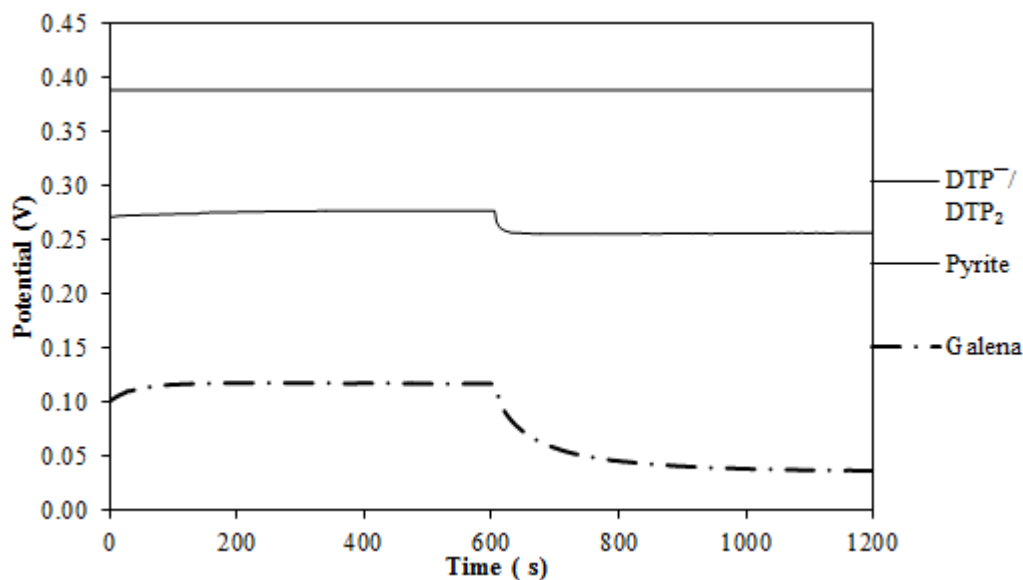


Figure 4.4. Rest potential of Galena and Pyrite at pH 9.2 in the presence and absence of diethyl dithiophosphate.

4.2.3 Rest Potential Measurements of Platinum Group Minerals in SEX

The same mixed potential measurements were applied to Pt and Pd minerals. This section provides results of the rest potential measurements for the platinum group minerals measured under acidic (pH 4.2) and alkaline conditions (pH 9.2). Results are presented for Pt, PtTe₂ and PtS as well as the palladium minerals Pd, PdTe₂ and PdS.

4.2.3.1 Rest Potential Measurements of Pt Minerals

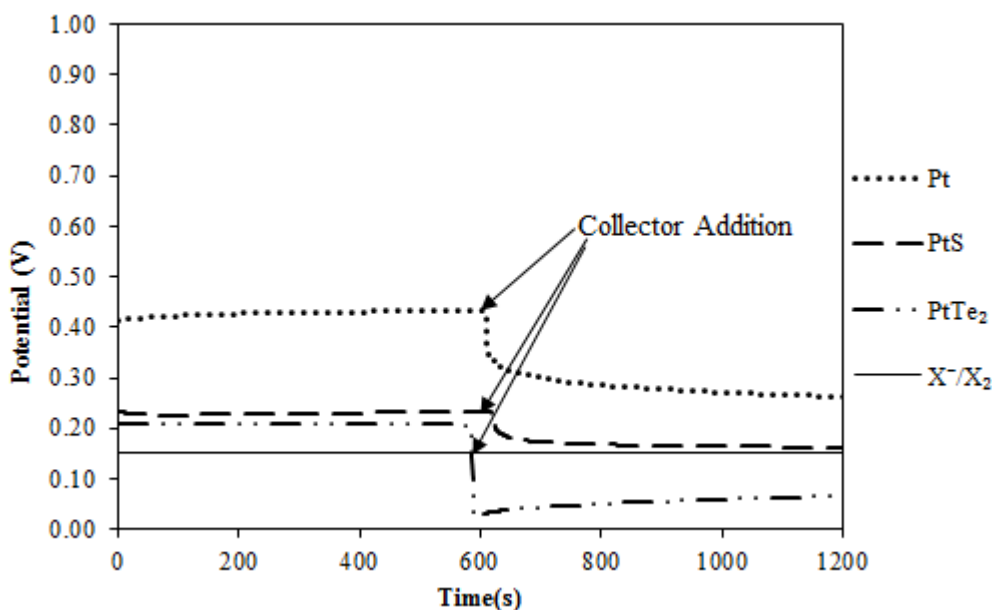


Figure 4.5. Rest potential of platinum minerals at pH 9.2 in the presence and absence of SEX

Figure 4.5 shows the rest potentials of the Pt minerals at pH 9.2. The most positive rest potential was that of Pt followed by PtTe₂ and PtS. After collector addition a gradual reduction in rest potential for Pt and PtS occurred with the resulting rest potentials being above the equilibrium potential for dixanthogen formation. PtTe₂ on the other hand, decreased in potential to a minimum potential below the dixanthogen equilibrium potential before the profile increased to an average value.

At a pH value of 4.2 rest potential measurement results for Pt minerals are shown in Figure 4.6. These potential values prior to collector addition were observed to be more anodic (positive) under acidic conditions than under alkaline conditions (cf. Figure 4.5). Unlike that for pH 9.2 in the presence of collector the resulting rest potentials for all minerals converged to within 0.2 V of one another and in all cases were more positive than the dixanthogen formation potential. Similarity was maintained however between the potentials of the minerals in acidic and alkaline conditions with the order of decreasing rest potential being Pt followed by PtS and then PtTe₂.

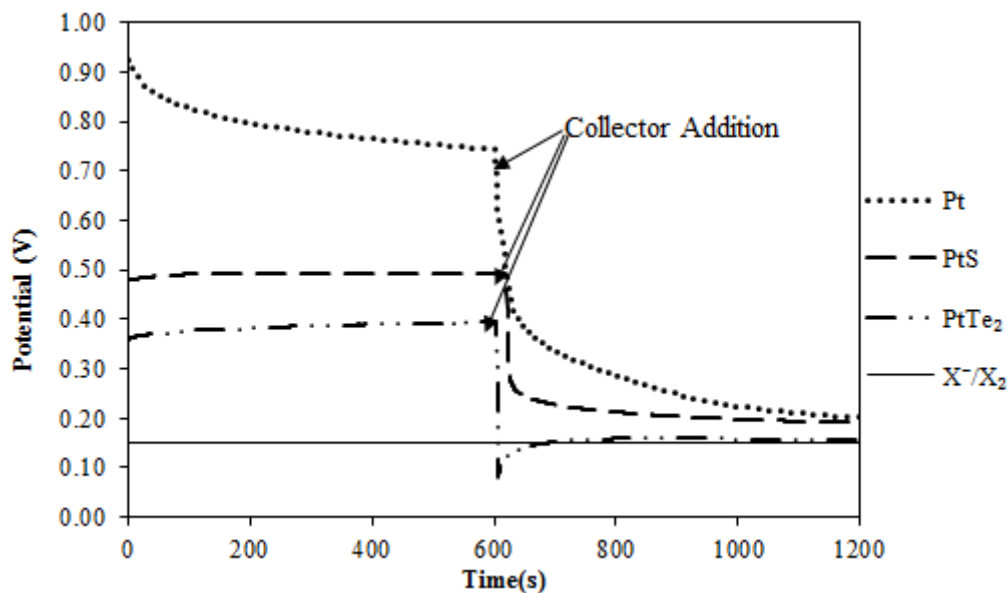


Figure 4.6. Rest potential of platinum minerals at pH 4.2 in the presence and absence of SEX

4.2.3.2 Rest Potential of Pt Minerals Polarised at Anodic and Cathodic Potentials

The effect of oxidation of the mineral surface can be investigated by polarising the minerals at potentials more anodic and cathodic with respect to the rest potential of the mineral. Potentials of 0.4 V, -0.4 V, 0.6 V and -0.6 V were applied to PtTe₂ and PtS.

Results for PtTe₂ after polarisation at different potentials are shown in Figure 4.7. It was observed that polarisation at potentials of 0.6V, 0.4 V, -0.4 V and -0.6 V had little difference on the final rest potential prior to collector addition at 600s. A difference in the rest potentials was only observed subsequent to collector addition, where the rest potential of the mineral after polarisation at 0.6 V was observed to have lower potential values compared to the other measurements.

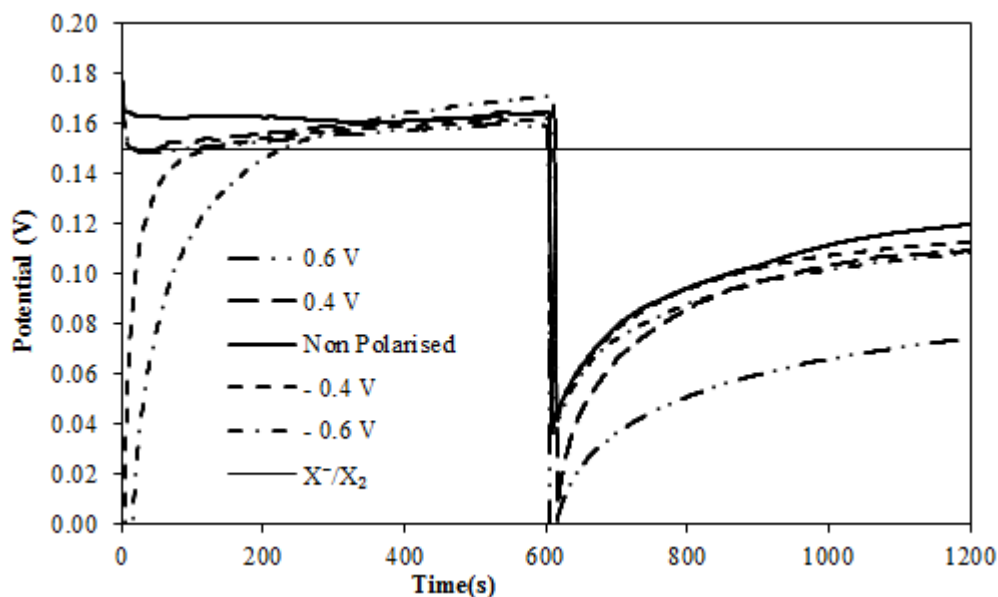


Figure 4.7. Rest potential results for PtTe₂ under different anodising conditions at pH 9.2 and with SEX collector addition after 600 s

Figure 4.8 shows the rest potentials for PtS after polarisation at the same potentials as were used in the results shown in Figure 4.7. There was no observed effect of polarisation of the mineral subsequent to collector addition but differences were observed prior to addition of SEX. The order of decreasing rest potential on the mineral prior to SEX addition was 0.6 V, 0.4 V, non-polarised, -0.4 V and -0.6 V. These observed changes in rest potential are indicative of varying oxidation behaviour at different potentials for the mineral.

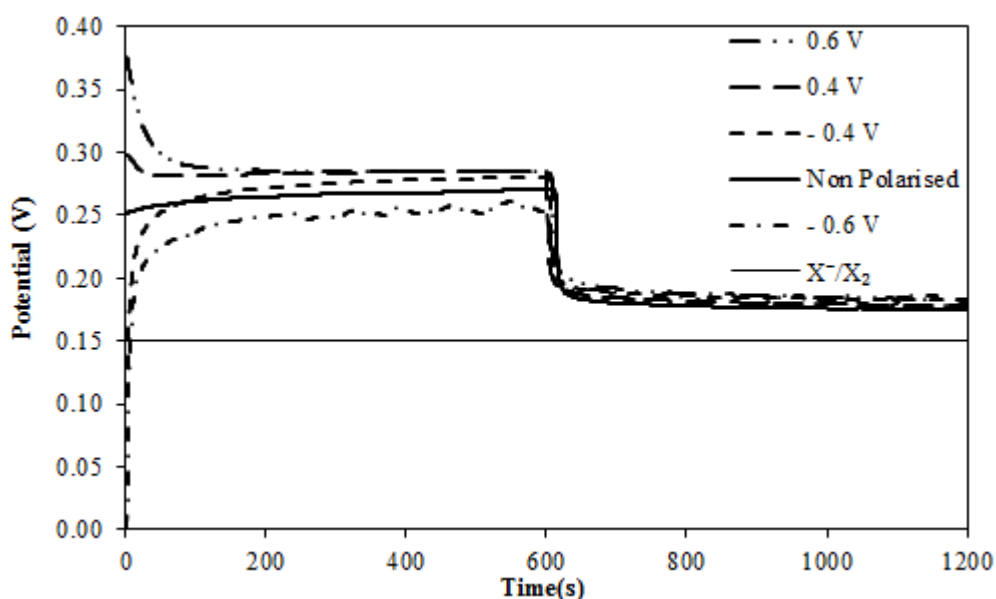


Figure 4.8. Rest potential results for PtS under different anodising conditions at pH 9.2 and with SEX collector addition after 600 s

4.2.3.3 Rest Potential Measurements of Pt Minerals in Platreef Pulp

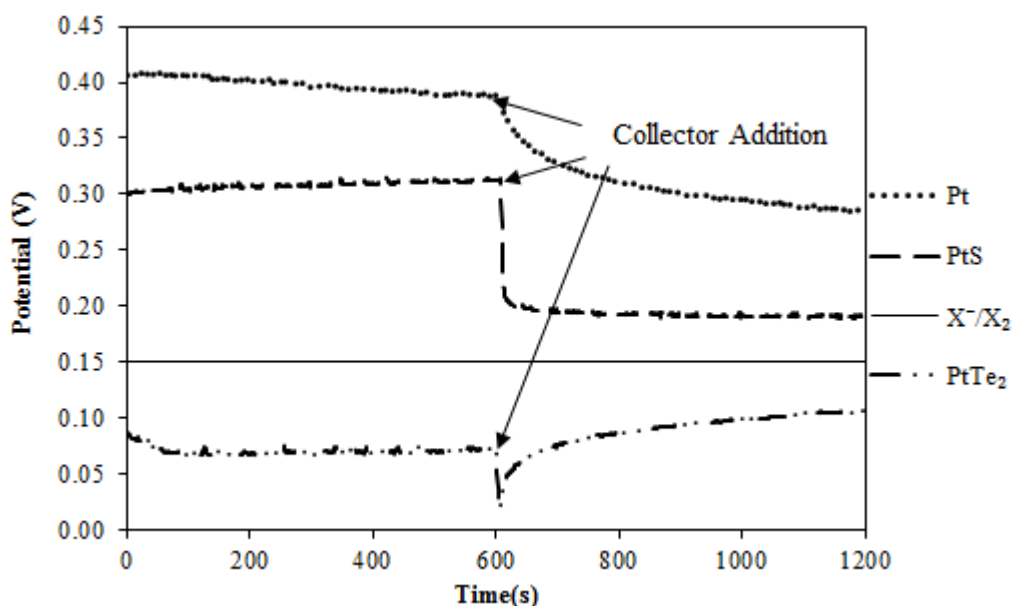


Figure 4.9. Rest potential results for Pt minerals in pulp at pH 7 before and after collector addition of SEX

Measurements of the rest potentials of minerals in the presence of solid were made in a simulated Platreef pulp. The procedure used has been described in Section 3.5.2. For Pt, PtTe₂ and PtS, the rest potentials within a reconstituted pulp are shown in Figure 4.9.

Under these conditions the rest potential of Pt in the pulp was the same as that for a solids free solution at pH 9.2 (cf. Figure 4.5) before and after SEX addition. PtS showed a more positive rest potential compared to that at pH 9.2 in the absence of solids whereas for PtTe₂ the rest potential that was more negative than that shown in Figure 4.5. The mineral developed a rest potential that was below the dixanthogen equilibrium potential both before and after collector addition indicating it to be the most significantly affected by the addition of solids to the system. Also notable was the final rest potential for PtTe₂ achieved after collector addition which was higher in magnitude than that for the mineral prior to collector addition.

4.2.3.4 Rest Potential Measurements of Pd Minerals

Rest potentials of the Pd minerals in solution without solids are shown in Figure 4.10 for pH 9.2. Pd had the most positive rest potential followed by PdTe₂ and PdS prior to collector addition. Pd metal's rest potential was significantly more positive than that of PdS and PdTe₂ which were within 0.05 V of each other. After collector addition the rest potentials of Pd and PdS decreased sharply to constant values. Pd has a potential after collector addition which was above the dixanthogen reduction potential (indicated at 0.15 V) whilst that of PdS was below 0.15 V. PdTe₂ decreased in potential sharply in the

same manner as the other minerals however the potentials became more positive resulting in a final rest potential which lay just above the dixanthogen line.

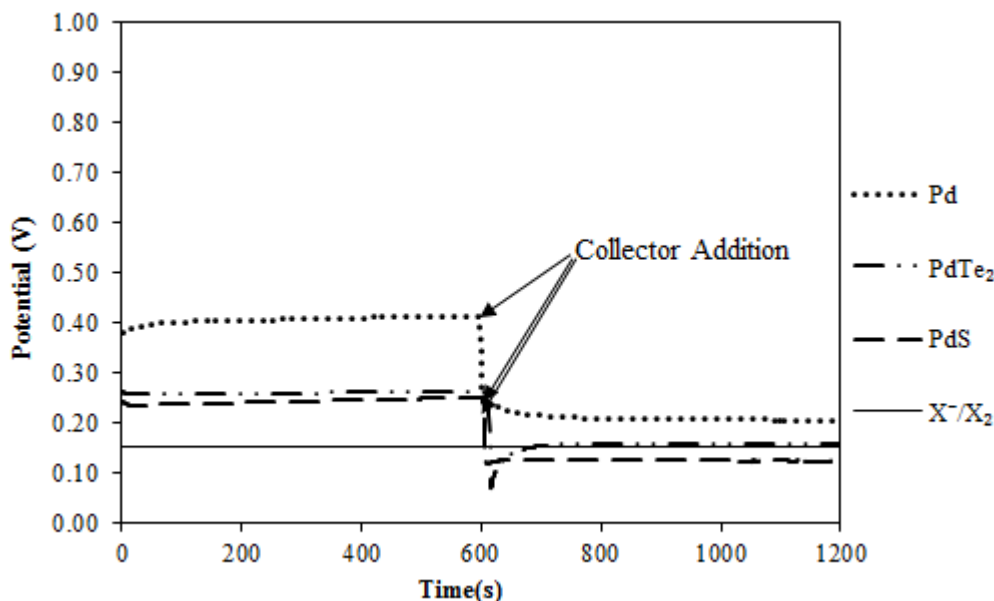


Figure 4.10. Rest potential of palladium minerals at pH 9.2 in the presence and absence of SEX

Under acidic conditions (pH 4.2) the rest potentials for the Pd minerals are shown in Figure 4.11. Rest potentials for all the minerals prior to collector addition were more positive at pH 4.2 than at pH 9.2. The rest potential of Pd shown in Figure 4.11 was found to have potentials of the same order as those of PdS and PdTe₂ at pH 4.2 unlike that of the metal at pH 9.2. After collector addition the rest potentials of the minerals were once again within a similar potential range. Even though the final rest potential values achieved were within 0.1 V of each other the rest potential of PdS fell below the dixanthogen equilibrium line.

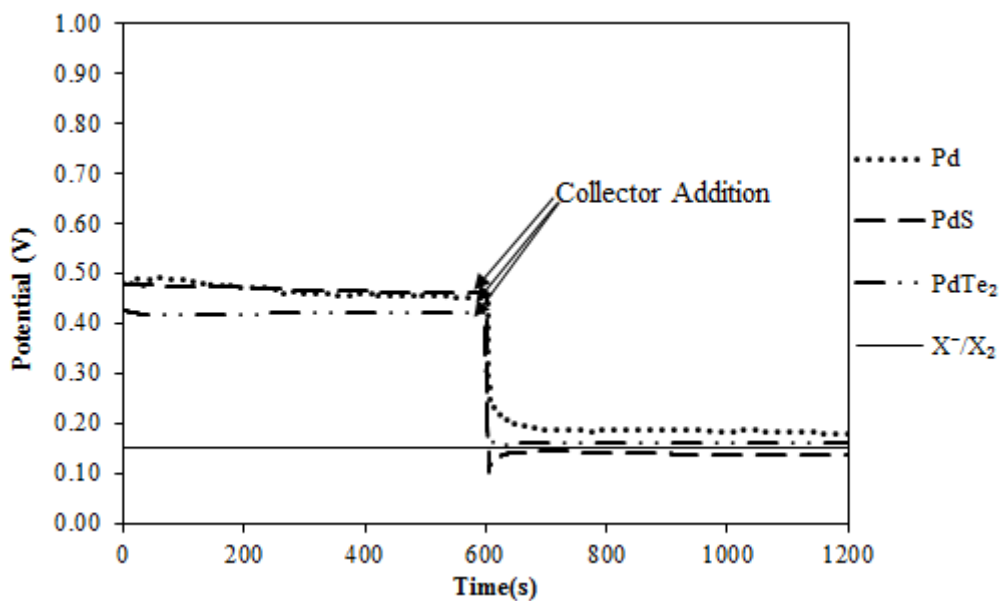


Figure 4.11. Mixed potential of palladium minerals at pH 4.2 in the presence and absence of SEX

4.2.3.5 Rest Potential of Pd Minerals Polarised at Anodic and Cathodic Potentials

In a manner similar to the case of the Pt minerals (cf. Figure 4.7 and 4.8) PdS and PdTe₂ were polarised at ± 0.4 V and ± 0.6 V prior to measurement of resulting rest potentials. The rest potentials for PdTe₂ are shown in Figure 4.12.

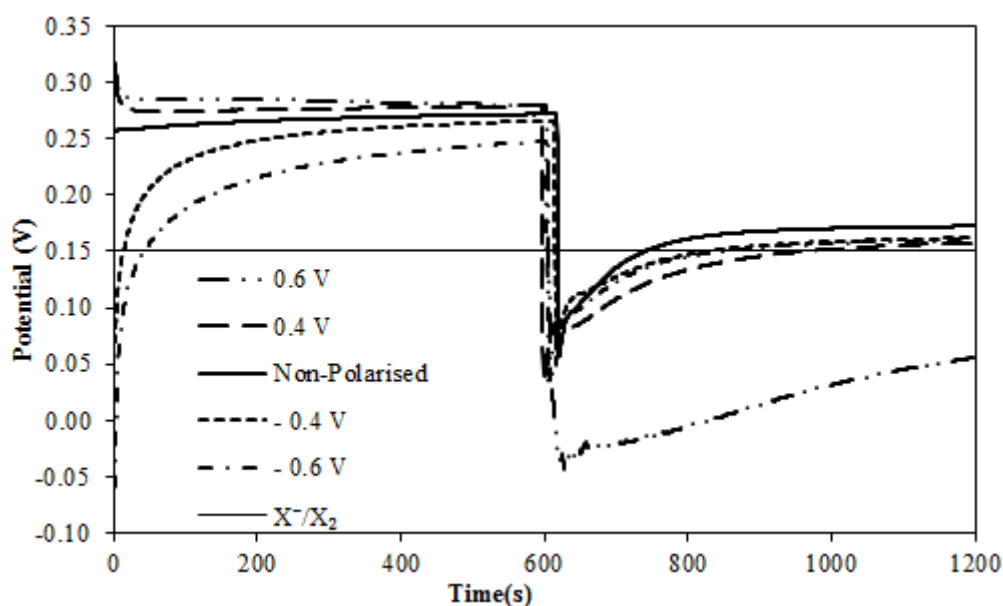


Figure 4.12. Rest potential results for PdTe₂ under different anodising conditions at pH 9.2 and with SEX collector addition after 600 s

The polarised mineral surface produced the same rest potential values after polarisation at potentials of 0.6 V, 0.4 V and -0.4 V prior and subsequent to collector addition. Subsequent to collector addition the final rest potential was above that of the dixanthogen formation potential for all conditions whilst after polarisation of the mineral at 0.6 V the final rest potential was significantly below this potential indicating the effect of oxidising conditions above a potential of 0.6 V.

In Figure 4.13 the results for the effect of polarisation for PdS are shown. Rest potentials of the mineral polarised at -0.6 V and ± 0.4 V were within the same potential range prior to collector addition whilst that for the mineral polarised at 0.6 V had a significantly more anodic rest potential. Subsequent to collector addition the mineral had a rest potential below the dixanthogen equilibrium potentials under all polarisation conditions. The order of decreasing rest potential can be observed to be 0.4 V, 0.6 V, -0.4 V, non-polarised and -0.6 V.

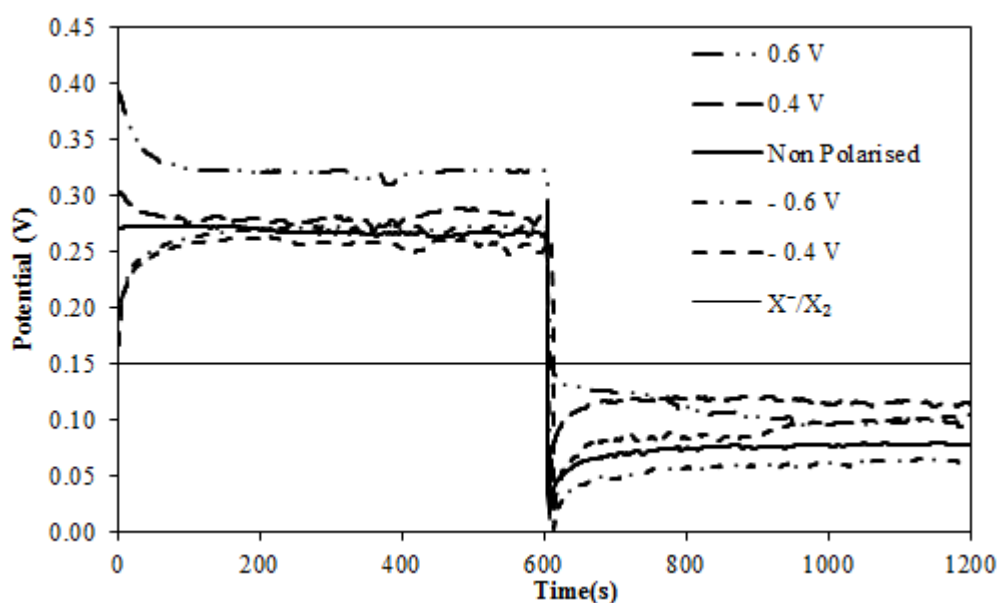


Figure 4.13. Rest potential results for PdS under different anodising conditions at pH 9.2 and with SEX collector addition after 600 s

4.2.4 Rest Potentials of Platinum Group Minerals in DTP

4.2.4.1 Rest Potentials of Pt Minerals

Rest potentials of the Pt Minerals were measured under acidic and alkaline conditions with DTP addition after 600 s. The equilibrium potential for the formation of a DTP dimer is shown as a solid straight line at 0.388 V in all the figures. At pH 9.2 Figure 4.14 shows the rest potentials of the three minerals Pt, PtTe₂ and PtS. This Figure shows Pt to have had the only rest potential above the equilibrium line for DTP before collector addition and after collector addition the resulting rest potential was slightly lower than the rest potential for the DTP dimer formation, viz. 0.388 V. PtS and PtTe₂ rest

potentials before and after collector addition were well below 0.388 V, viz. approximately 0.128 V and 0.188 V respectively. Changes in rest potentials for PtTe₂ and PtS were observed after collector addition and they were of lower magnitude compared to those observed for these minerals after SEX addition (Figure 4.5).

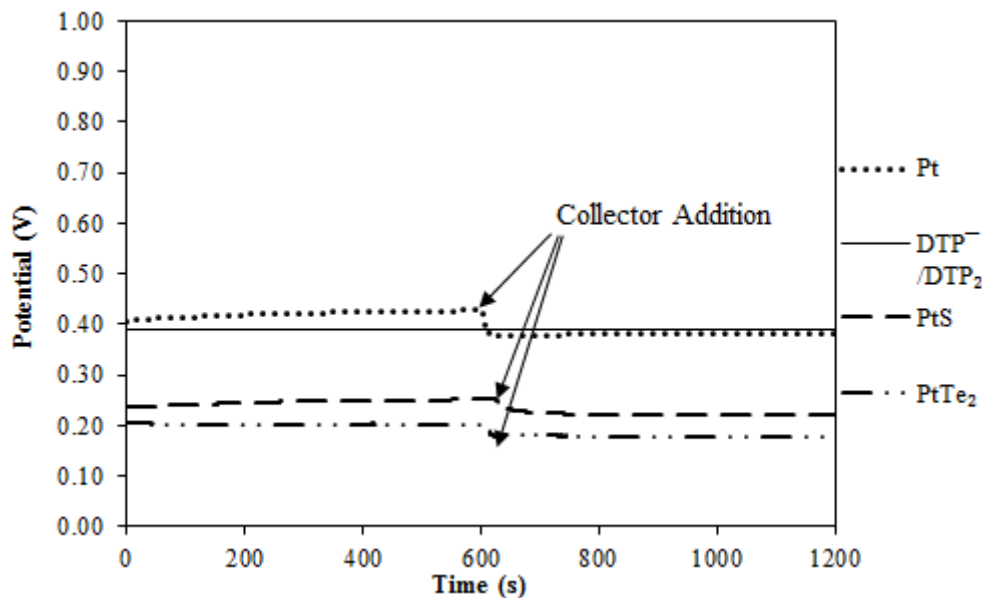


Figure 4.14. Rest potential of platinum minerals at pH 9.2 in the presence and absence of diethyl dithiophosphate

Under acidic conditions (Figure 4.15), the rest potentials measured were significantly higher than those observed for the minerals at alkaline conditions. Prior to collector addition the rest potential of PtTe₂ was equivalent to the equilibrium potential for the formation of a DTP dimer. Pt and PtS however had higher rest potential values. Following collector addition PtS and PtTe₂ had resulting rest potentials lower than 0.388 V whilst the rest potential of Pt metal was significantly above this potential.

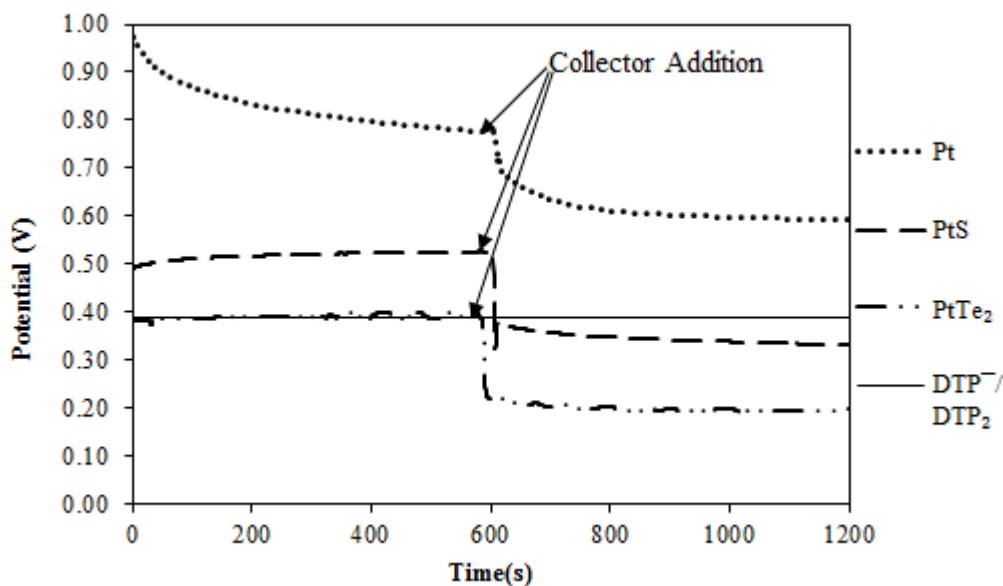


Figure 4.15. Rest potential of platinum minerals at pH 4.2 in the presence and absence of diethyl dithiophosphate.

4.2.4.2 Rest Potentials of Pd Minerals

The rest potentials of the Pd minerals, viz. Pd metal, PdTe₂ and PdS, were also measured under alkaline and acidic conditions. Results at pH 9.2 are presented in Figure 4.16. The equilibrium potential for formation of the dimer is 0.388 V and is indicated as a solid line on the figure. It was observed that Pd metal had a rest potential prior to collector addition that was above the equilibrium potential for dimer formation of DTP whilst the sulphide and the telluride minerals had rest potentials below this potential prior to collector addition. Subsequent collector addition resulted in rest potentials that were below the dimer equilibrium potential for DTP, for all the minerals.

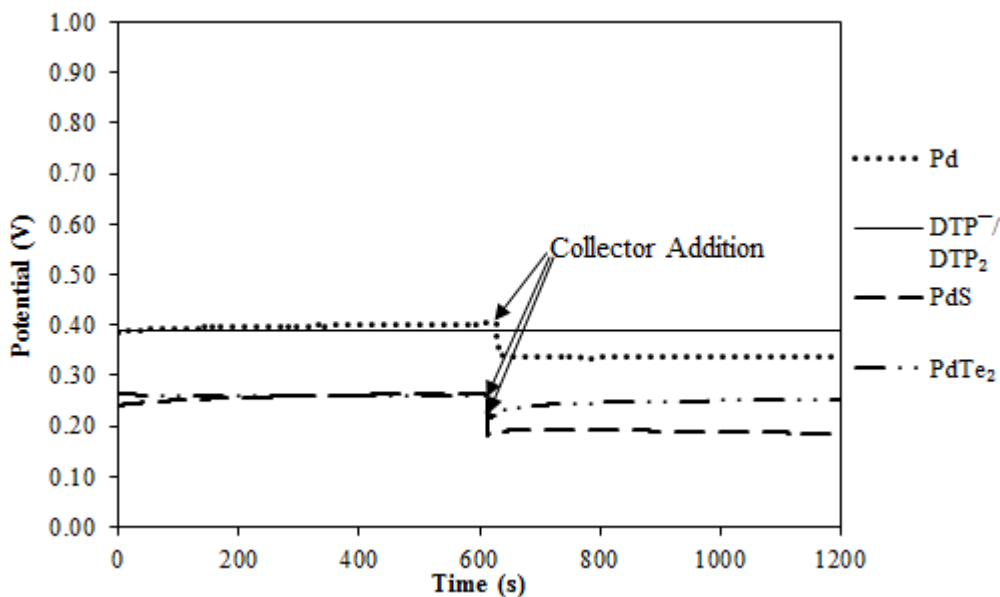


Figure 4.16. Mixed potential of palladium minerals at pH 9.2 in the presence and absence of diethyl dithiophosphate.

At pH 4.2 (Figure 4.17) all the Pd minerals exhibited rest potentials that were positive with respect to the dimerization potential of DTP prior to collector addition. From the point of collector addition all the minerals decreased in rest potential. Pd had a rest potential in the presence of DTP that was just above the dimerization potential of DTP, whilst those of PdTe₂ and PdS were below this potential. The change in potential for these minerals upon collector addition was found to be greater in magnitude than that observed at pH 9.2.

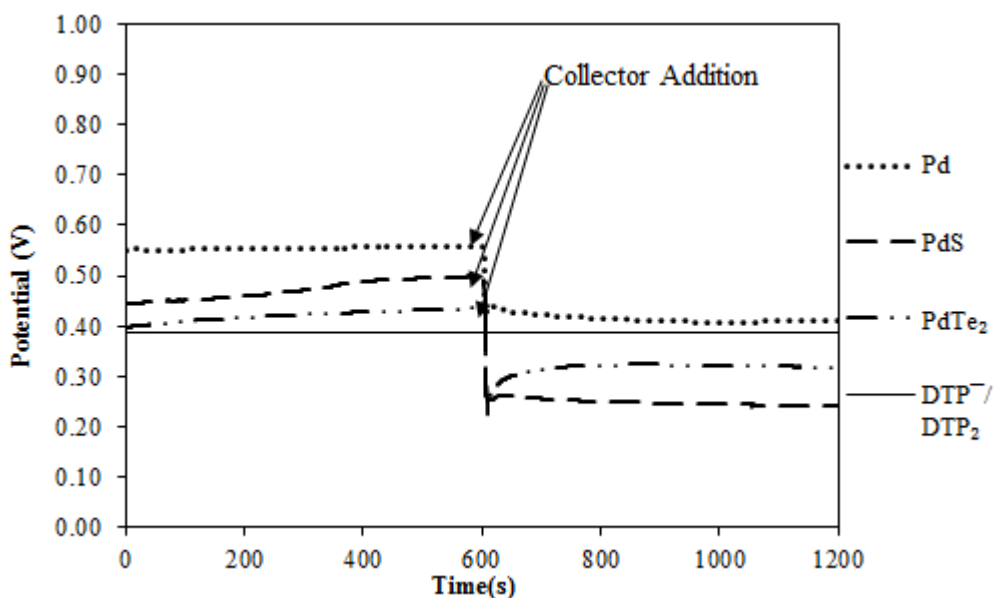


Figure 4.17. Mixed potential of palladium minerals at pH 4.2 in the presence and absence of diethyl dithiophosphate.

4.2.5 Rest Potentials of platinum minerals in MTP and DTPI

MTP and DTPI were also studied and rest potentials were determined for only the Pt minerals. Collector concentration was maintained as 6.24×10^{-4} M and the pH level was maintained at pH 9.2.

4.2.5.1 Rest Potentials of Pt Minerals in MTP and DTPI

Monothiophosphates belong to the phosphate group of thiol collectors. This collector was studied so as to be able to make a comparison with widely used dithiophosphate (DTP). Results shown in Figure 4.18 for the Pt minerals are presented with the equilibrium potential at which the dimer of MTP forms shown as a solid line. It can be seen that before and after collector addition, the rest potentials of all the minerals were significantly more negative with respect to this equilibrium potential. After collector addition it was observed that the changes in potential due to collector addition were not relatively very large and are lower in magnitude than those observed in the case of DTP.

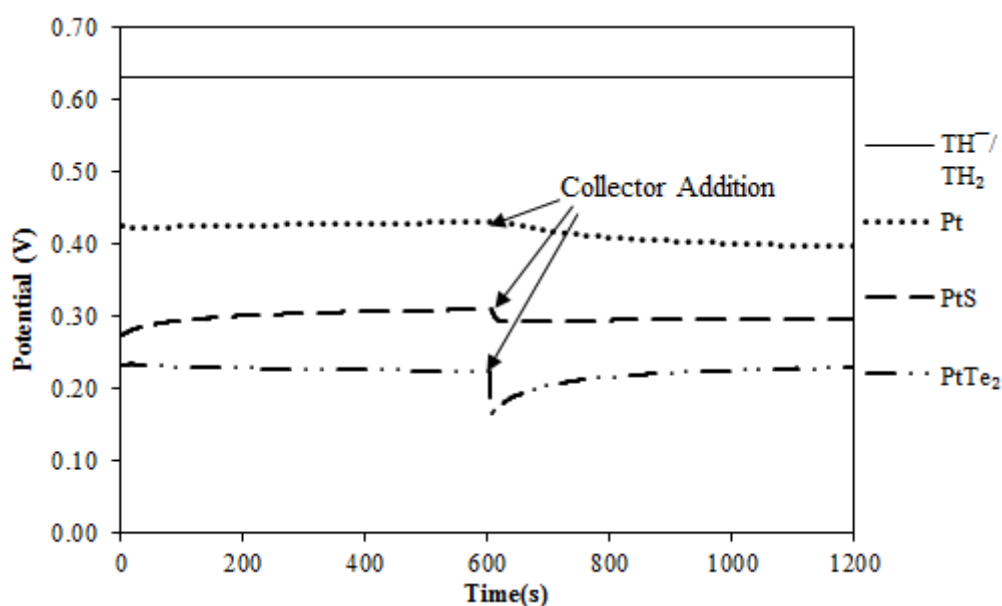


Figure 4.18. Mixed potential of platinum minerals at pH 9.2 in the presence and absence of monothiophosphate.

In Figure 4.19 the rest potentials of the Pt minerals are shown with sodium dithiophosphate DTPI at pH 9.2. The measured equilibrium potential for dimer formation of DTPI is shown on the graph as a solid line and this is significantly more positive than MTP and DTP. The rest potentials measured for the minerals prior to collector addition were all less positive than the dimerization potential as was the case for DTP and MTP. Once collector was added at 600s there was no change in the rest potential of pure Pt. PtTe₂ and PtS however showed changes in rest potential and these changes were observed to be relatively larger in magnitude than those observed after MTP addition.

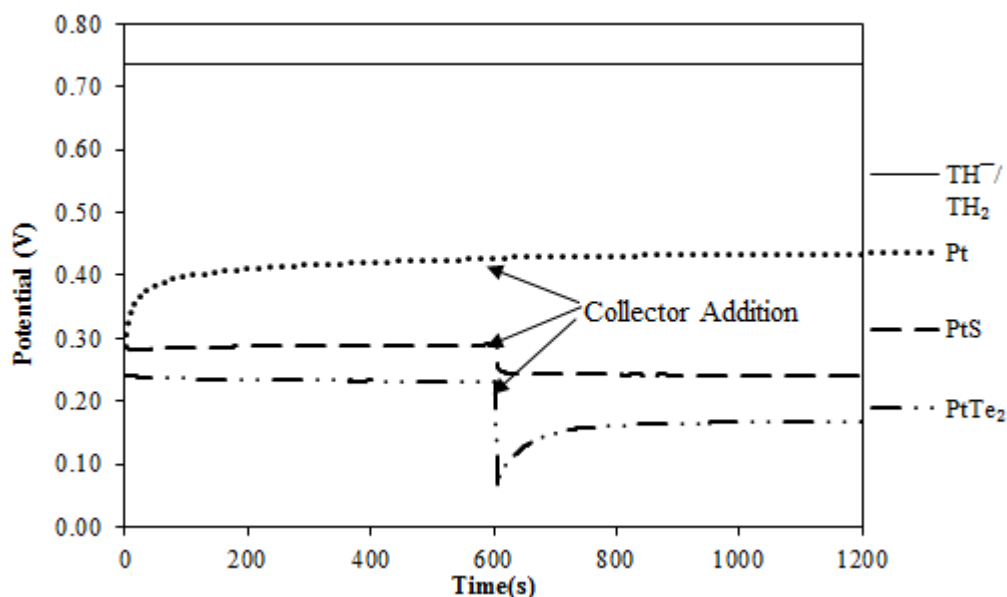


Figure 4.19. Mixed potential of platinum minerals at pH 9.2 in the presence and absence of diethyl dithiophosphate.

A comparison of Figure 4.14, Figure 4.18, Figure 4.19 indicates that the significant differences between the Pt minerals with changing phosphate collector are observed for Pt metal alone. Rest potentials for PtS and PtTe₂ do not change significantly and therefore no cyclic voltammetry measurements were made for DTPI and MTP. Due to the oxidising potential of both DTPI and MTP being so high it was not expected that Pd minerals will differ greatly from Pt minerals and were therefore not investigated.

4.3 Cyclic Voltammetry Study of Platinum Group Minerals with Thiol Collectors

As explained in Section 3.5.3 voltammetry methods employ a linear change in potential with time. The technique was used to attempt to identify and/or propose the mechanisms by which species react at the surfaces of electrodes. These results complement the results observed when rest potential measurements were made. In the context of this work, thiol collectors and activators in solution interacting with the surfaces of the platinum group minerals studied. Various conditions have been studied in order to form a basis for the determination of the reactions occurring due to chemical species in solution at the mineral surface and these are;

- Sweep rate
- Switching potential (cycling potential limits)
- Varying pH
- Varying collector concentration
- Dissolved oxygen concentration
- Number of cycles

Cyclic voltammograms were measured in forward going (increasing positive potential) and negative going (decreasing potential) directions. Sodium ethyl xanthate (SEX) was used in this study as a basis for the study of reactions of thiol collectors with PGMs. DTP which is a commonly used co-collector was also studied in order to establish its interactions with PGM surfaces. All the conditions were applied to PtTe₂ and PtS and as a result of the results obtained in these experiments, it was decided that only switching potential and number of cycles were varied in the case of Pt, Pd, PdTe₂ and PdS.

4.3.1 Validation of Cyclic Voltammetry Experiments – Galena and Pyrite Measurements

In order to validate that the technique employed for measurement of voltammograms was giving results similar to those previously reported in the literature, the technique was applied to the measurement of galena (PbS) and the resulting voltammograms were compared to those reported by Woods, (1971). The results from the present study are shown in Figure 4.20. Voltammograms for galena were measured in the absence and presence of collector in an aerated solution. Solution conditions used were the same as those used by Woods, (1971) and therefore the buffer used was of 0.1 M Na₂B₄O₇, concentration which is not the concentration generally used in this study.

At sweep rates of 10 mV/s (Figure 4.20(a)) and 40 mV/s (Figure 4.20(b)) the voltammograms generated produced similar current profiles. It is expected and was observed that the currents measured at 10 mV/s were lower in magnitude than those at 40 mV/s. A current peak was observed on both Figure 4.20(a) and (b) in the potential range of -0.1 V and 0.1 V which was followed by an increase in current in the presence of SEX. A reduction current peak was also observed in the cathodic sweep. These features of the generated voltammograms for the mineral were similar to those for the voltammogram generated by Woods (1971) for galena and this validates the experimental procedures used in this study.

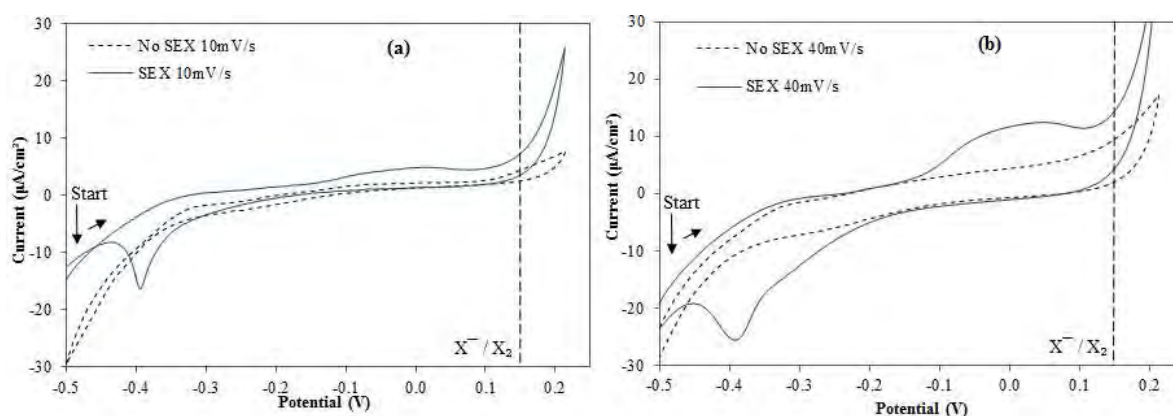


Figure 4.20. Cyclic voltammograms for galena (PbS) with forward starting sweeps measured for a single sweep in the absence and presence of collector, 1×10^{-2} M SEX in an aerated solution of 0.1 M Na₂B₄O₇ (a) 10 mV/s sweep rate and (b) 40 mV/s sweep rate. The oxidation potential for dixanthogen is indicated as a dotted line at 0.15 V.

4.3.2 Sodium Ethyl Xanthate Study

4.3.2.1 Cyclic Voltammetry Measurements of Pt

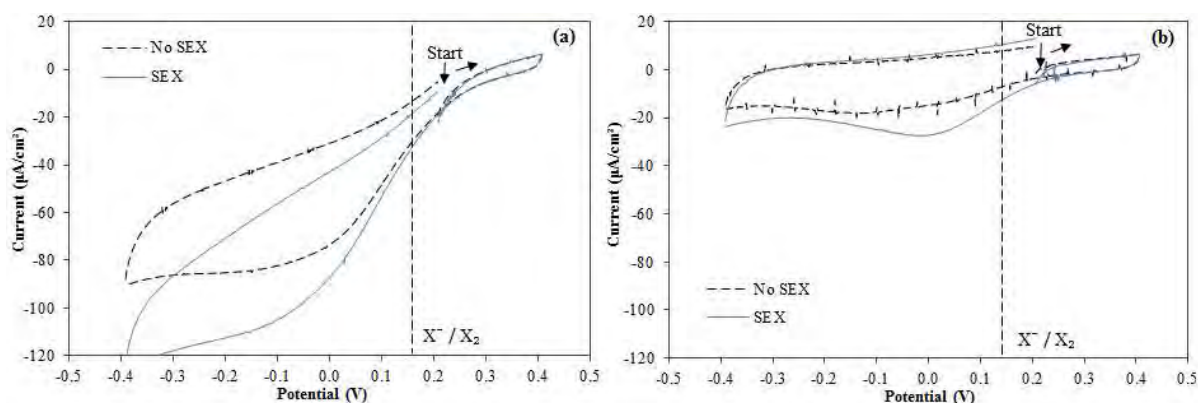


Figure 4.21. Cyclic voltammograms for Pt with forward starting sweeps measured for two sweeps in the absence and presence of collector, 6×10^{-4} M SEX (a) aerated solution conditions and (b) nitrogen saturated solution conditions. The oxidation potential for dixanthogen is indicated as a dotted line at 0.15 V.

Figure 4.21 shows the cyclic voltammograms for Pt metal over a potential range of ± 0.4 V under aerated and de-aerated solution conditions. Figure 4.21(a), which is the voltammogram for Pt metal measured in aerated solution (D.O levels cf. 3.5.3) shows that the anodic currents generated on the metal in the presence and absence of collector were almost identical. However the reduction currents generated differed with respect to the effect of collector addition. In the absence of collector a reduction current commenced from 0.2 V and reached a limiting current of approximately $-90 \mu\text{A}/\text{cm}^2$. In the presence of collector a similar reduction current commencing from 0.2 V results in more negative reduction currents reaching values around $-120 \mu\text{A}/\text{cm}^2$ was observed.

Anodic currents in a nitrogen purged solution (Figure 4.21(b)) also resulted in the metal producing identical anodic currents in the presence and absence of collector. Differences were observed in the reduction currents. A reduction current peak was observed to occur in the absence of collector over a potential range of 0.2 V and -0.4 V, whilst a similar current peak was observed in the presence of collector over a potential range of 0.2 V and -0.3 V. The difference between the reduction currents generated in the presence of collector however was that more negative current densities (minimum $-30 \mu\text{A}/\text{cm}^2$) were observed than those in the absence of collector (minimum $-20 \mu\text{A}/\text{cm}^2$).

The effect of aeration vs de-aeration was observed through the presence of more prominent reduction currents under aerated conditions than in nitrogen purged solution conditions. It will be later discussed in Chapter 5 that these reduction currents are a result of the reduction of oxygen.

4.3.2.2 Cyclic Voltammetry Measurements of PtTe₂

4.3.2.2.1 Cyclic voltammetry measurements over a potential range of ± 0.6 V

Voltammograms for PtTe₂ in the absence and presence of SEX at a sweep rate of 10 mV/s under aerated and de-aerated solution conditions are shown in Figure 4.22 (a) and (b) respectively. Two cycles were measured for the mineral in forward going sweeps.

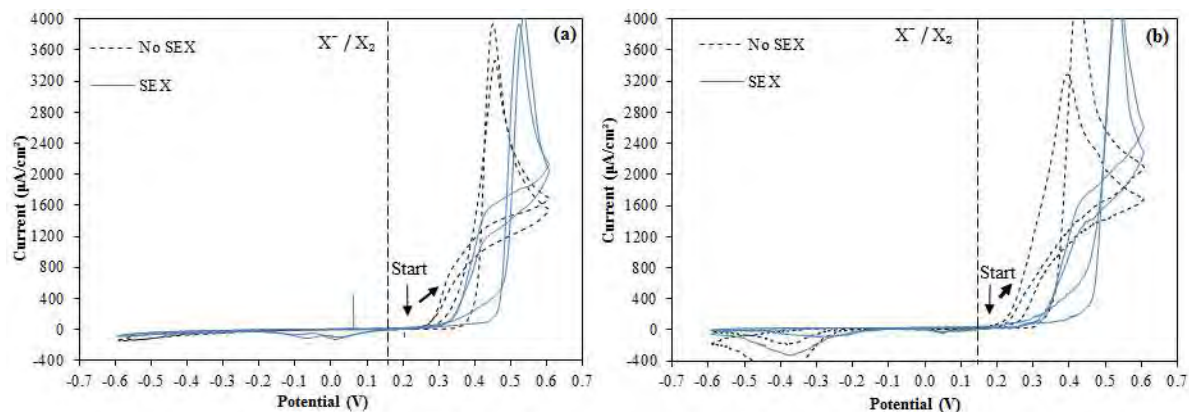


Figure 4.22. Cyclic voltammograms for PtTe₂ with forward starting sweeps measured for two sweeps in the absence and presence of collector, 6.24×10^{-4} M SEX (a) aerated solution conditions and (b) nitrogen saturated solution conditions. The oxidation potential for dixanthogen is indicated as a dotted line at 0.15 V.

In the absence of collector in aerated solution (Figure 4.22(a)) a sharp anodic current peak occurred at a potential of 0.4 V whilst in the reverse cathodic sweep, the current dissipated gradually approaching 0 $\mu\text{A}/\text{cm}^2$ at a potential of ≈ 0.25 V which was notably more negative than the potential on which the anodic current commenced. A second cycle measured in the absence of collector resulted in a similar profile to that of the first cycle.

Under de-aerated solution conditions (Figure 4.22(b)) the current profiles for PtTe₂ follow the same trend as observed in Figure 4.22(a) for aerated solution conditions. However both in the presence and absence of collector two reduction peaks, one in each cycle, were observed from a potential of -0.25 V. It is observed that the first cycle generated a larger peak current than the second cycle.

In the presence of collector a sharp anodic current similar to that observed in the absence of collector occurred from a potential of 0.5 V. This anodic current dissipated on the cathodic sweep to reach a current of 0 $\mu\text{A}/\text{cm}^2$ at a potential of 0.3 V. On a second cycle the anodic current generated both under aerated and de-aerated solution conditions was observed to commence from a potential of 0.3 V and increasing into a peak at 0.5 V. Two reduction current peaks were observed on both voltammograms from cathodic sweeps. Under aerated conditions these two peaks occurred between 0.1 V and -0.2 V whilst under de-aerated conditions these peaks occurred between 0.1 V and 0 V although they are very small in magnitude compared to the reduction peak commencing from 0.4 V.

4.3.2.2.2 Cyclic voltammetry measurements over a potential range of ± 0.4 V

Based on the results observed for switching potential of ± 0.6 V a narrower potential range of ± 0.4 V was chosen. Voltammetry measurements were made in aerated and de-aerated solution conditions with forward and reverse going sweeps being measured. Measurements under de-aerated conditions were found to produce similar voltammograms to those under aerated conditions for PtTe₂ and are therefore not shown in this chapter but are shown in Appendix B.

At a sweep rate of 10 mV/s Figure 4.23 shows the voltammograms in the presence and absence of collector for PtTe₂ measured for two reverse going sweeps. A reduction current commenced from a potential of -0.1 V in the absence of collector, with no visible peaks on this first cycle. The subsequent anodic sweep resulted in a sharp anodic current that commenced at 0.3 V and reaching a maximum value at 0.4 V. Following from this, the second cycle for the mineral did not show any changes in the current profile from the first cycle in both anodic and cathodic sweeps.

In the presence of collector the reduction current followed the same current potential profile as that of the mineral in the absence of collector up to 0 V when an anodic current commenced. This anodic current increased gradually until rising sharply from 0.2 V up to 0.4 V. Two reduction peaks were observed in the ensuing sweep between 0.25 V and 0 V which have been labelled P1 and P2 on the voltammogram. The first reduction peak potential occurred at a potential positive to the reversible potential for SEX to X₂ whilst the second peak potential occurs at a potential negative to the reversible potential for SEX to X₂. No further reduction peaks were observed on the cathodic sweep.

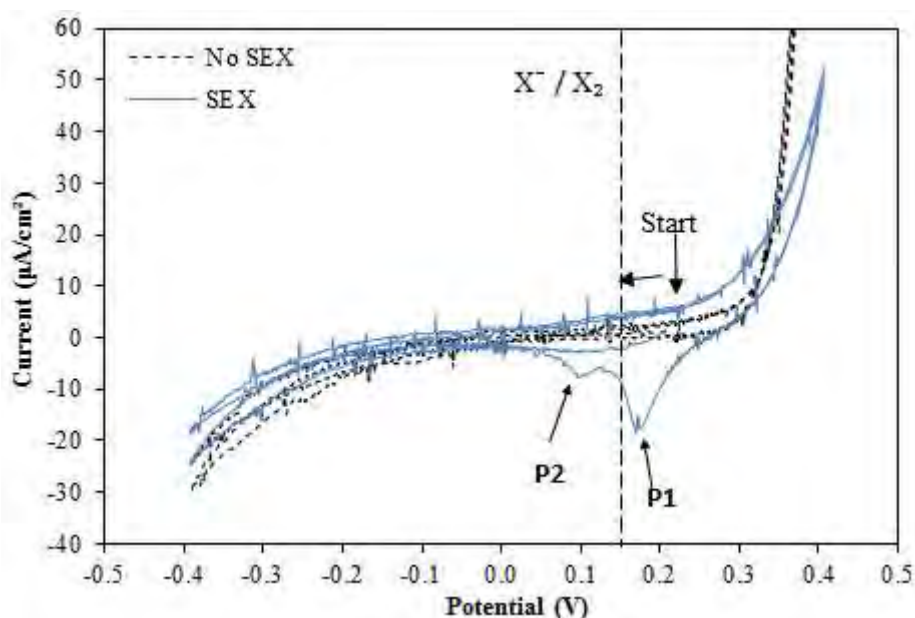


Figure 4.23. Cyclic voltammograms for PtTe₂ with a reverse starting sweep measured for two sweeps in the absence and presence of SEX, 6.24×10^{-4} M, in an aerated solution. The oxidation potential for dixanthogen is indicated as a dotted line at 0.15 V.

In Figure 4.24 shows that under aerated solution conditions at a sweep rate of 10 mV/s a single forward going sweep is observed in the absence and presence of SEX. From the starting potential of ≈ 0.207 V in the presence of collector an anodic current reached a maximum current of $\approx 80 \mu\text{A}/\text{cm}^2$. The cathodic sweep then yielded two reduction current peaks, labelled P1 and P2, in the potential region between 0.3 V and 0.1 V. Peak P1 was observed to be positive with respect to the reversible potential for the formation of X_2 whilst P2 was negative with respect to the reversible potential. Alternatively, in the absence of collector, the voltammogram shows a sharp peak current at a potential of 0.35 V and a reduction current in the region of the switching potential without evidence of reduction peaks. Comparing peaks P1 and P2 in Figure 4.23 and Figure 4.24 shows that P1 and P2 in Figure 4.24 are of similar magnitude in current whilst those in Figure 4.23 are not and P1 is larger in magnitude of current than P2.

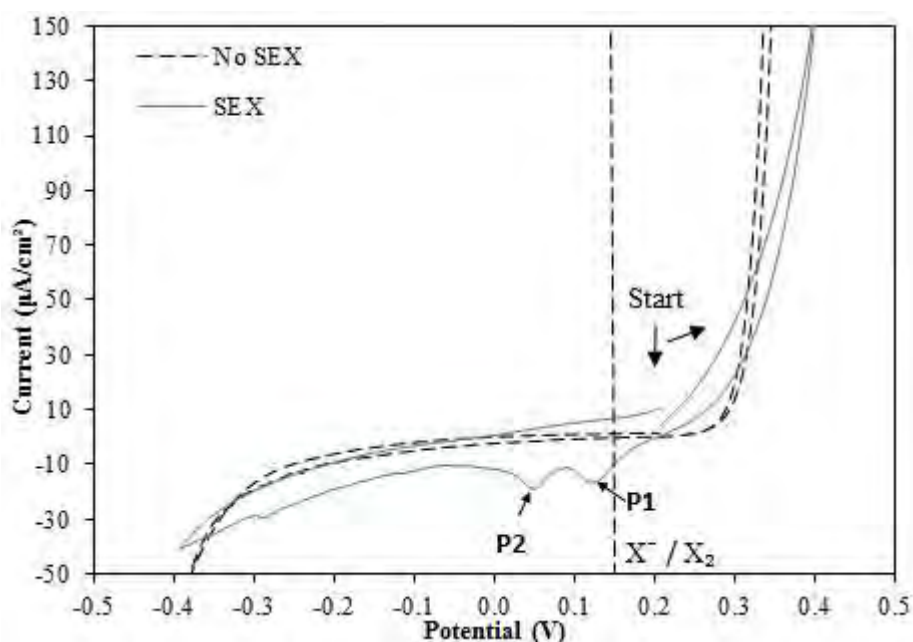


Figure 4.24. Cyclic voltammograms for PtTe_2 with a forward starting sweep measured for one sweep in the absence and presence of 6.24×10^{-4} M SEX, in an aerated solution. The oxidation potential for dixanthogen is indicated as a dotted line at 0.15 V.

4.3.2.2.3 Linear sweep voltammograms after polarisation of mineral

A study was conducted to further investigate the nature of Peaks P1 and P2 identified in Figure 4.23 and Figure 4.24 using linear sweep voltammetry. PtTe_2 was polarised at an anodic potential of 0.207 V for 15 minutes before a reverse linear sweep voltammogram (Figure 4.25(b)) was measured. A forward linear sweep voltammogram to a potential limit of 0.207 V was also measured before another reverse sweep (Figure 4.25(a)). In Figure 4.25 (a) the cathodic linear sweep produced two reduction current peaks labelled P1 and P2 that are separated by the dixanthogen reduction potential. P1 was less

distinct than P2. Figure 4.25(b) also shows two reduction currents P1 and P2 both of which are more distinct than in Figure 4.25(a).

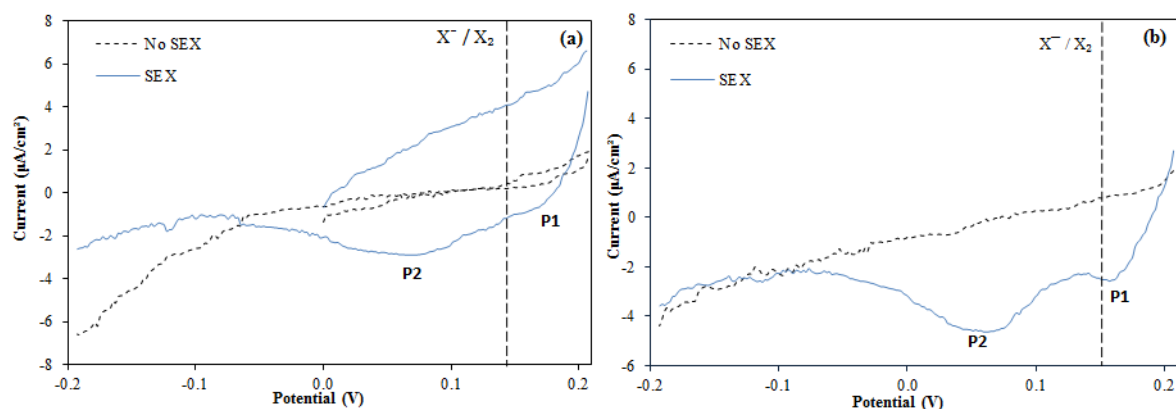


Figure 4.25. Linear sweep voltammograms in the presence and absence of 6.24×10^{-4} M SEX collector in aerated solution (a) oxidation sweep and subsequent reduction sweep (b) reduction sweeps generated after applying an anodic potential of 0.207 V for 15 minutes.

4.3.2.2.4 Investigation of the Effect of pH

The effect of pH was investigated for three other levels viz. pH 11.2, 7.0 and 5.2. These results are shown along with the results for pH 9.2 in the presence and absence of collector in Figure 4.26. In the absence of collector an anodic current was observed to occur towards the switching potential of 0.4 V. This current rose with increasing pH. Cathodic sweeps on the other hand at all pH levels did not generate any reduction current peaks.

Figure 4.26 shows that voltammograms generated for PtTe₂ at pH 5.2 and pH 7.0 had similar current potential profiles. An anodic current occurred for these minerals in the presence of collector that commenced at the starting potential (0.207 V). A single reduction current peak between 0.2 V and -0.1 V was generated following this anodic peak. PtTe₂ at pH 9.2 has already been discussed and for this mineral at pH 11.2 a sharp anodic current was observed to occur at positive potentials resulting in the highest current density observed for all pH levels 667 $\mu\text{A}/\text{cm}^2$. In the reverse cathodic sweep a single reduction current peak was observed between the potentials of 0 V and 0.05 V.

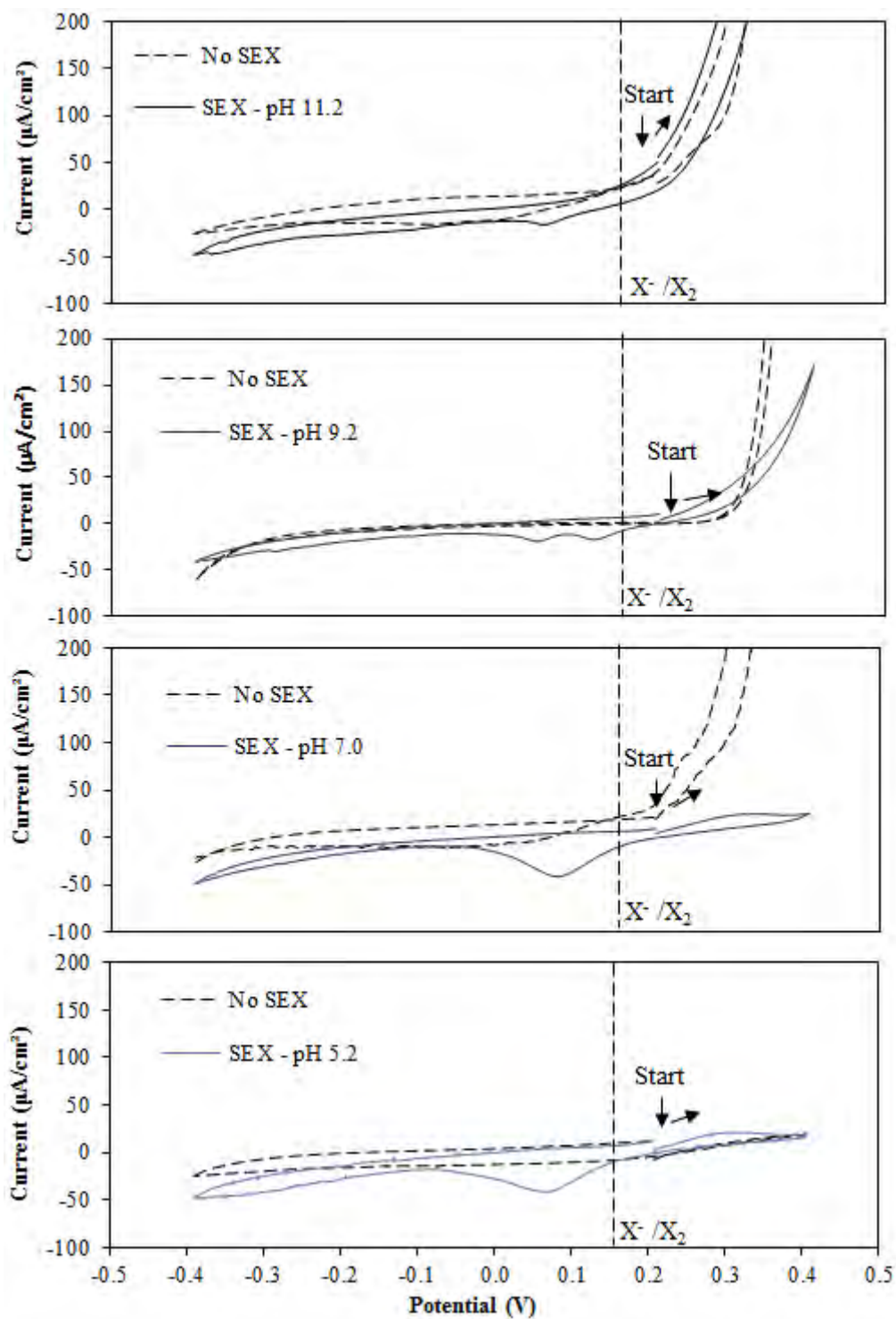


Figure 4.26. Cyclic voltammogram for PtTe₂ with forward starting sweeps in the absence and presence of 6.24×10^{-4} M SEX measured in aerated solution conditions. Voltammograms presented for varying pH conditions, pH 5.2, pH 7, pH 9.2 and pH 11.2 (starting potential of 0.207 V).

4.3.2.2.5 Investigation of the Effect of Concentration

As previously mentioned, collector concentration of 6×10^{-4} M was used as the concentration for most experiments. An investigation was conducted to determine the effect of concentration on the voltammograms for PtTe₂. The concentrations used were 2.5×10^{-3} M and 2.5×10^{-2} M.

Figure 4.27(a) shows the voltammograms for PtTe₂ in aerated solution in the presence of collector for two forward going cycles at a concentration of 2.5×10^{-4} M. An anodic current was observed to increase as the switching potential of 0.4 V was reached. Three reduction current peaks resulted during the reduction sweep at potentials of 0 V, -0.18 V and -0.25 V. A second anodic sweep yielded a current profile that differed from that generated in the first cycle. An anodic current commenced at 0 V and increased to develop into an anodic current peak at 0.25 V. The second cathodic sweep yielded the same reduction currents as were observed in the first cycle although the generated currents were lower in magnitude.

Figure 4.27(b) shows the voltammogram for PtTe₂ in a single forward going sweep at an SEX concentration of 2.5×10^{-3} M SEX. An anodic current peak was generated which occurred at a potential of 0.3 V. The following reduction current produced a reduction current from 0.1 V and formed a peak between 0 V and -0.1 V.

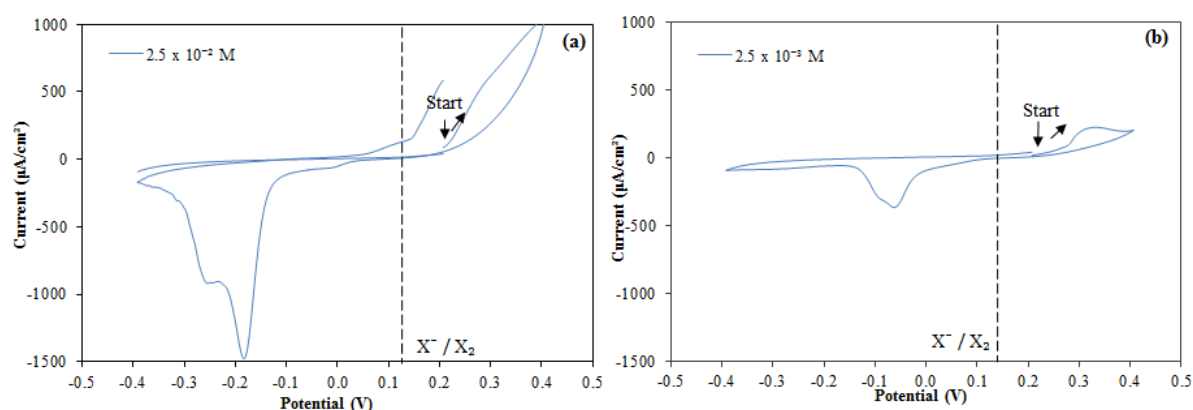


Figure 4.27. Cyclic voltammograms for PtTe₂ in forward starting sweeps in the presence of (a) 2.5×10^{-2} M SEX measured for two sweeps and (b) 2.5×10^{-3} M SEX measured for a single sweep in aerated solution. The oxidation potential for dixanthogen is indicated as a dotted line at 0.15 V.

4.3.2.2.6 Investigation of the Effect of Sweep Rate

In this study 10 mV/s was used as the base case sweep-rate for cyclic voltammetry measurements. An upper limit sweep-rate of 50 mV/s was also measured to investigate the effect of sweep-rate as well as a lower limit sweep-rate of 1 mV/s. The results are shown in Figure 4.28 for the three sweep-rates investigated. The highest anodic current was generated at 50 mV/s without showing any evidence of the peaks observed at 10mV/s. The figure also shows voltammograms obtained at sweep rates of 10

mV/s and 1 mV/s. Two reduction currents were observed to occur in all instances. At 50 mV/s the reduction current at 0.08 V was larger in magnitude than the second peak occurring at a potential of 0 V. A 10 mV/s sweep rate has already been discussed for Figure 4.24 where two reduction peaks of similar magnitude are identified. At a sweep rate of 1 mV/s the reduction current peaks were the lowest in magnitude and were observed to be less distinguished in shape than those for the higher sweep rates.

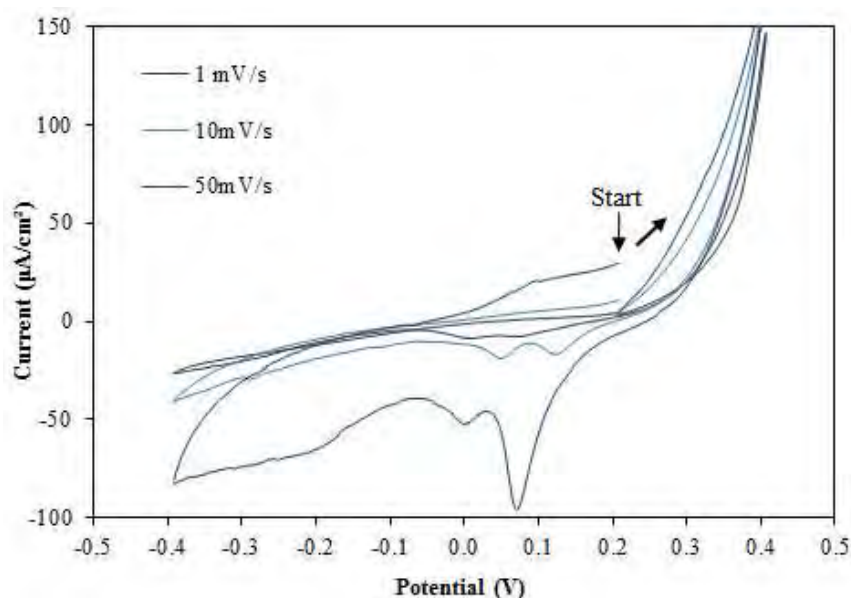


Figure 4.28. Cyclic voltammograms for PtTe₂ in a forward started sweep for a single sweep in the presence of 6.24×10^{-4} M SEX measured in an aerated solution. Voltammograms measured at sweep-rates of 1 mV/s, 10 mV/s and 50 mV/s.

4.3.2.3 Cyclic Voltammetry Measurements of PtS

The following section of results are for potential sweep measurements made on PtS. Similar measurements as those made for PtTe₂ were made in order to establish a basis of comparison between the two minerals.

4.3.2.3.1 Cyclic voltammetry measurements over a potential range of ± 0.6 V

Voltammograms for PtS under aerated and de-aerated solution conditions in the absence and presence of SEX at a sweep rate of 10 mV/s and potential range of ± 0.6 V are shown in Figure 4.29 (a) and (b). Two cycles were measured in each figure for forward going sweeps. In the absence of collector under aerated conditions (Figure 4.29(a)) an anodic current produced a peak at a potential of 0.5 V, which was not repeated in the second sweep. Reduction currents measured for both sweeps were similar in profile, commencing from a potential of 0.15 V and reaching a steady reduction current from a potential of -0.2 V to -0.6 V. Although in the presence of collector there were no anodic current peaks, a current increase

was measured at positive potentials which did not vary for the two sweeps measured. Reduction currents in the presence of collector were observed to occur from less negative potentials than those in the absence of collector (-0.1 V).

Under de-aerated solution conditions and in the absence of collector (Figure 4.29(b)) an anodic current was generated resulting in two peaks occurring in the initial sweep between the potentials of 0.4 V and 0.5 V. In a similar manner to Figure 4.29(a) a second anodic sweep did not yield any peaks. Cathodic sweeps did not yield any current peaks although a reduction current was present.

In the presence of SEX for Figure 4.29(b) an anodic peak coinciding with that observed in the absence of collector occurred in the first sweep. Current densities however were higher in magnitude than those observed in the absence of collector. Although the peak was not repeated in a second anodic sweep the current remained larger in magnitude in the presence of collector than in its absence. No significant reduction peaks were observed for the cathodic sweeps following each of these anodic sweeps.

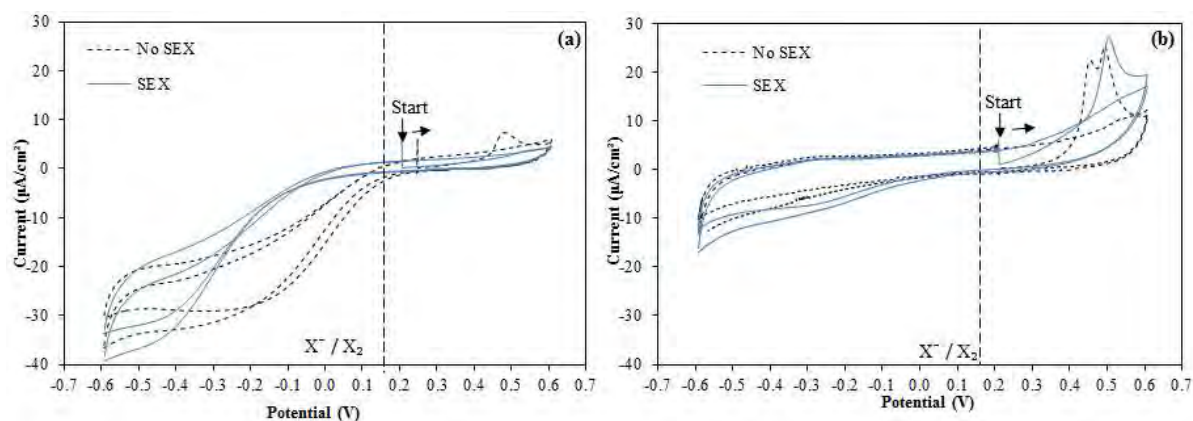


Figure 4.29. Cyclic voltammograms for PtS with a forward starting sweep measured for two sweeps in the absence and presence of collector, 6.24×10^{-4} M under aerated solution conditions. The oxidation potential for dixanthogen is indicated as a dotted line at 0.15 V.

4.3.2.3.2 Cyclic voltammetry measurements over a potential range of ± 0.4 V

A potential range of ± 0.4 V was applied to the cyclic voltammograms measured under aerated conditions for two reverse sweeps (Figure 4.30).

In the absence of collector, a reduction current occurred from a potential of 0.2 V. A steady current was reached similar to that in Figure 4.29(a) from a potential of ≈ -0.05 V to -0.4 V. At positive potentials an anodic current occurred from a potential of 0.2 V to 0.4 V. Both sweeps generated in the absence of collector exhibited the same current potential profile.

In the presence of collector PtS yielded reduction currents similar to those generated in the absence of collector. These reduction currents however commenced at potentials less positive than those occurring

in the absence of collector. The anodic currents generated were more positive than those in the absence of collector and commenced from a potential of 0 V.

In the presence of SEX anodic currents occurred for the two cycles which were higher in current than those generated in the absence of collector. Reduction currents generated were similar to those observed in the absence of collector, however the potential at which these currents commenced was 0.2 V less negative than those in the absence of collector at 0 V.

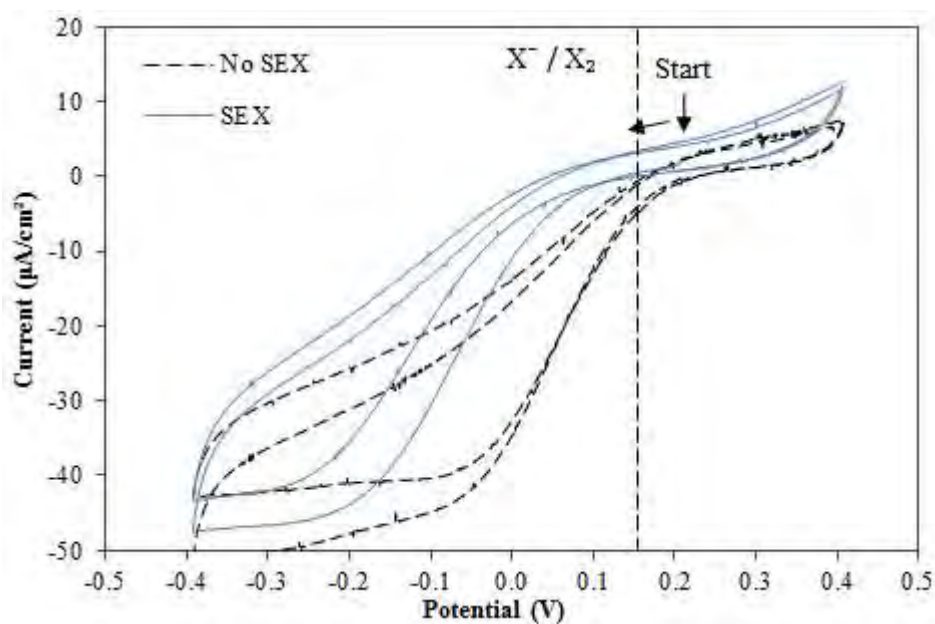


Figure 4.30. Cyclic voltammograms for PtS with a reverse starting sweep measured for two sweeps in the absence and presence of 6.24×10^{-4} M SEX, under aerated solution conditions. The oxidation potential for dixanthogen is indicated as a dotted line at 0.15 V.

Forward going single cycle voltammograms measured for PtS are shown in Figure 4.31 in the absence and presence of SEX. The potential range measured was ± 0.4 V. Although the cycles measured for PtS were forward going there was no significant difference between the voltammograms generated in Figure 4.31 and Figure 4.30. In the absence of collector the voltammogram generated for PtS showed a low anodic current followed by a reduction current starting from 0.2 V that reached a steady current at a potential of ≈ -0.05 V. In the presence of collector the anodic current generated at positive potentials achieved higher current densities than those in observed in the absence of collector as seen in Figure 4.30. The following reduction current generated on the cathodic sweep occurred at a potential less negative than that observed on the mineral in the absence of collector. This current also reached a steady current from a potential of ≈ 0.2 V to 0.4 V as was observed in Figure 4.30.

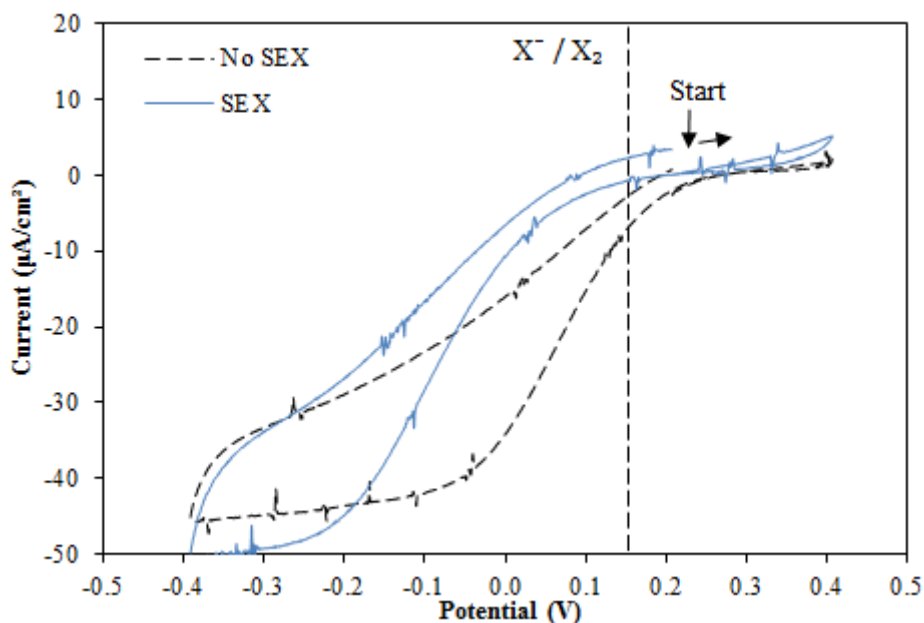


Figure 4.31. Cyclic voltammograms for PtS with a forward starting sweep measured for one sweep in the absence and presence of 6.24×10^{-4} M SEX, under aerated solution condition. The oxidation potential for dixanthogen is indicated as a dotted line at 0.15 V.

4.3.2.3.3 Investigation of the Effect of pH

The effect of pH on the interaction between PtS and SEX was investigated at pH 11.2, 9.2, 7.0, and 5.2. The results are shown in Figure 4.32 for aerated solution conditions, results for de-aerated solution conditions can be found in Appendix B. In the absence of collector the anodic current generated was low and almost insignificant, the reduction current generated however increases from a potential region of about 0.2 V. At pH 5.2 the current showed a reduction current from 0.3 V. This potential of commencement for this current became less negative with increasing pH values. In the presence of SEX the reduction current generated on the mineral was not affected by changes in pH and had the same profile. Anodic currents generated in the presence of collector were more anodic than those in the absence of collector. Additionally these currents became more positive with increasing pH values.

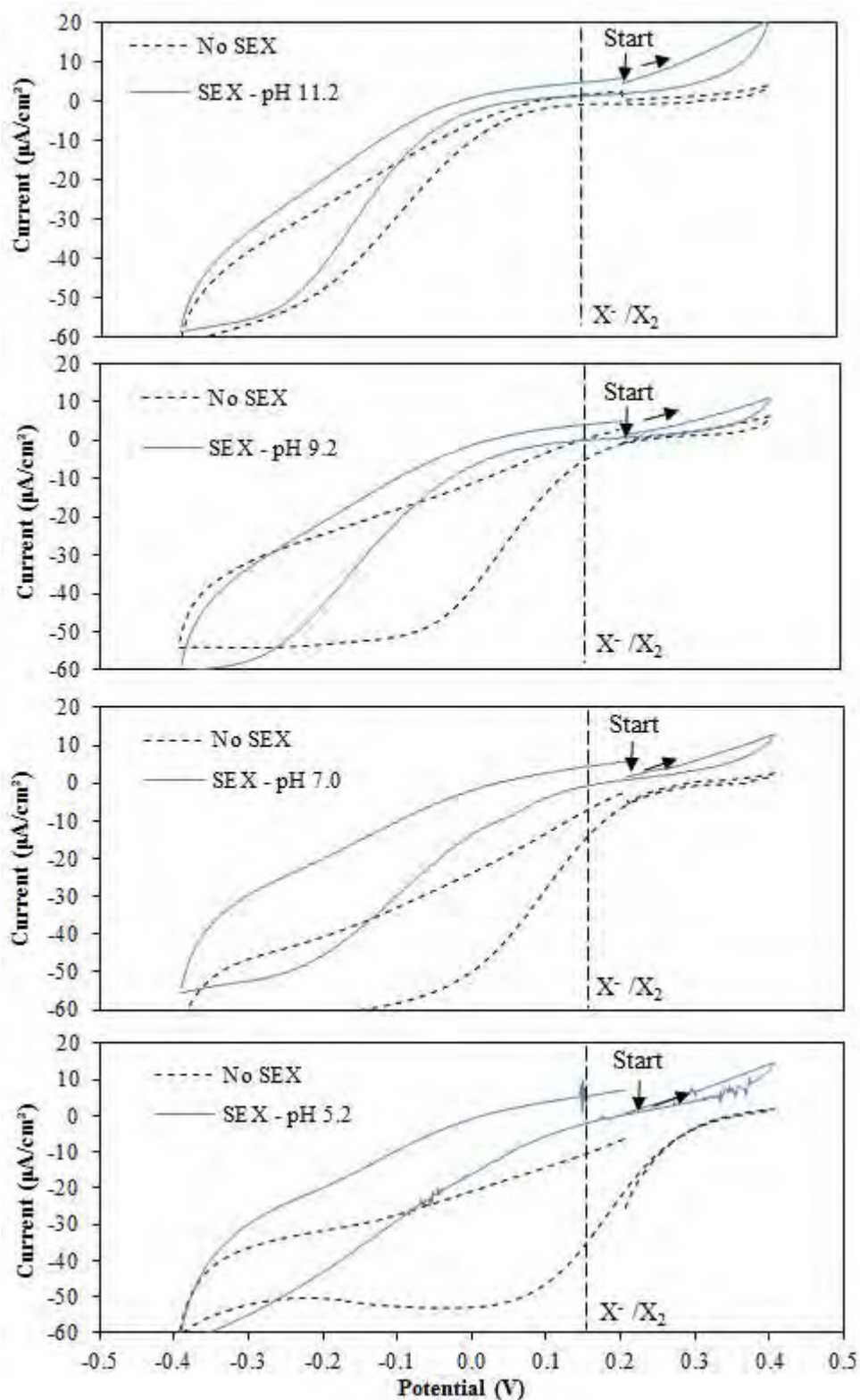


Figure 4.32. Cyclic voltammogram for PtS with forward starting sweeps in 6.24×10^{-4} M SEX in aerated solution. Voltammograms are shown for varying pH conditions, pH 5.2, pH 7, pH 9.2 and pH 11.2 and the potential for dixanthogen formation is indicated as a vertical dotted line at 0.15 V.

4.3.2.3.4 Investigation of the Effect of Concentration

Collector concentrations of 2.5×10^{-3} M and 2.5×10^{-2} M were used for PtS to compare voltammograms observed with that for PtS at a concentration of 6×10^{-4} M. Resulting voltammograms under aerated solution conditions are shown in Figure 4.33(a) and (b).

A voltammogram of PtS at a concentration of 2.5×10^{-2} M SEX is shown in Figure 4.33(a). Two forward cycles were measured from a potential of 0.207 V. In this figure the first anodic sweep yielded higher anodic current densities than the second anodic sweep. Reduction currents were also observed in the cathodic sweeps and commenced from a potential of -0.1 V to -0.4 V. These currents did not exhibit any peaks but were of the same magnitude in both sweeps.

Figure 4.33(b) shows the voltammogram for PtS measured in the presence of 2.5×10^{-3} M SEX for a single forward going cycle. An anodic current was generated which increased up to a potential of 0.4 V. This current had a lower current density than that for the mineral in a collector concentration of 2.5×10^{-3} M and higher in magnitude than that for the mineral at a concentration of 6.24×10^{-4} M. From 0.4 V a reduction current is generated in the cathodic sweep which commences from a potential of -0.1 V. The significant difference observed between the voltammograms in Figure 4.33 and that for PtS in a collector concentration of 6.24×10^{-4} M (Figure 4.31) was the development of steady reduction currents observed at collector concentration of 6.24×10^{-4} M.

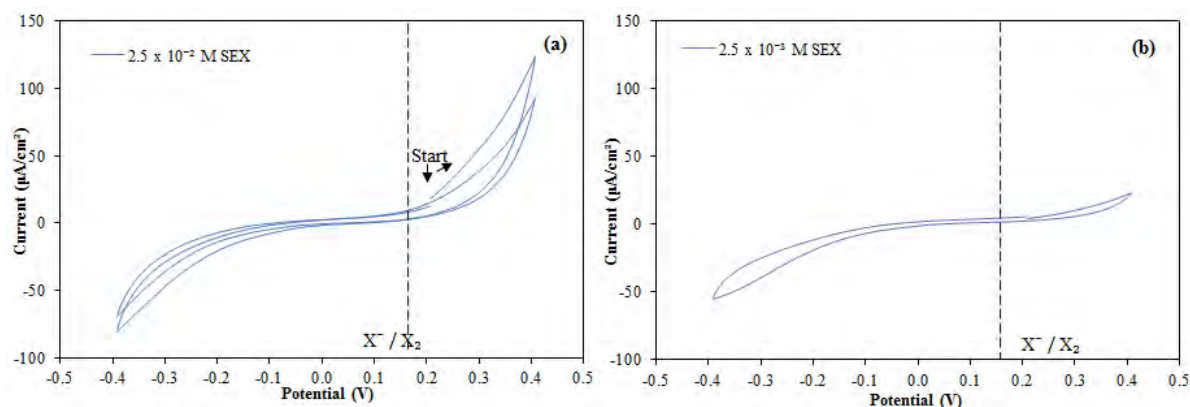


Figure 4.33. Cyclic voltammograms for PtS in forward starting sweeps in the presence of (a) 2.5×10^{-2} M SEX measured for 2 sweeps and (b) 2.5×10^{-3} M SEX measured for a single sweep in aerated solution. The reduction potential for xanthate to dioxanthone is superimposed at the potential of 0.15 V as a dotted line.

4.3.2.3.5 Investigation of the Effect of Sweep Rate

The effect of sweep rate was investigated for an upper limit sweep rate of 50 mV/s and a lower limit of 1 mV/s for PtS. Resulting voltammograms for the three sweep rates (i.e. including 10mV/s) in an aerated solution for single cycle forward starting sweeps are shown in Figure 4.34. These voltammograms showed 50 mV/s as producing the highest anodic and cathodic current densities. A sweep rate of 10

mV/s generated the next highest current densities with the lowest current densities being observed at a sweep rate of 1 mV/s. There were no significant differences in the shape of the current potential profiles other than the absence of a steady reduction current at a sweep rate of 50 mV/s.

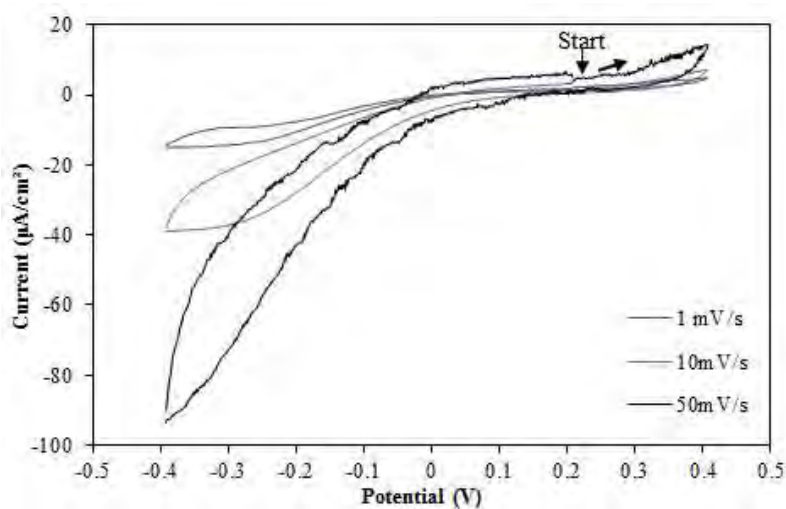


Figure 4.34. Cyclic voltammogram for PtS with forward starting sweeps in the presence of 6.24×10^{-4} M SEX for forward starting sweeps at sweep-rates of 1 mV/s, 10 mV/s and 50 mV/s measured in an aerated solution.

4.3.2.4 Cyclic Voltammetry Measurements of Pd

4.3.2.4.1 Cyclic voltammetry measurements over a potential range of ± 0.6 V

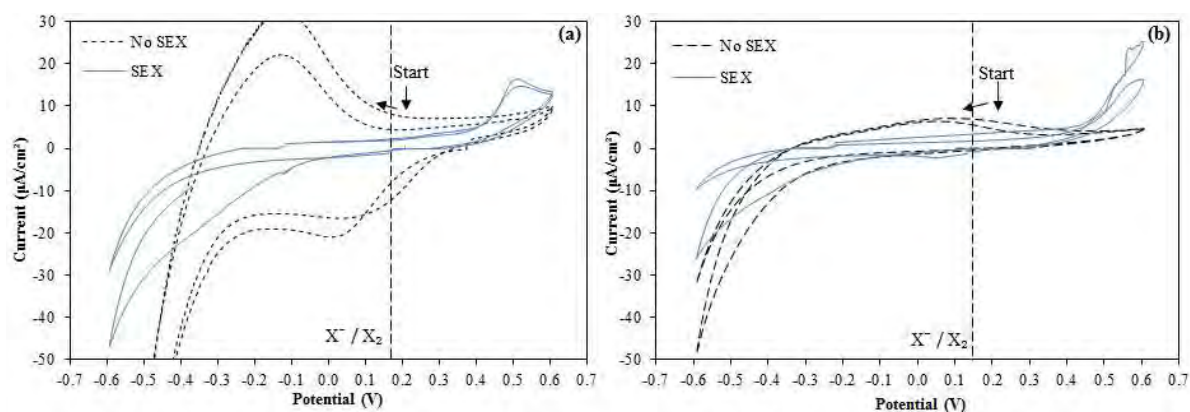


Figure 4.35. Cyclic voltammograms for Pd with reverse starting sweep measured for two sweeps in the absence and presence of 6.24×10^{-4} M SEX (a) in aerated solution conditions and (b) nitrogen saturated solution conditions. The oxidation potential for dixanthogen is indicated as a dotted line at 0.15 V.

The voltammograms for Pd metal were measured over a potential range of ± 0.6 V in aerated and nitrogen saturated solution conditions and are shown in Figure 4.35(a) and (b). In the absence of collector there were currents at the mineral surface in the aerated and de-aerated solution conditions between -0.4 V and 0.4 V. These currents were more pronounced under aerated solution conditions

showing high positive currents and low reduction currents. The reduction currents however, were not pronounced in de-aerated solution conditions. Absence of these currents in the presence of collector indicates that the collector is playing a role in inhibiting the mineral surface as will be discussed in Chapter 5.

4.3.2.4.2 Cyclic voltammetry measurements over a potential range of ± 0.4 V

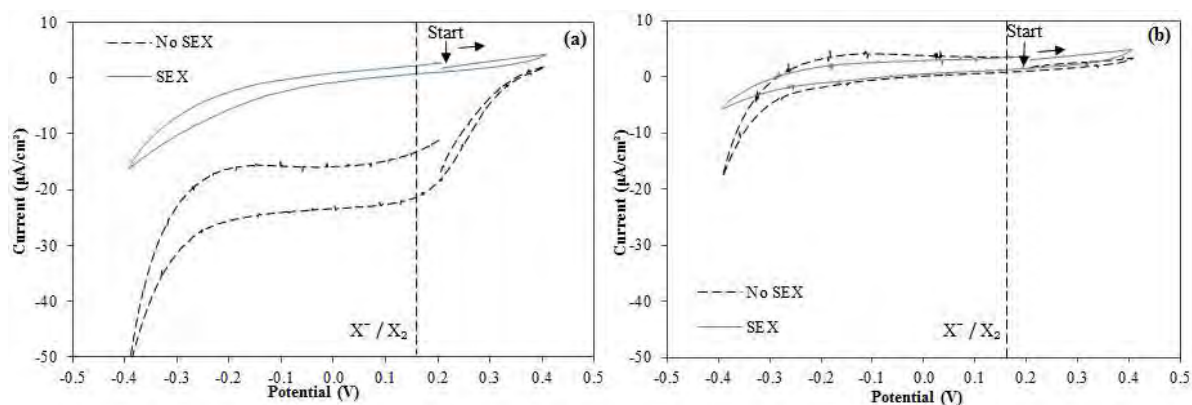


Figure 4.36. Cyclic voltammograms for PdTe₂ with forward starting sweep measured for two sweeps in the absence and presence of 6.24×10^{-4} M SEX (a) in aerated solution conditions and (b) nitrogen saturated solution conditions. The oxidation potential for dixanthogen is indicated as a dotted line at 0.15 V.

Over a potential range of ± 0.4 V the voltammograms generated on Pd metal were almost identical in the presence of SEX. Anodic currents at anodic potentials were higher in magnitude than in the absence of collector. The voltammogram generated in the absence of collector in aerated solution showed negative currents in the potential range from -0.4 V to 0.3 V, the shape of these currents becoming more negative in a cathodic sweep and less negative in an anodic sweep. In de-aerated solution conditions and the absence of collector the shape of the voltammogram followed that of the metal over a potential range of ± 0.6 V.

4.3.2.5 Cyclic Voltammetry Measurements of PdTe₂

PdTe₂ was investigated at a single sweep-rate of 10 mV/s under aerated and de-aerated solution conditions. Two switching potentials were investigated viz. ± 0.6 V and ± 0.4 V. Measurements were conducted in order to draw comparison with PtTe₂.

4.3.2.5.1 Cyclic voltammetry measurements over a potential range of ± 0.6 V

For a switching potential of ± 0.6 V, voltammograms for PdTe₂ under aerated and de-aerated solution conditions in the absence and presence of SEX are shown in Figure 4.37 for reverse going cycles. Figure

4.37(a) shows the voltammogram for PdTe₂ under aerated conditions. No reduction currents were observed in the initial reverse sweep of the mineral whilst an anodic current was generated which commenced from a potential of 0.35 V forming a peak at 0.5 V, in the anodic sweep. Current gradually dissipated to 0 $\mu\text{A}/\text{cm}^2$ at 0.35 V in the following cathodic sweep which is the same potential region from which the anodic current commenced. The second cathodic sweep resulted in a cathodic current in the potential region of -0.5 V to -0.6 V.

In the presence of collector the first cathodic sweep did not generate any reduction currents. The following anodic sweep yielded an anodic current from a potential of 0.45 V and a peak was observed at 0.5 V. A second cycle yielded a similar current profile albeit at lower current densities whilst the second cathodic sweep had yielded a reduction current peak at -0.45 V.

Under de-aerated solution conditions (Figure 4.37(b)), the initial cathodic sweep for PdTe₂ did not show any reduction currents. Current was generated in the following anodic sweep increasing from a potential of 0.35 V and yielding two peaks at ≈ 0.45 V. These were similar to those observed in Figure 4.37(a). Current dissipated from the switching potential (0.6 V) in the return cathodic sweeps and reduction current densities in the same potential region from which anodic currents commenced were generated. At negative potentials a reduction current peak similar to that occurring on the mineral in aerated conditions at 0.50 V was observed. The anodic current generated in the second cycle was similar to that observed in the first cycle except that it generated a single peak.

In the presence of collector, anodic currents generated commenced at potentials which were more positive than those generated in the absence of collector and formed peaks at 0.55 V. The reduction current generated in the second cycle occurred at -0.45 V which corresponds to the reduction current peak in the absence of collector. Current density in the presence of collector was however larger in magnitude than in its absence.

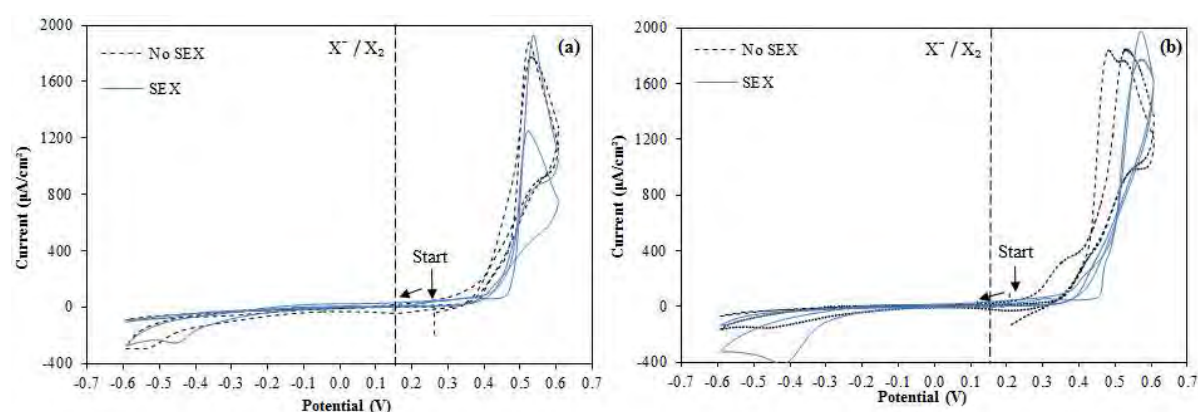


Figure 4.37. Cyclic voltammograms for PdTe₂ with reverse starting sweep measured for two sweeps in the absence and presence of 6.24×10^{-4} M SEX (a) in aerated solution conditions and (b) nitrogen saturated solution conditions. The oxidation potential for dixanthogen is indicated as a dotted line at 0.15 V.

4.3.2.5.2 Cyclic voltammetry measurements over a potential range of ± 0.4 V

The switching potential was changed to ± 0.4 V and voltammograms were generated for reverse and forward going sweeps in the absence and presence of collector.

Voltammograms generated for two reverse going sweeps in the absence and presence of collector are shown in Figure 4.38. Reduction currents similar in magnitude were generated at negative potentials whilst at positive potentials anodic currents were generated above a potential of 0.3 V which in turn showed similarities in current densities achieved.

In the presence of SEX, a reduction current with no current peaks occurred. However anodic sweeps resulted in currents generated from 0 V to form a current peak at 0.35 V. Two reduction current peaks labelled P1 and P2 developed after the first anodic cycle which were not present in the initial reduction cycle. The second anodic cycle had a current peak that was less prominent than the first peak generated in positive potential regions although the current profiles were identical up until the point of peak formation.

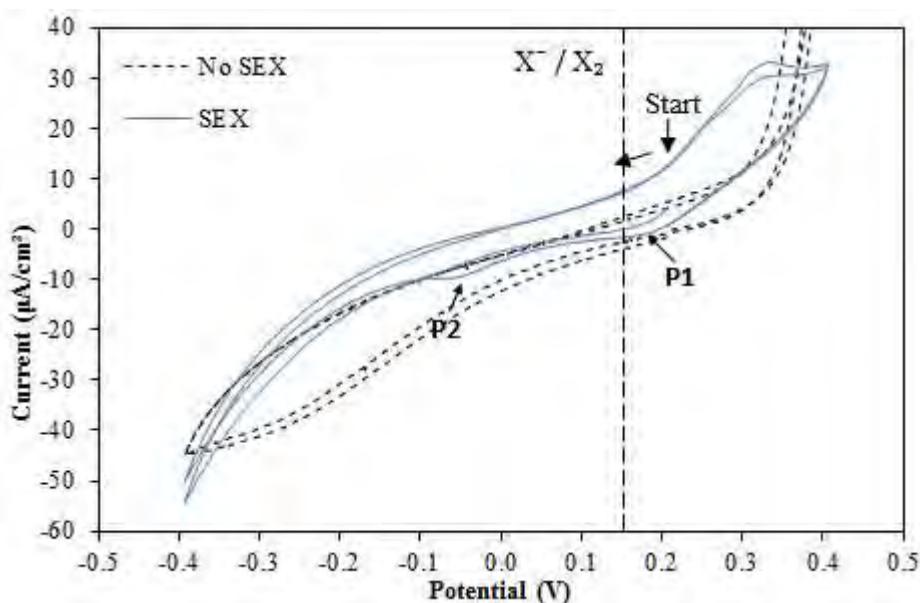


Figure 4.38. Cyclic voltammograms for PdTe₂ with a reverse starting sweep measured for two sweeps in the absence and presence of 6.24×10^{-4} M SEX, in aerated solution. The oxidation potential for dixanthogen is indicated as a dotted line at 0.15 V.

Voltammograms for PdTe₂ in a forward going sweep under aerated solution conditions are shown in Figure 4.39. The voltammogram generated in the absence of collector followed the same current potential profile as that generated in Figure 4.38. An anodic current was observed from a potential of 0.3 V and a reduction current was generated without the presence of reduction current peaks in the following cathodic sweep. In the presence of collector an anodic current was observed in Figure 4.38 which had a distinct peak at 0.3 V. Two reduction current peaks occurred during the cathodic sweep and have been labelled P1 and P2 owing to their similarity to those in Figure 4.38. P1 was found to be

positive with respect to the dixanthogen reduction potential, indicated as a dotted line, whilst P2 was less negative.

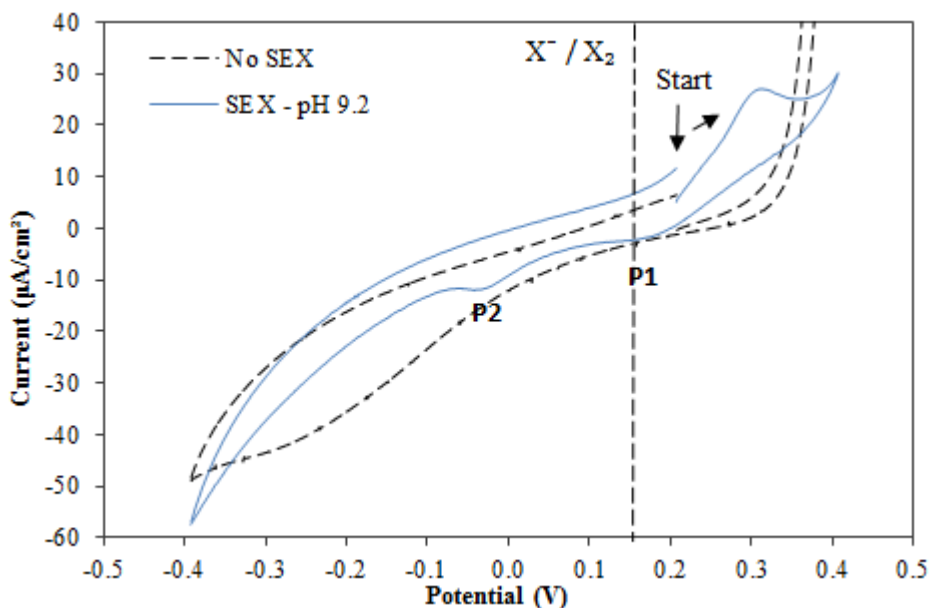


Figure 4.39. Cyclic voltammograms for PdTe₂ with a forward starting sweep measured for one sweep in the absence and presence of 6.24×10^{-4} M SEX, in aerated solution. The oxidation potential for dixanthogen is indicated as a dotted line at 0.15 V.

4.3.2.6 Cyclic Voltammetry Measurements of PdS

Switching potential ranges of ± 0.6 V and ± 0.4 V were also investigated for PdS under aerated and de-aerated solution conditions.

4.3.2.6.1 Cyclic voltammetry measurements over a potential range of ± 0.6 V

For a potential range of ± 0.6 V, measurements were made using cyclic voltammetry in two reverse going cycles. Voltammograms generated in the presence and absence of collector are shown in Figure 4.40. Voltammograms measured under aerated solution conditions are shown in Figure 4.40(a). In the absence of collector, reduction currents arose from the first cathodic sweep and similar currents were also observed in the second cycle measured. Anodic sweeps for the same voltammogram yielded identical currents. In the presence of SEX an initial reduction current was observed from 0 V to -0.4 V. A current peak was generated in the ensuing anodic sweep at 0.5 V which was not present in the second sweep. Cathodic sweeps yielded a reduction current that reached lower current densities than those generated in the first reduction peak.

Under de-aerated solution conditions (Figure 4.40b) anodic currents arose at positive potentials in the absence and presence of collector. Anodic currents generated in the presence of collector were higher in magnitude than those generated in the absence of collector. Conversely, cathodic sweeps in the presence of collector did not yield any peaks whilst in the absence of collector a reduction peak was generated in the potential range of 0 V and -0.4 V.

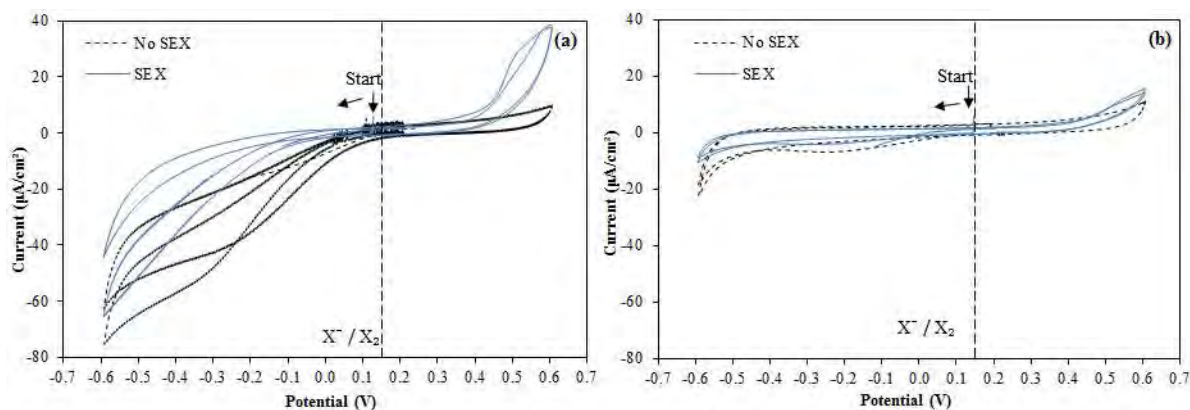


Figure 4.40. Cyclic voltammograms for PdS with forward starting sweep measured for two sweeps in the absence and presence of 6.24×10^{-4} M SEX (a) in aerated solution conditions and (b) nitrogen saturated solution conditions. The oxidation potential for dixanthogen is indicated as a dotted line at 0.15 V.

4.3.2.6.2 Cyclic voltammetry measurements over a potential range of ± 0.4 V

For a switching potential of ± 0.4 V the voltammogram for PdS was measured under aerated solution conditions for two reverse cycles. These voltammograms are shown in Figure 4.41. It is evident from comparison with Figure 4.40(a) (voltammograms for PdS at switching potentials of ± 0.6 V) that the generated voltammograms produced the same current potential profiles. Anodic currents generated at positive potentials are more positive in the presence of collector compared to those generated in the absence of collector. Ensuing cathodic currents in negative potential regions are also found to commence at more negative potentials in the presence of SEX than in its absence and these currents are lower in magnitude. Reduction currents generated in the absence of collector resemble those generated by PtS for the same conditions (cf. Figure 4.30) and, although a steady current was not observed, the rate of change of current reduced from a potential ≈ -0.1 V for PdS.

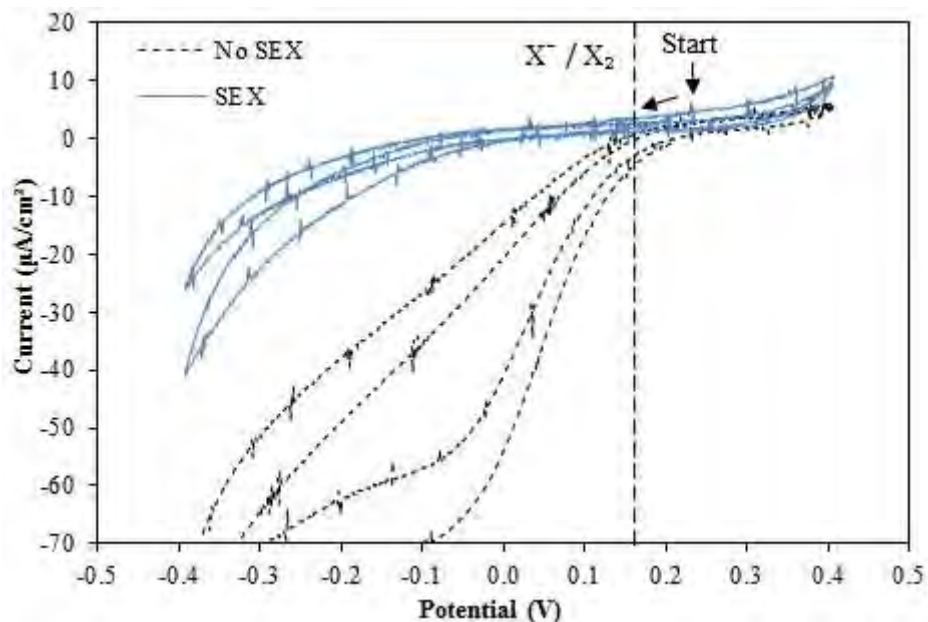


Figure 4.41. Cyclic voltammograms for PdS with a reverse starting sweep measured for two sweeps in the absence and presence of collector 6.24×10^{-4} M SEX, in aerated solution. The oxidation potential for dixanthogen is indicated as a dotted line at 0.15 V.

In a single forward going cycle the voltammogram generated for PdS over a potential range of ± 0.4 V (Figure 4.42) was not significantly different from that observed for reverse going sweeps. Anodic currents on the mineral in the presence of SEX were found to be more positive than those generated in the absence of SEX and notably these currents all occurred at potentials above the dixanthogen reduction potential (0.15 V) which is indicated in Figure 4.42 as a vertical dotted line. Reduction currents were observed to occur at potentials negative with respect to the X_2 reduction potential.

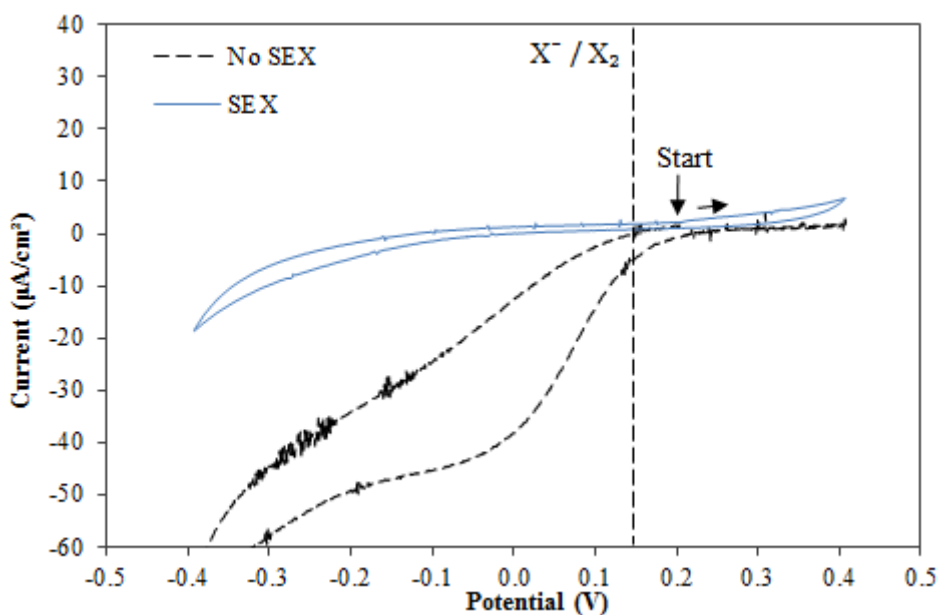


Figure 4.42. Cyclic voltammograms for PdS with a forward starting sweep measured for one sweep in the absence and presence of 6.24×10^{-4} M SEX, under aerated solution conditions. The oxidation potential for dixanthogen is indicated as a dotted line at 0.15 V.

4.3.3 Sodium Diethyl Dithiophosphate Study

Electrochemical interactions between Sodium Diethyl Dithiophosphate and the PGMs of this study were also investigated after the SEX study. Variables, including sweep rate (10 mV/s and 1 mV/s) and aeration/de-aeration were used to determine the electrochemical nature of interactions. Measurements were also made in the presence and absence of collector. The reversible potential for the formation of the dimer of DTP was measured to be 0.388 V c.f. Section 4.1.2. This potential is indicated on all voltammograms as a vertical line at 0.388 V.

4.3.3.1 Cyclic Voltammetry Measurements for PtTe₂

In Figure 4.43 the voltammograms for PtTe₂ in the absence and presence of collector for a forward going cycle are shown. A sweep rate of 10 mV/s was applied to the voltammograms. The behaviour of the mineral in the absence of collector was shown in Figure 4.24.

In the presence of DTP an anodic current increased from the starting potential to the potential limit of 0.4 V. This anodic current commenced at the same potential as that generated in the absence of collector. However the rate of increase of current in the presence of collector is lower resulting in the current increasing sharply at a potential of 0.35 V rather than 0.25 V in the absence of collector. The maximum current generated at the switching potential in the presence of collector was also observed to be significantly reduced compared that obtained on the mineral in the absence of collector. It will later be discussed in Chapter 5 that this is an effect of the collector on the mineral surface. Cathodic sweeps on the mineral both in the presence and absence of collector resulted in reduction currents of similar magnitude with no evidence of any current peaks.

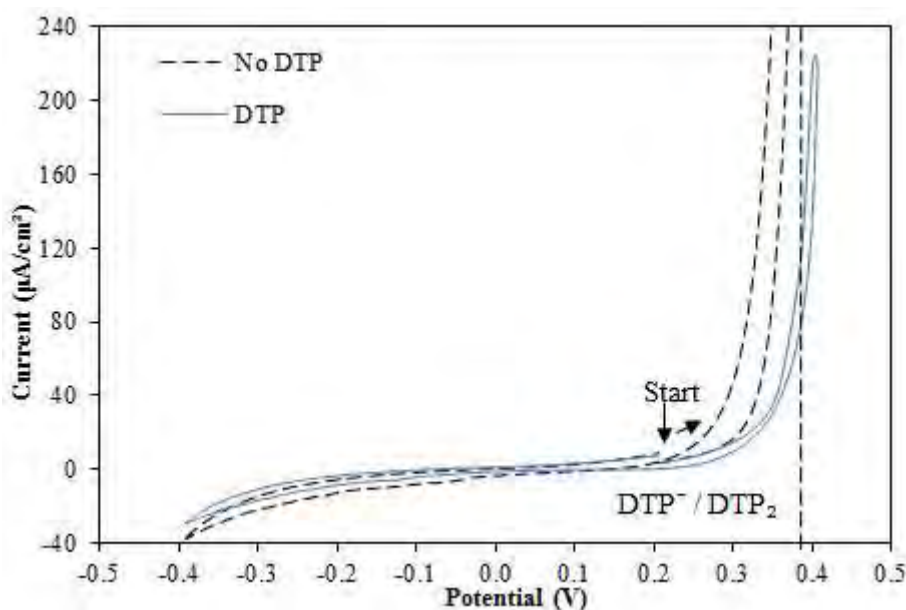


Figure 4.43. Cyclic voltammograms for PtTe₂ with a forward starting sweep at a sweep rate of 10 mV/s measured for one sweep in the absence and presence of 6.24×10^{-4} M DTP, under aerated solution conditions. The oxidation potential for DTP₂ is indicated as a dotted line at 0.388 V.

In Figure 4.44(a) and (b), a sweep rate of 1 mV/s was applied to the mineral in the presence and absence of collector and under aerated (a) and deaerated (b) solution conditions and results are shown.

Under aerated solution conditions in the absence of collector an anodic current similar to that generated at a sweep-rate of 10 mV/s commenced from a potential of 0.3 V up to 0.4 V. Subsequent current dissipation from 0.4 V on the cathodic sweep resulted in the current density reaching $\sim 0 \mu\text{A}/\text{cm}^2$ at potential values less negative than that for the commencement of the anodic sweep. A reduction current was generated on the mineral during this cathodic sweep but did not show any current peaks.

In the presence of collector the anodic currents generated on PtTe₂ were significantly lower in magnitude than those generated in the absence of collector as was observed in Figure 4.43. A peak was however from the anodic current region at a potential only fractionally higher than the dimerization potential for DTP.

Under de-aerated conditions (Figure 4.44(b)), results obtained were similar to those obtained under aerated solution conditions in the absence of collector. The current rose at 0.35 V and continued to rise until the switching potential was reached then dissipated in the cathodic sweep following a path resulting in the current density reaching $\sim 0 \mu\text{A}/\text{cm}^2$ at a potential 0.15 V. More significant differences were observed in the absence of oxygen than in the presence of dissolved oxygen. Reduction currents generated in de-aerated solution showed reduced currents compared to those generated in aerated solution.

In the presence of DTP, an anodic current commenced from 0.35 V to form a peak at ≈ 0.375 V. From this peak the current continued to rise before reaching the switching potential of 0.4 V. Despite the increase in current after the peak which is unlike Figure 4.44(a), the maximum current reached in the presence of DTP was lower in magnitude than that reached in the absence of DTP. Current dissipation followed the same order as that observed in the absence of collector but the reduction current generated in the presence of DTP was more negative than that generated in the absence of DTP. In addition a current peak was observed in the region of -0.38 V and -0.4 V (the potential limit).

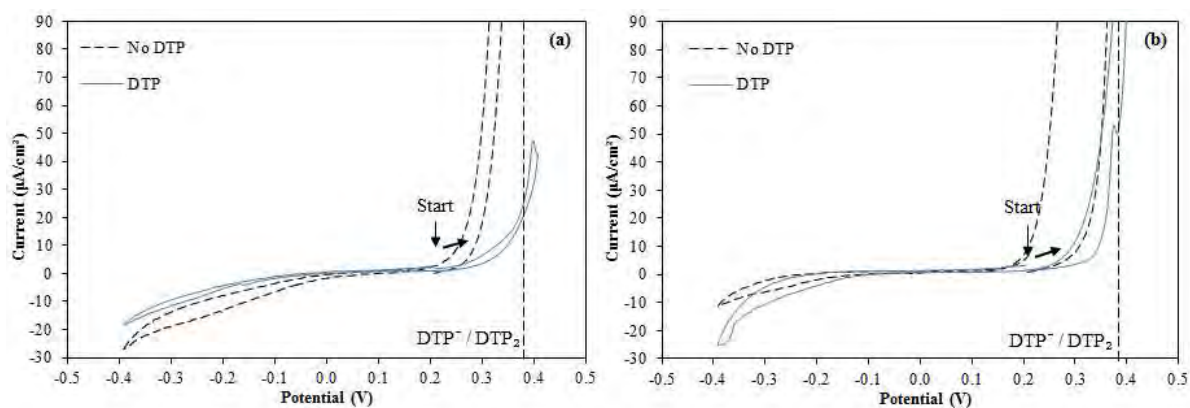


Figure 4.44. Cyclic voltammograms for PtTe₂ with a forward starting sweep at a sweep rate of 1 mV/s measured for a single sweep in the absence and presence of 6.24×10^{-4} M DTP, (a) in aerated solution conditions (b) in Nitrogen saturated solution conditions. The oxidation potential for DTP₂ is indicated as a dotted line at 0.388 V.

4.3.3.2 Cyclic Voltammetry Measurements of PtS

PtS was measured at sweep rates of 10 mV/s and 1 mV/s in the absence and presence of DTP. Both measurements were made under aerated conditions and are presented in this section.

At a sweep rate of 10 mV/s the voltammograms for PtS in the presence and absence of DTP for a forward going cycle are shown in Figure 4.45. In the absence of DTP anodic currents were present at positive potentials and reduction currents were evident from a potential of 0.2 V to the negative potential limit of -0.4 V as indicated in Figure 4.31. In the presence of DTP anodic currents were also observed and reduction currents similar in profile to those observed in the absence of collector were generated. At positive potentials the currents generated were more positive than those in the absence of collector and although there was a similar current potential profile, reduction currents commenced at potentials more negative than those observed for the mineral in the absence of collector.

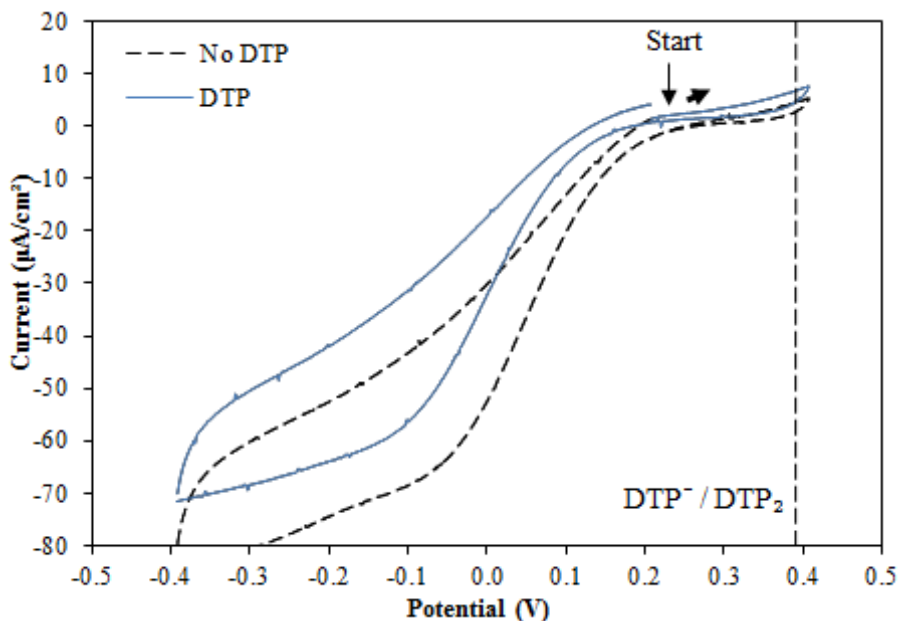


Figure 4.45. Cyclic voltammograms for PtS with a forward starting sweep at a sweep rate of 10 mV/s measured for a single sweep in the absence and presence of 6.24×10^{-4} M DTP, in aerated solution. The oxidation potential for DTP_2 is indicated as a dotted line at 0.388 V.

For a sweep rate of 1 mV/s (Figure 4.46) a significant difference was observed between the reduction currents generated in the absence and in the presence of collector. Anodic currents were observed to be higher in the presence of DTP than in its absence whilst the reduction currents generated in the absence of DTP were $\approx 50 \mu\text{A}/\text{cm}^2$ more negative than those arising in the presence of DTP. In both these voltammograms it was observed however that the rate of current reduction was reduced significantly in the potential region of -0.25 V and -0.4 V.

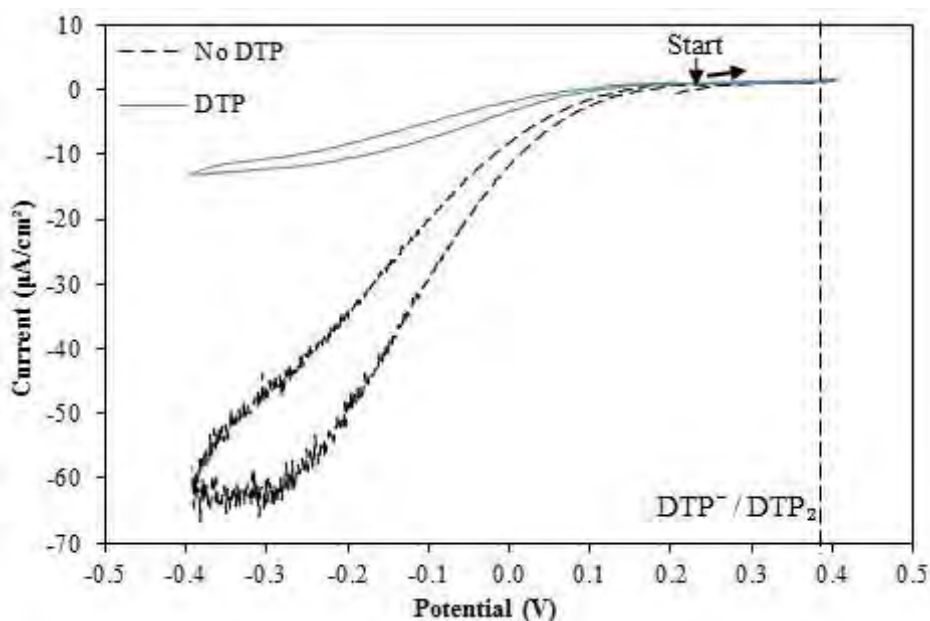


Figure 4.46. Cyclic voltammograms for PtS with a forward starting sweep at a sweep rate of 1 mV/s measured for a single sweep in the absence and presence of 6.24×10^{-4} M DTP, in aerated solution conditions. The oxidation potential for DTP_2 is indicated as a dotted line at 0.388 V.

4.3.3.3 Cyclic Voltammetry Measurements for PdTe₂

Voltammograms of PdTe₂ in the presence of DTP were only measured for a sweep-rate of 10 mV/s in the absence and presence of DTP. Results are shown in Figure 4.47.

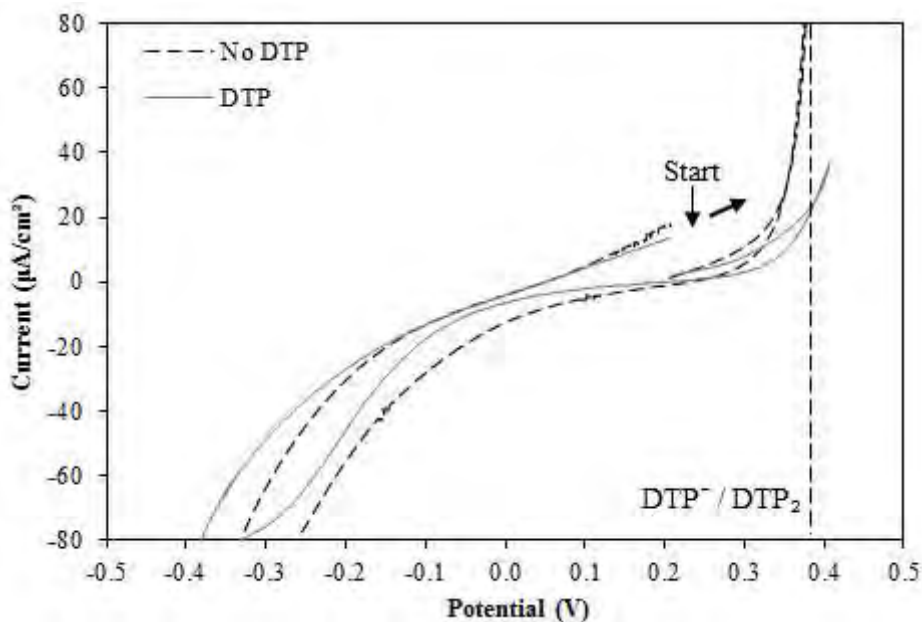


Figure 4.47. Cyclic voltammograms for PdTe₂ with a forward starting sweep at a sweep rate of 10 mV/s measured for a single sweep in the absence and presence of 6.24×10^{-4} M DTP, in aerated solution. The oxidation potential for DTP₂ is indicated as a dotted line at 0.388 V.

The behaviour of the mineral in the absence of collector has been shown previously (cf. Figure 4.39). In the presence of collector the anodic current occurring at positive potentials was significantly lower ($\approx 50 \mu\text{A}/\text{cm}^2$) than that generated in the absence of DTP. No anodic current peaks were generated on the mineral. A reverse sweep yielded a reduction current which was lower in magnitude than that generated in the absence of collector. It was also noted that the reduction current commences at potentials negative with respect to those in the absence of collector viz. -0.1 V in the presence of collector compared to 0.2 V in the absence of collector.

4.3.3.4 Cyclic Voltammetry Measurements for PdS

Voltammograms for PdS were also measured for a single sweep-rate of 10 mV/s and are shown in Figure 4.48 under aerated solution conditions. In the presence of collector anodic currents were generated which were larger in magnitude than those measured in the absence of collector. Under both conditions of the presence and absence of collector, reduction currents were generated. Figure 4.48 shows that the current generated in the absence of collector commenced at 0.15 V whilst that for the mineral in the presence of collector commenced at -0.1 V. Further differences can be noted for these

reduction currents from the change in the rate of reduction in the absence of collector at -0.1 V which was not observed in the presence of collector.

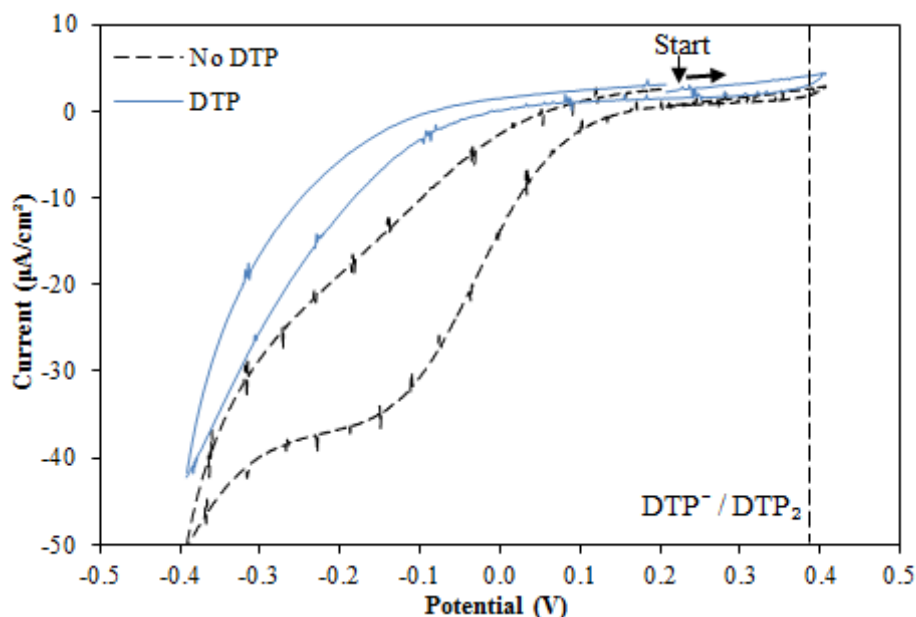


Figure 4.48. Cyclic voltammograms for PdS with a forward starting sweep at a sweep rate of 10 mV/s measured for a single sweep in the absence and presence of 6.24×10^{-4} M DTP, in aerated solution conditions. The oxidation potential for DTP_2 is indicated as a dotted line at 0.388 V.

4.4 Interaction of Platinum Group Minerals with Copper Sulphate (CuSO_4)

An electrochemical study comprised of mixed potential and cyclic voltammetry measurements was conducted for PtTe_2 and PtS in the presence of CuSO_4 . CuSO_4 is widely used as an activating agent in the flotation of PGMs and therefore measurements were made to investigate the effect of the presence of copper sulphate. Cyclic voltammograms were measured under de-aerated conditions for three different pH levels due to the different speciation of copper at pH 10, 8 and 6.

4.4.1 Mixed Potential measurements of PtS and PtTe_2

Mixed potential/rest potential measurements were made with addition of CuSO_4 before SEX addition. CuSO_4 was added after 600 s and SEX added after 1200 s.

In Figure 4.49 the rest potentials of both PtS and PtTe_2 at pH 10 are shown. From the point of copper sulphate addition there was an increase in the rest potential of PtS whilst there was no significant change in the rest potential of PtTe_2 . SEX addition at 1200 s resulted in an initial change of rest potential for both minerals. The potential subsequently rose with PtS achieving rest potential values within the same

range as the potential prior to collector addition and PtTe₂ achieving rest potential values slightly positive relative to that prior to SEX addition. All rest potentials were observed to be more positive than the dixanthogen reduction potential of 0.15 V which is shown as a straight line on Figure 4.49.

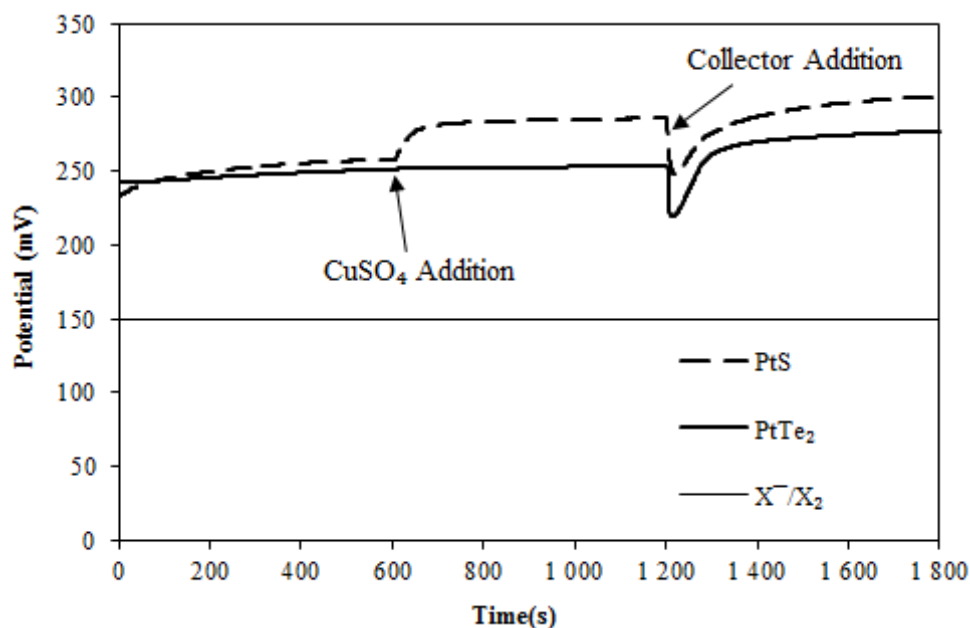


Figure 4.49. Mixed potential of platinum minerals at pH 10 in the absence of SEX and CuSO₄ followed by the addition of CuSO₄ and SEX.

Rest potentials of the minerals at pH 8 are shown in Figure 4.50. Rest potentials for the minerals at this pH level were more positive than those for the minerals at pH 10 (Figure 4.49). CuSO₄ addition resulted in an increase in rest potential for both minerals, although that for PtS was more significant than in the case of PtTe₂. SEX addition at 1200 s resulted in an initial decrease in potential on both minerals which was a greater change than that observed at pH 10. The potential increased after reaching a minimum value on both minerals and the final rest potential achieved on both PtS and PtTe₂ was more positive than the potentials observed on the mineral prior to collector addition.

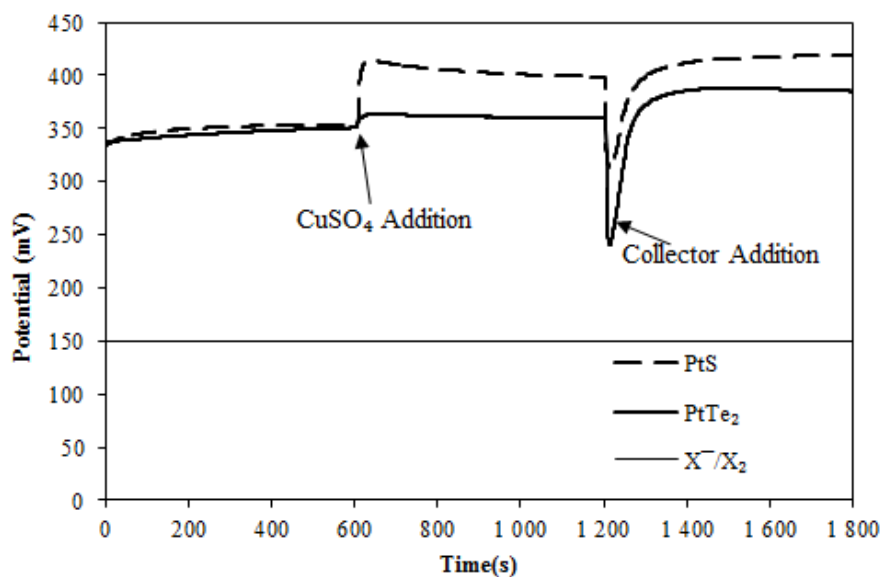


Figure 4.50. Mixed potential of platinum minerals at pH 8 in the absence of SEX and CuSO_4 followed by the addition of CuSO_4 and SEX.

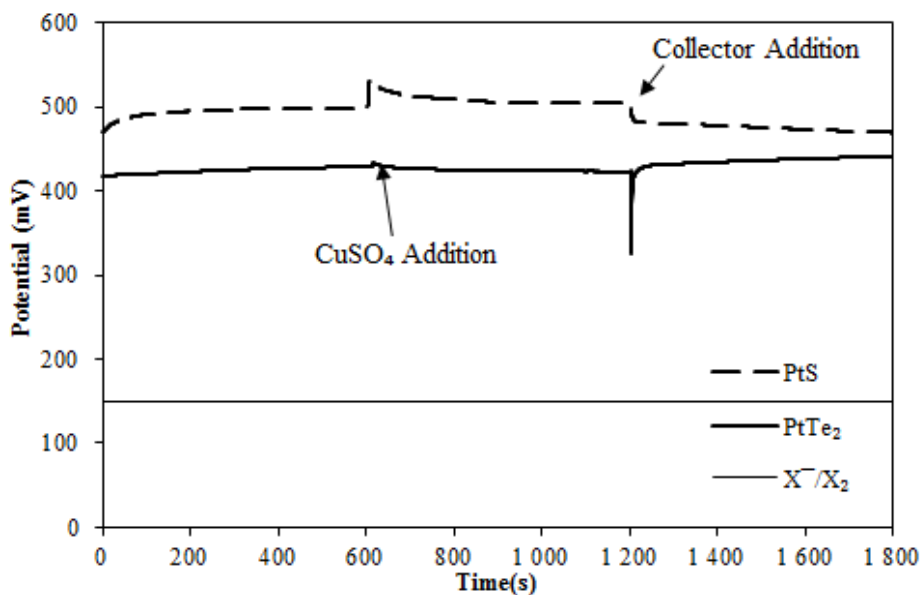


Figure 4.51. Rest potential of platinum minerals at pH 6 in the absence of SEX and CuSO_4 followed by the addition of CuSO_4 and SEX.

At pH 6 results of the rest potentials of the minerals after copper and collector addition are shown in Figure 4.51. It was observed that rest potentials for PtTe_2 and PtS decreased to 0.09 V prior to collector addition with the potential of PtS being more positive. These potentials were all positive with respect to the dixanthogen reduction potential of 0.15 V and more positive than the potentials for the mineral at pH 10 and pH 8. After copper sulphate addition to PtTe_2 the rest potential of the mineral did not change and whilst there was an initial change in potential after collector addition, the resulting rest potential was not significantly different from the potential before CuSO_4 and SEX addition. On the

other hand the rest potential of PtS increased when copper was added to the system. Collector addition resulted in the rest potential decreasing to potential more negative than after CuSO_4 addition and was only slightly lower than the potential of the mineral prior to any reagent addition.

4.4.2 Cyclic Voltammetry Measurements of PtTe_2

Cyclic voltammograms were measured for PtTe_2 at pH 10, 8 and 6 under four conditions viz. absence of reagents, 10^{-4} M CuSO_4 , 10^{-4} M EX and combined CuSO_4 and SEX.

4.4.2.1 Investigations of Interactions of PtTe_2 with CuSO_4 at pH 10

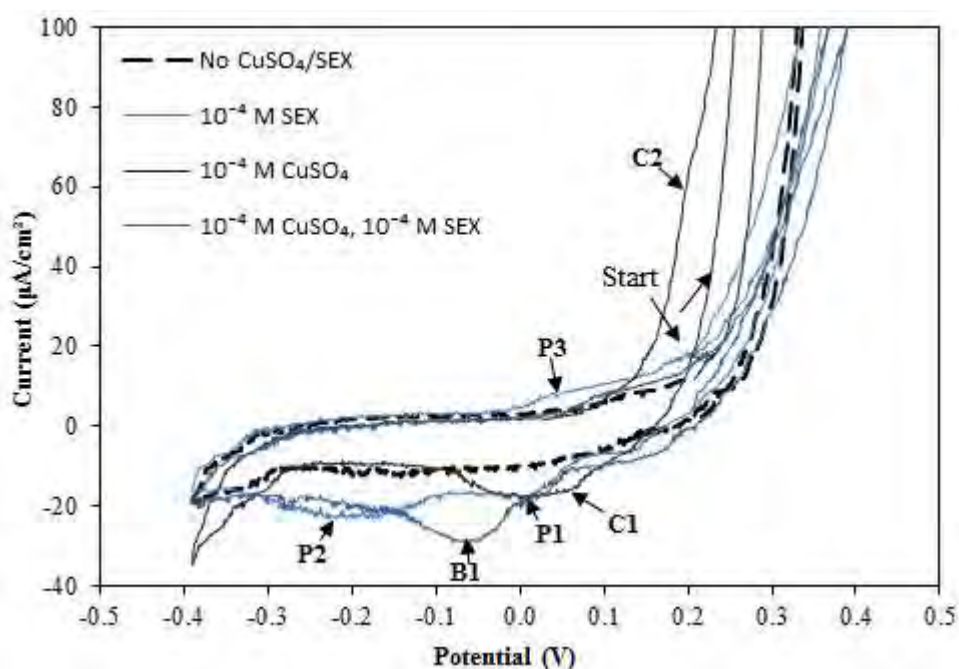


Figure 4.52. Cyclic voltammograms for PtTe_2 with a forward starting sweep at a sweep rate of 10 mV/s measured for a single cycle in the absence and presence of 1×10^{-4} M SEX, in the presence of 1×10^{-4} M CuSO_4 and in the presence of a both 1×10^{-4} M SEX and 1×10^{-4} M CuSO_4 in de-aerated solution at pH 10.

Forward going voltammograms for PtTe_2 at pH 10 are shown in Figure 4.52 measured under de-aerated conditions. In comparison with the absence of SEX and CuSO_4 the voltammogram generated in the presence of SEX showed a reduction current peak in the negative potential region. The first reduction current peak occurred in the region of 0 V and the second current peak between -0.1 V to -0.3 V. No reduction current peaks were present in the voltammogram generated in the absence of SEX.

Unlike the voltammogram for PtTe₂ measured in the absence of reagents; voltammograms generated in the presence of CuSO₄ and in the presence of both CuSO₄ and SEX both yielded reduction currents. With CuSO₄ present the initial anodic sweep yields an anodic current similar to that observed for the mineral in the absence of reagents, albeit occurring at differing potentials. Reduction current peak (C1) in the region of 0.1 V and -0.1 V was generated in a cathodic cycle. Return anodic sweeps also yielded an anodic current peak at 0.18 V (C2).

In the presence of both CuSO₄ and SEX the anodic currents generated were lower in magnitude in comparison to those generated under all other conditions. A single reduction current peak was observed in the following cathodic sweep at a peak potential of ≈ -0.08 V and is labelled (B1) on Figure 4.52.

4.4.2.2 Investigations of Interactions of PtTe₂ with CuSO₄ at pH 8

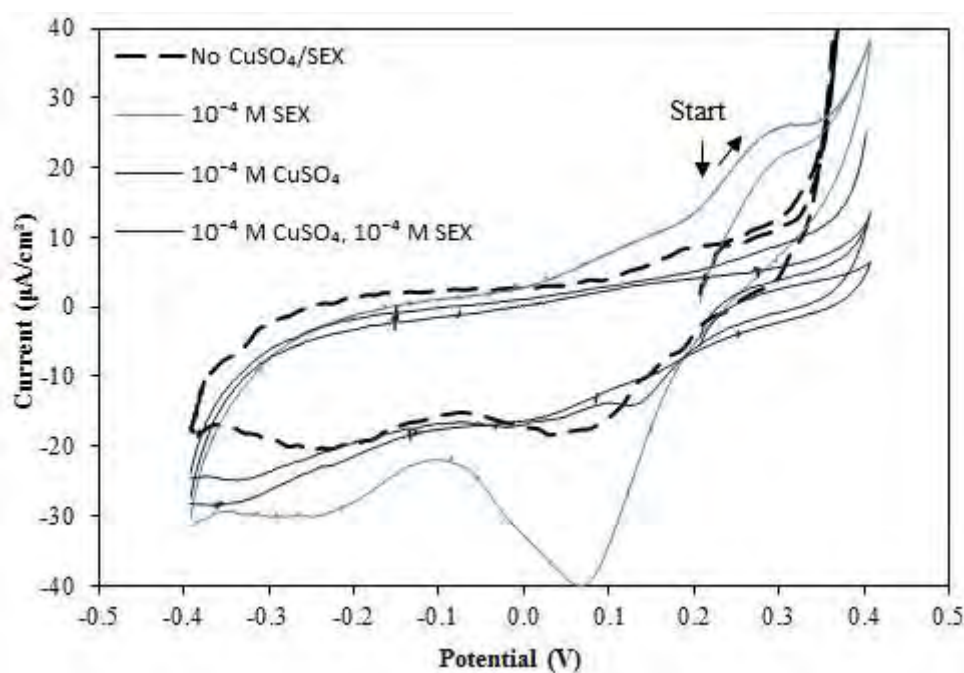


Figure 4.53. Cyclic voltammograms for PtTe₂ with a forward starting sweep at a sweep rate of 10 mV/s measured for a single cycle in the absence and presence of 1×10^{-4} M SEX, in the presence of 1×10^{-4} M CuSO₄ and in the presence of a both 1×10^{-4} M SEX and 1×10^{-4} M CuSO₄ in de-aerated solution at pH 8.

Voltammograms for PtTe₂ at pH 8 under de-aerated conditions in the presence and absence of SEX, presence of CuSO₄ and presence of both CuSO₄ and SEX, are shown in Figure 4.53. These voltammograms showed that at positive potentials, anodic current were present in the absence of collector from a potential of 0.05 V forming a current peak at 0.2 V followed by an increase in anodic current up to the switching potential of 0.4 V. Two reduction current peaks at potentials of ≈ 0.05 V and ≈ -0.25 V resulted from the cathodic sweep.

In the presence of SEX an anodic current peak was generated at a potential of 0.25 V from a current arising from the starting potential. The second anodic sweep showed a current generated from 0 V to form a peak at ≈ 0.25 V. Two reduction current peaks were generated in the following cathodic sweep, the first and most prominent peak being formed at 0.08 V and the second current peak at a potential of ≈ -0.25 V which coincided with that occurring in the absence of reagents.

In the presence of CuSO_4 , initial anodic currents were lower than those for the mineral in the absence of reagents and in the presence of SEX only. A reduction current commencing from 0.25 V forming a current peak at 0.15 V was followed by a reduction current that diminished up to -0.4 V.

In the presence of both CuSO_4 and SEX anodic currents were of the same magnitude as those measured in the presence of CuSO_4 and no significant reduction current peaks were observed from this voltammogram.

4.4.2.3 Investigations of Interactions of PtTe_2 with CuSO_4 at pH 6

Voltammograms for PtTe_2 obtained at pH 6 are shown in Figure 4.54. In the absence of collector anodic currents generated were significantly lower in magnitude than those generated in the presence of SEX. A cathodic sweep in the absence of SEX yielded a reduction current peak which reached a minimum current at a potential of -0.2 V. In the presence of collector an anodic current peak was generated at 0.3 V. Reduction currents were subsequently generated from 0.2 V with a change in current being observed between 0 V and 0.1 V.

In the presence of CuSO_4 , the first anodic sweep resulted in a slight anodic current which was followed by a cathodic sweep that had two changes in current. The first current change occurred in the potential range of 0.2 V and -0.1 V whilst the following change resulted in a peak within the potential range of -0.1 V and -0.4 V. A return anodic sweep from this cathodic sweep resulted in a sharp current occurring from a potential of 0.2 V.

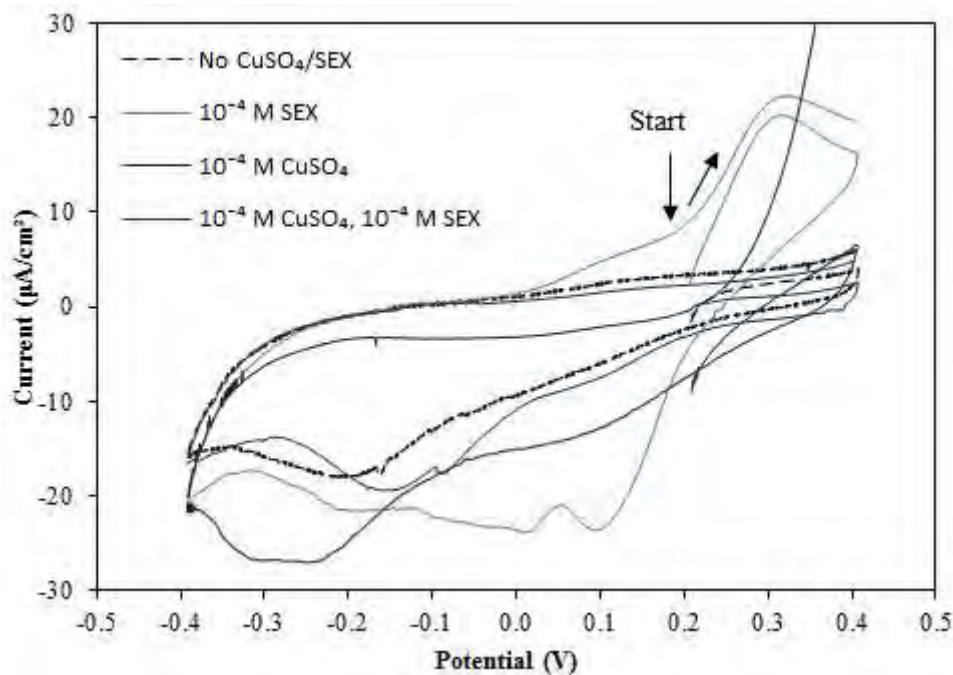


Figure 4.54. Cyclic voltammograms for PtTe₂ with a forward starting sweep at a sweep rate of 10 mV/s measured for a single cycle in the absence and presence of 1×10^{-4} M SEX, in the presence of 1×10^{-4} M CuSO₄ and in the presence of a both 1×10^{-4} M SEX and 1×10^{-4} M CuSO₄ in de-aerated solution at pH 6.

Anodic currents in the presence of CuSO₄ and SEX were the lowest in magnitude as shown on Figure 4.54. A reduction current exhibited a current change between the potentials of 0.2 V and 0 V followed by a current peak with a minimum at a potential of ≈ -0.15 V.

4.4.3 Cyclic Voltammetry Measurements of PtS

The following results are for PtS measured in the absence of reagents, presence of SEX, presence of CuSO₄ and presence of CuSO₄ and SEX at pH levels 10, 8 and 6.

4.4.3.1 Investigations of Interactions of PtS with CuSO₄ at pH 10

Figure 4.55 shows the results for PtS under the conditions measured. In the absence of SEX an anodic current was observed in positive potential regions without current peaks and a reduction current occurred without current peaks, in negative potential regions. The anodic current generated in the presence of SEX was higher in magnitude than that in the absence of collector and the return cathodic sweep in the presence of SEX resulted in a current peak at -0.1 V and thereafter achieving a minimum potential at -0.4 V.

In the presence of CuSO_4 the anodic current had a similar potential profile to that observed in the absence of CuSO_4 and SEX with no peaks being identified. A reduction current was generated in the ensuing cathodic sweep forming a peak at 0.18 V. The lowest anodic currents on PtS were produced in the presence of CuSO_4 and SEX, these did not also deviate significantly from those measured in the absence of CuSO_4 and SEX.

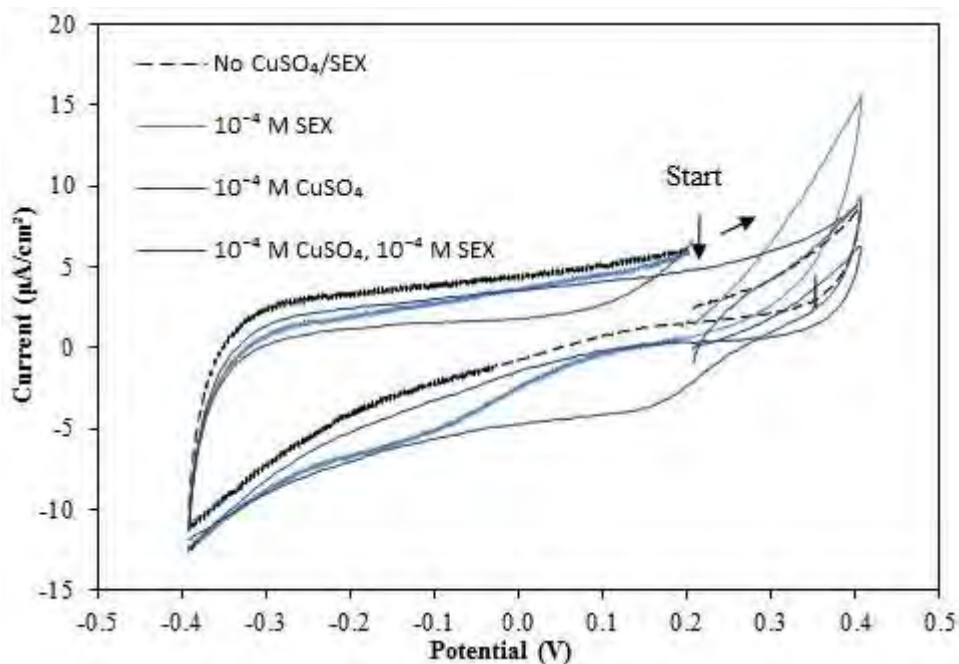


Figure 4.55. Cyclic voltammograms for PtS with a forward starting sweep at a sweep rate of 10 mV/s measured for a single cycle in the absence and presence of 1×10^{-4} M SEX, in the presence of 1×10^{-4} M CuSO_4 and in the presence of both 1×10^{-4} M SEX and 1×10^{-4} M CuSO_4 in de-aerated solution at pH 10.

4.4.3.2 Investigations of Interactions of PtS with CuSO_4 at pH 8

At pH 8 the voltammograms for PtS are shown in Figure 4.56. No current peaks were observed on any of the voltammograms generated at this pH level. In the absence of reagents and in the presence of CuSO_4 and in a mixture of CuSO_4 and SEX the anodic currents generated were of a similar magnitude. Reduction currents were also observed to be similar for the presence of CuSO_4 and CuSO_4 and SEX but the return anodic sweep resulted in higher current densities in the absence of CuSO_4 and SEX than in the presence of both CuSO_4 and SEX. In the presence of CuSO_4 at positive potentials the mineral responded differently resulting in a sharper rate of increase of current than was observed for the mineral in the absence of CuSO_4 and SEX. This behaviour of the mineral in the presence of CuSO_4 was similar to that of the mineral in the presence of SEX alone at this pH level. In Figure 4.56 the voltammogram shows that an anodic current density that is larger in magnitude than that of the mineral under the other conditions investigated was generated. This was followed by a reduction current that did not show any

peaks but notably reaching the same current densities as all other reduction currents measured at this pH level.

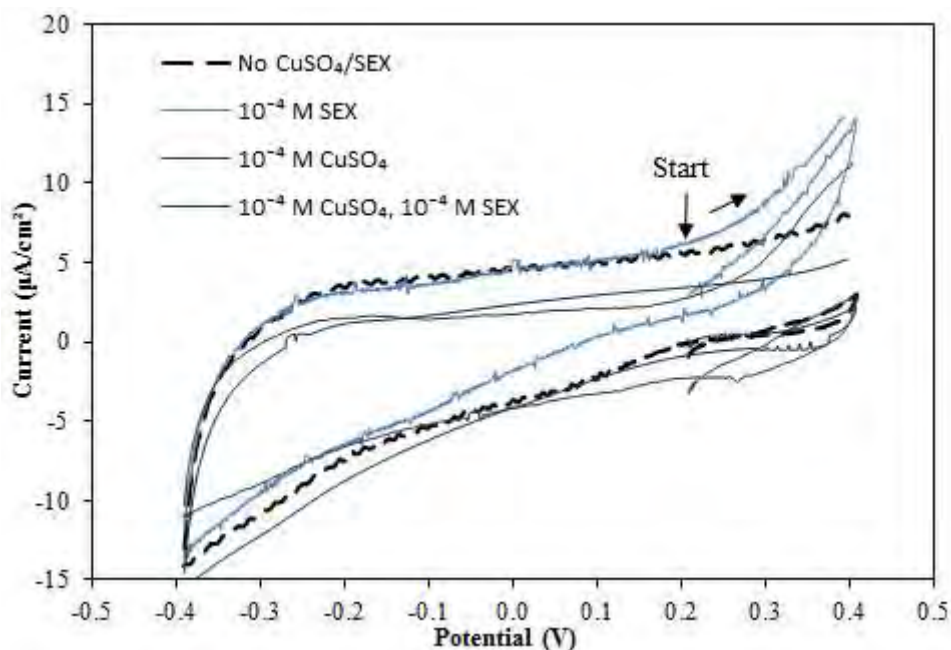


Figure 4.56. Cyclic voltammograms for PtS with a forward starting sweep at a sweep rate of 10 mV/s measured for a single cycle in the absence and presence of 1×10^{-4} M SEX, in the presence of 1×10^{-4} M CuSO_4 and in the presence of a both 1×10^{-4} M SEX and 1×10^{-4} M CuSO_4 in de-aerated solution at pH 8.

4.4.3.3 Investigations of Interactions of PtS with CuSO_4 at pH 6

At pH 6, Figure 4.57 shows the results for PtS. Anodic currents generated in the absence of CuSO_4 and SEX and in the presence of CuSO_4 and SEX were very low almost negligible. Similar reduction current potential profiles were generated for which there were no visible peaks. Reduction currents generated in the presence of SEX alone also exhibited similar behaviour to those observed in the absence of SEX and CuSO_4 and in the presence of both SEX and CuSO_4 . The anodic behaviour of the mineral in the presence of SEX was however not the same and it was observed that anodic currents were higher in magnitude and the rate of increase of these currents was also higher.

The current response of the mineral to the presence of CuSO_4 alone, was significantly different from the other voltammograms shown in Figure 4.56. At positive potentials, the anodic current produced had a high rate of increase despite the maximum current density reached being lower than that of the mineral in the presence of SEX alone. This anodic current was immediately followed by a reduction current peak during the cathodic sweep that occurred at 0.28 V. A return anodic sweep resulted in anodic activity from a potential of 0.2 V which resulted in the highest current density measured on the mineral at pH 8.

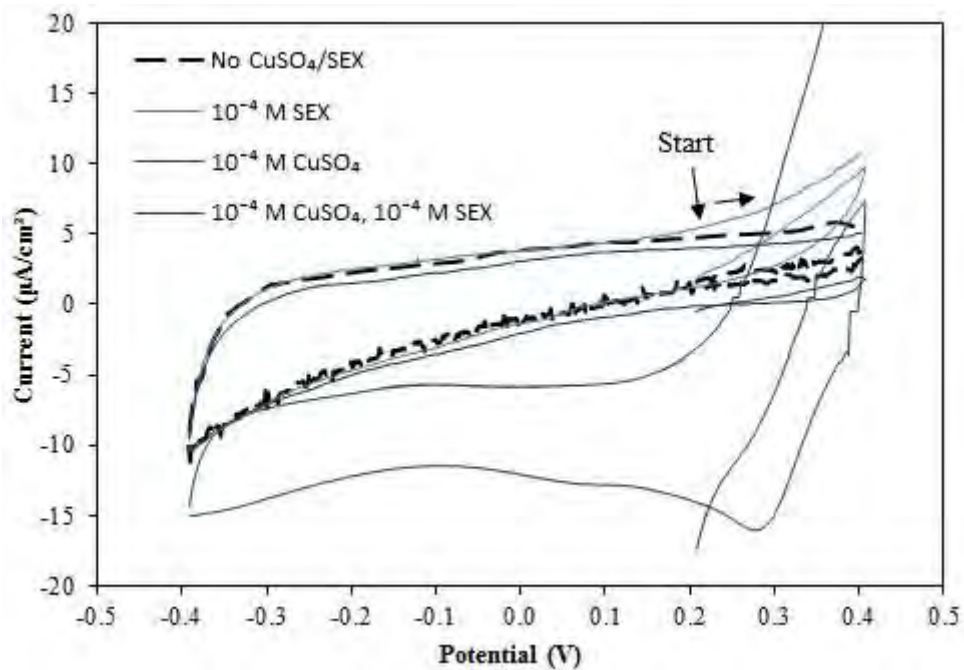


Figure 4.57. Cyclic voltammograms for PtS with a forward starting sweep at a sweep rate of 10 mV/s measured for a single cycle in the absence and presence of 1×10^{-4} M SEX, in the presence of 1×10^{-4} M CuSO_4 and in the presence of a both 1×10^{-4} M SEX and 1×10^{-4} M CuSO_4 in de-aerated solution at pH 6.

Chapter 5

5 Discussion

In this chapter a discussion of the results obtained for this study is presented. The interactions of the different PGMs (PtTe₂, PdTe₂, PtS and PdS) with thiol collectors and CuSO₄ are discussed and mechanisms are proposed. All the discussion is based on mixed potential theory which forms the basis of this electrochemical study (cf. 2.4.3).

The dominant cathodic reaction leading to adsorption of collector in solution is known to be the reduction of oxygen according to Reaction (5.1) (Rao and Leja, 2004).



The anodic reaction involves the oxidation of collector species to form one of three species, chemisorbed thiolate, a metal thiolate species and a dithiolate species.

Oxidation reactions at the mineral surface involving collector or oxidation of the mineral surface are driven by an over-potential at the mineral surface. At the open circuit condition, the reduction of oxygen occurs at a potential above the equilibrium potential for oxidation of the mineral. The difference in potential (over-potential) drives oxidation of the mineral to occur at the rate of reduction of oxygen (Kocabağ and Güler, 2008).

Hence it is possible through the knowledge of rest potential and equilibrium potential of possible oxidation reactions to make proposals regarding;

- Oxidation species formed at the surface of the mineral
- The relative rates of formation of species

The rest potential changes following the addition of oxidative and reductive species as illustrated in Figure 5.1. Anodic processes are the result of collector or mineral oxidation whereas cathodic processes are a result of reduction of oxygen. In the case where copper was added the reduction of copper is a cathodic process.

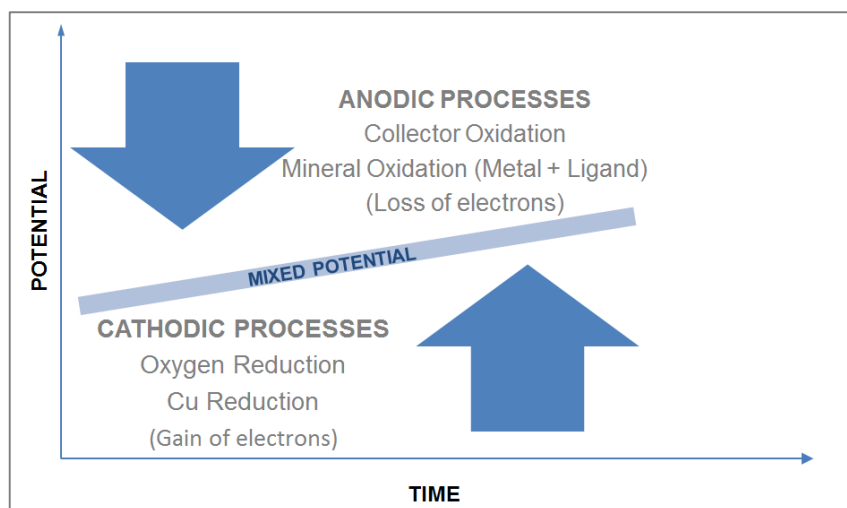


Figure 5.1. Mixed potential response to the addition of reductive and oxidative reactions.

Gibbs energy of reaction is a measure of the spontaneity of a reaction. The relationship between Gibbs free energy and standard potential for electrochemical reactions is given by Equation (5.2).

$$\Delta G_R = - nFE \quad (5.2)$$

where n = stoichiometric coefficient, F = Faradays constant

The spontaneity of a reaction increases in the direction of decreasing Gibbs energy. According to Equation (5.2) the potential will have an opposite sign to the Gibbs energy of reaction.

Analysis of the electrochemical measurements made experimentally involves prediction of reactions and calculation of the equilibrium potential at which these reactions would occur by calculating the Gibbs energy of reaction from literature values for the species. Data for the calculations of equilibrium potentials are presented in Appendix C. It should be noted that the equilibrium potential for the formation of the dimers of the thiol collectors were however measured experimentally these results are discussed later. All reactions in this chapter have been expressed following IUPAC conventions of representing reactions as reduction reactions, whilst the equilibrium potentials are calculated from standard potentials.

The structure of this study was therefore in three parts. The first part involves the study of the equilibrium potentials for the formation of oxidised collector and mineral species. The second part relates to measurements of rest potential to investigate the formation of bulk species at the mineral surface under various conditions at the open circuit. The third part involves cyclic voltammetry which was used to determine the possible mechanisms of formation of the oxidised species at the surface.

5.1 Equilibrium Potential Results

Anodic polarisation of a platinum electrode in a solution of SEX was used as a technique to determine the equilibrium potential for the dimerization of the collector at given solution conditions. The open circuit potential after anodic polarisation is the dimerization potential of the collector. The time dependent profile of the potential measured is also an indicator of the stability of the species formed i.e. dixanthogen etc at the metal surface. Three different concentrations for each collector were investigated and the Nernst equation was used to determine the standard potential. It has already been shown by Majima and Takeda, (1968) that the oxidation of SEX is known to follow Nernstian behaviour. The results obtained in this study are consistent with that observation. Figure 5.2 shows that in the case of the oxidation of SEX and DTP on a Pt electrode, a very good fit was observed between Nernstian behaviour (dotted line) and the experimental data points. A standard deviation of 0.001 V was calculated from data in Table 4.1. Figure 5.2 also shows that there is decreasing correlation between the experimentally measured results for MTP and DTPI and Nernstian behaviour. Given that the focus of this study was specifically aimed at the study of SEX and DTP and not MTP and DTPI, this poor correlation was not investigated further.

Allison et al. (1972) state that the standard oxidation potential (E°) for SEX to dixanthogen lies between -0.037 and -0.060 V, whilst Majima and Takeda, (1968) measured this potential to be -0.049 V. In this work the potential was measured to be -0.040 V which falls within the range given by Allison et al. (1972) and is within 0.009 V of the value given by (Majima and Takeda, 1968).

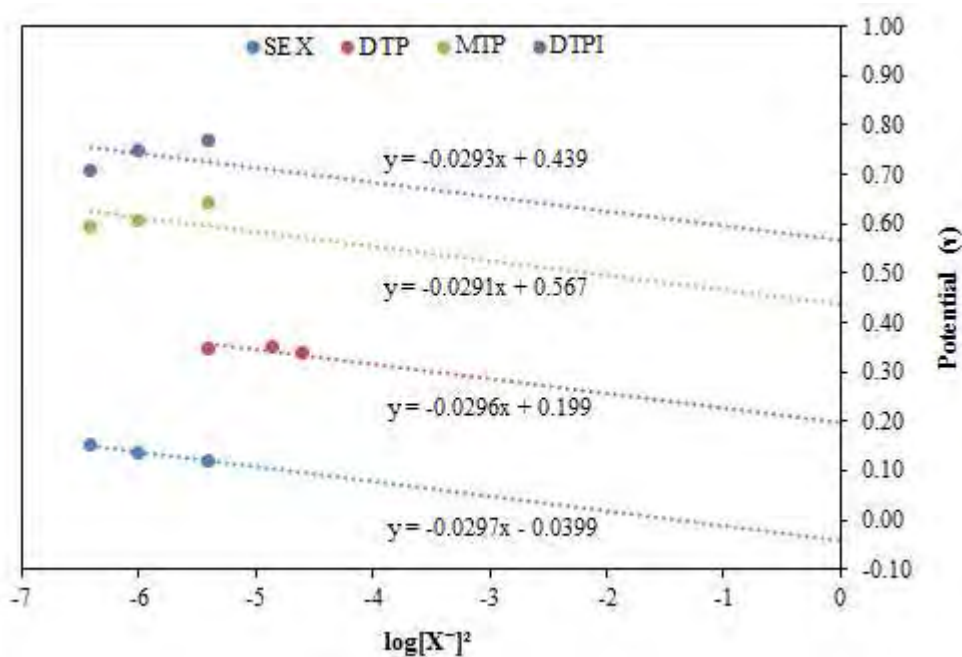


Figure 5.2. Oxidation potentials of the thiolate/dithiolate formation potential of SEX, DTP, MTP and DTPI at pH 9.2.

The dimer of DTP is bis-(diethoxythiophosphyl)-disulphide (DTP_2) which is reported to form at a standard potential of 0.260 V in Chander and Fuerstenau, (1974) and 0.250 V in Finkelstein and Goold, (1972). Values for this standard potential obtained in this work show a scatter in the experimentally determined equilibrium potentials such that the calculated standard potentials from the Nernst equation have an error of 0.011 V between them. These were used to extrapolate the equilibrium potential of DTP_2 formation at a concentration of 6.24×10^{-4} M by taking the arithmetic mean of the calculated standard potentials. The standard potential of DTP_2 determined in this manner was 0.199 V (Table 4.4) which compares reasonably well with the literature values reported above. The difference observed may be attributed to the fact that DTP_2 is an unstable compound and decomposes albeit slowly to form (MTP) diethyl monothiophosphate, diethyl dithiophosphoric acid (HDTP) and bis(diethoxyphosphoryl)-trisulphide (DTP_2S) (Chander and Fuerstenau, 1974).

The high oxidation potentials observed in the formation of the dimer of the phosphate collectors used in this study signifies that under strongly reducing conditions it is unlikely that the dimer will be present. Xanthates on the other hand have significantly lower oxidation potentials and therefore it is expected and has been shown in the literature that most minerals can catalyse the dimerization of SEX.

5.2 Rest Potential Measurements

5.2.1 Validation of rest potential measurement technique

Validation of the rest potential measurement technique was done to reproduce the work of Allison et al. (1972) and also to establish the degree of reproducibility of the experimental procedure. A comparison was made between the results obtained in this study and those of Allison et al. (1972). A summary of these results was shown in Table 4.6 and indicated a standard deviation of the three repeats to be 0.005 V for pyrite and 0.017 V for galena. The table also shows that the results are similar to those reported in the literature. Figure 4.1 and Figure 4.2 showed repeatability of the rest potentials to be within ± 0.005 V of one another.

The rest potential measurements determined for the galena-SEX and pyrite-SEX systems are shown in Figure 4.3 before and after collector addition. It should be noted that these measurements were made at pH 9.2 under aerated solution conditions. When the rest potential of a mineral in a solution is positive relative to the equilibrium potential of the collector (SEX - 0.15 V) this is indicative of possible oxidation of the collector on the mineral surface to form, in the present study, the dithiolate. When the mixed potential is negative relative to the collector equilibrium potential, oxidation of the collector to form the dithiolate is not possible.

Results obtained in this study for galena (Figure 4.3) are similar to the rest potential values obtained by Finkelstein and Poling, (1977) viz-0.035 V noting that their experiments were carried out in an oxygenated solution at an SEX concentration of 10^{-4} M. The potential measured in Figure 4.3 were determined at an SEX concentration of 6.24×10^{-4} M. From a thermodynamic point of view Figure 4.3 indicates that dixanthogen is the likely species formed on the pyrite surface after collector addition unlike galena. For reasons explained above, dixanthogen would not be the dominant species on galena surfaces but rather the metal xanthate (PbX_2). This is consistent with previous results shown in the literature (Allison et al., 1972; Finkelstein and Poling, 1977; Woods, 1971; Yoon and Basilio, 1993).

In Figure 4.4 the addition of DTP to both galena and pyrite shows an interaction of the collector with both minerals. The oxidation potential of DTP is however more anodic than the rest potentials of both minerals and therefore it is unlikely that any interaction would yield DTP_2 . This is consistent with the findings of Finkelstein and Poling, (1977) who reported that the metal thiol species was found on the surface. On pyrite surfaces the species formed by DTP is reported to be the dimer by Finkelstein and Goold (1972). In this work it was found that the rest potential of the DTP-pyrite system was 0.250 V which was lower than the equilibrium potential of DTP which was measured to be 0.388 V under these conditions. This indicates that, the dimer is not likely to form on pyrite and is therefore not consistent with the proposals of Finkelstein and Goold, (1972). It should be noted that in the latter study no direct measurements were made of this system.

The magnitude and rate of decrease in potential upon collector addition is a possible indicator of the extent to which the collector interacts with the mineral (Buswell et al., 2002). Figures 4.3 and 4.4 show that the change in potential when DTP is added to the solution for both galena and pyrite is lower than when SEX is added. Therefore this indicates that DTP is a weaker collector than SEX i.e. it does not react as extensively with mineral surfaces as, for example, xanthates. This is consistent with what has been proposed in the literature (Somasundaran, 2006). The weaker interaction of DTP with pyrite and galena may be due to the high dimerization potential of DTP compared to SEX.

Results obtained in the investigation of the interactions between xanthates and dithiophosphate with galena and pyrite serve to confirm that the experimental procedure used in this study produces results which are consistent with those of previous similar studies reported in the literature.

5.2.2 Rest potentials of platinum minerals in the presence of SEX

Rest potentials for Pt minerals at pH 9.2 and pH 4.2 are shown in Figure 4.5 and Figure 4.6 respectively. Pt metal has the most anodic rest potential in the presence and absence of collector which is consistent with the inert characteristics of Pt metal that make it useful as a counter electrode in electrochemical

processes. Within a certain potential range Pt metal does not oxidise but forms an electrical double layer in solution. Chemisorption of dissolved oxygen occurs on Pt surfaces followed by a reaction to form PtO (Reaction (5.3)) with the corresponding reduction reaction being the cathodic reduction of oxygen (Reaction (5.1)).



Equilibrium potentials for the formation of PtO on Pt metal surfaces are thermodynamically calculated to be 0.464 V and 0.760 V at pH 9.2 and pH 4.2 respectively. The increase in the equilibrium potential for the formation of PtO at lower pH values is expected because the reduction of oxygen increases by 0.059 V with each unit decrease in pH. A combination of the chemisorption of oxygen to form Pt-OH and subsequent formation of PtO is attributed to the rest potentials in the absence of collector for Pt as observed in Figure 4.5 and Figure 4.6.

Rest potentials of the minerals PtS and PtTe₂ in solution are less negative than that of Pt metal. A lower rest potential indicates greater ease of oxidation of these minerals. Oxidation of these minerals can result in the formation of PtO on the mineral surface. Unlike Pt metal, however additional oxidation reactions occurring on PtS and PtTe₂ at potentials less negative than the oxidation of Pt result in lower rest potentials. It is proposed that the oxidation reaction of PtS could follow that of base metal sulphides to form a metal oxide at the surface, Reaction (5.4);



Equilibrium potentials for this reaction are calculated to be 0.021 V at pH 9 and 0.317 V at pH 4, which are lower than those for the PtO/Pt couple. The equilibrium potential decreases as a result of the oxidation of sulphur to sulphate species. This results in the oxidation of PtS occurring at lower potentials than the PtO/Pt couple.

Reactions for PtTe₂ likewise are also determined by the oxidation of tellurium present within the mineral. It was reported by Elvy et al. (1996) that PdTe oxidises to form a TeO₂ layer at the surface of the mineral, indicating the oxidation of tellurium from the surface of the mineral. Since Pd and Pt have fairly similar elemental properties (both in the same group) it can be expected that tellurium at the mineral surface of PtTe₂ will form a similar species in aqueous solution. Pourbaix speciation diagrams for Te-O-H₂O system indicate that the TeO₃²⁻ species is stable over a pH range of 3 – 14 and an Eh above 0 V. As a result this is the species most likely to be formed at a telluride mineral surface in the solution conditions used in this study since the Eh was above 0 V as indicated by the rest potential of Pt (Figure 4.5).

In the presence of collector the rest potential of Pt and PtS are above that of the xanthate dixanthogen potential indicating the likelihood of the formation of dixanthogen at the mineral surface. As already

indicated previously potential-time transients on addition of the collector is indicative of the rates of the surface reactions occurring, viz. the reduction of oxygen and oxidation of SEX. In the case of Pt and PtS, the exponential decrease of the potential, which reflects a high rate of the surface reaction, will probably result in increasing coverage of the platinum surface by dixanthogen which inhibits electron transfer processes for both of these reactions. The higher rest potential for Pt at pH 9.2 can be attributed to the greater electro-catalytic activity of Pt resulting in higher rate of oxygen reduction and therefore higher mixed potential compared to PtS.

The final rest potential of PtTe₂ shows that collector oxidation to dixanthogen is not thermodynamically favoured and as a result this species is not likely to adsorb on this mineral surface. The shape of the potential-time transient observed in Figure 4.5 shows a rapid decrease in potential followed by an increase in potential. Since the reaction responsible for the rapid decrease in potential cannot be the formation of dixanthogen on the surface there are two alternative reactions that can occur. The mechanism of xanthate adsorption has been described as occurring through a chemisorption reaction. According to Buckley and Woods, (1997) chemisorption is thermodynamically favoured and thus occurs at lower potentials than that for formation of the dithiolate. Chemisorption could thus be responsible for the rapid decay of the potential on addition of the collector. It is also possible that a Te-thiolate complex could be the product of reaction in addition to the PtX₂. The slow subsequent increase in potential could reflect conversion of the chemisorbed Thiolate species into one or both of these thiolate complexes on the surface.

In acidic solution conditions (pH 4.2), the effect of collector is significantly different and results shown in Figure 4.6 identify dixanthogen to be the thermodynamically preferred species adsorbing on the mineral surface. Rest potentials of Pt and PtS decrease in potential compared to those occurring at pH 9.2 whilst that of PtTe₂ increases. Dixanthogen is formed by the catalytic effect of the mineral surface, and therefore it is evident that under acidic conditions PtTe₂ has a greater electro-catalytic capability to facilitate the formation of dixanthogen than under alkaline conditions.

5.2.2.1 Cathodic and Anodic Polarisation of PtTe₂ and PtS

Figure 4.7 and Figure 4.8 show the effect on the rest potentials of PtTe₂ and PtS after cathodically and anodically polarising the mineral surface. Cathodic polarisation of the mineral surface has a cleaning effect on the mineral whilst anodic polarisation simulates the oxidation of the mineral.

Results show that anodic polarisation had no significant effect on the rest potential of PtTe₂ surface before and after collector addition. The result indicates that the mineral surface remains the same even after oxidation at potentials up to 0.6 V. Such behaviour can be attributed to the occurrence of the same

oxidation reaction/reactions occurring within the potential range up to 0.6 V. No evidence of passivation due to oxidation products is observed. Similar to the anodic polarisation condition, that for cathodic polarisation showed that no significant change was observed for the rest potential of the mineral prior to collector oxidation. Thus there is an indication that there were no oxidised species at the mineral surface prior to rest potential measurements.

After collector addition the rest potential of PtTe₂ was below 0.15 V and the rest potential profile did not deviate significantly except at 0.6 V. After anodic polarisation of the mineral at 0.6 V the rest potential profile of the mineral after collector addition lies below that of the mineral at all other conditions. This indicates a lower rate of oxidation of initially adsorbed species to the formation of what is proposed to be a PtX₂ species.

On a PtS surface anodic and cathodic polarisation have a more significant effect on the rest potential of the mineral prior to collector addition than after collector addition. Rest potentials show that anodic polarisation increases the rest potential in the solution and cathodic polarisation has the effect of reducing the rest potential. Increase in rest potential is due to oxidation of the mineral surface resulting in passivation of the surface whilst cathodic polarisation of the mineral surface results in cleaning of the mineral surface. This is evidence of the fast oxidation kinetics of the PtS surface. The mineral surface generated after oxidation of the mineral has no effect on the final rest potential after collector addition.

5.2.3 Rest potential measurements of palladium minerals in SEX

For Pd minerals the equilibrium potential for the oxidation of Pd metal given by Reaction (5.5) is lower than that for Pt, viz. 0.560 V at pH 4 and 0.265 V at pH 9.2.



Thus, the mixed potentials of the Pd electrode in the absence of collector are lower than those of Pt. For the Pd minerals it can be seen from Figures 4.10 and 4.11 that the changes in mixed potential measured in the case of pure Pd after the addition of SEX was not significantly affected by changes in pH, although at pH 4.2 a more positive mixed potential is observed in the absence of collector on the mineral surface compared to pH 9.2. Since Pt and Pd belong to the same valence group (10) they may be expected to have similar electro-catalytic properties with the kinetics of oxygen reduction being slower on Pd than Pt. This may account for the results in Figures 4.10 and 4.11 which show Pd to have a lower rest potential (0.204 V) than Pt (0.264 V) after collector addition. Rest potentials of PdTe₂ and PdS in SEX free solution are very similar to those of the corresponding Pt minerals. As in the case of PtS, the

potential of PdS in the absence of a collector could be due to oxidation of the sulfide to the oxide by Reaction (5.6) that has an equilibrium potential at pH 4 of 0.256V and -0.040 V at pH 9.2



In the presence of collector at pH 9.2 the final rest potential of the Pd minerals in a solution of SEX indicates that dixanthogen is favoured to form on Pd and PdTe₂, whose rest potentials are positive relative to the potential required to form the dithiolate. The same is not true for PdS which has a final rest potential which is slightly lower than this potential. The reverse was found to be true for PtS and PtTe₂. In the case of PdTe₂ the rest potential is almost the same as the equilibrium potential of xanthate, viz. 0.153 V. It is of interest that the variation in the mixed potential of PdTe₂ with time (potential transient) is similar to that of PtTe₂, and that this is also possible evidence of two reactions in series. As previously proposed, the initial reaction may be chemisorption of collector. This is followed by a second reaction which is the oxidation of the adsorbed species. For the sulphide mineral the final mixed potential of PdS is slightly negative to the equilibrium potential of SEX and this indicates that the collector will not oxidise to the dithiolate on this mineral surface. This is unlike PtS which did favour the oxidation of the collector to its dimer and is possibly an indication of differences in the rate of oxygen reduction on both surfaces. Under acidic conditions, high potentials relative to those under alkaline conditions prior to collector addition are observed as expected and as shown in Figure 4.11. The rest potentials of all the minerals exhibit the same behaviour under acidic conditions as in alkaline conditions, indicating that the nature of the final species at the mineral surface possibly remains unchanged by pH.

5.2.3.1 Cathodic and Anodic Polarisation of PdTe₂ and PdS

Anodic polarisation of the mineral showed no significant effect on the rest potential profile of PdTe₂ except at a potential of -0.6 V which results in lower rest potential prior to collector addition. After collector addition dixanthogen was observed to be thermodynamically favoured at the mineral surface. The mineral surface after oxidation at 0.6 V has a resulting rest potential that is below the dixanthogen oxidation formation potential. It is evident that the extent of oxidation reduces the probability of formation of dixanthogen at the mineral surface.

Polarisation of PdS surface has the most significant effect on the mineral prior to collector addition at 0.6 V. Polarisation of PdS cathodically and anodically has an effect on the rest potential of the mineral after collector addition. Rest potentials indicate resulting passivation due to oxidation of the mineral surface. After collector addition the rest potentials on the mineral vary in potential but remain below the dixanthogen formation equilibrium potential line. The rest potentials after anodic polarisation are

higher in the presence of collector than after cathodic polarisation but this has no bearing on the bulk collector species formed on the surface.

5.2.4 Rest potential of platinum group minerals in the presence of DTP

5.2.4.1 Rest potential of platinum minerals in DTP

With the exception of possibly Pt the rest potentials in the presence of the collector show that the formation of the dithiolate is not favoured on the mineral surfaces at pH 9.2 and pH 4.2 as seen in Figure 4.14 and Figure 4.15. Chander and Fuerstenau, (1974) conducted an electrochemical study of the interaction of DTP on Pt metal and they proposed that the mechanism of collector adsorption initialised with chemisorption of DTP to form Pt-DTP which further oxidises to form DTP_2 at the metal surface. Taking note of the fact that the rest potential of Pt is close to the equilibrium potential of DTP then the mechanism resulting in the formation of DTP_2 , as reported by Chander and Fuerstenau, (1974), is a possibility on Pt metal. $PtTe_2$ and PtS are likely to form $PtDTP_2$ since the rest potentials are well below the dimerization oxidation potential at both acidic and alkaline conditions.

5.2.4.2 Rest potential of Pd minerals in DTP

The rest potentials of Pd minerals being lower than those of Pt yield significantly different results in the presence of DTP than in the presence of SEX. The dithiolate form of DTP is only favoured on Pd metal at acidic conditions (pH 4.2). At pH 9.2 the metal thiol species ($Pd(DTP_2)$) is most likely to be the preferentially formed and adsorbed species on Pd, PdS and $PdTe_2$ whilst the species is likely to be responsible for the rest potential of PdS and $PdTe_2$ at pH 4.2.

5.2.5 Summary of Rest Potential Results

Species present at PGM surfaces at the rest potential are collector species formed in multi-layers. Final rest potentials under the given conditions have shown the species likely to be the dominant species on the mineral surface. Comparison with pure metal behaviour, oxidation potential for dimer formation of the collector has enabled the determination of what would be the bulk collector species formed at the mineral surface. Whereas the telluride minerals exhibited similar behaviour as far as rest potential profiles were concerned, the potential region of the final rest potential exhibited differences suggesting that dixanthogen was more likely to be formed on $PtTe_2$ than on $PdTe_2$ at pH 9.2. A change in the potential transient on telluride minerals suggests that multiple species are formed at the surface due to

xanthate and that the species formed can oxidise further to form a secondary species. Sulphide minerals on the other hand exhibited a steady rest potential due to formation of oxidised collector species. At pH 9.2, PtS had greater rest potential than that of PdS and was more likely to form dixanthogen than the latter mineral.

Tellurides and sulphides show differences in the mechanisms of collector interaction with SEX at pH 9.2. At pH 4.2 the reactions due to any collector on the mineral surfaces all yielded the same response with rest potentials falling in the same regions. This suggests that at pH 4.2 dixanthogen in the presence of SEX is the favoured species formed. DTP on the other hand did not show any distinction with respect to the species formed on mineral surfaces, resulting in formation of the metal thiolate species on all minerals. This is however attributed to the high dimerization potential of the collector rather than the catalytic capabilities of the mineral surfaces.

5.3 Cyclic Voltammetry Study

5.3.1 Validation and Reproducibility of Measurements

Woods, (1971) measured the cyclic voltammogram for galena in a 0.1 M $\text{Na}_2\text{B}_4\text{O}_7$ solution in the absence and presence of 9.5×10^{-3} M SEX. In the voltammogram measured by Woods, (1971) an oxidation peak between -0.2 V and 0.2 V was observed prior to an increase in current which was attributed to a second reaction. Woods attributed these two reactions to, firstly, chemisorption of xanthate ions on the galena surface to form Pb-X, where X denotes a xanthate molecule. The second reaction was attributed to the formation of a metal thiolate species (PbX_2) on the galena surface. Figure 4.20 shows the results obtained in this study in which the system used by Woods was replicated. Two sweep rates were investigated which showed, as expected, an increase in currents measured with increasing sweep rate. The reduction peak shown in Figure 4.20 which is due to the reduction of chemisorbed xanthate occurs at -0.4 V which is occurring in the same potential range as that observed by Woods, (1971). The similarity between these results and those observed by Woods serve to validate the experimental procedures being used in this investigation. Moreover, it was also observed that the system used in this study yielded reproducible results. A significant number of the voltammograms measured in this study were duplicated with a view to ensuring on an ongoing basis the reproducibility of the measurements made.

5.3.2 Cyclic voltammetry measurements using SEX

5.3.2.1 Pt metal measurements

The voltammograms for Pt in the presence of SEX have been measured by Woods, (1971) and in the presence of DTP by Chander and Fuerstaneau, (1974). In the present work measurements for Pt metal were made over a potential range of ± 0.4 V from a starting potential of 0.22 V which is the open circuit potential of Pt prior to the measurement of the voltammograms. Woods, (1971) ascribed the peaks occurring between -0.46 and 0 V to the adsorption and desorption of hydrogen. Chander and Fuerstaneau, (1974) ascribed the peaks occurring above 0 V to the adsorption and desorption of oxygen. In the region of 0 V there are no currents because Pt is inert and it establishes a double layer before reaction (Chander and Fuerstaneau, 1974). In the current work, in an aerated solution from a potential of 0.2 V the anodic currents in the absence and presence of collector did not show any significant differences (Figure 4.21). This does not however disregard reactions taking place at the surface and differences in the reduction currents generated during reverse sweeps gave evidence that such reactions may be occurring. Reduction of dissolved oxygen is responsible for cathodic currents (Figure 4.21(a)) since the solution was aerated allowing for oxygen to react on the mineral surface. As would be expected these cathodic currents were significantly reduced in the de-aerated solution (Figure 4.21(b)) since the dissolved oxygen concentration under these conditions was $\approx < 0.50$ ppm compared to the value observed for an aerated system of approximately 8 ppm. This very low concentration of oxygen could however account for the reduction current in the absence of collector. Greater reduction currents in the presence of SEX (Figure 4.21(b)) are indicative of the reduction of an oxidised collector species. The potential region viz. < 0.2 V is consistent with this reduction current being due to the reduction of dixanthogen which is the oxidised collector species. It has already been shown via rest potential measurements that dixanthogen does form on Pt metal.

5.3.2.2 Cyclic voltammetry of PtTe₂

5.3.2.2.1 Reactions of PtTe₂ in the absence of SEX

The reactions of PtTe₂ in solution have been previously studied using cyclic voltammetry (Vermaak et al., 2005, Vermaak et al., 2007) and it was observed that PtTe₂ exhibited significant anodic activity at potentials greater than 0.3 V in the absence of SEX. It was previously suggested (Section 5.2.2) that oxidation of PtTe₂ might result in the formation of tellurite ions (TeO₃²⁻) (Figure 4.5 and Figure 4.6).

By using the standard Gibbs energy of formation the equilibrium potentials of the oxidation of PtTe₂ can be estimated. Potentials shown below (Reactions 5.7 – 5.10) are estimates for the equilibrium

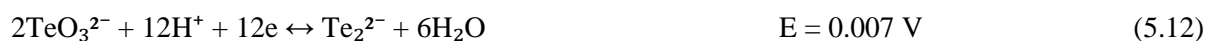
potentials for reactions of PtTe₂ resulting in the formation of tellurite ions calculated at pH 9.2 and a concentration of soluble tellurite ions of 10⁻⁴ M.



In aerated and de-aerated solutions solution conditions anodic currents starting from 0.3 V (Figure 4.22(a) and (b)) can be attributed to any of the Reactions (5.7) – (5.10). The commencement of the second sweep from a potential of 0.2 V suggests that Reactions (5.7) and (5.8) were more likely to be responsible for the anodic currents observed. Furthermore it is unlikely that reactions (5.9) and (5.10) were occurring because the over-potentials would have to be very low to account for measurable current at potentials only slightly higher than the equilibrium potentials.

The proposal that Reaction (5.7) is due to the oxidation of PtTe₂ is supported by the study conducted by (Elvy et al., 1996) (cf. 5.2.2). It is therefore likely that Reaction (5.7) is also responsible for the rest potential of the mineral in a solution where no collector is present (cf. Figure 4.5). It was also found (Figure 4.7) that anodic polarisation of the mineral up to a potential of 0.6 V did not yield any passivating products on the mineral surface and had no significant effect on the collector species subsequently formed. Therefore the formation of a soluble tellurite species from the oxidation of PtTe₂ is supported and that Reaction (5.7) is the preferred reaction occurring at the mineral surface.

Although the tellurite species likely to be formed would dissolve into the aqueous phase reactions involving the species at the mineral surface cannot be discounted. Reactions (5.11) – (5.13) were proposed by Mishra et al., (1990) for the reduction of a tellurite species in aqueous solution. Potentials were calculated at pH 9.2 and a tellurite concentration of 10⁻⁴ M.



There is no evidence of Reaction (5.11) and Reaction (5.13) occurring on the mineral surfaces in any of the voltammograms measured for PtTe₂ in the absence of collector. Reaction (5.12) could account for the reduction currents observed (Figure 4.22(b)) from a potential of -0.3 V thus indicating that it is possible that reactions involving tellurite species may be occurring at the mineral surface. Specifically

this implies that in the reverse sweep tellurite species present at the mineral solution boundary may be reduced according to Reaction (5.12).

In order to reduce the effect of mineral oxidation the anodic activity of PtTe_2 was measured over a potential range of ± 0.4 V (Figure 4.23 and Figure 4.24). The shape of these voltammograms remains unchanged for two consecutive potential sweeps showing that over this potential range the surface of PtTe_2 was not permanently altered. A reduction current which can be attributed to Reaction (5.12) was also observed to commence from -0.3 V in de-aerated solution over a potential range of ± 0.4 V (Figure B.3(a) and (b), Appendix B) thus indicating the possibility of the reduction of TeO_3^{2-} to Te_2^{2-} .

Low cathodic currents on PtTe_2 surfaces in aerated solutions (cf. Figure 4.21(a), Figure 4.22 and Figure 4.23) are also due to reduction of dissolved oxygen and the commencement of these currents below a potential of about 0.2 V indicates that PtTe_2 surface is a poor promoter of oxygen reduction. This contrasts with the behaviour of Pt metal as discussed in Section 5.3.2.1 where it was shown that large cathodic currents are due to high rate of oxygen reduction.

Reactions (5.7) to (5.10) predict increased anodic activity at high pH values which is shown in Figure 5.3. Comparison of the cathodic currents at all pH values in aerated (Figure 5.3) solutions in the absence of SEX shows little difference at potentials below about 0.1 V which suggests that reduction of oxygen to OH^- is slow on an oxidised PtTe_2 surface.

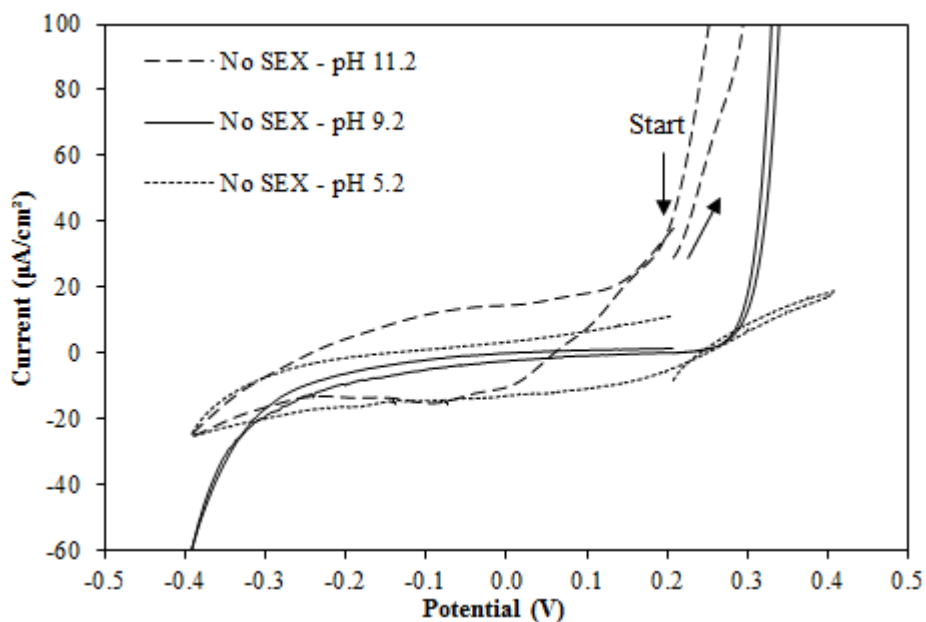


Figure 5.3. Cyclic voltammograms for PtTe_2 in an aerated solution in the absence of collector over varied pH levels.

5.3.2.2.2 Reactions of PtTe₂ in the presence of SEX

In the presence of SEX (Figure 4.22(a) and (b)) over a potential range of ± 0.6 V, anodic currents commenced at potentials more positive than those observed in the absence of collector indicating that the presence of collector at the surface appeared to inhibit the oxidation of the mineral. Over the narrower potential range of ± 0.4 V, reduced anodic currents were also observed in the presence of SEX (cf. Figure 4.23 and Figure 4.24) confirming the presence of SEX at the surface. The second indicator of collector oxidation at the mineral surface is the presence of two reduction current peaks which were observed (Figure 4.22(a), Figure 4.23 and Figure 4.24) and are due to the presence of oxidised collector species. These peaks are observed between the potentials of 0 V and 0.2 V.

In the presence of SEX the mineral was linearly polarised up to 0.207 V from the starting potential of 0 V using linear sweep voltammetry (Figure 4.25(a)) or anodically polarised at 0.207 V for 15 minutes (Figure 4.25(b)). This was followed by subsequent stripping of the surface in both cases using linear sweep voltammetry. Figure 4.25(a) shows that there are negligible currents due to mineral oxidation but positive currents due to the presence of SEX. The return linear sweep clearly indicated that collector oxidation occurs at potentials below 0.207 V. In Figure 4.25(b) the two reduction peaks P1 and P2 are observed once again. Figure 5.4 shows current time transients for PtTe₂ during anodic polarisation at a potential of 0.207 V. The measurements were made in duplicate as shown in Figure 5.4 and indicate that there are oxidation reactions taking place at the mineral surface which are identified as current peaks. Currents in Figure 5.4 occurring before ≈ 20 s can be attributed to the formation of P2 which is instantaneous whilst the formation of P1 occurs after the formation of P2.

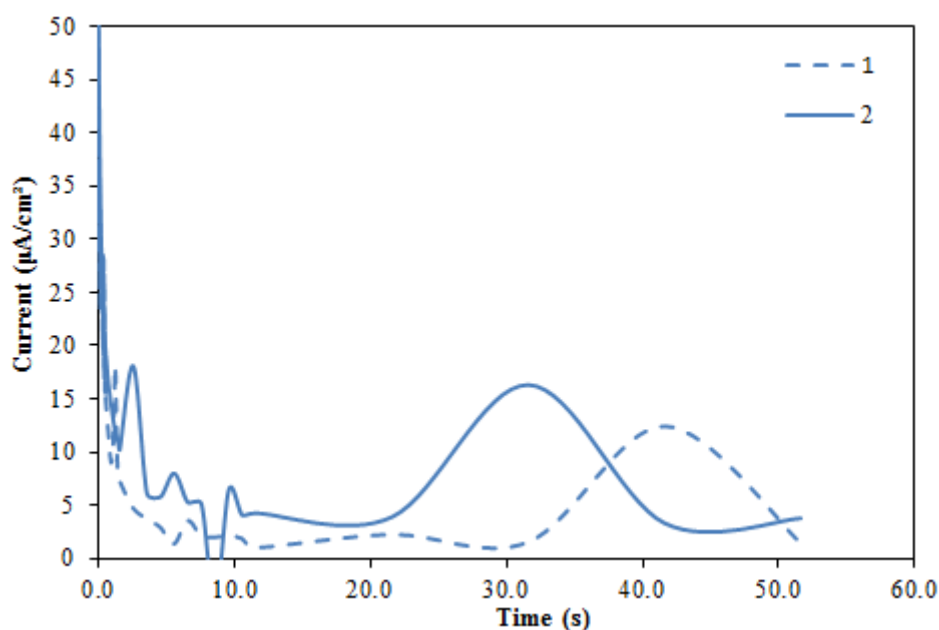
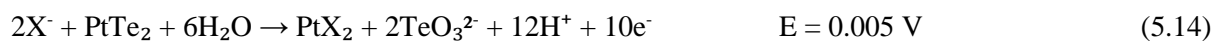


Figure 5.4. Current – time curves for PtTe₂ anodically polarised at 0.207 V in an aerated solution for Figure 4.25(b). The solid line and dotted line represent repeat measurements.

The effect of sweep-rate (cf. Figure 4.28) on the voltammograms generated on PtTe₂ was investigated by increasing the sweep-rate to 50 mV/s and reduced to 1 mV/s. No significantly notable changes to the peaks generated on the mineral surface are observed indicating that the reactions occurring are reversible and that there are only two species present on the PtTe₂ surface and these will be shown to be PtX₂ and X₂.

Oxidation of SEX to form dixanthogen has already been established as taking place at a potential of 0.15 V. Formation of the metal thiolate PtX₂ species from PtTe₂ is proposed to take place according to Reaction (5.14) which has an equilibrium potential calculated from Gibbs energy of formation to be 0.005 V. According to Buckley and Woods, (1993), Chander et al. (1979) and Woods, (1971) chemisorption occurs at potentials less negative than the formation of a metal thiolate species formation and the formation of dixanthogen and therefore would occur on PtTe₂ at potentials less negative than 0.005 V.



In Figure 4.23, which shows two sweeps for the mineral for a reverse going initial sweep under aerated conditions, the return cathodic sweep yields P1 commencing from a potential of ≈ 0.25 V whilst P2 occurs below 0.15 V. In Figure 4.24, for a single forward going sweep, P1 occurs below 0.15 V and P2 at ≈ 0.045 V and this was the same under de-aerated solution conditions. Due to the proximity of the peak P1 to the reduction potential for dixanthogen this peak can be attributed to the reduction of dixanthogen formed at the mineral surface during the anodic sweep. Reaction (5.14) predicts the potential at which the formation of PtX₂ is more thermodynamically favourable than the formation of dixanthogen and therefore P2 can be attributed to the reduction of a metal thiolate species.

The results illustrated in Figure 4.25(b), which show the reduction of species formed from anodic polarisation of the mineral at 0.207 V, also indicate that the collector species formed are within the potential region for dixanthogen reduction and the potential region for metal thiolate reduction. These voltammograms show that peak P2 is far more prominent than P1 which indicates that the formation of PtX₂ is more thermodynamically favoured at 0.207 V. These results show that at these conditions dixanthogen formation would be limited by the low over-potential (0.207 V – 0.150 V) available for formation of the species.

Higher collector concentration results in a higher concentration gradient between the bulk phase and the mineral surface. It was thus expected that the current measured would be greater at increased concentrations and the results shown in Figure 4.27(a) and (b) confirm this. Higher concentration of collector at the mineral surface completely inhibited mineral oxidation and it was observed that the oxidation current peaks generated at the mineral surface were consistent with dixanthogen formation. This was because the peaks occurred at potentials above the dixanthogen oxidation potential. Reduction

current peaks showed the dominance of dixanthogen at the mineral surface because the reduction current associated with this oxidation i.e. first reduction peak, was much greater than the second reduction peak.

The reduction reaction responsible for P1 is given by the reverse of dixanthogen formation to result in xanthate ions according to Reaction (1.17). It is however not possible to make a definitive assignment to the reaction associated with the reduction of PtX_2 . The reverse of Reaction (5.14) is unlikely as this would constitute the re-formation of the mineral surface. A prediction of the formation of Pt metal and xanthate ions was made for the reduction of PtX_2 according to Reaction (5.15) and the equilibrium potential for three different concentrations was calculated. Calculated equilibrium potentials for this reaction are -0.230 V at 6.25×10^{-4} M SEX, -0.263 V at 2.5×10^{-3} M SEX and -0.322 V at 2.5×10^{-2} M SEX. The potential at which reduction current peak P2 occurs in Figures 4.23 and 4.24 (± 0.4 V potential range) indicates that this reaction cannot be due to Reaction (5.15). However the reduction currents observed at higher concentrations in Figure 4.27(a) and 4.27(b) can coincide with this reaction.



The effect of pH on the reaction mechanisms of SEX on the mineral was shown in Figure 4.26. In the presence of SEX the anodic peak observed at about 0.3 V at pH 5.2 was probably due to oxidation of the collector to the dithiolate because the potential is above the dixanthogen formation potential. This anodic peak was not present in the absence of SEX. Reduction of the dithiolate was observed as a cathodic peak at about 0.08 V. The roughly equal areas under the anodic and cathodic peaks confirm this assignment as did the observation that oxidation of SEX occurred at potentials positive relative to the equilibrium potential (shown as the vertical dotted line) and reduction at potentials negative relative to the equilibrium potential. The same applied to the voltammogram generated at pH 7.0. At pH 11.2, it appeared that no dithiolate was formed as there was only one small cathodic peak at the same potential as P2 measured at pH 9.2. The electrochemical behaviour of $PtTe_2$ might have connotations on the flotation behaviour of $PtTe_2$ at pH above 11.2. Should flotation of a telluride mineral not be observed at these pH levels then it would indicate that dixanthogen which is shown to be absent at these conditions is a critical species to flotation of the mineral.

5.3.2.3 Cyclic Voltammetry of PtS

5.3.2.3.1 Reactions in the absence of SEX

Base metal sulphides and their reactions have been extensively studied, for example, PbS , $CuFeS_2$ and FeS_2 (Buckley and Woods 1987, Buckley and Woods 1994, Gardner and Woods 1979). In each case at pH 9.2 the oxidation product has been found to be an oxidised metal species such as the hydroxide or

oxide form of the metal, and sulphur oxidising to form either a sulphate or sulphite ion. Formation of PtO has already been proposed to account for the rest potential of PtS at pH 9.2 and 4.2 in the absence of collector (Reaction (5.4)). Thermodynamic potentials at which this reaction and other reactions possibly occur on PtS were calculated at pH 9.2 and a concentration for Pt ions of 10^{-4} mol/L. These reactions are as follows;



The reactions above indicate that the formation of the oxide can occur at potentials close to 0 V while dissolution of PtS can occur at potentials higher than ~ 0.15 V which is the equilibrium potential for dixanthogen formation. Oxidation of PtS is evident (Figure 4.29 (a) and (b)) for a potential range of ± 0.6 V, with a peak being formed that can be attributed to Reaction (5.16). Oxidation to Pt^{2+} is less evident over a potential range of ± 0.4 V (cf. Figure 4.30 and Figure 4.31). These two figures show the oxidation of the mineral over a potential range of ± 0.4 V.

In Figure 4.29(a), Figure 4.30 and Figure 4.31 cathodic currents similar to those observed on Pt were observed at potentials below 0.2 V and are due to reduction of dissolved oxygen to OH^- in the aerated solution. These currents indicate a fast initial rate of oxygen reduction which reaches a constant rate at negative potentials. Reduction currents are significantly reduced in de-aerated solution conditions (Figure 4.29(b)) showing that the currents being referred to are indeed a result of dissolved oxygen reduction.

The equilibrium potential for oxygen reduction increases with decreasing pH and as a result oxygen reduction on PtS is observed to commence at more positive potentials at pH 5.2 compared to pH 11.2 (Figure 5.5). Although the changes in anodic activity are not highly significant on the mineral, pH 5.2 has lowest anodic activity which is consistent with the fact that mineral oxidation according to Reaction 5.16 and Reaction (5.4) are expected to occur at more positive potentials in lower pH regions. Decrease in anodic activity on PtS with decreasing pH is more evident in de-aerated solution as shown in Figure 5.6 which compares voltammograms for pH 5.2, 7, 9.2 and 11.2. Reactions (5.4) and (5.16) have equilibrium potentials of -0.009 V and 0.148 V at pH 9.2 respectively whilst they have potentials of 0.287 V and 0.355 V at pH 4.2 respectively.

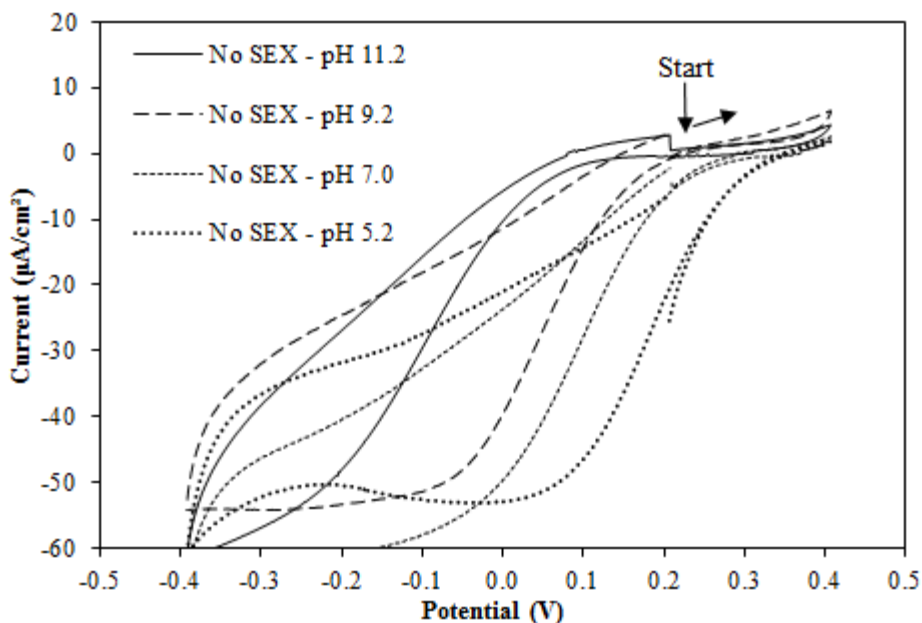


Figure 5.5. Cyclic voltammograms for PtS in an aerated solution in the absence of collector over varied pH levels.

Figure 5.6 shows that at pH 5.2 there is anodic and cathodic activity present between -0.1 V and 0 V, which is not observed at higher pH values. According to the S-H₂O speciation diagrams and speciation diagrams for PtS (cf. Section 2.2.2.2, Figure 2.6) this electrochemical activity at the mineral surface could be due to the oxidation and reduction of sulphate species according to Reaction (5.17) which was calculated to occur at a potential of -0.089 V (10⁻⁴ M SO₄²⁻).

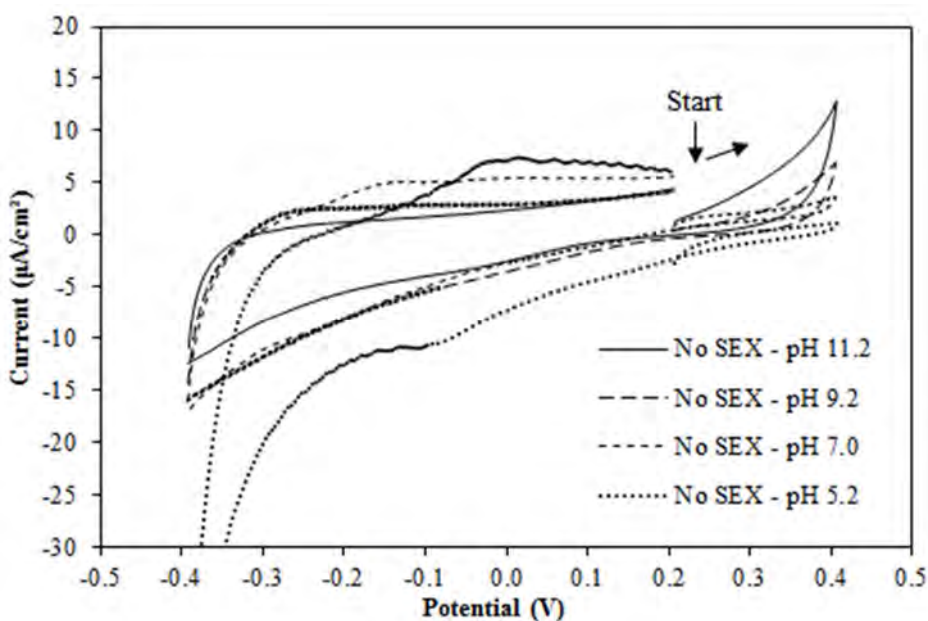
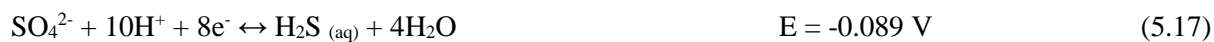


Figure 5.6. Cyclic voltammograms for PtS in an aerated solution in the absence of collector over varied pH levels.

5.3.2.3.2 Reactions in the presence of SEX

As has been discussed, PtS possibly oxidises at potentials above 0.4 V to form Pt^{2+} as indicated in Figure 4.29(a) and (b). In the presence of SEX anodic currents due to formation of Pt^{2+} were inhibited but they were present in de-aerated solution showing that collector coverage did not inhibit this oxidation reaction. Increased anodic currents in de-aerated solution in the presence of SEX compared to the currents observed in the absence of SEX indicate that the collector is oxidised at the mineral surface in the de-aerated case. Since the oxidation currents for the collector were above the dixanthogen formation equilibrium potential the species being formed was more than likely to be dixanthogen.

Lower reduction currents which occur at more negative potentials in Figure 4.29, Figure 4.30 and Figure 4.31 in the presence of SEX compared to those observed in the absence of SEX indicate the inhibition of a reaction that has been concluded to be oxygen reduction. This implies that species formed from oxidation of SEX at PtS surface cover the surface. PtX_2 formation from PtS is predicted from thermodynamic data to occur at a potential of -0.211 V (Reaction (5.18)).



The equilibrium potential for this reaction suggests that it is more thermodynamically favoured than dixanthogen formation and can therefore not be discounted from occurring on the mineral surface. There was no significant electrochemical activity at the PtS surface to suggest that there was any reduction of the species formed at the mineral surface. A study at higher concentrations was made in order to determine whether the lack of reduction currents due to collector species was due to low collector coverage or lack of electrochemical activity of the species. Figure 4.33 showed increasing anodic activity with increasing concentration for SEX, which was due to collector oxidation. There were notably no reduction current peaks due to the collector either. It is clear from Figure 4.33 that the oxidation of SEX favours dixanthogen formation at increasing coverage at higher concentrations. This is consistent with rest potential measurements (cf. Figure 4.5). The lack of reduction currents means that dixanthogen remains at the mineral surface and is the species which imparts hydrophobicity to the mineral.

It was also observed that dixanthogen is the preferred species formed on PtS over a pH range from 5.2 to 11.2. Figure 4.32 showed that increased anodic activity with increasing pH resulted in the species having a greater surface coverage at alkaline conditions than at acidic conditions. Lower collector coverage at acidic conditions might also be due to decomposition of SEX at acidic conditions to its formation components. This is unlike PtTe_2 which showed increased coverage of dixanthogen at acidic conditions which might be due to faster kinetics than PtS.

5.3.2.4 Cyclic Voltammetry of Pd

The behaviour of Pd metal in the absence of SEX is as expected from the literature. The reduction of oxygen is responsible for reduction currents observed from 0.3 V and hydrogen adsorption is responsible for anodic currents at -0.2 V (Figure 4.35(a)). As expected, Figure 4.35(b) shows the absence of the reduction of oxygen in de-aerated solution, but shows hydrogen adsorption currents in aerated and de-aerated solution.

In the absence of SEX, reduction of dissolved oxygen was observed over a potential range of ± 0.4 V (Figure 4.36(a)). The cathodic currents observed are similar to those observed on platinum (cf. Figure 4. 21a). Oxygen reduction currents were absent in de-aerated solution in the absence of SEX (Figure 4.36b). Large cathodic currents at potentials below about -0.3 V are due to the reduction of water to hydrogen thus producing absorption currents.

In Figure 4.35 anodic currents within the region for dixanthogen formation were observed and these occurred at a significantly high over-potential i.e. at potentials significantly above the dixanthogen formation potential. Occurrence of the oxidation peak above 0.3 V indicates that below 0.4 V dixanthogen formation would not be as significant. Consequently dixanthogen formation peaks were not identified in Figure 4.36(a) or (b). Increased anodic activity of the metal in the presence of SEX compared to its absence suggests that the species responsible for SEX oxidation might be the metal thiolate. Although no reduction peaks were identified in the presence of collector, hydrogen evolution was inhibited due to collector coverage on the minerals surface. This behaviour is contrary to what would have been expected of Pd, which was expected to exhibit similar characteristics to Pt metal, given their equivalent valence group number, which showed reduction of dixanthogen at the surface. Although the presence of dixanthogen at the Pd surface within this potential range is not discounted it is more likely that PdX₂ is the more dominant species.

5.3.2.5 Cyclic Voltammetry of PdTe₂

5.3.2.5.1 Reactions in the absence of SEX

PdTe₂ is expected to react in a similar manner to PtTe₂ because it belongs to the same crystal structure group and because Pt and Pd belong to the same valence group. Moreover Pd has been observed to exhibit similar behaviour to Pt metal in the presence of SEX albeit at higher over-potentials. Oxidation reactions for PdTe₂ calculated from thermodynamic data also show that they occur at higher potentials compared to corresponding reactions for PtTe₂. Oxidation reactions for PdTe₂ are given in Reactions (5.19) – (5.23) along with the equilibrium potentials at which they are calculated to occur.





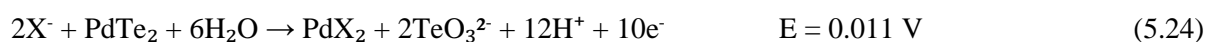
Any or all of these reactions could be responsible for the anodic oxidation currents observed in Figure 4.37(a) and 4.37(b), above a potential of 0.3 V. The almost identical behaviour of PtTe₂ and PdTe₂ is proof that these minerals have almost identical reaction behaviour. Reduction currents are not significant compared to anodic currents and, in a similar manner to that suggested for PtTe₂, are likely to be due to Reaction (5.12).

Oxidation of the mineral is still observed to occur at a high rate from 0.3 V over a narrower range of \pm 0.4 V. Within this range Reactions (5.19) and (5.23) are most likely to be responsible for the oxidation of the mineral.

5.3.2.5.2 Reactions in the presence of SEX

In Figure 4.37 unlike PtTe₂, PdTe₂ does not exhibit clear reduction peaks due to collector species reduction. However, there is evidence of collector interaction on the mineral surface which is identified by mineral oxidation commencing at higher potentials in the presence of collector. Mineral oxidation has more of a significant effect on the Pd mineral than the Pt mineral.

Figure 4.38 and Figure 4.39 are measured under the same conditions as Figure 4.23 and Figure 4.24, for a potential range of \pm 0.4 V. Figure 4.38 and Figure 4.39 for PdTe₂ showed distinct oxidation current peaks due to collector oxidation. These peaks were generated at potentials above the dixanthogen formation potential and it can therefore be concluded that dixanthogen formation occurs. Two reduction current peaks were identified during cathodic sweeps and labelled P1 and P2 and are analogous to those formed on PtTe₂. The same assignment of reactions to P1 and P2 can be made to the PdTe₂ mineral viz. P1 being reduction of dixanthogen and P2 reduction of the metal thiolate species having been formed according to Reaction (5.24).



The more defined anodic X₂ peak on PdTe₂ compared to PtTe₂ is evidence of higher rate of oxidation on PdTe₂ surface than on PtTe₂. Likewise the rate of oxygen reduction is greater on a PdTe₂ surface than on a PtTe₂ surface.

5.3.2.6 Cyclic voltammetry of PdS

5.3.2.6.1 Reactions in the absence of SEX

PdS was measured over a potential range of ± 0.6 V and the results shown in Figure 4.40(a) and (b) for the aerated and de-aerated condition show that oxidation of the mineral in the absence of collector is not significant. Under de-aerated solution conditions (D.O < 0.50 ppm) the oxidation of PdS is accompanied by reduction currents in the reverse sweep between 0 and -0.4 V. Reactions 5.25 and 5.26 may be responsible for this behaviour.



Oxygen reduction is observed to be dominant under aerated solution conditions, much like PtS as was observed in Figure 4.40(a). The behaviour of PdS did not deviate significantly from that of PtS and this may be expected since they both have the same crystal structure and Pd and Pt metal belong to the same valence group. In the absence of collector Figure 4.41 and Figure 4.42 show the voltammograms for PtS over a potential range of ± 0.4 V which are similar to what was observed on Figure 4.40, which in turn shows the same behaviour as that of Pt and PtS.

5.3.2.6.2 Reactions in the presence of SEX

In Figure 4.41 and Figure 4.42 the voltammograms for PdS are similar to those observed for PtS under the same conditions. Increased anodic currents in the presence of SEX compared to those observed in its absence is a clear indication of SEX oxidation occurring at the surface. The potential at which these currents appear is above the dixanthogen formation potential indicating that the species formed is likely to be dixanthogen. Absence of reduction current peaks indicates that the species was not reduced in the cathodic sweep. Consequently reduction of oxygen at the mineral surface was almost completely inhibited. Unlike PdS the reduction of oxygen was not completely inhibited on PtS suggesting that PdS might have greater surface coverage of dixanthogen. In addition, anodic currents on PdS are more distinguished in the presence of SEX than on PtS. It should be noted however that from these voltammograms it is not possible to exclude the occurrence of PdX₂. Calculation of the equilibrium potential of formation indicates that this species forms at a potential of -0.226 V (Reaction (5.27)) which makes the species more thermodynamically favoured than the formation of dixanthogen.



5.3.3 Reactions in DTP

5.3.3.1 Reactions on PtTe₂

Reactions in the absence of collector for all the minerals studied have already been discussed above. Figure 4.43 shows the voltammogram for PtTe₂ in the absence and presence of DTP. In the absence of DTP it has already been shown that oxidation of the mineral surface results in the formation of a soluble tellurite species. At a sweep rate of 10 mV/s in the presence of DTP no oxidation current peaks were identified however the current associated with mineral oxidation was reduced. It would seem that in the presence of DTP, species associated with the collector inhibit mineral oxidation and thus the reduced currents were observed.

A slower sweep rate of 1mV/s was measured on the assumption that the kinetics of DTP oxidation might be slower than those for SEX. Results shown in Figure 4.44 indicate this to be true and an anodic current peak was observed in aerated and de-aerated solution near the dimerization potential of the collector. The rest potential of Pt was found to be close to the dimerization potential of DTP. The peak observed occurs from a potential of about 0.35 V which would not suggest that it is the dimer of DTP. Rest potential measurements showed that dimer formation on the mineral surface is not favoured and it can be proposed that the species formed is the metal thiolate species without discounting a chemisorption reaction. The peak observed however could still be due the dimer being formed at an under-potential enhanced by a low sweep rate. There is no evidence to support the reduction of the adsorbed collector species in the form of current peaks. It is notable that in Figure 4.44a, oxidation of the mineral is more greatly inhibited in the presence of DTP for the aerated condition than for the de-aerated condition, possibly suggesting the importance of the role of oxygen.

5.3.3.2 Reactions on PtS

The behaviour of PtS in the presence of DTP does not differ from that of PtS in the presence of SEX for a sweep rate of 10 mV/s (Figure 4.45). Increased anodic currents in the presence of DTP support the fact that DTP is adsorbed at the mineral surface. Rest potential measurements supported the formation of a metal thiolate species and the high dimerization potential of DTP also excludes the formation of the dimer within this potential range. PtDTP₂ is therefore proposed to be the species responsible for collector oxidation. At a slower sweep rate of 1mV/s the reduction of oxygen at the mineral surface is very significantly inhibited by the presence of DTP at the mineral surface. This suggests that the kinetics of DTP interaction with PtS are slow relative to interaction with SEX and thus greater surface coverage is achieved in Figure 4.46 than in Figure 4.45.

5.3.3.3 Reactions on PdTe₂ and PdS

Voltammograms for PdTe₂ (Figure 4.47) and PdS (Figure 4.48) were measured in aerated solution at a sweep rate of 10 mV/s. The significantly inhibited anodic currents on PdTe₂ in the presence of DTP were evidence of DTP oxidation on the mineral surface. These were more significantly inhibited than on PtTe₂ showing that once again PdTe₂ has greater tendency to oxidise the collector than PtTe₂. Within this potential range it can be concluded that the species responsible for inhibition of mineral oxidation is PdDTP₂ as was concluded from the rest potentials. On PdS, increased anodic currents in the presence of DTP compared to the absence are, as in the case of PtS, attributed to the formation of PdDTP₂. Like PtS reduction of oxygen similarly is inhibited by the presence of DTP at the mineral surface.

5.3.4 Comparison of telluride and sulphide mineral reactions

The objective of this work was not to determine the reactivity of telluride and sulphide minerals in aqueous solutions and therefore an extensive study into the behaviour of these minerals in the absence of collector was not conducted. It is however not possible to determine collector - mineral interactions without having a prior knowledge of the behaviour of the mineral surface before collector attachment or non-attachment of the collector.

In previous work by Vermaak et al. (2005) it was found that the order of decreasing reactivity towards oxidation was PdBi > PdTeBi > PdTe. This was ascribed to electronegativity differences between Bi and Te atoms where Bi is a larger less electronegative atom than Te and therefore a Pd-Bi bond would be weaker than a Pd-Te bond. Similarly Te atoms are less electronegative than S atoms and therefore an M-Te bond is expected to be weaker than a M-S bond (Livingstone, 1965). The difference in bond strength between an M-Te and an M-S bond has been observed in the present study in the anodic behaviour of the telluride minerals which showed larger activity over the potential ranges studied compared to that of the sulphide minerals. Despite this however, this increased anodic activity was shown to not be detrimental to the adsorption of SEX and DTP on tellurides. There was also no evidence to suggest that anodic oxidation reactions on the sulphides in solution had any influence on the adsorption of collector. In fact oxidation of the sulphide mineral was minimal compared to that of the telluride mineral. This was previously noted in Figure 4.8 and Figure 4.13 where anodic polarisation was found to have little effect on the rest potentials of PtS and PdS in the presence of SEX.

Reduction of dissolved oxygen is a key characteristic of the mineral surface which can affect collector adsorption and therefore flotation. It was determined that Pt which is known to be a catalyst for oxygen reduction showed strong reduction currents for dissolved oxygen. Sulphide minerals showed similar behaviour to Pt metal potentially indicating that the catalytic capability of these minerals is comparable

to that of Pt. Although telluride minerals on the other hand exhibited slow rates of oxygen reduction, based on the flotation results of Shackleton, (2007) for micro-flotation tests on PtTe₂ and PdTe₂ (99 % recoveries) this did not have an adverse effect on flotation.

The electrochemical behaviour of tellurides and sulphides in the presence of SEX was different. The relative ease of oxidation of telluride minerals resulted in measurable anodic currents in the presence of SEX due to oxidation of the collector and/or formation of a metal xanthate. The currents observed on sulphide minerals showed little difference compared to those of the mineral in the absence of SEX. Collector adsorption however was identified through the inhibition of oxygen reduction. The reduction of oxygen occurring on sulphide minerals however indicates that there was incomplete coverage of the mineral surface due to the adsorption of collector resulting in the original surface reducing oxygen. PdS showed greater inhibition of oxygen reduction than PtS suggesting a greater coverage on PdS surfaces than the corresponding Pt mineral. Oxidation of collector on telluride minerals indicated that the collector species which formed on telluride minerals were electrochemically active for reduction whereas reduction was not identified on sulphide minerals suggesting that the species formed on sulphides are either not electrochemically active for reduction or do not remain present at the mineral surface. This observation represents a significant difference between the sulphide and telluride minerals and notably the behaviour of the telluride minerals can be likened to that of Pt with regards to the reduction of oxidised dixanthogen species formed at the mineral surface as observed in Figure 4.21(b).

From a flotation perspective all the collector species identified are expected to produce hydrophobicity of the mineral. The hydrophobic character of a xanthate-mineral species is dependent on the difference in electronegativity between the xanthate species and the metal with which it is interacting. In the case of metal thiolate species, it has also been observed that this in turn is related to the solubility of the metal – xanthate species. The order of decreasing solubility for some metal xanthate species has been found to be as follows, Hg₂X₂ > Cu₂X₂ > PbX₂ > ZnX₂ (Rao and Leja, 2004). This decreasing order is equivalent to a decreasing order of hydrophobicity i.e. Hg₂X₂ results in the highest hydrophobicity for this series. The solubility product of PtX₂ is reported by to be 1×10^{-54} which is smaller than that for Hg₂X₂ (2.5×10^{-38}) (Chanturiya and Vigdergauz, 2008). This suggests that the PtX₂ species would have an even higher degree of hydrophobicity than Hg₂X₂. Dixanthogen is believed to be the most hydrophobic of the products of reduction of the xanthate species (Rao and Leja, 2004). The results observed for PtTe₂ at pH 9.2 indicate that both X₂ and PtX₂ are simultaneously present at the mineral surface. These two species are expected to be sufficiently hydrophobic in character to facilitate flotation. Likewise the presence of dixanthogen on sulphide mineral surfaces indicates that these will be sufficiently hydrophobic for flotation to occur. Previous studies by Shackleton, (2007) on the micro-flotation of PtS show that the mineral seemingly has sufficient natural hydrophobicity, i.e. in the absence of collector, producing recoveries of 94 % and producing the same recoveries in the presence of SIBX. Hydrophobicity in the absence of collector is assumed to occur due to the formation of a metal

deficient surface supporting the occurrence of Reaction (5.16) at PtS surfaces. PdS which has been found to possibly form PdX_2 at rest under the conditions studied did not impart significant natural hydrophobicity in the absence of collector compared to the presence of SIBX giving recoveries of 64% compared to 94 % in the presence of SIBX. Shackleton, (2007) found that the telluride minerals were significantly less hydrophobic in the absence of collector giving micro-flotation recoveries lower than 63 % compared to recoveries of 99 % in the presence of SIBX. Evidently telluride minerals produced higher recoveries signifying possibly greater extent of hydrophobicity than sulphide minerals. This clearly indicates that the rate of oxygen reduction is not a rate determining step in determining the hydrophobicity of these mineral surfaces.

Cathodic currents on telluride minerals enable calculations of surface coverage to be determined although this was only applied to the telluride minerals. These results are shown in Table 5.1.

Table 5. 1. Calculation of fractional coverage of SEX on PtTe₂ surfaces. Γ (mol) denotes total coverage in mols and (Γ/Γ_m) denotes the fraction of a monolayer that the collector coverage results in.

Peak	Charge (μC)	Γ (mol)	Fractional Coverage (Γ/Γ_m)
PtTe ₂ - P1	-16.32	8.46×10^{-11}	1.12
PtTe ₂ - P2	-19.92	0.11×10^{-11}	1.37

The results shown in Table 5.1 indicate that the amount of dixanthogen formed on the surface of the mineral would be equivalent to slightly more than a pseudo - monolayer while the overall coverage by collector is about 2 pseudo-monolayers. At this stage it is not possible to say whether dixanthogen is present as a single layer or in multi-layers as this is dependent on the mineral crystal surface and the availability of bonding sites. It is very likely that at multi-layers dixanthogen is the dominant species at the surface indicating that differences between sulphide and telluride minerals exist below two pseudo-monolayers of collector coverage.

5.3.4.1 Rest potentials of Pt minerals in a pulp

Given that in an operational environment the minerals studied in this investigation must interact with the reagents in a complex pulp, tests were carried out in which a real Platreef ore was used in the pulp environment in which measurement of rest potentials of the Pt minerals were made. These results were presented in Figure 4.6. In the presence of a pulp made up of Platreef ore at pH 7 the rest potential of Pt and PtS did not differ significantly from what was observed under controlled solution conditions in the absence of the ore (pulp). The pulp phase did not have an oxidative effect on either Pt and PtS. PtTe₂ however was significantly affected and the rest potential prior to collector addition became significantly more negative. This drop in the rest potential indicates that the mineral surface experienced increased

oxidation in the presence of the pulp. With such a complex system it is difficult to speculate what the cause of the potential change on PtTe₂ could be. Collector addition in the presence of pulp showed no difference to that in the absence of ore on Pt and PtS however PtTe₂ which was already significantly affected in the absence of collector. An initial interaction was measured on the mineral as a decrease in potential which was followed by an increase in potential until it reached the potential region measured prior to collector addition. Further studies such as spectroscopic studies would have to determine whether there is any collector present at the mineral surface after a prolonged period of time. It has already been determined through cyclic voltammetry that in sufficiently reducing conditions adsorbed collector species can be reduced and thereby released into solution from the mineral surface. The behaviour of PtTe₂ in the presence of pulp would therefore be an important subject for further study because under flotation conditions the rest potential of the mineral should favour the formation of oxidised collector species.

5.4 Reactions of Pt Minerals with CuSO₄

The classic mechanism for the activation of sulphide minerals using copper sulphate has been described in Chapter 3. It is evident from the literature concerning the mechanism of copper activation that there are significant factors affecting activation. Arguably the most important factor in determining the copper sulphate activation of minerals is pH which would affect the nature of the species present. Speciation diagrams (cf. Figure 5.7) show that the dominant copper species at acidic, neutral and alkaline conditions are as follows (Gustafsson, 2011):

- at pH 6 the dominant copper species is Cu²⁺
- at pH 8 the dominant copper species are Cu(OH)₂aq, Cu(OH)⁺aq, (Cu)₂(OH)²⁺aq and Cu(OH)₂s
- at pH 10 the dominant copper species are Cu(OH)₂s and Cu(OH)₂aq.

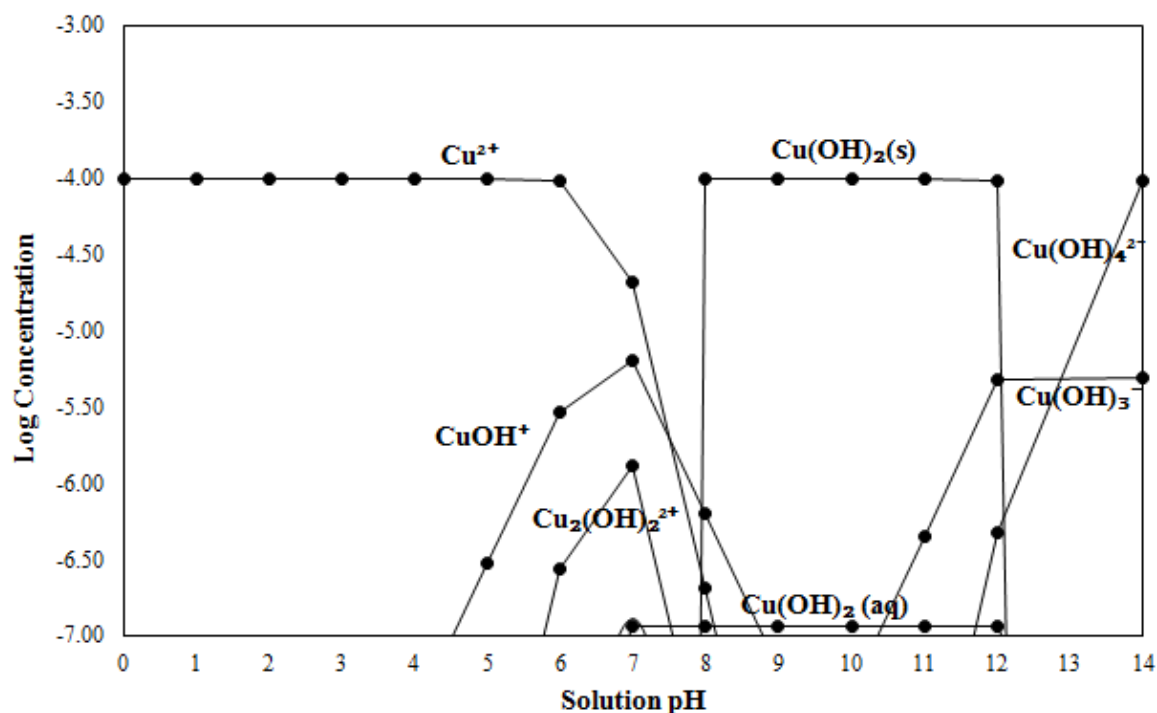
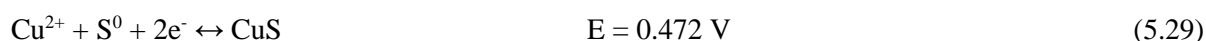


Figure 5.7 Speciation diagram for copper species in solution at a collector concentration of 1×10^{-4} M CuSO_4

There are two modes of interaction of copper species with mineral surfaces identified in the literature (Finkelstein, 1997; Wang et al., 1989; Wang et al., 1989). These two mechanisms involve precipitation and electrochemical oxidation and reduction of species. Precipitation of copper species on sulphide mineral surfaces is proposed to be accompanied by formation of CuS which is considered to be one of the species responsible for activation in the absence of collector. It has also been observed that formation of a CuS surface product could be followed by oxidation of this species to form Cu_2S (Finkelstein, 1997; Hu et al., 2009; Wang et al., 1989). At pH 6, Cu^{2+} is presumed to react with S dissolved from the mineral surface to form CuS which is subsequently adsorbed on the mineral surface. Uptake of Cu^{2+} ions at the mineral surface has been found to occur as the initial step in a sequence of reactions leading to activation of mineral surfaces (Ralston and Healy, 1980a, Ralston and Healy, 1980b). Reaction (5.28) has been reported to be the electrochemical mechanism by which CuS is formed on sulphide mineral surfaces, which occurs via reduction of sulphur at the mineral surface.



Reduction reactions leading to the activation of sulphide mineral surfaces have been described using the mixed potential model (cf. Section 2.5). From a mixed potential perspective reduction reactions involving CuSO_4 in addition to oxygen reduction results in an increase of the rest potential of the mineral from the condition of the absence of CuSO_4 (Wang et al., 1989).

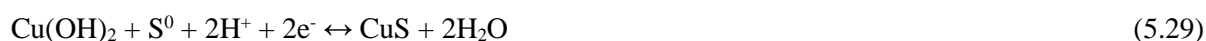
Under alkaline conditions (pH 10) the dominant copper species are hydrolysed species which adsorb onto the mineral surface (Ralston and Healy, 1980(b)). It is proposed that ion exchange within the crystal lattice subsequently results in the formation of a CuS surface (Finkelstein, 1997; Ralston and Healy, 1980). It should be noted however, that in order for ion exchange to occur within the crystal lattice the ions in question need to be geometrically similar i.e. have the same ionic radius.

The mechanisms that have been described for sulphide minerals cannot be directly translated to telluride minerals but CuSO₄ reactions which are independent of the mineral surface can be identified electrochemically. It was not the objective of this work to determine whether activation leads to hydrophobicity but to identify interaction mechanisms. Previous work conducted by Shackleton, (2007) on the interaction of these minerals Cooperite (PtS) and Moncheite (PtTe₂) with CuSO₄, is used to assist in the determination of the species identified electrochemically.

5.4.1 Mixed Potential Measurements of PtS and PtTe₂ with CuSO₄ and SEX addition

5.4.1.1 Rest potential measurements at pH 10

Cu(OH)_{2s} and Cu(OH)_{2aq} are the dominant species present in solution at pH 10. Previous studies indicated that activation at pH 10 occurs by surface coverage of hydroxyl species (Ralston and Healy, 1980b, Weisner and Gerson, 2000). Figure 4.49 shows that PtTe₂ is unaffected by the addition of CuSO₄ to the system whilst the increase in rest potential of PtS indicates that CuSO₄ was reduced at the mineral surface resulting in a more anodic rest potential. Reduction of Cu(OH)₂ species at pH 10 is proposed to occur via the reduction of sulphur according to Reaction (5.29) (Hu et al., 2009; Wang et al., 1989). This would result in activation of the mineral surface by CuS.



According to Figure 5.7, at pH 10 and relatively high Eh, Cu-OH-X(s) is stable and at lower Eh values, CuX is the stable species. Addition of SEX into solution was accompanied by a yellow precipitate which is characteristic of the formation of CuX confirming the formation of this species in the vessel. From rest potential measurements it is evident that the initial reaction on addition of collector showed oxidation of the collector at the mineral surface as indicated by the immediate decrease in rest potential. Species formed at the mineral surface due to SEX were either subsequently oxidised to form new species or migrated from the surface of the mineral as indicated by a rise in the rest potential on both minerals. Reactions (5.30) and (5.31) could account for the depletion of SEX from solution and oxidised SEX species on the mineral surface. The resulting rest potential of PtS after collector addition and formation of the CuX species is the rest potential of the mineral in the presence of CuSO₄. Chen and Yoon, (2000) measured rest potentials for ZnS at pH 9.2 in the presence of 1x10⁻⁴ M CuSO₄ and

compared these rest potentials to that of CuS and Cu₂S. They found that the rest potential of sphalerite increased to a value similar to that of a CuS surface. In this work the more anodic rest potential of the PtS surface in the presence of CuSO₄ might also be due to the formation of a CuS surface. On PtTe₂ however, the rest potential of the mineral after collector addition is slightly higher than that of the mineral prior to collector addition. This increased rest potential value might be considered insignificant compared to the rest potential prior to collector addition showing that there is no interaction of collector at the mineral surface in the presence of CuSO₄. Alternatively the increased rest potential may be due to passivation of the mineral surface by CuX₂ or CuX species.



On both the sulphide and the telluride mineral it was observed that CuSO₄ was detrimental, to the adsorption of collector on the mineral surface although CuX₂ might have been present on the surface. These results are of considerable importance because the microflotation study by Shackleton, (2007) showed that the presence of CuSO₄ reduced recoveries. Shackleton could not present an explanation for these results but it seems that these rest potentials show that there is no interaction of CuSO₄ and SEX to impart hydrophobicity to the mineral surfaces.

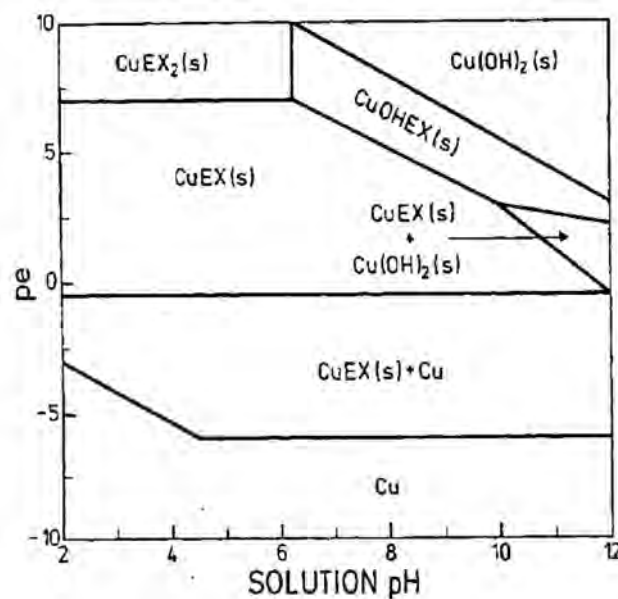


Figure 5. 8 pE- pH diagram for the Cu – EX system for Cu and EX concentration of 10⁻⁴M where pE=E°/0.059 (Wang et al., 1989).

5.4.1.2 Rest potential measurements at pH 8

At near neutral solution conditions (pH 8), the behaviour of PtS as shown in Figure 4.50 follows that observed at pH 10. The increase in rest potential after CuSO_4 addition is indicative of the reduction reactions involving CuSO_4 in solution with the possible formation of CuS . The complexity of the copper species present at these conditions however makes it difficult to speculate as to which species are formed at the surface. The response of PtTe_2 at pH 8 to the addition of CuSO_4 was also an increase in rest potential. This increase in potential is likely to be due to additional reduction reactions at the mineral surface in addition to reduction of oxygen.

Whereas a CuS like surface may exist on sulphide minerals after CuSO_4 is added, interactions on telluride mineral surfaces could lead to similar species to CuS comprising of tellurium e.g. the formation of a copper telluride or tellurite. A study conducted by Pathan et al. (2003) showed formation of Cu_2Te and CuTe from CuSO_4 and Na_2TeO_3 by a method of chemical deposition. The work of Pathan et al. (2003) was an example of the possible reactions between CuSO_4 and TeO_3^{2-} species generated from oxidation of the mineral. It should be noted however that in that work CuSO_4 was at pH 9 and Na_2TeO_3 was at pH 5 and the final pH of the mixture was not reported. In speculating on the species present at PtTe_2 mineral surface it is also noted that the change in rest potential in the presence of CuSO_4 is not significantly large and therefore extensive reaction is unlikely to be occurring.

A yellow precipitate was once again formed on the addition of SEX into the solution. Once again on both minerals, collector interaction with the mineral surface occurs immediately and is faster than CuX_2 precipitation as indicated by the decrease in potential after collector addition. In this pH region CuX is stable and so is CuX_2 . According to Reaction (5.32) reduction of CuX_2 to CuX may be accompanied by the oxidation of xanthate ions to form dixanthogen. It is therefore possible that such a reaction could yield hydrophobic dixanthogen at the mineral surface, since it is also stable in this potential region.



The final rest potential of PtS after collector addition (following copper sulphate addition) is characteristic of the surface prior to SEX addition as is the case for PtTe_2 . Slightly more anodic potentials are likely to be due to partial passivation by the CuX species formed. No evidence of bulk collector oxidation at the mineral surface was observed however, leading to the conclusion that CuSO_4 is detrimental to adsorption of collector by conventional collector adsorption mechanisms.

5.4.1.3 Rest Potential Measurements at pH 6

Cu^{2+} is the dominant species in solution at pH 6 and therefore reactions involving this species are expected to be dominant. Increase in potential identified in Figure 4.51 after copper sulphate addition is consistent with the reduction of Cu^{2+} , possibly resulting in the formation of CuS (Reaction (5.28)) at the PtS mineral surface. PtTe_2 however does not show any evidence of copper reduction indicating that oxygen reduction remains the dominant reaction contributing to the rest potential on the mineral surface. This lack of reactivity between copper ions and the telluride mineral may also be as a result of the reduced anodic activity of the mineral at this pH which has been identified previously in this work.

Although SEX addition on the PtTe_2 surface does indicate instantaneous interaction of collector with the mineral surface as shown by a decrease in rest potential, this decrease in rest potential is not sustained and the final rest potential of the mineral remains unchanged from that prior to collector addition. This is evidence of the speed of reaction between Cu^{2+} and xanthate ions so as to completely inhibit any reaction between the mineral surface and SEX. Although CuX_2 was identified in the vessel as a yellow precipitate there is no evidence from rest potential results to support further oxidation to yield dixanthogen.

SEX addition on PtS results in the reduction of rest potential and a sustained lower value rest potential due to oxidation of SEX at the mineral surface. CuX_2 precipitation was observed. It is possible that dixanthogen formation also occurs at the mineral surface as the potential region is favourable towards its formation.

5.4.2 Cyclic Voltammetry Measurements for PtS and PtTe_2 in the presence of CuSO_4 and SEX

Voltammograms were generated from the minerals PtTe_2 and PtS under de-aerated solution conditions for four conditions;

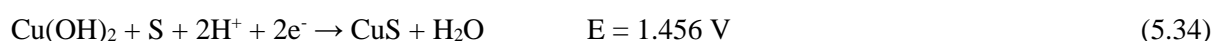
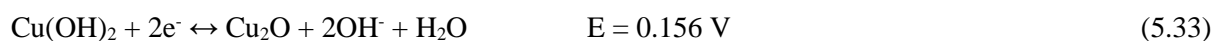
- Absence of SEX and CuSO_4
- Presence of SEX
- Presence of CuSO_4
- Presence of both CuSO_4 and SEX

The first two conditions were measured in order to establish a base line for distinguishing interactions of CuSO_4 species and CuX_2/CuX species at the mineral surface. These measurements were conducted at the three different pH levels studied for rest potentials in order to provide more information regarding the species formed. There is no known open literature on electrochemical investigations involving PtTe_2 and PtS using CuSO_4 , the most common work on CuSO_4 having been done on ZnS. Cyclic voltammetry

measurements on ZnS in the presence of 1×10^{-4} CuSO₄ are used to assist in interpreting the voltammograms generated on PtTe₂ and PtS. Such work includes that of Chen and Yoon, (2000) who measured voltammograms for ZnS in CuSO₄ at pH 9.2 and the work of Hu et al. (2009) who measured voltammograms for ZnS at pH 6, pH 9.5 and pH 12.8 in a CuSO₄ concentration of 1.1×10^{-4} M. It is noted that the pH values differ with those used in this work and that the method of undertaking the voltammograms differs from this work, however insight regarding the possible reactions can still be gained.

5.4.2.1 Cyclic voltammetry measurements of PtS

Cyclic voltammetry measurements for PtS at pH 10 were shown in Figure 4.55. It was proposed that the increased anodic activity of PtS in the presence of SEX compared to its absence was due to collector interaction resulting in the formation of dixanthogen and possibly PtX₂. In the presence of CuSO₄ reduction of copper species was evident between 0.1 V and 0.2 V. This was probably due to the reduction of Cu(OH)₂aq. Reaction (5.33) which involves the reduction of Cu(OH)₂ to form Cu₂O and Reaction (5.34) which involves the reduction of S and reaction with Cu(OH)₂ to form CuS can possibly account for this peak. The high reduction potential of Reaction (5.34) indicates that it is highly favoured. XPS results from Shackleton, (2007) show that there is indeed Cu²⁺ present on PtTe₂ in the presence of CuSO₄ alone at pH 9.



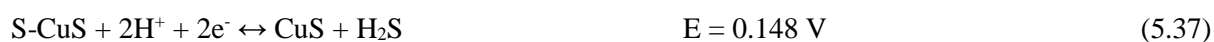
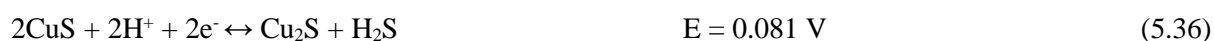
Inhibition of anodic currents observed in the presence of both CuSO₄ and SEX verifies the presence of CuX at the mineral surface. This species is not electrochemically active and inhibits oxidation of the mineral surface. No evidence of oxidation of SEX at the mineral surface was shown and this might suggest, as shown by XPS results by Shackleton, (2007) that CuX₂ and not CuX is formed.

At pH 8, PtS shows significant oxidation due to SEX interaction compared to that observed in the absence of CuSO₄. Anodic currents measured in the presence of CuSO₄ and those in the presence of CuSO₄ and SEX were initially the same as those measured when no collector was present. The similarity between these anodic currents suggests that oxidation of the mineral surface is the dominant reaction at the mineral surface. The return anodic sweep after oxidation in the presence of CuSO₄ yielded significant oxidation currents which were not due to mineral oxidation and were possibly due to oxidation of a CuS species present at the mineral surface. Chen and Yoon, (2000) identified oxidation peaks at pH 9.2 which commenced from above 0.3 V which they attributed to Reaction (5.35) which they calculated to occur at potentials above 0.303 V at pH 9.2;



According to the Nernst equation it is expected that such a reaction will decrease by 0.059 V for every unit increase in pH and therefore based on the potential quoted by Chen and Yoon, (2000) at pH 8 Reaction 5.35 will occur at ≈ 0.362 V. This reaction may account for currents observed at PtS surface. Absence of this oxidation current in the presence of SEX and CuSO_4 is attributed to the depletion of copper species by the formation of CuX.

In Hu et al. (2009), the cyclic voltammograms for ZnS in the presence of 1.1×10^{-4} M CuSO_4 at pH 6 were analysed. Similar behaviour to that observed in Figure 4.57 for PtS at pH 6, in the presence of CuSO_4 between 0 V and 0.4 V was observed. The following reactions due to oxidation and reduction of CuS and Cu_2S were proposed in Hu et al. (2009) to be occurring and the reduction potentials are given in Reactions (5.36) – (5.37). In Reaction (5.37), S-CuS represents a polysulphide.



At pH 6 Cu^{2+} is predominant in solution and the formation of CuS is reported to occur readily. In the presence of CuSO_4 initial oxidation can therefore be attributed to the formation of a polysulphide on PtS surface whilst the following reduction current is attributed to any or both of the reverse of Reactions (5.38) and (5.39). A strong anodic oxidation current in the return anodic sweep can be attributed to oxidation of Cu_2S back to CuS and oxidation of the polysulphide back to CuS according to Reactions (5.36) and (5.37). This behaviour is not exhibited in the presence of SEX and CuSO_4 and no reactions due to SEX, copper species or CuX can be electrochemically identified. It however cannot be discounted that CuX solid which was observed in solution could have been present at the mineral surface albeit to a limited extent.

5.4.2.2 Cyclic Voltammetry Measurements of PtTe_2

At pH 10 the voltammograms generated for PtTe_2 are shown in Figure 4.52. Peak C1 on Figure 4.52 can be attributed to copper reduction on the mineral surface and the current change C1 is likewise due to oxidation of copper species. Reaction (5.33) for the reduction of $\text{Cu}(\text{OH})_2$ to Cu_2O occurs within the same potential region at pH 10 and can be attributed to peaks C1 and C2. With regards to tellurium chemistry it is found that in strongly alkaline solutions Te^{4+} reduces to Te^0 and further to Te^{2-} as indicated

in Reaction (5.40) (Mishra et al., 1990; Sarala and Jayarama Reddy, 1986). It has been previously noted that this reduction is inhibited in the presence of collector (cf. Section 5.3.2.2). In the presence of reduced Te^{2+} species reduction of $\text{Cu}(\text{OH})_2$ may be accompanied by the formation of a CuTe species. C1 can thus be attributed to oxidation of this species according to Reaction (4.40) which could be an alternative to the occurrence of Reaction (5.33).



In the presence of both CuSO_4 and SEX peak B1 occurred at potentials between -0.1 V and 0 V. Peaks P1 and P2 were similar to those obtained on PtTe_2 in the presence of SEX at pH 9.2 which were due to reduction of X_2 and PtX_2 respectively. Peak B1 commenced at the same potential as peak P1 and can therefore be assigned to the reduction of dixanthogen at the mineral surface. It has been established that the formation of dixanthogen on PtTe_2 in the presence of both CuSO_4 and SEX can occur via two mechanisms viz. oxidation of xanthate ions and oxidation of CuX_2 to form CuX and X_2 . It will be shown later that XPS results from Shackleton, (2007) indicated the presence of both Cu^{2+} and Cu^+ indicating the reduction of CuX_2 to CuX species as illustrated in Reaction (5.32). The extent of xanthate interaction in the presence of CuSO_4 and SEX was notably reduced from that in the presence of SEX alone as indicated by reduced anodic currents.

At pH 8 the voltammograms for PtTe_2 are shown in Figure 4.53. In the absence of reagents anodic currents due to the oxidation of the mineral were accompanied by reduction current changes between -0.4 V and 0.1 V. In the presence of SEX alone it was observed that there were two anodic current changes which correspond to oxidation of the collector forming dixanthogen. In the presence of CuSO_4 anodic currents showed that mineral oxidation was inhibited. Inhibition could be due to copper hydroxyl species. The speciation of CuSO_4 in this pH region is too complex to definitively assign species to the various peaks. In the presence of CuSO_4 the small peak occurring at 0.15 V may be attributed to the reduction of some copper species. In the presence of CuSO_4 and SEX anodic currents are further reduced compared to the condition of the presence of CuSO_4 and this may be due to surface coverage by a non-electrochemically active species such as CuX .

In Figure 4.54 reduced anodic activity of PtTe_2 in the absence of CuSO_4 and SEX was identified. Cu^{2+} should be the dominant species at these conditions and therefore it is expected that in the presence of CuSO_4 the reduction currents observed in the region of 0 V and 0.2 V were due to the reduction of Cu^{2+} prior to reduction of mineral oxidation species. It can be hypothesised that CuTe would be formed via the reduction steps of Te^{4+} to Te^{2-} . The absence of this reduction current in the presence of CuSO_4 and SEX possibly confirms this hypothesis. The reduction current in the presence of CuSO_4 is difficult to assign but the currents are similar to those for the mineral in the presence of SEX albeit occurring at lower potentials. This might suggest that collector oxidation might have taken place at PtTe_2 surface, possibly due to Reaction (5.32).

5.4.3 Summary

In this part of the study the electrochemical behaviour of PtS and PtTe₂ in the presence of have shown that the behaviour of PtS follows the classical method of activation which is documented in the literature for base metal sulphides, whilst that for the telluride mineral did not follow the same behaviour. Previous work to study the interactions of these minerals with CuSO₄ and thereafter SIBX in the presence of CuSO₄ was conducted by Shackleton, (2007). In that investigation studies of Zeta Potential at pH 6, 8 and 10 were conducted. ToF SIMs and XPS measurements were made at pH 9 in synthetic plant water with micro-flotation test work conducted as a measure of hydrophobicity. A summary of these findings is presented here and a discussion of the comparison with the electrochemical data obtained in the present investigation is also given.

Zeta potential data for PtS and PtTe₂ showed that both minerals had negative zeta potential in synthetic plant water at all pH levels with PtTe₂ exhibiting a more negative zeta potential than PtS. Addition of CuSO₄ into solution resulted in the Zeta Potential of all the minerals becoming more positive across the potential range.

Perhaps most significant is the zeta potential of PtS which went from having a negative value to having a positive value at pH 10. At pH 10 the greatest change in zeta potential was noted on PtTe₂. This was taken as evidence of the neutralisation of charge at this pH by adsorbed Cu(OH)₂ species. At pH 8 and pH 6, Cu²⁺ and Cu-hydroxy species were presumed to be responsible for the neutralisation of charge in the presence of CuSO₄.

The change in zeta potential in the presence of CuSO₄ and SIBX had the effect of making the zeta potential of PtS also less negative than in the absence of CuSO₄ and SIBX and a negligible change in zeta potential was observed on PtTe₂. The negligible change in the zeta potential of PtTe₂ was consistent with the mixed potential results obtained which showed that the change to the mineral surface due to the CuSO₄ and SEX was not significant.

On PtS the zeta potential in the presence of CuSO₄ was less negative than that of the mineral in the absence of CuSO₄ and this could be consistent with the observation from the mixed potential study that the final rest potential values indicate possibly a CuS like surface.

ToF SIMS and XPS were conducted on the mineral surfaces at pH 9. ToF SIMS results showed that the amount of copper ions in the presence of CuSO₄ was lower on PtS than in the presence of both CuSO₄ and SIBX whilst the reverse was found to be true on the PtTe₂ sample. With respect to xanthate ions, a higher amount was also identified on PtS in the presence of SIBX and CuSO₄ than in the presence of CuSO₄ whilst the reverse was found to be true for PtTe₂. Shackleton, (2007) attributed this to the adsorption of CuX₂ on PtS surface thereby increasing the amount of copper ions as well as xanthate

ions on the surface. At pH 9 copper ions on PtTe₂ were attributed to coverage by Cu(OH)₂(s) and the presence of xanthate was attributed to the adsorption of CuX₂. In Figure 4.49 at pH 10 where Cu(OH)₂(s) is the dominant species in solution there was no change in rest potential for PtTe₂ to indicate passivation or interaction with copper ions in solution. It is possible however that Cu(OH)₂ present at the mineral surface had no electrochemical effect on the mineral surface. Increased rest potential of the mineral after collector addition can be attributed to the presence of CuX₂ and CuX solid at the mineral surface resulting in passivation of part of the mineral surface.

Results of the XPS study are summarised in Table 5.2 below. Results for the minerals in the presence of synthetic water alone and SIBX were consistent with what was determined by the cyclic voltammetry and rest potential measurements regarding the behaviour and reactions of PtTe₂. XPS corroborates the fact that the oxidation of PtS in solution is limited and lower in extent compared to that of the telluride minerals. In the presence of CuSO₄ copper is present as Cu²⁺ on PtTe₂ consistent with the formation and presence of Cu(OH)₂ at the surface of the mineral. In the presence of CuSO₄ + SIBX the mineral surface showed evidence of both CuX₂ and CuX as well as dixanthogen. Rest potential measurements did not contradict this finding nor corroborate it but cyclic voltammograms measured and shown in Figure 4.52 corroborated this finding as reduction currents consistent with the reduction of dixanthogen were exhibited. Formation of these species would be according to Reaction (5.32). CuX is electrochemically inactive and this would account for the electrochemical inactivity of PtS in the presence of CuSO₄ and SIBX.

Table 5.2. Summary of XPS data obtained by Shackleton, (2007) for PtS and PtTe₂ adapted from (Shackleton, 2007)

	Moncheite (PtTe ₂)	Cooperite (PtS)
In Synthetic Water	Ions present in the synthetic water are not strongly adsorbed Some oxidation – TeO ₄ ion or Te(OH) ₂ Ratio of TeO ₄ :Te(OH) ₂ is 60:40	Specifically adsorbs Mg ²⁺ Limited oxidation from synthetic water
With CuSO₄ addition	Copper is detected at 1.0 at.% 100% Cu as Cu ²⁺	Copper is detected at 1.6 at.%
With CuSO₄+SIBX addition	Cu is present at 0.7 at.% 64% Cu ²⁺ with 36 % Cu ⁺ Xanthate adsorption (2.8%S). Some production of oxidised dixanthogen. Less oxide or hydroxide after xanthate addition	Cu is present at 1.6 at.% 100% Cu ⁺ Xanthate adsorption (5%S increase)
With SIBX Addition	Xanthate adsorption (3.8%S). More xanthate adsorbed without CuSO ₄ addition. For the copper xanthate system, the area estimate is 960 c/s compared with the xanthate alone at 1780 counts	Xanthate adsorption lower (3%S increase) compared with copper activation

- Reduced activity of collector oxidation at the mineral surface in the presence of SEX and CuSO₄ is significant towards the reduction of hydrophobicity.
- Higher reactivity of telluride minerals resulted in the oxidation of the collector species at the mineral surface whilst this was less likely on PtS surfaces except at low pH viz. pH6
- Whilst PtS follows a classical method of activation in collectorless solution leading to formation of CuS it is likely that a similar mechanism might occur on telluride minerals leading to formation of CuTe, further investigations particularly with regards to identification of species would be required.

Chapter 6

6 Conclusions

In this study the interactions between Moncheite (PtTe_2), Merenskyite (PdTe_2), Cooperite (PtS) and Vysotskite (PdS) with SEX, DTP and CuSO_4 were investigated. These minerals are arguably some of the key minerals relevant to the PGM industry, at present and in the future. It is projected that the beneficiation of Platreef ores will be an integral part of all future developments in the PGM industry. The recovery of the arsenide, telluride and sulphide platinum group minerals is thus of critical importance in the recovery of PGMs in what is known as the Platreef ore body. This study therefore contributes fundamental knowledge which will be a key contribution to the understanding of the optimum processes to be used in the concentration of these minerals by flotation. The present investigation has focussed specifically on the telluride and sulphide minerals and due to the virtual impossibility of obtaining real samples from the ore body, synthetic minerals have been studied as was the case in previous investigations by Shackleton, (2007) and Vermaak et al. (2007).

Electrochemical techniques are a classical method for the study of collector-mineral interactions and represent an excellent technique for such studies. This is because the fundamental mechanisms relating to the surface mineral-reagent interactions all relate to a process in which electrons are transferred across the mineral solution boundary between the mineral, and the collector species in the presence of an oxidising agent such as oxygen. Thus an electrochemical study was undertaken in order to determine collector- mineral interactions. CuSO_4 is widely used as an activator in flotation operations treating these minerals and thus its effect on the interactions between minerals and collectors was also studied.

It has been shown in the present study that at anodic potentials above 0.3 V the oxidation of telluride minerals is more significant than that which occurred on the sulphide minerals, and this was observed for both PtTe_2 and PdTe_2 PGMs. From cyclic voltammetry results, oxidation of PtTe_2 and PdTe_2 was proposed to result in the formation of a soluble tellurite species leaving a PtTe or PdTe surface available for reaction in the absence of any flotation reagents such as a thiol collector or an activator such as CuSO_4 . This was consistent with previous findings of Vermaak et al. (2007) and Elvy et al. (1996). On the other hand for the sulphide mineral investigations, the results indicated that PtO or PdO surface was thermodynamically favoured.

Dixanthogen is the most hydrophobic species responsible for flotation. However the other thiolate species such as a metal thiolate and a chemisorbed thiolate are also responsible for imparting hydrophobicity to the minerals. Rest potential and cyclic voltammetry studies using SEX as a collector showed that on PtTe_2 and PdTe_2 mineral surfaces at pH 9.2, a metal xanthate species (PtX_2 or PdX_2) was formed prior to the formation of dixanthogen. Rest potential measurements and cyclic voltammetry

experiments also indicated that dixanthogen was the predominant species formed on sulphide minerals although the formation of a metal xanthate species could not be discounted. This was particularly in the case of PdS which had a rest potential below the dixanthogen formation equilibrium potential.

pH was found to be an important parameter in the present study. It was found that the species formed by SEX on telluride minerals were significantly affected by changes in pH. Dixanthogen was found to be the dominant species at pH 4.2 and pH 7, whilst at pH 9.2 metal xanthate was present on the surface and was seemingly the dominant species at pH 11.2. On the other hand, on sulphide minerals dixanthogen was seemingly the dominant species at all pH levels from pH 4.2 to pH 11.2.

Interactions of the telluride and sulphide minerals with DTP were observed to differ from interactions with SEX at pH 9.2 and pH 4.2. Rest potential measurements and cyclic voltammetry showed that the metal thiolate was the dominant species of DTP formed on both mineral types. This was attributed to higher oxidation potential of DTP than SEX which makes formation of the dimer unlikely at the rest potential of the minerals under the conditions studied.

It was hypothesised at the commencement of this study that minerals with similar crystal structures would possibly demonstrate similar electrochemical behaviour. It has been found that rest potential and cyclic voltammograms were indeed similar for PtTe₂ and PdTe₂ which have similar crystal structures. The same observation was made in the case of the sulphide minerals of Pt and Pd. It thus appears that there is some correlation between crystal structure of minerals and their electrochemical behaviour.

Neither PtTe₂, PdTe₂, PtS nor PdS were found to behave in exactly the same manner as their metal constituents, Pt and Pd which was proposed as an hypothesis in this study. A rest potential comparison of the minerals and the metals showed that, as expected, the minerals were more susceptible to oxidation than the pure metals. Rest potentials also showed that dixanthogen was readily formed on the metal surfaces whilst the potentials for the minerals (PtS and PdTe₂) which formed dixanthogen were significantly lower and closer to the dixanthogen equilibrium potential. This is an indicator of lower rates of dixanthogen formation on the mineral surfaces compared to its formation on the metal surfaces. Cyclic voltammograms on PtTe₂ are more similar to Pt in the presence of SEX than in the absence of SEX. On the other hand cyclic voltammograms for PtS were more similar to Pt metal in the absence of SEX than in the presence of SEX. These observations indicate that it is not possible to draw conclusions on the behaviour of the minerals from the behaviour of the respective metals.

In the study to investigate the effect of CuSO₄ on collector-mineral interactions, the rest potential study showed interaction between a PtS surface and CuSO₄ at pH 6, pH 8 and pH 10. There was, however, no significant interaction between PtTe₂ and CuSO₄ at the mineral surface over the same pH range. Whilst reduction of the mineral surface to form a CuS like surface could be extended to PtS, this was not the case with PtTe₂. Notably, there were no significant interactions between both sulphide and

telluride minerals with SEX in the presence of CuSO_4 . CuX species were physically observed to be formed in solution when both CuSO_4 and SEX were present in solution and therefore it is possible that the species could have resulted in some coverage of the mineral surface via non-electrochemical processes. Ultimately, CuSO_4 was shown to inhibit the electrochemical interactions of both sulphide and telluride mineral surfaces with SEX. This result was consistent with observations made by Shackleton, (2007) who found that the presence of CuSO_4 inhibited recoveries of these minerals during micro-flotation experiments.

Cyclic voltammetry results for both the telluride and sulphide minerals consistently showed that the presence of both CuSO_4 and SEX resulted in reduced activity of collector at the mineral surface. Except for PtTe_2 at pH 10, there was no evidence of SEX oxidation or reduction at the mineral surface on both PtTe_2 and PtS in the presence of CuSO_4 . It should also be noted that the reduction peak observed on PtTe_2 at pH 10 in the presence of both CuSO_4 and SEX was not as significant as that occurring in the presence of SEX alone.

With the bulk of this study having been conducted in the absence of solids, it was of interest to investigate how these mineral collector interactions are affected by the presence of solids and ultimately other minerals in solution, since those conditions are more representative of the interactions occurring in a flotation cell. A preliminary study of rest potentials of Moncheite and Cooperite in solids typical of the Platreef showed that Pt metal and PtS were less significantly affected by the presence of solids than PtTe_2 . Notably, the oxidation behaviour of PtTe_2 in the absence of collector was significantly affected, resulting in a lowered rest potential in the presence of solids than that in the absence of solids. As a result, the collector species formed were significantly affected whilst those for PtS and Pt were not affected. Results obtained showed that in the presence of solids SEX species might not adsorb onto the mineral surface at all, which would have significant ramifications to a flotation operation in which these minerals are to be recovered. This presents an opportunity for further study.

Chapter 7

7 References

- ALLISON, S.A., GOOLD, L., NICOL, M. and GRANVILLE, A., 1972. A determination of the products of reaction between various sulfide minerals and aqueous xanthate solution, and a correlation of the products with electrode rest potentials. *Metallurgical and materials transactions.A, Physical metallurgy and materials science*, **3**(10), pp. 2613-2618.
- ARMITAGE, P.E.B., MCDONALD, I., EDWARDS, S.J. and MANBY, G.M., 2002. Platinum-group element mineralization in the Platreef and calc-silicate footwall at Sandsloot, Potgietersrus District, South Africa. *Transactions. Section B, Applied earth science*, **111**(1), pp. 36-45.
- BARD, A.J. and FAULKNER, L.R., 1980. *Electrochemical methods: fundamentals and applications*. Wiley New York.
- BARNES, S.J., 2004. Platinum-group element distribution in the main zone and upper zone of the Bushveld Complex, South Africa. *Chemical Geology*, **208**(1), pp. 293.
- BARNES, S., MAIER, W.D. and ASHWAL, L.D., 2004. Platinum-group element distribution in the Main Zone and Upper Zone of the Bushveld Complex, South Africa. *Chemical Geology*, **208**(1-4), pp. 293-317.
- BERLINCOURT, L.E., HUMMEL, H.H. and SKINNER, B.J., 1981. Phases and Phase Relations of the Platinum-Group Elements. In: L.J. CABRI, ed, *Platinum-Group Elements: Mineralogy, Geology, Recovery*. Special Volume 23 edn. Canadian Institute of Mining and Metallurgy, pp. 19-45.
- BOCKRIS, J.O. and REDDY, A.K., 1973. *Modern electrochemistry: an introduction to an interdisciplinary area*. Springer.
- BOUROUSHIAN, M., 2010. *Electrochemistry of metal chalcogenides*. Springer.
- BOZKURT, V., XU, Z. and FINCH, J., 1998. Pentlandite/pyrrhotite interaction and xanthate adsorption. *International Journal of Mineral Processing*, **52**(4), pp. 203-214.
- BUCKLEY, A. and WOODS, R., 1993. Underpotential deposition of dithiophosphate on chalcocite. *Journal of Electroanalytical Chemistry*, **357**(1), pp. 387-405.
- BUCKLEY, A. and WOODS, R., 1990. X-ray photoelectron spectroscopic and electrochemical studies of the interaction of xanthate with galena in relation to the mechanism proposed by Page and Hazell. *International Journal of Mineral Processing*, **28**(3), pp. 301-311.

- BUCKLEY, A.N. and WOODS, R., 1997. Chemisorption—the thermodynamically favoured process in the interaction of thiol collectors with sulphide minerals. *International Journal of Mineral Processing*, **51**(1–4), pp. 15-26.
- BUCKLEY, A.N. and WOODS, R., 1994. Xanthate chemisorption on lead sulfide. *Colloids and Surfaces A: Physicochemical and Engineering Aspects*, **89**(1), pp. 71-76.
- BUCKLEY, A.N. and WOODS, R., 1987. The surface oxidation of pyrite. *Applied Surface Science*, **27**(4), pp. 437-452.
- BULATOVIC, S.M., 2007. *Handbook of Flotation Reagents: Chemistry, Theory and Practice*. Burlington: Elsevier.
- BUSWELL A M, 1998. *An Electrochemical Investigation into the Floatability of Pyrrhotite*, University of the Witwatersrand.
- BUSWELL, A.M., BRADSHAW, D.J., HARRIS, P.J. and EKMEKCI, Z., 2002. The use of electrochemical measurements in the flotation of a platinum group minerals (PGM) bearing ore. *Minerals Engineering*, **15**(6), pp. 395-404.
- BUSWELL, A.M. and NICOL, M.J., 2002. Some aspects of the electrochemistry of the flotation of pyrrhotite. *Journal of Applied Electrochemistry*, **32**(12), pp. 1321-1329.
- CAWTHORN, R.G., 1999. The platinum and palladium resources of the Bushveld Complex. *South African Journal of Science*, **95**(11/12), pp. 481-489.
- CAWTHORN, R.G., LEE, C.A., SCHOUWSTRA, R.P. and MELLOWSHIP, P., 2002. Relationship between PGE and PGM in the Bushveld Complex. *Canadian mineralogist*, **40**(2), pp. 311-328.
- CAWTHORN, R.G., 2011. Geological interpretations from the PGE distribution in the Bushveld Merensky and UG2 chromitite reefs. *The Journal of the South African Institute of Mining and Metallurgy*, **111**, pp. 67-79.
- CHANDER, S. and FUERSTENAU, D.W., 1974. The effect of potassium diethyldithiophosphate on the electrochemical properties of platinum, copper and copper sulfide in aqueous solutions. *Journal of Electroanalytical Chemistry and Interfacial Electrochemistry*, **56**(2), pp. 217-247.
- CHANDER, S., KAR, G. and FUERSTENAU, D.W., 1979. The corrosion and wetting behaviour of copper in the presence of some thiol reagents. *Corrosion Science*, **19**(6), pp. 405-416.
- CHANTURIYA, V. and VIGDERGAUZ, V., 2008. Sulfide Electrochemistry. *Flotation Theory and Practice*.

DAI, D., KOO, H.-. WHANGBO, M.-. SOULARD, C., ROCQUEFELTE, X. and JOBIC, S., 2003. Trends in the structure and bonding in the layered platinum dioxide and dichalcogenides PtQ₂ (Q=O, S, Se, Te). *Journal of Solid State Chemistry*, **173**(1), pp. 114-121.

DALTRY, V.D.C. and WILSON, A.H., 1997. Review of platinum-group mineralogy: Compositions and elemental associations of the PG-minerals and unidentified PGE-phases. *Mineralogy and petrology*, **60**(3), pp. 185-229.

ELVY, S.B., WILLIAMS, P.A. and BUCKLEY, A.N., 1996. XPS Evidence for the Incongruent Surface Oxidation of Minerals in the Pd²⁺Te²⁺Bi System. *Surface and Interface Analysis*, **24**(9), pp. 641-646.

FINKELSTEIN, N.P. and POLING, G.W., 1977. The Role of Dithiolates in the Flotation of Sulphide Minerals. *Minerals Science Engineering*, **9**(4), pp. 177-197.

FINKELSTEIN, N., 1997. The activation of sulphide minerals for flotation: a review. *International Journal of Mineral Processing*, **52**(2), pp. 81-120.

FINKELSTEIN, N. and ALLISON, S., 1976. Chemistry of Activation, Deactivation and Depression in the Flotation of Zinc Sulfide--Review. *Flotation--A.M.Gaudin Memorial*.

FINKELSTEIN, N. and GOOLD, L., 1972. The reaction of sulphide minerals with thiol compounds. *National Institute of Metallurgy, South Africa.Report*, (1439).

FINKELSTEIN, N.P. and POLING, G.W., 1977. Role of Dithiolates in the Flotation of Sulphide Minerals. *Miner Sci Eng*, **9**(4), pp. 177-197.

GARDNER, J.R. and WOODS, R., 1979. An electrochemical investigation of the natural flotability of chalcopyrite. *International Journal of Mineral Processing*, **6**(1), pp. 1-16.

GARDNER, J.R. and WOODS, R., 1979. A study of the surface oxidation of galena using cyclic voltammetry. *Journal of Electroanalytical Chemistry*, **100**, pp. 447-459.

GRANVILLE, A., FINKELSTEIN, N. and ALLISON, S., 1972. Review of reactions in the flotation system galena-xanthate-oxygen. *Trans.Inst.Min.Metall*, **81**, pp. C1-C30.

GÜLER, T., HIÇYILMAZ, C., GÖKAĞAÇ, G. and EKMEKÇI, Z., 2004. Voltammetric and drift spectroscopy investigation in dithiophosphate–chalcopyrite system. *Journal of colloid and interface science*, **279**(1), pp. 46-54.

- GÜLER, T., HIÇYILMAZ, C., GÖKAĞAÇ, G. and EKMEKÇI, Z., 2005. Electrochemical behaviour of chalcopyrite in the absence and presence of dithiophosphate. *International Journal of Mineral Processing*, **75**(3–4), pp. 217-228.
- GUSTAFSSON, J., 2011. Visual MINTEQ ver. 3.0. *KTH Department of Land and Water Resources Engineering, Stockholm, Sweden. Based on de Allison JD, Brown DS, Novo-Gradac KJ, MINTEQA2 ver. 4*, pp. 1991.
- HAMILTON, I.C. and WOODS, R., 1981. An investigation of surface oxidation of pyrite and pyrrhotite by linear potential sweep voltammetry. *Journal of Electroanalytical Chemistry and Interfacial Electrochemistry*, **118**(0), pp. 327-343.
- HANSON, J.S. and FUERSTENAU, D.W., 1991. The electrochemical and flotation behavior of chalcocite and mixed oxide/sulfide ores. *International Journal of Mineral Processing*, **33**(1–4), pp. 33-47.
- HELMY, H.M., BALLHAUS, C., BERNDT, J., BOCKRATH, C. and WOHLGEMUTH-UEBERWASSER, C., 2007. Formation of Pt, Pd and Ni tellurides: experiments in sulfide–telluride systems. *Contributions to mineralogy and petrology*, **153**(5), pp. 577-591.
- HOLWELL, D.A., ARMITAGE, P.E.B. and MCDONALD, I., 2005. Observations on the relationship between the Platreef and its hangingwall. *Transactions - Institution of Mining and Metallurgy. Section A. Mining industry*, **114**(4), pp. 199-209.
- HOLWELL, D.A., MCDONALD, I. and ARMITAGE, P.E.B., 2006. Platinum-group mineral assemblages in the Platreef at the Sandsloot Mine, northern Bushveld Complex, South Africa. *Mineralogical magazine*, **70**(1), pp. 83-101.
- HU, Y., SUN, W. and WANG, D., 2009. *Electrochemistry of Flotation of Sulphide Minerals*. Tsinghua University Press and Springer.
- KHAN, A. and KELEBEK, S., 2004. Electrochemical aspects of pyrrhotite and pentlandite in relation to their flotation with xanthate. Part-I: Cyclic voltammetry and rest potential measurements. *Journal of Applied Electrochemistry*, **34**(8), pp. 849-856.
- KINLOCH, E.D., 1982. Regional trends in the platinum-group mineralogy of the critical zone of the Bushveld Complex, South Africa. *Economic Geology*, **77**(6), pp. 1328-1347.
- KINNAIRD, J. and MCDONALD, I., 2005. An introduction to mineralisation in the northern limb of the Bushveld Complex. *Transactions - Institution of Mining and Metallurgy. Section A. Mining industry*, **114**(4), pp. 194-198.

KISSINGER, P.T. and HEINEMAN, W.R., 1983. Cyclic voltammetry. *Journal of chemical education*, **60**(9), pp. 702.

KLIMPEL, R., 1984. Froth Flotation: the Kinetic Approach. *MINTEK 50: International Conference on Mineral Science and Technology*. 1984, pp. 385-392.

KOCABAĞ, D. and GÜLER, T., 2008. A comparative evaluation of the response of platinum and mineral electrodes in sulfide mineral pulps. *International Journal of Mineral Processing*, **87**(1), pp. 51-59.

LIDE, D.R., 2004. *CRC handbook of chemistry and physics*. CRC press.

LIVINGSTONE, S.E., 1965. Metal complexes of ligands containing sulphur, selenium, or tellurium as donor atoms. *Quarterly Reviews, Chemical Society*, **19**(4), pp. 386-425.

MABBOTT, G.A., 1983. An introduction to cyclic voltammetry. *Journal of chemical education*, **60**(9), pp. 697.

MAJIMA, H. and TAKEDA, M., 1968. Electrochemical studies of the xanthate-dixanthogen system on pyrite. *Trans.AIME*, **241**, pp. 431-436.

MCDONALD, I., HOLWELL, D.A. and ARMITAGE, P.E.B., 2005. Geochemistry and mineralogy of the Platreef and "Critical Zone" of the northern lobe of the Bushveld Complex, South Africa: implications for Bushveld stratigraphy and the development of PGE mineralisation. *Mineralium Deposita*, **40**(5), pp. 526-549.

MILLER, J.D., LI, J., DAVIDTZ, J.C. and VOS, F., 2005. A review of pyrrhotite flotation chemistry in the processing of PGM ores. *Minerals Engineering*, **18**(8), pp. 855-865.

MISHRA, K., HAM, D. and RAJESHWAR, K., 1990. Anodic Oxidation of Telluride Ions in Aqueous Base: A Rotating Ring-Disk Electrode Study. *Journal of the Electrochemical Society*, **137**(11), pp. 3438-3441.

MOSLEMI, H., SHAMSI, P. and HABASHI, F., 2011. Pyrite and pyrrhotite open circuit potentials study: Effects on flotation. *Minerals Engineering*, **24**(10), pp. 1038-1045.

NAGARAJ, D.R., 1988. The Chemistry and Application of Chelating or Complexing Agents in Minerals Separations. In: P. SOMUSANDARAN and B.M. MOUDGIL, eds, *Reagents in Mineral Technology*. Marcel Dekker, Inc, pp. 257-334.

PATHAN, H.M., LOKHANDE, C.D., AMALNERKAR, D.P. and SETH, T., 2003. Preparation and characterization of copper telluride thin films by modified chemical bath deposition (M-CBD) method. *Applied Surface Science*, **218**(1–4), pp. 291-297.

PECINA, E.T., URIBE, A., FINCH, J.A. and NAVA, F., 2006. Mechanism of di-isobutyl dithiophosphate adsorption onto galena and pyrite. *Minerals Engineering*, **19**(9), pp. 904-911.

PENBERTHY, C.J., OOSTHUYZEN, E.J. and MERKLE, R.K.W., 2000. The recovery of platinum-group elements from the UG-2 chromitite, Bushveld Complex—a mineralogical perspective. *Mineralogy and petrology*, **68**(1), pp. 213-222.

POLING, G., 1976. Reactions between thiol reagents and sulphide minerals. *Flotation--A.M.Gaudin Memorial*.

POURBAIX, M., 1974. *Atlas of electrochemical equilibria in aqueous solutions*. Houston, Tex.: National Association of Corrosion Engineers.

RALSTON, J. and HEALY, T.W., 1980. Activation of zinc sulphide with Cu II, Cd II and Pb II: I. Activation in weakly acidic media. *International Journal of Mineral Processing*, **7**(3), pp. 175-201.

RAO, S.R. and LEJA, J., 2004. *Surface Chemistry of Froth Flotation: Reagents and mechanisms*. 2nd edn. Plenum Publishers.

ROINE, A., 1999. Outokumpu HSC chemistry for windows: chemical reaction and equilibrium software with extensive thermochemical database. *Pori, Finland: Outokumpu*, .

SARALA, Y. and JAYARAMA REDDY, S., 1986. Electrochemical reduction of tellurium(IV). *Journal of Electroanalytical Chemistry and Interfacial Electrochemistry*, **214**(1–2), pp. 179-190.

SCHOUWSTRA, R.P. and KINLOCH, E.D., 2000. A short geological review of the Bushveld Complex. *Platinum metals review*, **44**(1), pp. 33-39.

SHACKLETON, N.J., MALYSIAK, V. and O'CONNOR, C.T., 2007. Surface characteristics and flotation behaviour of platinum and palladium tellurides. *Minerals Engineering*, **20**(13), pp. 1232-1245.

SHACKLETON, N.J., 2007. *Surface Characterization and Flotation Behaviour of the Platinum and Palladium Arsenide, Telluride and Sulphide Mineral Species*, University of Cape Town.

SHAMAILA, S. and O'CONNOR, C.T., 2008. The role of synthetic minerals in determining the relative flotation behaviour of Platreef PGE tellurides and arsenides. *Minerals Engineering*, **21**(12-14), pp. 899-904.

SOMASUNDARAN, P., 2006. *Solution Chemistry, Volume 17: Minerals and Reagents*. Burlington: Elsevier.

STRUNZ, H. and NICKEL, E.H., 2001. *Strunz mineralogical tables: chemical-structural mineral classification system*. Stuttgart: Schweizerbart.

USUL, A. and TOLUN, R., 1974. Electrochemical study of the pyrite-oxygen-xanthate system. *International Journal of Mineral Processing*, **1**(2), pp. 135-140.

VERMAAK, M.K.G., MILLER, J.D. and LEE, J., 2007. Electrochemical interactions of industrially important platinum-containing minerals. *Minerals Engineering*, **20**(15), pp. 1337-1343.

VERMAAK, M.K.G., PISTORIUS, P.C. and VENTER, J.A., 2005. Electrochemical and Raman spectroscopic studies of the interaction of ethyl xanthate with Pd-Bi-Te. *Minerals Engineering*, **18**(6), pp. 575-584.

VERMAAK, M.K.G., PISTORIUS, P.C. and VENTER, J.A., 2007. Fundamental electrochemical and Raman spectroscopic investigations of the flotation behaviour of PtAs₂. *Minerals Engineering*, **20**(12), pp. 1153-1158.

VILJOEN, M.J. and SCHURMANN, L.W., 1998. Platinum-Group Metals. In: M.G.C. WILSON and C.R. ANHAEUSSER, eds, *The Mineral Resources of South Africa: Handbook*. 6 edn. Council for Geoscience, pp. 532-568.

WANG, J., 2006. *Analytical electrochemistry*. Wiley. com.

WANG, X., FORSSBERG, E. and BOLIN, N.J., 1989. The Aqueous and Surface Chemistry of Activation in the Flotation of Sulphide Minerals—A Review. Part I: An Electrochemical Model. *Mineral Processing and Extractive Metallurgy Review*, **4**(3-4), pp. 135-165.

WANG, X., FORSSBERG, E. and BOLIN, N.J., 1989. The Aqueous and Surface Chemistry of Activation in the Flotation of Sulphide Minerals—A Review. Part II: A Surface Precipitation Model. *Mineral Processing and Extractive Metallurgy Review*, **4**(3-4), pp. 167-199.

WESTLAND, A., 1981. Inorganic chemistry of the platinum-group elements. *Platinum-Group Elements: Mineralogy, geology, recovery*. Canadian Institute of Mining, Metallurgy, and Petroleum, *Special*, **23**, pp. 5-18.

WIESE, J., HARRIS, P.J. and BRADSHAW, D.J.:., 2005. The influence of the reagent suite on the flotation of ores from the Merensky reef. *Minerals Engineering*, **18**(2), pp. 189-198.

WILLS, B.A. and NAPIER-MUNN, T., 2005. 12 - Froth flotation. *Wills' Mineral Processing Technology (Seventh Edition)*. Oxford: Butterworth-Heinemann, pp. 267-352.

WOODS, R., 2010. Electrochemical Aspects of Sulfide Mineral Flotation. In: C.J. GREET, ed, *Flotation Plant Optimisation: A Metallurgical Guide to Identifying and Solving Problems in Flotation Plants*. Spectrum Series 16 edn. AuSIMM, pp. 123-134.

WOODS, R., 1971. Oxidation of ethyl xanthate on platinum, gold, copper, and galena electrodes. Relation to the mechanism of mineral flotation. *The journal of physical chemistry*, **75**(3), pp. 354-362.

WOODS, R., BASILIO, C.I., KIM, D.S. and YOON, R.H., 1992. Ethyl xanthate chemisorption isotherms and Eh-pH diagrams for the silver + water + ethyl xanthate system. *Journal of Electroanalytical Chemistry*, **328**(1-2), pp. 179-194.

WOODS, R., YOUNG, C.A. and YOON, R.H., 1990. Ethyl xanthate chemisorption isotherms and Eh-pH diagrams for the copper/water/xanthate and chalcocite/water/xanthate systems. *International Journal of Mineral Processing*, **30**(1-2), pp. 17-33.

YOON, R.H. and BASILIO, C.I., 1993. Adsorption of Thiol Collectors on Sulphide minerals and Precious Metals - A New Perspective, *XVIII International Mineral Processing Congress, Sidney 1993*, The Australasian Institute of Mining and Metallurgy, pp. 611 - 617.

APPENDICES

Appendix A

CT-Scanning Images for PtS

Scoping of X-Ray CT-Scans was done at 3 different resolutions namely 15 micron, 20 micron and 35 micron resolution. Two voltages 160 kV and 220 kV were applied to the nano-tube.



Figure A.1. PtS CT-Scanning surface image, 220kV, 20 micron resolution and 1hour scan.

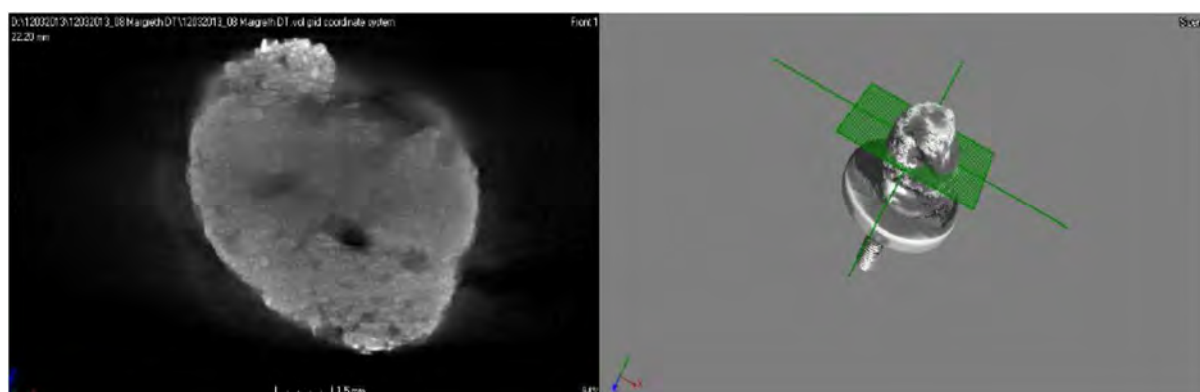


Figure A.2. Cross sectional slice through PtS electrode, 220 kV scan.

APPENDICES

Appendix B

Cyclic Voltammetry Results for Pt/Pd Minerals in De-aerated Solution

Cyclic voltammograms reported in Chapter 4 are reported for aerated solutions and corresponding voltammograms were measured in de-aerated solutions. The voltammograms generated indicate that there is no significant new information that can be determined from measurements under de-aerated solution conditions than aerated solution conditions. These results are presented for the minerals in the presence of SEX in this Appendix.

Voltammograms measured with 600 mV Switching Potential

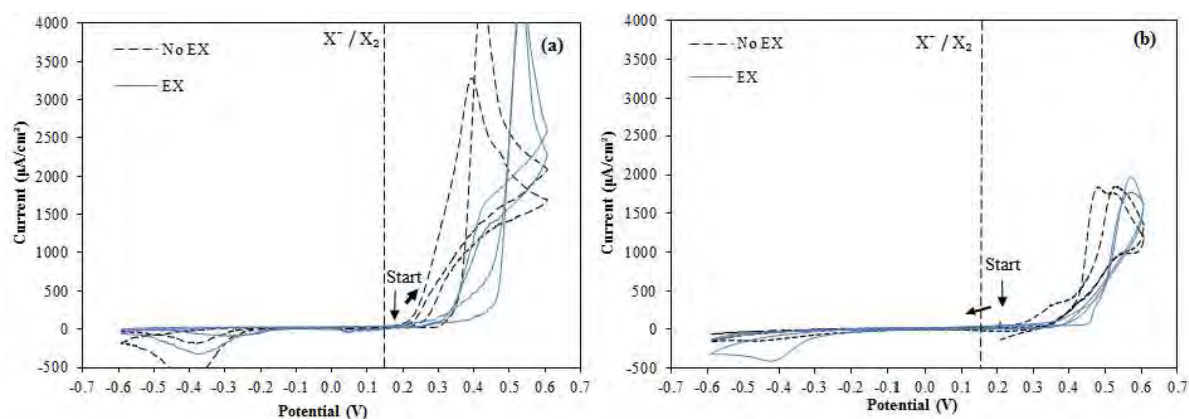


Figure B.1. Cyclic voltammograms for (a) PtTe₂ with a forward starting sweep and (b) PdTe₂ in a reverse starting sweep with two sweeps measured in the absence and presence of collector 6×10^{-4} M. The oxidation potential for dixanthogen is indicated as a dotted line at 0.15 V.

In Figure B.1 the voltammograms for PtTe₂ (a) and PdTe₂ (b) indicate that the behaviour of the mineral under de-aerated solution conditions is similar to that of the mineral in aerated conditions with increased anodic activity occurring for both minerals above a potential of 0.3 V. The presence of collector on the mineral surface inhibits this oxidation resulting in the anodic oxidation occurring at more positive potentials. Reduction currents are observed for the mineral in the region between -0.4 V and -0.3 V.

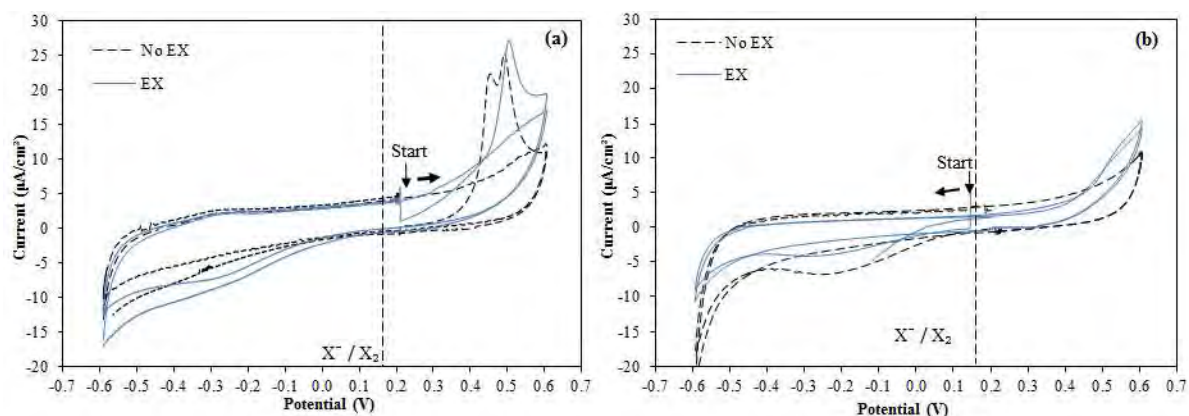


Figure B.2. Cyclic voltammograms for (a) PtS with a forward starting sweep and (b) PdS in a reverse starting sweep with two sweeps measured in the absence and presence of collector 6×10^{-4} M. The oxidation potential for dixanthogen is indicated as a dotted line at 0.15 V.

For the sulphide minerals over a potential range of ± 0.6 V Figure B.2 shows that an anodic oxidation current is present on PtS (a) in the absence of collector which is also present in the presence of collector. In the presence of collector, oxidation of SEX is identified by increased anodic currents. Increased anodic currents on PdS are also indication of collector oxidation at the surface. The initial reverse sweep of PdS in the absence and presence of collector indicates reduction of oxidised species on this mineral which is evidence of the fast kinetics of oxidation on this mineral.

Voltammograms Measured with 400 mV Switching Potential

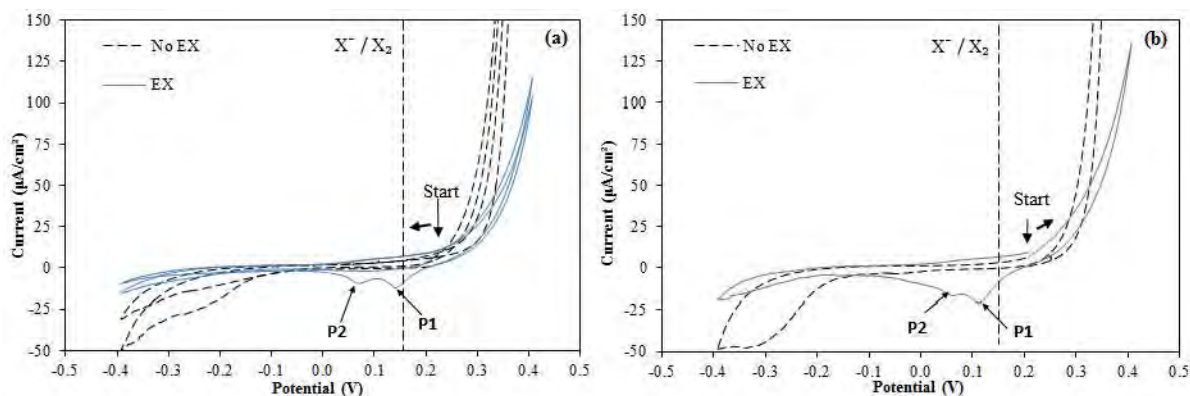


Figure B.3. Cyclic voltammograms for (a) PtTe₂ with a reverse starting sweep measured for two sweeps and (b) PdTe₂ with a forward starting sweep measured for one sweep in the absence and presence of collector 6×10^{-4} M. The oxidation potential for dixanthogen is indicated as a dotted line at 0.15 V.

Over a potential range of ± 0.4 V for reverse and forward starting sweeps the voltammograms for PtTe₂ are shown in Figure B.3 (a) and (b) respectively. Increased anodic activities that are characteristic of the mineral oxidation are identified as those in aerated solution conditions. Reduction currents are more distinguished in the absence of collector, however, as compared to the condition of an aerated solution. Voltammograms generated in the presence of collector indicate reduced anodic currents due to the presence of collector

and two reduction currents P1 and P2 attributed to the reduction of collector species occur below the reduction potential of xanthate to dioxanthone.

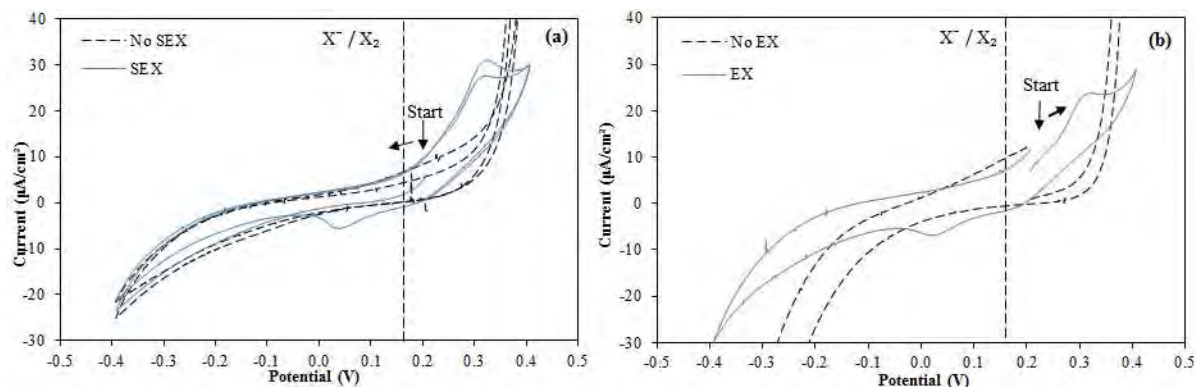


Figure B.4. Cyclic voltammograms for PdTe₂ (a) with a reverse starting sweep measured for two sweeps and (b) with a forward starting sweep measured for one sweep in the absence and presence of collector 6.24×10^{-4} M. The oxidation potential for dioxanthone is indicated as a dotted line at 0.15 V.

Voltammograms for PdTe₂ in Figure B.4 indicate distinct oxidation currents for the collector at anodic potentials with two reduction currents occurring on the reverse sweeps. Anodic oxidation of the mineral is inhibited by the presence of collector. These voltammograms are consistent with those occurring in aerated solutions.

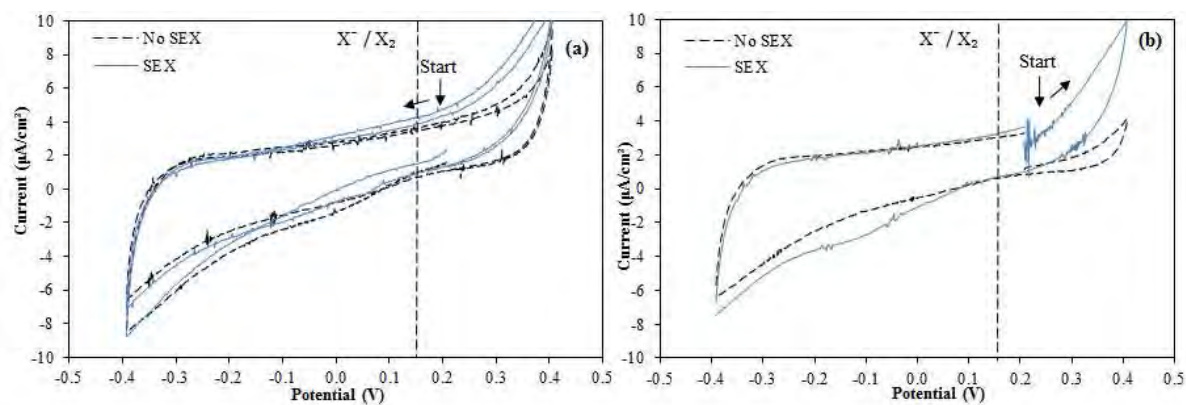


Figure B.5. Cyclic voltammograms for PtS (a) with a reverse starting sweep measured for two sweeps and (b) with a forward starting sweep measured for one sweep in the absence and presence of collector 6.24×10^{-4} M. The oxidation potential for dioxanthone is indicated as a dotted line at 0.15 V.

PtS under de-aerated solution conditions (Figure B.5) does not exhibit the reduction of oxygen. Increased anodic currents in the presence of collector indicate that collector oxidation takes place on the mineral surface. Distinct reduction currents do not occur to match the increased anodic activity and suggest reduction of oxidised collector species.

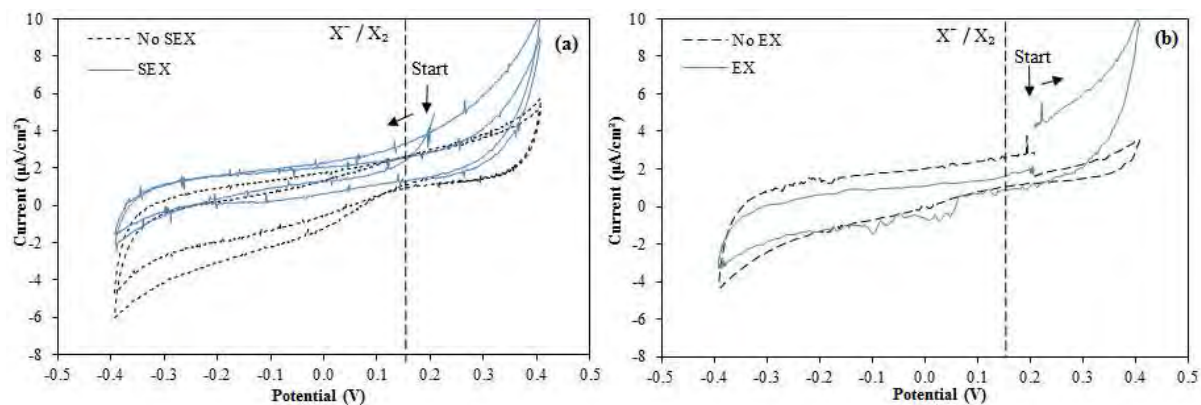


Figure B.6. Cyclic voltammograms for PdS (a) with a reverse starting sweep measured for two sweeps and (b) with a forward starting sweep measured for one sweep in the absence and presence of collector 6.24×10^{-4} M. The oxidation potential for dixanthogen is indicated as a dotted line at 0.15 V.

In Figure B.6, voltammograms generated on PdS similarly to PtS, result in the disappearance of the oxygen reduction currents. Oxidation of the mineral is observed by anodic currents at positive potentials. These currents are lower than those generated in the presence of collector indicating the oxidation of collector at the mineral surface. There is no evidence via the presence of reduction currents to suggest the reduction of oxidation collector species.

APPENDICES

Appendix C

Equilibrium Potential Calculations

The relationship between Gibbs energy of reaction and reaction potential is given by Equation C1.

$$E = - \Delta G_R / nF \quad (C1)$$

Where ΔG_R is the Gibbs free energy of reaction

n is the stoichiometric coefficient

F is Faradays constant (96 485C/mol)

The Nernst equation thus allows the relationship of standard potential to equilibrium potential at the given conditions.

$$E = E^0 + RT/nF \ln (A^{ox}/A^{red}) \quad (C2)$$

At sufficiently low concentrations such as those measured in this work the Nernst Equation can be written in terms of concentration and has been applied in this work as such.

$$E = E^0 + RT / nF \ln [Ox] / [Red] \quad (C3)$$

- Values for the standard equilibrium potential were obtained from HSC Chemistry software, from the Gibbs free energy of reaction. Values of standard equilibrium potential not obtained from HSC chemistry are obtained from the literature.
- Concentration of all soluble species was set at 1×10^{-4} M for calculation purposes
- In accordance with IUPAC conventions the reduction potential was calculated

Calculations for the reactions of the minerals, sulphur and tellurium are presented in Table C.1, which is presented below.

Table C.1. Electrochemical reactions with their standard equilibrium potentials and calculated equilibrium potentials for the conditions measured.

Reaction	E ⁰	Soluble [Te]=[Pt]=1		E(10 ⁻⁴ M TeO ₃ ²⁻) (10 ⁻⁴ M SO ₄ ²⁻)
		E (pH 9)	E (pH 4)	E (pH 9)
PtO + 2TeO₃²⁻ + 14H⁺ + 10e⁻ = PtTe₂ + 7H₂O	0.918 ^[1]	0.256	0.587	0.221
Pt(OH)₂ + 10e⁻ + 14H⁺ + 2TeO₃²⁻ = PtTe₂ + 8H₂O	0.932 ^[1]	0.270		0.235
Pt²⁺ + 2TeO₃²⁻ + 12H⁺ + 10e⁻ = PtTe₂ + 6H₂O	0.972 ^[1]	0.405		0.275
Pt²⁺ + 2Te + 2e⁻ = PtTe₂	1.539 ^[1]	1.539		
PtO + 2Te + 2e⁻ + 2H⁺ = PtTe₂ + H₂O	1.272 ^[1]	0.799		
PtTe + TeO₃²⁻ + 4e⁻ + 6H⁺ = PtTe₂ + 3H₂O	0.866 ^[1]	0.157		0.112
PtO₂ + 2TeO₃²⁻ + 12e⁻ + 16H⁺ = PtTe₂ + 8H₂O	0.940 ^[1]	0.310		0.280
PtO₂ + 2Te + 4e⁻ + 4H⁺ = PtTe₂ + H₂O	1.159 ^[1]	0.686		
PtO + TeO₃²⁻ + 6e⁻ + 8H⁺ = PtTe + 4H₂O	0.953 ^[1]	0.323		0.293
TeO₃²⁻ + 6H⁺ + 4e⁻ ↔ Te(s) + 3H₂O	1.071 ^[2]			0.317
2TeO₃²⁻ + 12H⁺ + 12e⁻ ↔ Te₂²⁻ + H₂O	0.494 ^[2]			0.007
TeO₃²⁻ + 3H₂O + 6e⁻ ↔ Te²⁻ + 6OH⁻	-0.795 ^[2]			-1.254
SO₄²⁻ + 8e⁻ + 10H⁺ = H₂S + 4H₂O	0.303 ^[3]			-0.089
PtO + S + 2e⁻ + 2H⁺ = PtS + H₂O	1.390 ^[1]	0.917	1.154	
PtO + SO₄²⁻ + 8e⁻ + 10H⁺ = PtS + 5H₂O	0.612 ^[1]	0.021	0.317	0.287
Pt²⁺ + SO₄²⁻ + 8e⁻ + 8H⁺ = PtS + 4H₂O	0.680 ^[1]	0.207		0.355
Pt²⁺ + S + 2e⁻ = PtS	1.660 ^[1]	1.660		
PtO + 2e⁻ + 2H⁺ = Pt + H₂O	0.996 ^[1]	0.464	0.760	
Pt + SO₄²⁻ + 6e⁻ + 8H⁺ = PtS + 4H₂O	0.484 ^[1]			0.129
PdO + 2TeO₃²⁻ + 14H⁺ + 10e⁻ = PdTe₂ + 7H₂O	0.885 ^[1]	0.223		0.188
Pd(OH)₂ + 10e⁻ + 14H⁺ + 2TeO₃²⁻ = PdTe₂ + 8H₂O	0.907 ^[1]	0.245		0.210
Pd²⁺ + 2TeO₃²⁻ + 12H⁺ + 10e⁻ = PdTe₂ + 6H₂O	0.910 ^[1]	0.343		0.213
Pd²⁺ + 2Te + 2e⁻ = PdTe₂	1.229 ^[1]	1.229		
PdO + 2Te + 2e⁻ + 2H⁺ = PdTe₂ + H₂O	1.110 ^[1]	0.637		
PdTe + TeO₃²⁻ + 4e⁻ + 6H⁺ = PdTe₂ + 3H₂O	0.887 ^[1]	0.178		0.133
PdO + TeO₃²⁻ + 6e⁻ + 8H⁺ = PdTe + 4H₂O	0.886 ^[1]	0.256		0.226
PdO + S + 2e⁻ + 2H⁺ = PdS + H₂O	1.143 ^[1]	0.670		
PdO + SO₄²⁻ + 8e⁻ + 10H⁺ = PdS + 5H₂O	0.551 ^[1]	-0.040		
Pd²⁺ + SO₄²⁻ + 8e⁻ + 8H⁺ = PdS + 4H₂O	0.58 ^[1]	0.107		
Pd²⁺ + S + 2e⁻ = PdS	1.262 ^[1]	1.262		
PdO + 2e⁻ + 2H⁺ = Pd + H₂O	0.797 ^[1]	0.265		

[1] (Roine, 1999)

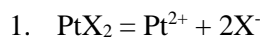
[2] (Mishra et al., 1990)

[3] (Bouroushian, 2010)

Equilibrium potential calculations for formation of metal xanthates

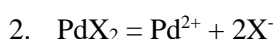
Equilibrium potentials for the formation of metal xanthates PtX_2 and PdX_2 from the minerals were calculated starting with the solubility products of these species using the following relation.

$$\Delta G^0 = -RT \ln K_{sp} \quad (C4)$$



$$\text{Solubility Product (SP)} = [Pt^{2+}][X^-]^2 = 10^{-54} \quad (\text{Chanturiya and Vigdergauz, 2008})$$

$$\Delta G^0 = 308.2 \text{ kJ/mol}$$



$$\text{Solubility Product (SP)} = [Pd^{2+}][X^-]^2 = 3.03 \times 10^{-43} \quad (\text{Chanturiya personal communication})$$

$$\Delta G^0 = 242.68 \text{ kJ/mol}$$

These standard Gibbs energy of formations were used to determine the standard Gibbs energy of reaction for the formation of metal xanthate species by reaction addition as follows;

PtS

	ΔG^0 kJ/mol	E^0 (V)	E (V) pH 9
$PtX_2 = Pt^{2+} + 2X^-$	308.2		
$Pt^{2+} + SO_4^{2-} + 8H^+ + 8e^- = PtS + 4H_2O$	-524.9	0.68	
$PtX_2 + SO_4^{2-} + 8H^+ + 8e^- = PtS + 2X^- + 4H_2O$	-216.7	0.281	-0.211

PtTe₂

	ΔG^0 kJ/mol	E^0 (V)	E (V) pH 9
$PtX_2 = Pt^{2+} + 2X^-$	308.2		
$Pt^{2+} + 2TeO_3^{2-} + 12H^+ + 10e^- = PtTe_2 + 6H_2O$	-937.9	0.972	
$PtX_2 + 2TeO_3^{2-} + 12H^+ + 10e^- = PtTe_2 + 2X^- + 6H_2O$	-629.7	0.653	0.005

PdS

	ΔG° kJ/mol	E° (V)	E (V) pH 9
$\text{PdX}_2 = \text{Pd}^{2+} + 2\text{X}^-$	242.7		
$\text{Pd}^{2+} + \text{SO}_4^{2-} + 8\text{H}^+ + 8\text{e}^- = \text{PdS} + 4\text{H}_2\text{O}$	-447.7	0.580	
$\text{PdX}_2 + \text{SO}_4^{2-} + 8\text{H}^+ + 8\text{e}^- = \text{PdS} + 2\text{X}^- + 4\text{H}_2\text{O}$	-205.0	0.266	-0.226

PdTe₂

	ΔG° kJ/mol	E° (V)	E (V) pH 9
$\text{PdX}_2 = \text{Pd}^{2+} + 2\text{X}^-$	242.7		
$\text{Pd}^{2+} + 2\text{TeO}_3^{2-} + 12\text{H}^+ + 10\text{e}^- = \text{PdTe}_2 + 6\text{H}_2\text{O}$	-878.1	0.910	
$\text{PdX}_2 + 2\text{TeO}_3^{2-} + 12\text{H}^+ + 10\text{e}^- = \text{PdTe}_2 + 2\text{X}^- + 6\text{H}_2\text{O}$	-635.4	0.658	0.011

Reduction of Metal Xanthate Species

Equilibrium potentials for the reduction of metal xanthate species were calculated by adding the standard Gibbs energy of formation of the reactions making up the species formed. Calculations are summarised below.

Reduction of PtX₂

	ΔG° kJ/mol	E° (V)	E (V) pH (9)
$\text{PtX}_2 = \text{Pt}^{2+} + 2\text{X}^-$	308.2		
$\text{Pt}^{2+} + 2\text{e}^- = \text{Pt}$	-227.7	1.180 ^[4]	
$\text{PtX}_2 + 2\text{e}^- = \text{Pt} + 2\text{X}^-$	80.46	-0.417	-0.227

Reduction of PdX₂

	ΔG° kJ/mol	E° (V)	E (V) pH (9)
$\text{PdX}_2 = \text{Pd}^{2+} + 2\text{X}^-$	242.7		
$\text{Pd}^{2+} + 2\text{e}^- = \text{Pd}$	-176.6	0.915 ^[4]	
$\text{PdX}_2 + 2\text{e}^- = \text{Pd} + 2\text{X}^-$	66.1	-0.343	-0.153

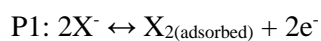
[4] (Lide, 2004)

APPENDICES

Appendix D

Collector coverage calculations

Collector coverage calculations were only made for PtTe₂ since the electrochemical responses obtained for the other minerals studied did not allow for reasonable determination of charge due to species oxidation or reduction. Collector coverage on the PtTe₂ mineral surface was calculated from reduction currents observed on the mineral surface. The assignment of reactions to each of reduction current peaks P1 and P2 are as follows;



P2: Reduction of PtX₂

N.B in order to make comparison with P1 it is assumed that P2 is due to a 2 electron reduction process.

	Peak Position	Charge (μC) ^[1]	Γ (mol) ^[2]	Coverage (Γ/Γ_m) ^[3]
P1	0.122 V, -3.16 μA	-16.28	8.44×10^{-11}	1.12
P2	0.055 V, -3.76 μA	-20.48	1.06×10^{-10}	1.41

1. Integrate the area under the peaks to obtain the amount of charge transferred. This was done using Gamry software (cf. Figure 2) which de-convolutes the voltammogram and defines limits of integration. The limits are shown by solid vertical lines

$$Q/A_{\text{mineral}} = \int_0^t \text{Current Density } dt$$

Where: Q = charge transferred (Coulombs)

A_{mineral} = Surface Area of mineral electrode (cm^2)

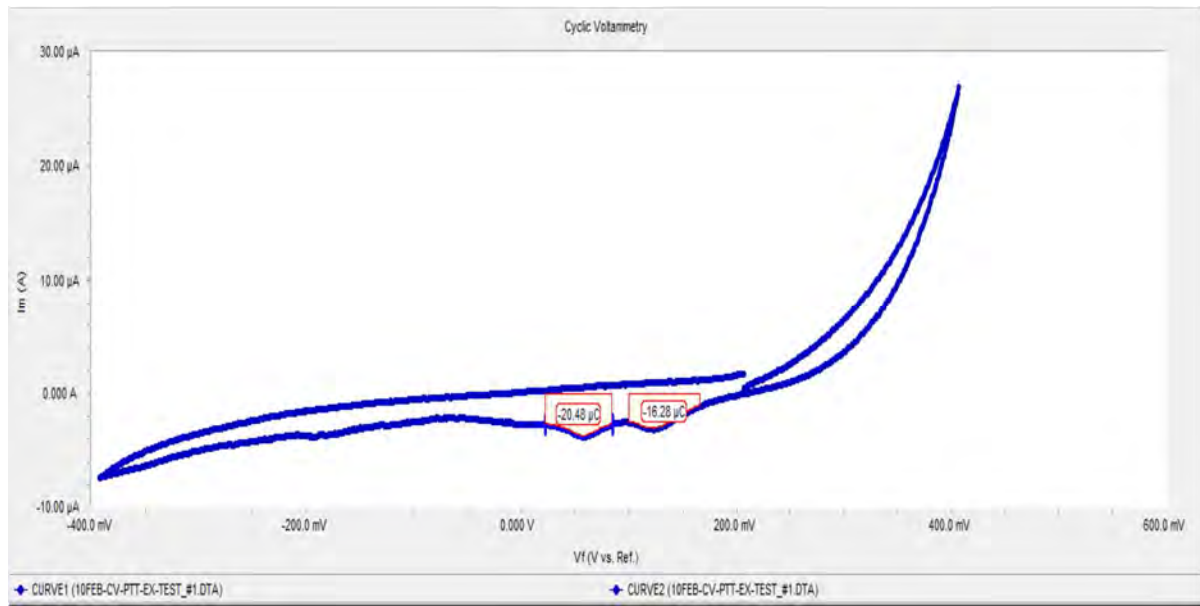


Figure D.1. Gamry software source file for PtTe₂ indicating integrated peaks.

- the number of moles covering the surface can be calculated using Faraday's Law,

$$\Gamma = Q/nFA_{\text{mineral}}$$

- the surface concentration to cover a monolayer is calculated from the area covered by a single collector molecule (for ethyl xanthate this is $3.7 \times 10^{-15} \text{ cm}^2$ (Granville et al., 1972))

$$\Gamma_m = A_{\text{mineral}} / (A_{\text{collector}} \times \text{Avogadro's No})$$

Where the surface area of the PtTe₂ electrode is given by $A_{\text{PtTe}_2} = 0.168 \text{ cm}^2$

And hence the total surface coverage of one layer is given by $\Gamma_m = 7.50 \times 10^{-11} \text{ mol}$